

**Investigation of the Transport of Lipophilic Drugs in
Structurally Diverse Lipid Formulations through Caco-2
Cell Monolayer Using Mathematical Modeling**

Inauguraldissertation

zur

Erlangung der Würde eines Doktors der Philosophie

vorgelegt der

Philosophisch-Naturwissenschaftlichen Fakultät

der Universität Basel

von

Marcel Schneider

aus Koppigen, Kanton Bern (Schweiz)

Basel, 2008

Genehmigt von der von der Philosophisch-Naturwissenschaftlichen Fakultät
auf Antrag von

Herrn Prof. Dr. Georgios Imanidis (Fakultätsverantwortlicher und Dissertationsleiter)

Herrn PD Dr. Peter van Hoogevest (Korreferent)

Basel, den 09.12.2008

Prof. Dr. Eberhard Parlow
Dekan

meinen Eltern und Esther

Acknowledgements

Herrn Prof. Dr. Hans Leuenberger danke ich für die Möglichkeit, dass ich meine Dissertation am Institut für Pharmazeutische Technologie der Universität Basel durchführen konnte.

Bei Prof. Dr. Georgios Imanidis möchte ich mich für die wissenschaftliche Betreuung der vorliegenden Arbeit bedanken. Er ließ mir die Freiräume, die Arbeit nach meinen Vorstellungen zu gestalten, war aber auch jederzeit mit interessanten und kritischen Diskussionen eine wertvolle Unterstützung. Ausserdem möchte ich ihm für den ermöglichten reibungslosen Wechsel an die FHNW danken.

Bedanken möchte ich mich bei PD Dr. Peter van Hoogevest für das Interesse an meiner Arbeit und die Übernahme des Korreferates.

Sabrina Toscano und Daniela Murer danke ich recht herzlich für das Engagement und die produktive Zusammenarbeit während Ihrer Masterarbeiten und das mir entgegengebrachte Vertrauen als Betreuer ihrer Masterarbeiten.

Stefan Winzap danke ich für jegliche technische Unterstützung und für seinen unverzichtbaren Beitrag zum reibungslosen Ablauf des Institutsalltages, Sonja Reutlinger für ihre immer wieder motivierende Art und ihre unverzichtbare Unterstützung beim Übertritt ins IPT der FHNW und ihrem Beitrag zum reibungslosen Ablauf des Institutsalltages.

Weiter möchte ich mich bei meinen Kollegen für die freundliche Atmosphäre und all die Dinge bedanken, die dazu beitragen, dass mir meine Zeit am Institut für pharmazeutische Technologie der Universität Basel und dem Institut Pharma Technology der Fachhochschule Nordwestschweiz in positiver Erinnerung bleiben wird. Besonders bedanke ich mich bei meinen Laborkollegen /-innen Susanne Reitbauer, David Blaser, Miriam Reiser und Constantinos Markopoulos sowie bei allen beteiligten für die Hilfe in der Durchführung des Studentenpraktikums in flüssig-sterilen Arzneiformen, im speziellen bei Johannes von Orelli, Heiko Nalenz und Maxim Puchkov.

Ein ganz spezieller Dank geht an „die letzten Mohikaner“ Thomas Meyer, Franziska Müller und Miriam Reiser

Ganz besonders aber bedanke ich mich bei Esther und meiner Familie für die Geduld und die unermessliche Unterstützung auf dem Weg zur Promotion

ABBREVIATIONS	10
1 SUMMARY	11
2 INTRODUCTION AND OBJECTIVES	14
2.1 Introduction	14
2.2 Objectives	16
3 THEORETICAL SECTION	18
3.1 Drug Absorption after Oral Application	18
3.2 The Gastro-Intestinal Tract and the Intestinal Epithelium	19
3.3 Mechanisms of Membrane Permeation	20
3.3.1 Passive Transcellular Permeation	21
3.3.2 Paracellular Transport	22
3.3.3 Drug Transporters: Carrier Mediated Influx and Efflux	22
3.3.4 Vesicular Transport	23
3.4 In Vitro Assessment of Drug Permeability: Models	23
3.4.1 Excised Tissue Models	23
3.4.2 Cell Models to Study Drug Absorption	24
3.4.3 In Vitro Models Without Cells	25
3.5 <i>In Vitro</i> Assessment of Drug Permeability: Data Analysis	25
3.6 Effect of Food on Drug Absorption	29
3.7 Absorption Enhancement by Solubility Enhancement for Oral Drug Delivery	29
3.8 Absorption Enhancement with Intestinal Permeation Enhancers	29
3.8.1 Permeation Enhancement by Tight Junction Opening	29
3.8.2 Permeation Enhancement by Inhibition of Efflux Transporters	30
3.8.3 Permeation Enhancement by Influencing the Cell Membrane	30
3.9 Influence of Pharmaceutical Formulations on Gastrointestinal Drug Absorption	31
3.10 Mass Transfer of Lipophilic Compounds Between Lipid Particles or Membrane Vesicles and Cell Membranes	32
3.11 Choice of Model Compounds	32
3.12 Choice of Model Formulations	34
4 EXPERIMENTAL SECTION	36
4.1 Influence of Structurally Diverse Lipid Containing Drug Formulations on the Transport of Lipophilic Drugs through Caco-2 Cell Monolayer (Publication Part)	36
4.1.1 Abstract	36
4.1.2 Introduction	36
4.1.3 Material and Methods	39
4.1.3.1 Material	39
4.1.3.2 Cell Culture Procedures	40
4.1.3.3 Drug Quantification	40
4.1.3.4 TEER Measurements	41
4.1.3.5 Drug Permeation Across Caco-2 Cell Monolayers	41

4.1.3.6	Cell Monolayer Drug Extraction	42
4.1.3.7	Drug Extraction out of Transwell Plates	42
4.1.3.8	Production and Characterization of Lipid Containing Drug Dosage Forms	43
4.1.3.8.1	Preparation of Liposomes	43
4.1.3.8.2	Preparation of Emulsions and Microemulsions	43
4.1.3.8.3	Particle Size Measurement	43
4.1.3.9	Equilibrium Dialysis for Free Fraction Determination	44
4.1.3.10	Theoretical Modeling	45
4.1.3.10.1	Mathematical Model for the Determination of Drug Absorption Parameters in Caco-2 Cell Monolayers Including a Term Describing Drug Partition between Donor, Acceptor, and Cell Compartment	45
4.1.3.10.2	Delineating the Components of Apparent Permeability Coefficient Based on a Biophysical Model	50
4.1.3.10.3	Analysis of the Permeation Data	54
4.1.4	Results	55
4.1.4.1	Formulation Characterization	55
4.1.4.2	Cell Permeation of Drugs from Aqueous Solutions and Formulations	57
4.1.4.3	Qualitative Influence of Lipid Phase Concentration on Apparent Permeability Coefficient	67
4.1.4.4	Quantitative Influence of Free Fraction on Apparent Permeability Coefficient	68
4.1.4.5	Effect of Lipid Containing Drug Formulations on Drug Fluxes	74
4.1.5	Discussion	76
4.1.5.1	Cell Permeation Kinetics	76
4.1.5.2	Influence of Lipid Containing Formulations on Carrier Mediated Efflux	77
4.1.5.3	Influence of Formulation and Free Fraction on Apparent Permeability Coefficient	78
4.1.5.4	Drug Flux: Consequences for In-Vivo Drug Delivery?	81
4.1.6	Conclusions	82
4.1.7	Acknowledgements	83
4.2	Screening of Several Lipophilic Compounds to Find a Poorly Soluble Compound with Low Membrane Permeability and No Carrier Mediated Efflux	84
4.2.1	Material and Methods	84
4.2.1.1	Material	84
4.2.1.2	Drug Quantification	85
4.2.1.3	TEER Measurements	86
4.2.1.4	Drug Permeation Across Caco-2 Cell Monolayers	86
4.2.1.5	Data Analysis	87
4.2.2	Results and Discussion	88
4.2.3	Conclusion	89
4.3	Screening of Different Emulsions and Microemulsions for their Suitability as Model Formulation	90
4.3.1	Material	90

4.3.2	Methods	91
4.3.2.1	Preparation of the Formulations	91
4.3.2.2	Particle Size Measurement	91
4.3.2.3	TEER Measurements	91
4.3.2.4	Determination of Transcellular Drug Permeation	91
4.3.2.5	Fluoresceine Quantification	92
4.3.2.6	Data Analysis	92
4.3.3	Results and Discussion	93
4.3.4	Conclusions	94
4.4	Maintaining TEER over Time of the Chosen Formulations: Determination of Duration of Transport Experiments	96
4.4.1	Material and Methods	96
4.4.1.1	Material	96
4.4.1.2	Preparation of Emulsions and Microemulsions	96
4.4.1.3	TEER Measurements	97
4.4.2	Results	97
4.4.3	Conclusions	98
4.5	Development of a Method to Determine the Free Fraction of a Drug Formulation Containing Lipids	99
4.5.1	Material and Methods	99
4.5.1.1	Material	99
4.5.1.2	Preparation of Liposomes	99
4.5.1.3	Preparation of Microemulsions	100
4.5.1.4	Particle Size	100
4.5.1.5	Ultrafiltration	100
4.5.1.6	Ultracentrifugation	100
4.5.1.7	Equilibrium Dialysis	100
4.5.1.8	Drug Quantification	101
4.5.2	Results and Discussion	101
4.5.2.1	Ultrafiltration	101
4.5.2.2	Ultracentrifugation	102
4.5.2.3	Equilibrium Dialysis	103
4.5.3	Conclusions	106
4.6	Calculation of the Free Fraction of Progesterone Liposome Formulations	107
4.6.1	Derivation of an Equation for the Calculation of a Partition Coefficient of a Drug Between Lipid Phase and Water Phase out of Equilibrium Dialysis Experiments	107
4.6.1.1	Results of the Calculated Partition Coefficients	110
4.6.2	Graphical Approach to Assess the Free Fraction of Liposome Formulations	111
4.6.3	Conclusions	112
4.7	Measurements of Cellular Drug Uptake	113
4.7.1	Material and Methods	113

4.7.1.1	Material	113
4.7.1.2	Preparation of the Emulsions	114
4.7.1.3	Measuring the Cellular Uptake to the Cellular Compartment	114
4.7.1.4	Drug Quantification	114
4.7.1.5	Calculation of the Permeability Coefficients	115
4.7.2	Results and Discussion	115
4.7.3	Conclusions	117
4.8	Measurements of Passive Cellular Efflux	118
4.8.1	Material and Methods	118
4.8.1.1	Material	118
4.8.1.2	Preparation of the Formulations	119
4.8.1.3	Determination of Passive Drug Efflux	119
4.8.1.4	Drug Quantification	119
4.8.1.5	Calculation of Permeability Coefficient Delineating Drug Efflux	120
4.8.2	Results and Discussion	120
4.8.3	Conclusions	122
5	CONCLUSIONS AND OUTLOOK	123
5.1	<i>Conclusions</i>	123
5.2	<i>Outlook</i>	125
6	APPENDIX	127
6.1	Determined TEER Values	127
6.1.1	Screening Experiments	127
6.1.2	Microemulsions	127
6.1.3	Emulsions	129
6.1.4	Liposomes	131
6.2	Drug Extraction from Caco-2 Cell Monolayer at the Endpoint of the Transport Experiments	134
6.3	Additional Figures of Qualitative Influence of Lipid Phase Concentration on Apparent Permeability Coefficient	138
6.4	Determination of Maximal Drug Solubility in Formulation Lipid Phases and Calculation of Theoretical Maximal Fluxes	141
6.4.1	Methods	141
6.4.2	Results	141
6.5	Determination of Inorganic and Organic Phosphate of the Acceptor Compartment after Equilibrium Dialysis of a Liposome Formulation	142
6.5.1	Material and Methods	142
6.5.2	Results	142
6.5.3	Conclusions	143
6.6	Detailed Derivations of Used Models and Additional Calculations	144
6.6.1	Detailed Derivation of Delineation of Apparent Permeability Coefficient Based on a Biophysical Model	144

6.6.2	Subdivision of the Apparent Permeability Coefficient Including Permeation through Diffusion Boundary Layer and through Cellular Membrane Including Model Extension for Non-Sink Conditions.	149
6.6.2.1	Fitting the Biophysical Model for the Subdivision of Apparent Permeability Coefficient Including Permeation through Diffusion Boundary Layer and through Cellular Membrane to Apparent Permeability Coefficients out of Cell Permeation Experiments	154
6.6.2.2	Model Extension for Non-Sink Conditions of the Subdivision of the Apparent Permeability Coefficient Including Permeation through Diffusion Boundary Layer and through Cellular Membrane	154
7	REFERENCES	159

ABBREVIATIONS

Å	Angstrom
ABC	ATP binding cassette
ADME	Absorption, Distribution, Metabolism, Elimination of a Drug
ATP	Adenosine triphosphate
AUC	Area under the curve
BCRP	Breast cancer resistance protein
BCS	Biopharmaceutics Classification System
D	Dalton
D-PBS	Dulbecco's Phosphate Buffered Saline
ER	Efflux ratio
HPLC	High performance liquid chromatography
HPLC-UV	High performance liquid chromatography with UV-Vis absorbance detection
HPLC-MS	High performance liquid chromatography with mass spectrometry detection
IAM	Immobilized artificial membrane column
KCts/s	kilo-counts per second
log D	Distribution coefficient (pH dependent ratio of the sum of the concentrations of ionized plus neutral compound in octanol water system).
log P	Partition coefficient (logarithm of the ratio of the concentrations of the un-ionized solute in octanol water system)
MRP 2	Multi resistance protein 2
P _a	Apparent permeability coefficient of the apical membrane
PAMPA	Parallel artificial membrane permeation assay
P _{app}	Apparent permeability coefficient of Caco-2 cell monolayer
P _b	Apparent permeability coefficient of the basal membrane
PCS	Photon Correlation Spectroscopy (dynamic light scattering)
Pgp	P-glycoprotein
pKa	Acid dissociation constant (equal to $-\log_{10} K_a$).
TEER	Trans epithelial electric resistance
SEDDS	Self emulsifying drug delivery system

1 SUMMARY

Introduction: To be absorbed from the gastrointestinal tract, a drug has to be sufficiently soluble, because, with some exceptions, passive diffusion of dissolved drug molecules from high to low drug concentration is the driving force of drug absorption. Different physicochemical and physiological properties determine the reasons for poor drug absorption, which are poor water solubility, low membrane permeability, carrier mediated drug efflux, drug metabolism, and pharmacological interactions. A successful strategy to improve the oral bioavailability of poorly water soluble drugs in vivo is the use of lipid containing dosage forms. Lipid formulation can reduce the inherent limitation of slow and incomplete dissolution of poorly water soluble drugs by facilitating the formation of solubilized phases containing the drug, from which absorption may occur. Only few commercially available products on this basis have been approved so far. Reasons for this small number of approved products may be the limited knowledge about formulation parameters that are responsible for good in vivo performance because of limited understanding of the underlying mechanisms. Compared to an aqueous suspension of lipophilic drug, it is generally agreed so far that improved drug absorption takes place because the drug is solubilized already in a lipid containing dosage form. There is little information in literature dealing with the effect of lipid containing dosage forms on the passive permeation. The objective of this thesis was to elucidate mechanisms by which a lipophilic drug that is contained in a lipid formulation is absorbed by the intestine. For this purpose, a theoretical model and experimental procedures were developed, using Caco-2 cell monolayer.

Methods: Different formulations were tested as model formulations. Since it is known that several formulation components may work as permeation enhancers by tight junction modulation, trans-epithelial electrical resistance (TEER) was used as criteria to test monolayer integrity. As model formulations phosphatidylcholine liposomes, an emulsion with a lipid phase consisting of 67% ($^m/m$) triglyceride (Captex 8000), 5% ($^m/m$) mixture of mono- and diglycerides (Capmul MCM), 18% ($^m/m$) surfactant (Cremophor EL), and 10% ($^m/m$) ethanol, and a microemulsion with a lipid phase consisting of 35.05% ($^m/m$) Captex 8000, 17.58% ($^m/m$) Capmul MCM, 36.84% ($^m/m$) Cremophor EL, and 10% ($^m/m$) ethanol were chosen. To determine the influence of these model formulations on the permeation of lipophilic drugs, different drugs were evaluated as suitable model compounds. Propranolol, progesterone, saquinavir, and triclabendazole were finally selected. An equilibrium dialysis method to determine the free fraction of the drugs in the different formulations was developed. The influence of liposomes, microemulsion, and emulsion on transport processes of the model drugs through Caco-2 monolayer was determined with a bi-directional Caco-2 assay, using purely aqueous drug solutions as reference. At least three different lipid concentrations for each formulation in the range of 0.1-50 mg/ml were tested. Within each lipid concentration at least three different drug concentrations were tested per drug. Apparent passive permeability coefficient of the apical (P_a) and of the basal membrane (P_b), formulation-to-cell partition coefficient, and carrier mediated apical efflux rate were deduced by fitting a mathematical model to the experimental concentration data of the bi-directional assay using Easy Fit[®] fitting software. Further, a biophysical model was developed to delineate the contribution of drug transport in the diffusion boundary layer and drug permeation through cell membrane to the

determined apparent permeability coefficient. Additionally, a differentiation was introduced between permeation of free drug through the cell membrane and permeation following direct drug transfer from the lipid particles to the membrane upon collision. Drug uptake and passive drug efflux for selected drugs and formulations were further studied in the Caco-2 cell monolayer.

Results and Discussion: Both, the model for the determination of absorption parameters in Caco-2 cells and the biophysical model for delineating the components of apparent permeability coefficient explained the experimental data satisfactorily. Generally P_a , P_b , and free fraction decreased with increasing lipid concentration. Within the same lipid concentration, no influence of drug concentration on P_a , P_b , and free fraction was determined. Triclabendazole showed lower P_b than P_a whereas permeability coefficients of all other drugs were equal for both membranes. Carrier mediated apical drug efflux was found for saquinavir only and its rate, when expressed as zero order, decreased with increasing lipid concentration and increased with increasing drug concentration. Formulation-to-cell partition coefficient increased with increasing lipid concentration for all drugs and formulations.

Deduced permeability coefficients of diffusion boundary layer, reflecting drug transport in the apical and basal solution, was smaller than overall permeability coefficient of cell membrane for all drugs except saquinavir for which values were comparable. This indicates that the compounds are good permeable for cell membrane. Permeability coefficient of the drug corresponding to direct mass transfer from lipid particle to cell membrane ($P_{m,L}$) was for progesterone greater than the permeability coefficient corresponding to permeation of free drug through cell membrane ($P_{m,d}$). For triclabendazole $P_{m,L}$ was smaller than $P_{m,d}$. For saquinavir $P_{m,L}$ was comparable or smaller than $P_{m,d}$. Finally for propranolol $P_{m,L}$ was smaller than $P_{m,d}$ for liposome formulation. For propranolol emulsion and microemulsion, no interaction of formulation and drug was observed, therefore no meaningful values were obtained for $P_{m,L}$. The rate limiting step of transport and the dominating mechanism of membrane permeation depend on the corresponding permeability coefficients and the free and lipid bound drug concentration. These observations apply to all three structurally different lipid formulations used in this study. Permeability coefficients of drug uptake of progesterone formulations and passive drug efflux of progesterone and triclabendazole formulations in the Caco-2 monolayer decreased with increasing lipid concentration, which was consistent with the permeation experiments.

Drug fluxes increased with increasing drug concentration within the same lipid concentration and decreased with increasing lipid concentration within the same drug concentration. Fluxes of progesterone in experiments with equal free drug concentration increased with simultaneously increasing drug and lipid concentration. This was demonstrated with progesterone liposomes and can be related to the larger $P_{m,L}$ compared to $P_{m,d}$ found for this drug.

Conclusions: Lipid formulations containing the drug in a molecular form provide the possibility to increase the concentration of poorly water soluble drugs in a macroscopically aqueous system. Apparent drug permeability coefficient for the cell membrane is decreased by these formulations. Apparent drug permeability coefficient depends on free fraction, whereas drug flux depends on absolute amount of free drug in water phase. Therefore simultaneous increase of drug and lipid concentration can provide an undiminished drug flux, which may improve bioavailability by prolonged

intestinal absorption at a sustained rate. These findings are independent of the composition and the structure of the lipid formulation lending support to the universal nature of this conclusion. In addition flux can be further increased by direct drug transfer from lipid particle to cellular membrane. This was observed for only one drug in the present work. The necessary drug properties for this direct transfer to take place should be investigated in the future. The results of this work shed light into the mechanism of drug absorption from lipid formulations and demonstrate potential beneficial effects of these formulations on absorption of lipophilic drugs in vivo. They may be used for the development of efficient oral dosage forms to improve bioavailability for these drugs.

2 INTRODUCTION AND OBJECTIVES

2.1 Introduction

After oral drug administration, which is the most accepted route for drug administration, a drug has to overcome several obstacles to reach the site of its pharmacological action. The drug has to be absorbed from the gut lumen to the blood stream which is the most important prerequisite for a compound to act as drug. The unchanged amount of absorbed drug determines the bioavailability and the systemic exposure of the body to the drug. Many in vitro highly active compounds, generated by modern drug discovery strategies, possess unfavorable biopharmaceutical properties including poor oral absorption, caused by poor solubility or low intestinal wall permeability. A general drug classification of the impact of drug solubility and membrane permeability on drug absorption has been done by the framework of the biopharmaceutics classification system (BCS) (1, 2). Different physiological properties determine the reasons for poor drug absorption such as carrier mediated drug efflux, drug metabolism, and pharmacological interactions. The most important cause for low permeability is the inability of the molecule itself to cross a biological barrier by passive diffusion. Several physicochemical properties are influencing the ability to cross biological barriers which are lipophilicity, molecular weight, hydrogen bonding capacity, and charge (3-6). Lipinski's "rule of five" assesses on the basis of these properties the ability of a drug to be absorbed after oral administration (7).

An increasing number of drugs have been identified to be subject of carrier mediated efflux which is limiting the trans-membrane permeability and finally oral bioavailability. Carrier mediated efflux is caused by proteins located in the apical cell membrane by pumping back drug molecules from the cellular lumen to the intestinal lumen. These efflux pumps have a broad substrate specificity which is a powerful mechanism to prevent the body from the uptake of toxic alimentary ingredients and, unfortunately, from the oral absorption of many drugs (8). Most important efflux transporters for drugs belong to the ATP-binding cassette (ABC) family, e.g. P-glycoprotein (Pgp), breast cancer resistance protein (BCRP) and MRP2 (9-13).

Drug metabolism may affect oral bioavailability by an extensive first pass metabolism of both, the intestinal epithelium and the liver. Drug metabolism is divided into phase I metabolism that includes degradation of the drug molecule by oxidative reactions catalyzed by enzymes, e.g. Cytochrome P450, and phase II metabolism that includes conjugation of the drug or its phase I metabolite with hydrophilic moieties such as glucuronic acid or sulfate (14-19). Because of a large pH-range from 1.5 to 7.4 in the intestinal tract, orally administered drugs may further undergo chemical degradation, which is limiting oral bioavailability too.

The water solubility of poorly water soluble drugs strongly influences absorption and oral bioavailability. It is generally agreed that one of the preconditions for diffusion through a biological membrane is dissolution of the compound in the occurring media. Consequently, water solubility of a compound is one of the most important parameters affecting drug absorption. If the solubility of poorly water soluble drugs is increased, an increase in absorption is observed (2, 20, 21). Several strategies have been developed to increase solubility of poorly water soluble compounds such as chemical

modification, use of salts of ionizable compounds, use of cosolvents, use of surfactants and the use of complexing agents like cyclodextrins. Another strategy is the formulation of poorly water soluble drugs with lipid containing formulations such as self emulsifying drug delivery systems (SEDDS). This strategy has been used successfully to improve the oral bioavailability of some drugs deemed to be hardly deliverable, like cyclosporine A, saquinavir or indinavir (22-28). Only a small number of approved oral lipid formulations are commercially available. Reasons for this small number may be the limited knowledge about formulation parameters that are responsible for good in vivo performance because of limited understanding of the underlying mechanisms. It is generally agreed so far that lipid formulation can reduce the inherent limitation of slow and incomplete dissolution of poorly water soluble drugs by facilitating the formation of solubilized phases containing the drug from which absorption may occur. The underlying molecular mechanisms besides the solubility enhancement and the possibility of direct lymphatic uptake of these lipid containing systems in vivo are rarely known (29, 30).

Many in situ and in vitro models of different levels of complexity and sophistication have been developed to assess and predict the absorption and permeation properties of compounds at different administration sites of the body (31). One of the best characterized and most used model to study drug absorption in the gastrointestinal tract is the Caco-2 cell model. The cells of human colon adenocarcinoma cell line Caco-2 spontaneously differentiate into enterocyte like cells. Seeded on semipermeable filter supports, a cell monolayer expressing a number of active transport proteins results, which permits to investigate simultaneously different absorption mechanisms e.g. passive diffusion and active carrier mediated efflux (32, 33). The Caco-2 model is a useful tool for a mechanistically understanding of drug absorption, which results in an increasing knowledge of the different mechanisms that are part of drug absorption (34).

Like all in vitro models the Caco-2 model has some disadvantages. Caco-2 cells require under standard culture conditions usually three weeks culture on filters before they can be used for drug permeation experiments. Because of their nature as tumor cells, Caco-2 cells may possess different expression levels of transporters and metabolic enzymes and may undergo spontaneous mutagenesis. Inter-laboratory variability and variation of morphological and biochemical properties depending on used passage numbers and culturing conditions are often encountered problems. Standardized cell culture conditions (media, seeding density), the use of established marker compounds, and the use of a predefined small number of passages may help to lower often reported differences of permeability measurements of selected compound for different labs (35-39).

The commonly used approach to assess cell permeability of drugs by the calculation of apparent permeability coefficient P_{app} possesses some limitations: The cell monolayer is modeled as a single rate limiting barrier, without taking into account the influence of a diffusion boundary layer on permeability of highly permeable compounds. This method is not sensitive to mass balance problems such as metabolism, cellular accumulation or nonspecific binding to the device surfaces, and drug stability, because it depends on the total mass transported to the receiver relative to initial mass. The use of this approach still requires the establishment of the linear phase of absorption because the method describes just the initial drug transport under sink conditions. Active apical efflux substrates are identified by comparison of the drug permeability coefficient from apical to basal compartment with

the drug permeability coefficient from basal to apical compartment, forming the efflux ratio (ER) and by performing transport experiments with inhibition of the carrier (40). To overcome unspecific adsorption of highly lipophilic drug molecules to the plastic made surface and to maintain sink conditions additives like albumin were commonly used, sometimes without taking into account a possible influence of these additives to drug permeation (41-43).

Few attempts have been undertaken to investigate complex drug formulations with the Caco-2 models, most of them by searching more physiologically relevant media. Most of these experiments were focusing on cell viability and qualitative effects of the tested formulation on various model drugs (44-53). Little systematical work on the quantitative interactions of lipid containing drug formulations on cellular drug permeation has been published so far.

2.2 Objectives

Because the mechanism of lipid formulations on drug absorption is not clear, in particular the pathway by which the drug that is contained in lipid particles is taken up by epithelial cells has been debated in literature.

The objective of this thesis was to elucidate mechanisms by which a lipophilic drug that is contained in a lipid formulation is absorbed by the intestine. For this purpose, a methodology for determining unbiased parameters in in-vitro cell culture models describing the absorption of lipid containing formulations of poorly soluble drugs in the Caco-2 system was developed. A mathematical model had to be developed and evaluated, describing the processes involved in this system. The aim was to provide a tool to investigate the influence of lipid containing drug formulations on drug permeation through the Caco-2 cell monolayers grown on permeable filter supports in Transwell plates. This methodology consisting of a mathematical model and an appropriate experimental design was developed to provide parameters that delineate passive, carrier mediated, and formulation induced effects on drug permeation and allows the study of different lipid containing drug formulations. It should be able to quantify the contribution of different transport parameters to the epithelial permeation. The model included additionally a partition coefficient describing drug partition of the formulation to the cell and should be used for the quantitative analysis of model compound bi-directional permeation through Caco-2 cell monolayer. Suitable lipophilic model drugs had to be found exhibiting different properties with respect to solubility and permeability. Model compounds with the following properties were identified: High permeability and high solubility (propranolol), high permeability and low solubility (progesterone), low solubility and low permeability (triclabendazole), low permeability, low solubility, and subject to carrier mediated efflux (saquinavir).

Different lipid containing drug formulations were investigated which had different properties concerning the nature of particles. It was of high importance to use formulations of simple composition out of components that are known to be compatible with the Caco-2 cell model. The used model formulations were liposomes, a microemulsion and an emulsion. The formulations were characterized for optical aspect, particle size and free fraction. Concerning free fraction, a reliable method had to be developed for the quantification of the free fraction of structurally different lipid containing dosage forms, which was equilibrium dialysis.

The final benefit of this work is to gain fundamental knowledge about the influence of lipid containing formulations on drug absorption by understanding the mechanism. The result of this work may be used for the development of efficient oral dosage forms to improve bioavailability of poorly water soluble drugs.

3 THEORETICAL SECTION

3.1 Drug Absorption after Oral Application

The oral delivery of drugs is the most accepted administration of drugs for patients. Orally administered drug formulations are preferred to their non-invasive alternatives like dermal or pulmonary delivery for different reasons. A tablet or capsule is very suitable for self medication and compliance; it can easily be swallowed and transported. For the industry, the low production costs, established formulation strategies and long shelf life are important issues.

To ensure an efficient oral delivery, a drug has to be suitable for oral administration. Several criteria have to be met. Due to the enormous pH-range of the gastrointestinal tract from 1.5 in the stomach up to 7-8 in the intestine, a drug has to resist to these conditions. Furthermore, a drug has to resist to high enzymatic activity, specially degradation and metabolism. To be absorbed from the gastrointestinal tract, a drug has to be sufficient soluble, because, with some exceptions, passive diffusion from high to low drug concentration of dissolved drug molecules is the driving force of drug absorption. Drug absorption is generally defined as the process by which unchanged drug proceeds from site of administration to site of measurement within the body (54). Consequently, this means that an orally administered drug has to be able to permeate sufficiently through the gastrointestinal epithelium to reach its active site.

A huge number of potentially new chemical entities have been generated since the introduction of modern drug discovery strategies like combinatorial chemistry and high throughput screening. Resulting compounds of these strategies are often more lipophilic, less soluble, and have a higher molecular weight than traditionally synthesized compounds. A lot of these in vitro highly active compounds possess unfavorable biopharmaceutical properties, which can lead to termination of the clinical development. If the drug development is stopped in an early clinical phase, because the candidate has a low oral bioavailability, an enormous financial effort was spent. One effort to improve properties of potential drug candidates was the introduction of the "Rule of 5" which defines a range of certain properties that a compound has to possess to be absorbed in gastrointestinal tract to achieve good oral bioavailability (7). Oral bioavailability is defined as the fraction of an oral dose reaching the systemic circulation (55).

A growing effort to predict the oral bioavailability at an early development stage is spent. Ideally, the bioavailability may be predicted out of the chemical structure of the compound. The most important predictive properties of a drug for the determination of the absorption are considered to be solubility and permeability. While a lot of strategies are available to increase the solubility of a drug, limited options to increase the membrane permeability are available. It is of enormous importance to assess the solubility and permeability of a new potential compound as early as possible during the development, to secure that the new compound achieves good solubility and good membrane permeability.

In recent years, the biopharmaceutics classification system (BCS) was proposed, established, and many commercial available drugs have been classified according to this system (1, 2). It classifies

drugs into four different classes according to their solubility and permeability. This theoretical classification enables an estimation of oral absorption if conclusive data are available. The BCS classifies compounds into 4 classes: Class I contains compounds with good solubility and high permeability, class II contains compounds with low solubility and high permeability, class III contains compounds with high solubility and low permeability, and class IV contains compounds with low solubility and low permeability (2). According to the BCS classification, a drug is highly soluble if the highest oral dose strength is soluble in 250 ml or less of aqueous media over a pH range of 1-7.5. A drug is highly permeable if the extent of absorption is determined 90% or more of the administered dose in vivo (2, 56).

Aqueous solubility of a drug is an important physicochemical parameter that has a significant role in various physical and biological processes. According to the simplest definition, the solubility of a drug is the maximum amount of the most stable crystalline form, which is molecularly dispersed in a solvent in equilibrium, in a given volume at a given temperature and pressure. Inadequate solubility of a drug results in incomplete and slow oral absorption in vivo. Through the various phases of discovery and development of a drug, solubility information serves a wide range of needs: At an early stage of development, solubility is an important parameter to decide that a compound is soluble enough to be used in activity screenings. Later, solubility data is extensively used to assess absorption of the drug and in formulation development for early and late clinical phases (20). Strategies to improve the solubility and the permeability of a drug will be discussed later in this section.

3.2 The Gastro-Intestinal Tract and the Intestinal Epithelium

After swallowing, an oral dosage form enters the stomach. The acidic environment of pH 1-2 in fasted state and 3-4 in fed state degrades bacteria as well as some drugs (57). A drug solution, drug suspension, or an intact dosage form enters then the duodenum and the small intestine, which are the main intestinal segments for absorption. The gastrointestinal tract is geometrically idealized a tube, covered with epithelia. In the duodenum and the small intestine, a macroscopic mucosal surface area magnification including circular folds, villi, and a microscopic surface area with brush border on the apical membrane, ensures a huge surface (around 200 m²) for absorption (see Figure 1). The mucosal membrane of the intestinal epithelial cells is regarded as the primary permeability barrier to drug absorption from oral administration. Epithelial tissues generally demarcate body entry points like skin, respiratory and gastrointestinal epithelia, predisposing a general barrier function. The gastrointestinal epithelia serve special function promoting efficient nutrient digestion and absorption. This dual absorption-protection function of the epithelia requires an efficient strategy to attenuate the entry of noxious solutes.

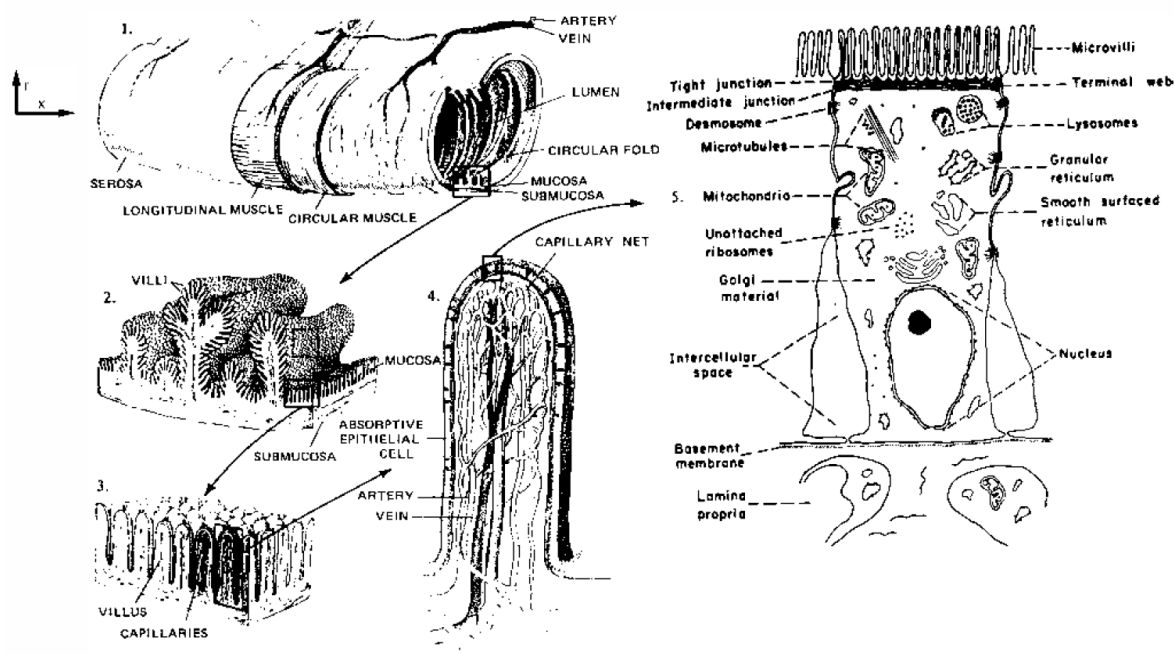


Figure 1 Increasingly magnified views of intestinal epithelia from cylindrical tube to enterocyte (Figure originally published in Friedmann, MH Principles and Models of Biological Transport, Springer-Verlag, Berlin 1986)

The gastrointestinal epithelia is composed of different cell types, namely paneth, goblet, endocrine, and absorptive cells. Enterocytes, the absorptive cells, dominate the cellular population of the epithelium and serve the major role in gastrointestinal solute transport. The enterocytes are highly polarized cells. The apical side, which is directed to the intestinal lumen, exhibits a microvillus brush border membrane. The paracellular space is sealed with tight junctions. Close to the basal membrane there are blood capillaries and lymphatic vessels to assure efficient absorption of nutrients. The mucosa is covered with a layer of intestinal mucus with a thickness between 50 and 450 μm and consists of water (>95%), glycoproteins (mainly mucine), and lipids (58).

The Intestinal mucus layer, the apical membrane of the enterocyte in parallel with the tight junction barrier, cytosol, basolateral membrane in parallel with the lateral intercellular space basement membrane, and parallel lamina propria endothelial membranes of blood vessels and lymphatic vessels contribute to the barrier function of the epithelia (59).

3.3 Mechanisms of Membrane Permeation

Different parameters are influencing pharmacokinetics and pharmacodynamics of drugs to reach their target in sufficient, therapeutic relevant concentration. The site of application is usually apart from the site of action, thus most drugs have to cross biological membranes after application. If the drug does not reach its molecular target, no therapeutic effect will take place. The ability of a drug to cross membranes is one of the most important properties for a successful systemical therapy because it influences the pharmacokinetic profile in absorption, distribution and elimination.

The main process to cross biological membranes is passive diffusion, which is influenced by both, the physicochemical properties of the drug and the biological barrier. For permeates, the main

physicochemical properties influencing the permeation through membranes are lipophilicity, molecular weight, size, hydrogen-bonding capacity, and charge. The presence of water pores, the lipophilic manner of the bilayer, and the membrane surface area are considered to be important factors influencing membrane transport. The transport through a biological barrier, e.g. the gastrointestinal epithelium, can be divided into passive transport through the cellular membrane (passive transcellular permeation), passive transport through tight junctions (paracellular transport) and active transport processes (carrier or vesicle mediated) (3, 60). These different mechanisms will be discussed in the next chapters.

3.3.1 Passive Transcellular Permeation

Our current understanding of the structure of biological membranes, consisting of a lipid-double-layer, is the fluid-mosaic model (61). The double layer structure is a result of the orientation of amphoteric lipids in aqueous medium. The double layer consists of phospholipids, glycolipids, and cholesterol. Major membrane constituents are different amphiphilic phospholipids. Phospholipids consist of a glycerol backbone, two fatty acids and a phosphorylated alcohol. Typical chain length of the fatty acids are 14-18 carbon atoms. Most important phospholipids are phosphatidylcholine, phosphatidylserine, and phosphatidylethanolamine. The double layer structure with a lipophilic core and a polar surface is highly flexible and allows its constituents lateral and transversal movements (3). Inner and outer leaflet of cellular membranes are differently composed. Additionally, there are many different proteins embedded in the membrane performing different functions. A cellular membrane is 7-8 nm thick and is permeable for neutral and lipophilic compounds and water. Ions are not able to pass the phospholipid barrier. Special trans-membranal proteins form selective ion channels. Membrane composition varies depending on tissue type and location.

The fluid mosaic model was further developed by the lipid raft hypothesis. Lipid rafts are membrane microdomains enriched in cholesterol and sphingolipids. These extremely small rafts are formed by highly dynamic clustering of sphingolipids and cholesterol and involve interactions of both proteins and lipids (62). The rafts have been implicated in processes as diverse as signal transduction, endocytosis, cholesterol trafficking, and altering of function of trans-membranal proteins. A lot of papers dealing with rafts were published but there is still skepticism about the real nature of existence and their functions. More work is still needed to confirm or neglect the raft hypothesis (63).

The passive transcellular transport can be divided into several steps. The partitioning of the permeant into the apical monolayer is considered to be the first step, followed by either partitioning and diffusion through the cytoplasm following partition into the basolateral membrane or translateral diffusion inside of the lipophilic core of the cell membrane. The resulting pathway is depending on the physicochemical properties of the permeate, as translateral diffusion is expected mainly for highly lipophilic molecules. After reaching basolateral membrane, the permeate partitions out of the membrane to the basolateral space. Diffusion to the membrane surface and through the cytoplasm are fast processes, whereas the rate of passive transcellular permeability is mainly determined by the transport across the cell membrane. Passive permeation depends to a large extent on three interdependent physicochemical properties, which were lipophilicity (independent of pKa: $\log P$, dependent of pKa: $\log D$), polarity (charge, hydrogen bonding), and molecular size of the permeant (3,

60). Gastrointestinal epithelial cells are polarized. The apical surface borders to the intestinal lumen and is covered with microvilli and the brush border, while basolateral plasma membrane faces the basal lamina and underlying tissue. To maintain an optimal physiological function, the two membranes are different in their protein and lipid compositions. The basolateral membrane is enriched e.g. in sphingomyelin and phosphatidylcholine (64, 65). Consequently, the membrane permeability coefficient of a compound may be different through apical and basolateral membrane.

3.3.2 Paracellular Transport

The passive paracellular pathway is an aqueous, extracellular route across the epithelium. The driving forces are the electrochemical potential gradients derived from differences in concentration, electrical potential, and hydrostatic pressure between the two sides of the epithelium. The main barrier to passive paracellular diffusion is the tight junction (66). The tight junction is an intracellular junctional structure that mediates adhesion between epithelial cells and is required for epithelial cell function. Tight junctions control paracellular permeability across epithelial cell sheets (67). The dimension of the paracellular space in tissues is between 10 and 30-50 Å suggesting that molecules with a molecular radius exceeding 15 Å (ca. 3.5 kD) will be excluded from this uptake route (68). The available pores of epithelial tissues, where cells are connected to each other by tight junctions are smaller. The calculated pore radii of the human intestinal tract tight junctions are 6-8 Å in jejunum, 2.9-3.8 Å in ileum, and less than 2.3 Å in colon (69). The pore radius of Caco-2 monolayer was determined to be 12 Å (59). The paracellular pathway is the preferred pathway of larger hydrophilic compounds and ions. The total contribution of the paracellular pathway to general drug transport is very low because of the low surface fraction of the pores to the total surface. The cell membrane surface is more than 1000 times larger than the paracellular surface area (70).

3.3.3 Drug Transporters: Carrier Mediated Influx and Efflux

The small intestinal mucosa expresses large numbers of absorption transporters responsible for absorption of nutrients and vitamins. In addition to their physiological function, these transporters have shown to mediate the absorption of some drugs, e.g. transporters for di- and tripeptides, amino acids, bile acids, nucleosides, and monocarboxylic acids. These influx transporters can increase the drug absorption by binding dissolved compounds from intestinal fluid and transport them through the epithelial membrane. Compounds that are substrates of these transporters exhibit intestinal absorption higher than expected from their diffusion across cell membranes.

In contrast to absorption transporters, efflux transporters can have the opposite effect by transporting compounds from the cell lumen or the inner membrane leaflet to the intestinal lumen. This process is called apical efflux and is mediated by transporters that belong to the ATP binding cassette (ABC) superfamily. P-glycoprotein (Pgp) is the most studied member of the apical efflux transporters and is the product of the MDR1 gene. Pgp has 2 subunits with 6 trans-membrane domains and two ATP binding sites. It is located on the apical cell membrane of enterocytes and also expressed in other tissues (66). Pgp was one of the first transporters that have been identified to be involved in the efflux of drugs. It has broad substrate specificity and transports a lot of structurally diverse drugs (12).

All of these described mechanisms and examples of transporters have in common, that carrier mediated transport can be directed against a concentration gradient, is energy dependent, and undergoes saturable transport kinetics. A saturable transport undergoes an increased passive transported fraction with increased dose. If the drug has a low permeability, a decreased fraction absorbed results (70).

3.3.4 Vesicular Transport

The vesicular transport process starts when the plasma membrane forms invaginations that pinch off and form small vesicles that migrate from the cell membrane inwards to the cellular lumen. These vesicles fuse with endosomes and if they undergo fusion with the basolateral side of the cell membrane followed by release of the vesicle lumen to the basolateral space the process is called transcytosis (66). This route is less attractive for drug transport, because of its low capacity, but it is an interesting transport pathway for large and highly potent molecules. In gastrointestinal tract transcytosis of macromolecules is mainly performed by M-cells that are overlying the lymphoid tissue in gastrointestinal tract (70).

3.4 In Vitro Assessment of Drug Permeability: Models

In vivo drug absorption in animals is generally a good predictor for human absorption, but with the increasing number of potential drug candidates resulting out of modern lead finding strategies, in vivo models are too complex and too inefficient to screen a large number of compounds. Due to the hazardous potential of unknown compounds, ethical concerns, complexity of the analytical methods, and the time and work intensive nature of the experiments are disadvantages of in vivo experiments. For an efficient strategy to test compounds of ADME properties, fast and easy in vitro models are of growing importance to the pharmaceutical research. The following section gives a brief overview over in vitro methods used in drug discovery.

3.4.1 Excised Tissue Models

Excised tissue models have been extensively used to study drug absorption. They have the big advantage that the architecture of the tissue is obtained. One of the common tissue models is the use of perfused intestinal segments. The isolated segment comprises the absorptive cells and the underlying muscle layers. Sampling is done only on the mucosal side which implies that drug disappearance is assumed to be equal to the drug absorption. Efflux, metabolism and accumulation in the tissue could lead to a wrong estimation of absorption. Because of physiological differences of intestinal segments, the number of intestinal segments obtained from one animal are limited. Additionally, the viability of a segment is limited. This technique is not suitable for a screening tool but may be useful in the evaluation of complex drug formulations (71, 72).

Another common tissue model is the everted sac model. A piece of intestine is inverted and the ends are tied. After filling the segment with buffer, the sac is placed in a solution of the test compound and samples are taken inside and outside of the sac. It suffers from similar problems as the perfused intestinal segments model (73, 74).

Diffusion cells with intestinal mucosa without muscle layer as barrier between the two compartments is used too. It allows the determination of transport polarity and the study of drug absorption within different intestinal segments. The complexity of this technique, specially the preparation of mucosa, is a big disadvantage compared with modern cell models (66, 72).

3.4.2 Cell Models to Study Drug Absorption

Numerous different cultured cells have been used to study intestinal absorption. Today, mainly Colon Adenocarcinoma Cells (Caco-2), HT-29, and Madin-Darby Canine Kidney Cells (MDCK) are used. Since drug transport studies in cell monolayers are easy to perform and require only small drug quantities, they are extensively used screening tools at an early stage of drug development (70).

Madin-Darby Canine Kidney cells form polarized monolayers and develop tight junctions under adequate culture conditions. They need short culture times and the Trans Epithelial Electrical Resistance (TEER) is similar to the in vivo situation. The cells are well characterized but the origin of this cell line is generally considered as disadvantage compared to intestinal cell lines (36, 66).

HT 29, a cell line derived from a human colonic adenocarcinoma, form under adequate culture conditions monolayers of polarized cells and differentiate into enterocytic or mucus secreting goblet cells. Different clones have been used to study intestinal absorption (66). One clone, the HT29-H clone, secretes mucus and may be an interesting model to study drug absorption but these cells grow very slowly. Culture times up to 43 days are needed (75).

Most drug transport studies in cell monolayers have been performed using Caco-2 cell monolayer. The Caco-2 cells were characterized as an intestinal permeability model in 1989. The cells were isolated from a colon adenocarcinoma. These intestinal epithelial cells differentiate into polarized cells with distinct mucosal and serosal cell membrane domains if seeded on porous polycarbonate membranes (32). The differentiation of the Caco-2 cells starts with reaching cell confluence between day 4 and 7 and is finished after 16 days in culture. Although they originate from colon cells, they have a lot of the properties of small intestinal absorptive cells, including microvilli, intercellular tight junctions, and many of the enzymes, nutrient transporters, and efflux transporters present in the small intestinal absorptive cells (76). Some of the most important transport proteins are expressed as P-glycoprotein, multidrug resistance protein, and transporters for glucose, amino acids, folic acids, biotin, peptides, nucleosides, and monocarboxylic acids. The cells also express enzymes for phase I and phase II metabolism like Cytochrome P450, sucrose isomaltase, lactase, amino-peptidase, alkaline peptidase, carboxylesterases, glucuronyltransferases, N-acetyltransferase, sulfotransferase, and glutathione S-transferase (38). Most studies investigating mechanistic drug transport focused on active drug transport, but a good correlation with intestinal tissue and in vivo oral absorption data was found too (70, 77).

One main disadvantage of the current Caco-2 cell model is the lack or underexpression of one of the most important oxidative metabolic enzyme in the gastrointestinal tract, the Cytochrome P450 3A4. Different approaches have been undertaken to increase Cytochrome P450 3A4 levels by transfection

or change of culture conditions (78, 79). Because of their nature as tumor cells, Caco-2 cells may possess different expression levels of transporters and metabolic enzymes and may undergo spontaneous mutagenesis. Morphological and biochemical properties vary with passage numbers (38). Standardized cell culture conditions (media, seeding density) and Transwell inserts, the use of marker compounds and the use of a small number of passages may help to lower inter-laboratory differences (35-37, 80). The long culture time of around 20 days may be disadvantageous but shorter protocols have been developed but not established (81). Despite these limitations, the Caco-2 cells constitute an excellent model to study the drug transport across the intestinal barrier, provided that its limitations are taken into account in interpreting the data.

3.4.3 In Vitro Models Without Cells

To classify compounds to their ability to simple passive membrane permeation, several methods that do not involve biological material have been developed. The advantages of these techniques are the higher throughput and better reproducibility.

A system to study relationship between molecular structures and lipophilicity is Immobilized Artificial Membrane Column (IAM). It consists of a special reverse-phase liquid chromatography column, where the support of the solid phase is coated with lipids. The correlation between membrane permeability and IAM is done by the retention time. A good membrane permeable compound has a long retention. The use and relevance of this method to study drug absorption is limited (66).

Parallel Artificial Membrane Permeation Assay (PAMPA) uses 96-well plates consisting of two parts. The bottom is a standard 96-well plate filled with buffer. A special top part contains filters impregnated with an organic solvent which are mimicking the cell membrane. The test compound is added to the top part and membrane permeation is measured. This fast and cheap method has shown a good correlation with Caco-2 and human absorption data (66, 82, 83). PAMPA allows studying passive membrane absorption only, but it ignores the possible role of active processes, enzymes, and drug metabolism. PAMPA and Caco-2 can be synergistically applied for efficient and rapid investigation of permeation mechanisms in drug discovery. During early discovery, all compounds can be rapidly screened using PAMPA to assess passive diffusion permeability to indicate potential for gastrointestinal and cell assay permeation. Later in drug discovery, a combination of PAMPA with Caco-2 assay for potentially interesting compounds may be reasonable to characterize completely permeation mechanisms (84).

3.5 In Vitro Assessment of Drug Permeability: Data Analysis

In vivo, several factors influence the rate of drug absorption from the intestine. Dissolution rate and solubility determine how fast a drug reaches its maximum plasma concentration c_{\max} . The permeability coefficient P_{wall} determines the rate of a drug crossing the biological barrier. Together, these factors comprise Fick's first law and describe the flux J_{wall} of a drug across a biological barrier:

$$J_{\text{wall}} = P_{\text{wall}} \cdot c_{\max}$$

Equation 1

If drug permeability is assessed with an in vitro model, the apparent permeability coefficient is described with the following approximated solution:

$$P_{app} = \frac{dc_R}{dt} \cdot \frac{V_R}{A \cdot c_{0D}}$$

Equation 2

Where P_{app} is the apparent permeability coefficient, dc_R/dt the change of drug concentration in receiver compartment over time, V_R the volume of the receiver compartment, A the area of the barrier surface, and c_{0D} the initial drug concentration in the donor compartment (85).

This approach has some limitations. The cell monolayer is considered as a single rate limiting barrier, without taking into account possible influence on permeability of a diffusion boundary layer on highly permeable compounds. Equation 2 is not sensitive to mass balance problems like metabolism, binding to cells or device surfaces, and drug stability, because it depends on the total mass transported to the receiver relative to initial mass. Equation 2 is accurate for an early time point, defined by linear drug transport with time, maintaining of sink conditions, and negligible backflow (86).

Since this approach does not directly show any involvement of carrier mediated processes, active apical efflux substrates are identified by comparison of the drug permeability from apical to basal compartment with the drug permeability from basal to apical compartment, building the efflux ratio (ER).

$$ER = \frac{P_{appa_b}}{P_{appb_a}}$$

Equation 3

The ER is calculated with Equation 3, where P_{appa_b} is the apparent permeability coefficient in apical to basal direction and P_{appb_a} the apparent permeability coefficient from basal to apical compartment. For compounds with an ER close to one, active efflux is implausible. If ER exceeds 2, involvement of carrier mediated efflux is presumably existent (34). This approach has some limitations and disadvantages. The ER is time dependent and sensitive to the extent of passive permeation, which means that a highly permeable compound may not be detected by this approach, because the ER is practically 1 compared to a low permeable compound with the same amount of carrier mediated transport. The approach to characterize drug transport through cell monolayer with equation 2 and 3 is not suitable to quantify directly the passive permeability of a substrate to carrier mediated transport. The common practice to calculate passive permeability for substrates to carrier mediated transport is to subtract passive transport curves, gained by using an inhibitor for the carrier, from the active transport curve. This might be an approximated semi quantitative solution at early time points, but neglects reversibility of transport, which is substantial over longer time periods. In the apical to basal direction is the calculated permeability lower than the real permeability because the carrier mediated transport is bigger than backdiffusion alone. In the basal to apical direction, the active transport results in higher drug concentrations in the apical compartment compared to passive diffusion alone leading to a higher permeability.

The use of these approximated equations still requires the establishment of the linear phase of permeability because the equation describes just the initial slope of the transport curve. To study substrates of carrier mediated transport or the influence of drug formulations on transport processes it is important to gain knowledge about the equilibrium conditions and the interaction with the cells.

Further, this method does not take into account a potential cellular retention of compounds, which is known for lipophilic drugs (42).

A more detailed model by Ho et al., describing transcellular diffusion of highly membrane interactive permeants and lipophilic molecules with a long membrane residence, differs from the previous described approximation by subdividing the transcellular transport into several single steps as shown in Figure 2.

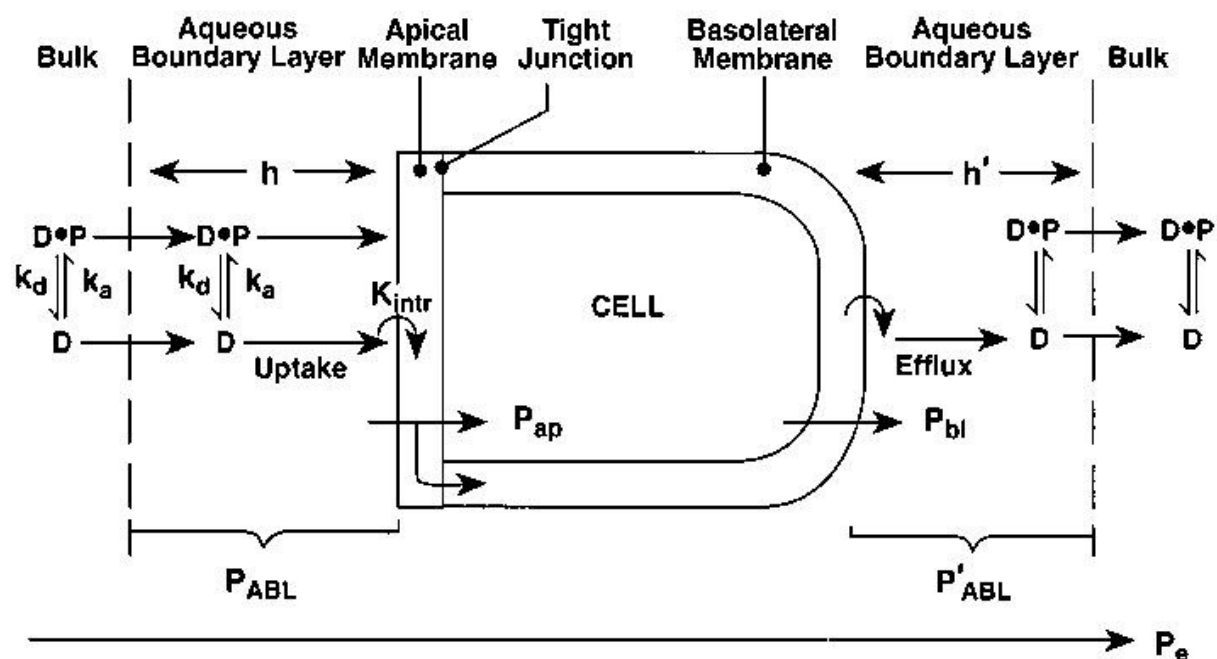


Figure 2 Sophisticated transcellular drug permeation model for highly lipophilic and membrane interactive drugs that takes into account protein binding of the drug, formulation to cell partitioning, influence of diffusion boundary layer, drug uptake and drug efflux. Legend: Highly lipophilic and membrane-interactive drug is denoted by D as it permeates through a cell within a continuous monolayer. h and h', thicknesses of the aqueous boundary layers. k_d and k_a , dissociation and association binding constants, respectively. P, protein molecule. Permeability coefficients: Effective, P_e ; aqueous boundary layer, P_{ABL} and P'_{ABL} ; apical membrane, P_{ap} ; basolateral membrane, P_{bl}

The model describes the transcellular diffusion of a drug solution containing albumin to a receiver compartment containing albumin as well. The model describes the uptake of unbound drug through diffusion boundary layer to the cell and the efflux from the cell into the acceptor compartment. The rate of disappearance of a drug from donor solution can be described as

$$\frac{dC_d}{dt} = -\alpha \cdot C_D + (\alpha\beta + \gamma) \cdot \left[C_D(0) - C_D - \left(\frac{V_R}{V_D} \right) \cdot C_R \right]$$

Equation 4

And the rate of appearance in the receiver sink is

$$\frac{dC_R}{dt} = \gamma \left(\frac{V_D}{V_R} \right) \cdot \left[C_D(0) - C_D - \left(\frac{V_R}{V_D} \right) \cdot C_R \right]$$

Equation 5

Where the apical uptake (α , [min⁻¹]) and basolateral efflux (γ , dimensionless) rate constants and the partition parameter (β , [min⁻¹]) are

$$\alpha = \frac{A \cdot P_e}{V}$$

Equation 6

$$\beta = \frac{V}{V_{cell} \cdot K}$$

Equation 7

$$\gamma = \frac{A \cdot P'_{bl}}{V_{cell}}$$

Equation 8

$$P'_{bl} = \frac{1}{\frac{1}{\epsilon P_{bl}} + \frac{1}{P_F} + \frac{1}{P_{ABL}}}$$

Equation 9

C_D and C_R are the total concentration (including free and bound drug) in the donor volume V_D and in the receiver solution V_R , respectively. V_{cell} is the volume of the cell monolayer, A the cross-sectional area of the monolayer and ϵ is the porosity of the filter. The effective membrane uptake permeability coefficient (P_e) for the apical membrane partition coefficient (K) are functions of protein concentration. The permeability coefficients of the basolateral membrane per se, filter support, and aqueous boundary layer on the filter side are P_{bl} , P_F , and P_{ABL} , respectively.

This model is applicable to quantify not only the transmonolayer kinetics of highly membrane interactive compounds but also the kinetics of less membrane interactive compounds. It also takes into account how a drug formulation influences the permeability (59, 87, 88). One of the disadvantages of this model is, that different experiments with different test assemblies are used to determine the permeability of a compound through a cell monolayer. The uptake experiments in apical to cell direction were performed in Petri dishes, whereas efflux from cell to basal compartment and transmonolayer permeability coefficients were determined using Transwell plates. The model was deduced for simple passive diffusion in the apical to basal direction but does not take into account substrates to carrier mediated efflux.

3.6 Effect of Food on Drug Absorption

The presence of food in the gastrointestinal tract may alter the oral bioavailability of drugs. Food leads to secretion of gastric acid, bile, and pancreatic fluids which may alter the rate and extent of absorption. A slowed gastrointestinal motility and alterations in blood and lymph flow have also an impact on absorption.

The digestion of dietary lipids decreases gastric motility and increases the secretion of bile and pancreatic fluids. Bile may improve the bioavailability of poorly water soluble drugs by enhancing the dissolution rate and the solubility. Bile and the products of lipid digestion (mono- and di-glycerides and free fatty acids) are effective emulsifying agents. Lipids and lipophilic drugs can also be absorbed by the lymphatic pathway, which bypasses the liver first pass metabolism and may increase the bioavailability. Examples for drugs with increased postprandial oral bioavailability are griseofulvin, danazol, and halofantrine (89).

3.7 Absorption Enhancement by Solubility Enhancement for Oral Drug Delivery

Drugs classified in BCS class II achieve high membrane permeability but a low solubility leading to a low dissolution, slow drug uptake, low blood and plasma levels, and poor bioavailability after oral drug uptake. If solubility may be increased with appropriate methods, higher dissolution accomplished by higher drug uptake, and increased plasma levels is achieved. Hence, a lot of strategies were developed in pharmaceutical technology to increase the solubility of drug solutions. Salts are used to increase the solubility of ionizable compounds. Some compounds were able to build complexes with appropriate complexing agents, e.g. cyclodextrins may be used to solubilize lipophilic compounds by embedding them. Cosolvents are used extensively to increase solubility of lipophilic poorly soluble compounds by disturbing the cluster structure of water. The use of surfactants increases the solubility of poorly soluble compounds by formation of micelles, which incorporate the drug molecules.

As mentioned before, oral drug intake after a fatty meal may increase bioavailability of diverse lipophilic compounds. It is obvious as a strategy to improve bioavailability of poorly soluble or poorly absorbed compounds by the use of lipid containing dosage forms (89).

3.8 Absorption Enhancement with Intestinal Permeation Enhancers

3.8.1 Permeation Enhancement by Tight Junction Opening

Hydrophilic, charged compounds are absorbed via the paracellular route. In epithelial tissues, tight junctions are limiting paracellular transport. A transient opening of tight junctions potentially increases paracellular transport and would seem less damaging than a disruption of cell membrane structure. Thus, it is important to develop an understanding of the mechanism of action of an absorption enhancing formulation or excipient.

Various fatty acids have been shown to have membrane permeation enhancing activity. Sodium caprate has been the most thoroughly characterized for use as an absorption enhancing excipient. It increases the Caco-2 permeabilities because of dilatation of tight junctions. In vivo, absorption

enhancement was shown. The absorption enhancing effect was higher in colon than in jejunum. Chitosan acts in vitro as an intestinal permeation enhancer by opening tight junctions in a concentration and pH dependent way. Chitosan reduced Caco-2 TEER values and increased apparent permeability of mannitol. Nevertheless a vehicle containing 1.5% chitosan at pH 6.7 increased the bioavailability of intraduodenally administered buserelin in rats (90).

Degradation products of phospholipids like lysophosphatidylcholine decrease significantly TEER compared to controls in cell models, indicating tight junction opening. Lysophosphatidylcholine may be formed out of phospholipids by the activity of Phospholipase A₂ which is expressed in the intestinal epithelia (91).

3.8.2 Permeation Enhancement by Inhibition of Efflux Transporters

An increasing number of drugs have been recognized as substrates to carrier mediated efflux, which may limit drug absorption. Inhibition of efflux transporters in the intestine offers a potential strategy to improve oral bioavailability. Strategies like coadministration of a drug with affinity to the efflux transporter, coadministration of a specific inhibitor without pharmacological effect, or nonspecific inhibition of the efflux transporter Pgp by pharmaceutical excipients are discussed. Some widely used pharmaceutical excipients, including surface active compounds, lipids, and polymers, are known to enhance the intestinal absorption by inhibiting nonspecifically efflux transporters (92). The underlying mechanisms of efflux inhibition of the pharmaceutical excipients are still under discussion. Several excipients can indirectly inhibit Pgp through effects on the lipid membrane because the activity of Pgp is modulated by the physical state of the lipid bilayer. For example PEG-300 alters the membrane fluidity by changing the microenvironment of the Caco-2 cell membranes, which perturbs the ability of efflux transporters to efflux substrates such as taxol and doxorubicin. PEG-300 causes almost complete inhibition of Pgp activity in an MDR1- transfected Madin-Darby Canine Kidney cell line (93). Also Tween 80 and Cremophor EL increase the membrane fluidity, whereas Vitamin E TPGS decreases the membrane fluidity (94). But changes in membrane fluidity alone may not be generalized as mechanism to reduce transporter activity (95). An alteration in the fluidity of the lipid membrane environment of Pgp modulates the drug efflux, by reduction of the ATPase activity (96). Other mechanism are discussed like energy depletion by decreasing the ATP pool available for Pgp which is together with membrane fluidization, that causes inhibition of Pgp ATPase activity, a critical factor contributing to the Pgp inhibition (97). Pluronic P85 inhibits P- glycoprotein mediated efflux of rhodamine 123 in Caco-2 cells (98).

Some of these in vitro effects have been also verified in vivo (99). In vitro, D- α -tocopheryl polyethylene glycol 1000 succinate (TPGS) acts as a reversal agent for P-glycoprotein multidrug resistance and inhibits Pgp mediated drug transport of paclitaxel and rhodamine 123 in a Caco-2 cell assay (100). In an in vivo intraduodenal perfusion study, low TPGS concentrations (0.04%) significantly increased the bioavailability of talinolol (99).

3.8.3 Permeation Enhancement by Influencing the Cell Membrane

The easiest way to evaluate the effectiveness, mechanism, and potential for toxicity of absorption enhancers is to use in vitro models of the intestinal epithelium (Caco-2 models or animal intestinal

segments). These *in vitro* studies can provide an initial consideration of the possible extent of permeation enhancement for a drug or excipient of interest and whether this can be accomplished without damaging the membrane. But many of the compounds examined *in vitro* as membrane permeation enhancers cause cytotoxicity or membrane damage. Intact intestinal tissues are found to be more resistant to the cytotoxic effects of permeation enhancer than cell culture models, because intact tissue has mechanisms for recovery and an additional physical barrier like intestinal mucus. Various nonionic, anionic, and cationic surfactants have been investigated as intestinal permeation enhancers. Nonionic surfactants influence absorption enhancing activity by size and structure of both the alkyl chain and the polar group. Generally these seem to affect membranes by solubilizing membrane components. Medium chain glycerides, e.g. mono- and diglycerides of caprylic and capric acid, are used as pharmaceutical excipients and as nutritional agents. Diglycerides are much less active than monoglycerides as membrane permeation enhancers. Steroidal detergents like physiologically occurring bile salts have membrane permeation enhancing effects. Many investigators explain membrane permeation enhancing effects with reversibly damaging the intestinal mucosa. The colon may be more sensitive than the small intestine to the absorption enhancing effect of bile acids, as shown in the effects of glycocholate on insulin absorptions in rats. Physiologically, bile salts are present in the intestinal lumen in the form of mixed micelles. The *in vitro* effects of bile salt on epithelial membranes can be quite different when they are incorporated with other agents in mixed micelles. For example the permeation-enhancing effects and cytotoxicity of taurocholate on Caco-2 monolayers was greatly reduced when incorporated with phospholipids or cholesterol in mixed micelles, but a mixed micelle composed of taurocholate and oleic acid had much more potent membrane effects than taurocholate alone (101).

3.9 Influence of Pharmaceutical Formulations on Gastrointestinal Drug Absorption

In previous chapters, the influence of different pharmaceutical excipients on gastrointestinal drug absorption was summarized. Similar effects have been expected, when complex pharmaceutical preparations have been investigated on their influence on gastrointestinal drug absorption. A successful strategy is the formulation of poorly water soluble drugs with lipid containing formulations like self emulsifying drug delivery systems (SEDDS). These orally administered lipid containing dosage forms generally consist of a drug dissolved in a mixture of two or more excipients like triglycerides, partial glycerides, surfactants and cosolvents. The underlying molecular mechanisms of the absorption enhancement are known partially (29, 30). It is generally agreed so far that improved dissolution compared to an aqueous suspension of lipophilic drug increases the absorption because the drug is solubilized in a lipid containing dosage form already (102-104). The dissolution is improved by facilitating the formation of solubilized phases from which absorption may occur. The presence of digestion products and bile salts in the intestine may facilitate diffusion through diffusion boundary layer and alter intrinsic permeability of the intestinal membrane via paracellular and transcellular permeation. It was observed that drug solubilization may decrease the free fraction of poorly soluble drugs. This could potentially lead to a decrease in absorption, if no other beneficial mechanisms are involved (105).

Lymphatic transport has been shown to be a contributor to the oral bioavailability of highly lipophilic drugs. The formation of lipoproteins in the intestinal tract is a prerequisite for lymphatic transport. If highly lipophilic drugs are formulated with suitable lipid containing vehicles, intestinal lymphatic transport may be promoted (106).

Self emulsifying drug delivery systems contain large amounts of surfactants that have been described to have absorption enhancing effects by inhibiting drug efflux (107).

Few commercially available products have been approved so far, where this strategy has been used successfully to improve the oral bioavailability of some drugs deemed to be hardly deliverable, e.g. Neoral[®] (cyclosporine), Norvir[®] (ritonavir), Fortovase[®] (saquinavir), and Agenerase[®] (amprenavir) (22-28, 104). Reasons for this small amount of approved products on this basis may be the limited knowledge about formulation parameters that are responsible for good in vivo performance. Some partially successful attempts have been done for the oral administration of liposomes, most in the field of protein and peptide delivery like vaccine or insulin delivery, only few in the field of poorly water soluble drugs (108).

Of special commercial interest are soft gelatin capsules filled with concentrates of lipid phases, that form fine oil in water emulsions or microemulsions when they are diluted by aqueous solutions under mild agitation (106).

3.10 Mass Transfer of Lipophilic Compounds Between Lipid Particles or Membrane Vesicles and Cell Membranes

As membrane biochemistry studies with liposomes as model membranes were performed, an inter-membrane transfer phenomenon was described where lipophilic molecules were transferred from a liposomal carrier system to model membranes.

Two models have been proposed to explain the transfer of lipophilic molecules between two lipid domains. The first model proposes molecule transfer through water phase as postulated by cholesterol transfer (109). This transfer is mathematically described as first order model, suggesting that the transfer was independent from donor and acceptor vesicle concentration (110). This model follows the “free fraction dogma” in pharmacokinetics, which describes that only unbound drug has a pharmacological effect.

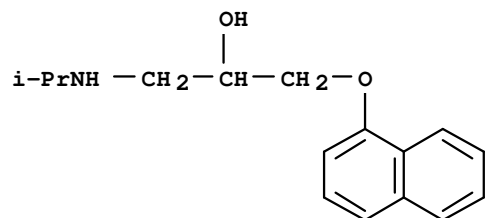
The second model proposes a transfer of lipophilic molecules from lipid domain to lipid domain by collision of lipid vesicles in addition to transfer through the aqueous phase. This collision-model is mathematically described as a second order model originally modeled for cholesterol and phosphatidylcholine transfer between phospholipid vesicles (111). Transfer of lipophilic drugs from lipid containing particles to cell membranes may be subject of the same underlying mechanism (112). The role of these in vitro models for the in vivo situation, has still to be discovered.

3.11 Choice of Model Compounds

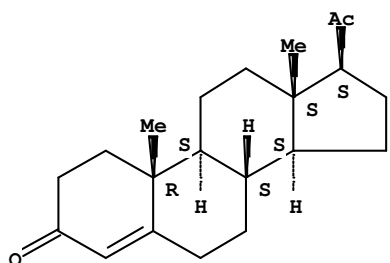
It was the aim of this work to investigate lipophilic drugs with different properties. Literature was searched for lipophilic compounds with high or low permeability according to the biopharmaceutical classification system (BCS). We focused on BCS class I, II, and IV compounds which means high

permeability and high solubility in class I, low solubility and high permeability in class II, and low permeability and low solubility in class IV (2).

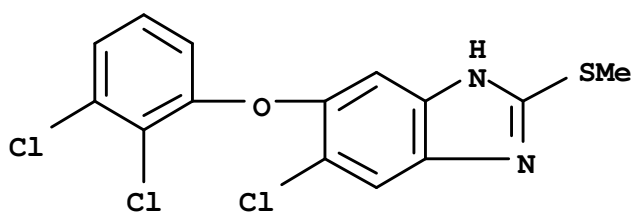
A



B



C



D

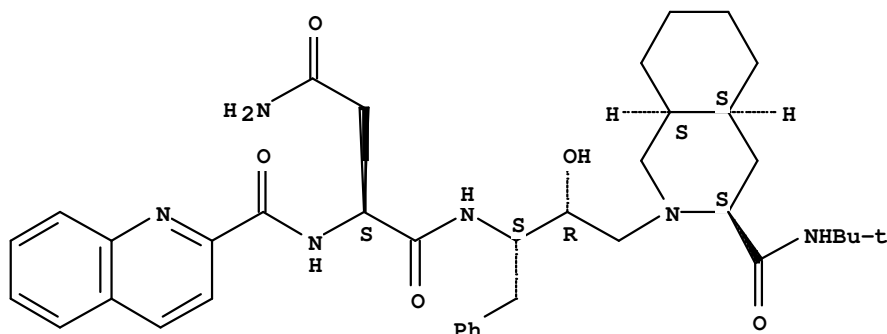


Figure 3 Used model compounds for the determination of the influence of lipid containing dosage forms on Caco-2 cell permeation. Propranolol (panel A), progesterone (panel B), triclabendazole (panel C), and saquinavir (panel D) were used.

Propranolol was chosen as model compound for BCS class I (2). Propranolol is a widely used marker compound for transcellular transport in the Caco-2 assay with a log P of 2.53 (42).

Progesterone was chosen as model compound for BCS class II. It is very slightly soluble in water exhibiting a log P of 3.8-3.87 and no carrier mediated transport is known (42, 113).

As a model compound for BCS class IV, triclabendazole was chosen. It is insoluble in water and exhibits a calculated log P of 5.969 (calculated using Advanced Chemistry Development Software V8.14 for Solaris [1994-2008 ACD/Labs]). The permeability classification is inconclusive and is described in literature as high or low (1). It undergoes strong first liver pass if orally administered (114). As complement, saquinavir was chosen as model compound of BCS class IV, possessing low solubility, exhibiting a log P of 4.1, low permeability, and it is subject of carrier mediated transport (1, 115, 116).

3.12 Choice of Model Formulations

Macroscopically aqueous but microscopically structurally diverse lipid formulations were studied in this work. Liposomes, microemulsions and emulsions were used as model formulations.

Liposomes are spherical vesicles consisting of one or more phospholipid bilayer that are similar to cellular membranes. The formation of these vesicles occur spontaneously if phospholipids were dispersed in aqueous media with appropriate methods. The properties of the liposomes, such as size can be influenced by the membrane composition and the manufacturing process. Liposomes have suitable properties as drug carriers, which are low systemic toxicity, ability to incorporate lipophilic and hydrophilic drugs, and high stability (108). The liposomes, which have been chosen for this work, were tested for their compatibility with the Caco-2 model in previous work of our group already (115). These liposomes consist mainly of Lipoid S100, which is phosphatidylcholine (>94%) isolated from soy lecithin.

Microemulsions are disperse systems of two not miscible phases. They consist typically of one or more lipid, a surfactant, a cosolvents and an aqueous phase. The formation of microemulsions occurs spontaneously if the lipid phase is dispersed under mild agitation in the water phase. Microemulsions are optically clear or exhibit weak opalescence. Typical particle sizes are 5-140 nm (102, 105). The chosen microemulsion was tested already concerning cytotoxicity and compatibility with the Caco-2 model in previous work of our group. The lipid phase was consisting of 35.05% (^m/_m) triglyceride (Captex 8000), 17.58% (^m/_m) mixture of mono- and diglycerides (Capmul MCM), 36.84% (^m/_m) surfactant (Cremophor EL), and 10% (^m/_m) ethanol (117).

Emulsions are disperse systems of two not miscible phases and are composed of a lipid phase and water phase. Emulsions are stabilized by adding an emulgator. Emulsions have bigger particles than microemulsions, are optically turbid and their formation consumes energy. An emulsion, representing the third model formulation, was newly developed for this work. Regarding compatibility with the Caco-2 model, a formulation out of components, which were tested already for their compatibility with the Caco-2 model in previous work of our group, was developed using Cremophor EL, Captex 8000, Capmul MCM, and ethanol. Cremophor EL is a nonionic surfactant and consists of the product of the reaction of ethylene oxide with castor oil. It was chosen for this study because it shows no cell damage up to high concentrations (up to 10%) and shows an inhibiting effect on apical carrier

mediated efflux (94). Captex 8000 consists of >99% tricaprylin, which is a triglyceride substituted with three caprylic acid moieties. Caprylic acid is a C-8 fatty acid. Capmul MCM is a mixture of mono- and diglycerides. The fatty acids consist of 3.2 % capronic acid (C-6), 66.8% caprylic acid (C-8), 29.6% caprinic acid (C-10), and traces of laurinic acid and palmitinic acid. Additionally, ethanol was used as cosolvent.

For this study, it was very important to use formulations with small influence on the tight junctions, because the influence of formulations on the intact membrane barrier should be studied. Since it is known that several formulation components may work as permeation enhancers by tight junction modulation, trans-epithelial electrical resistance (TEER) was used as criteria to test monolayer integrity.

4 EXPERIMENTAL SECTION

The experimental section is divided into different parts which are a publication part (section 4.1), preliminary experiments, and additional work. Each part is discussed separately.

4.1 Influence of Structurally Diverse Lipid Containing Drug Formulations on the Transport of Lipophilic Drugs through Caco-2 Cell Monolayer (Publication Part)

4.1.1 Abstract

Introduction: To overcome poor bioavailability of poorly water soluble drugs, lipid containing drug formulations were used. We determined the influence of structurally diverse lipid containing drug formulations, including liposomes, a microemulsion, and an emulsion, on transport processes of lipophilic model drugs (propranolol, progesterone, saquinavir, and triclabendazole) through Caco-2 monolayers. **Methods:** Drug absorption was determined in a bi-directional Caco-2 assay, using purely aqueous drug solutions as reference. Passive permeability coefficient of the apical (P_a) and of the basal membrane (P_b), formulation-to-cell partition coefficient, and carrier mediated efflux kinetics were deduced by fitting a mathematical model to the transport data with the software Easy Fit[®]. At least three different lipid concentrations for each formulation in the range of 0.1-50 mg/ml were tested. Within each lipid concentration at least three different drug concentrations were tested per drug. The formulations were characterized for free fraction of drug by equilibrium dialysis. Further, a biophysical model was developed to delineate the contribution of drug transport in the diffusion boundary layer and drug permeation through cell membrane to the determined apparent permeability coefficient. Additionally, a differentiation was introduced between permeation of free drug through the cell membrane and permeation following direct drug transfer from the lipid particles to the membrane upon collision. **Results and Discussion:** P_a , P_b and free fraction decreased with increasing lipid concentration. Within one lipid concentration, no influence of drug concentration on P_a , P_b , and free fraction was determined. No effect on permeability and free fraction was observed with propranolol emulsions and microemulsions. Triclabendazole showed lower P_b whereas permeability coefficients of all other drugs were equal for both membranes. Free fraction of drug plays an important role for intestinal cell permeation but direct transfer of lipophilic drugs from lipid phase of the formulation to cell membrane can also make an essential contribution to drug permeation. The relative significance of these two processes may depend on the drug and the formulation. These observations apply to structurally different lipid containing drug formulations. This could explain differences in permeability coefficients of the drugs.

4.1.2 Introduction

The modern drug discovery strategies like combinatorial chemistry and high throughput screening prefer lipophilic, poorly soluble compounds. These compounds show often solubility and oral bioavailability problems in vivo. To ensure an efficient oral delivery, a drug has to be suitable for oral

administration. To be absorbed from the gastrointestinal tract, a drug has to be sufficient soluble, because, with some exceptions, passive diffusion from high to low drug concentration of dissolved drug molecules is the driving force of drug absorption. Drug absorption is generally defined as the process by which unchanged drug proceeds from site of administration to site of measurement within the body (54). A general drug classification of the impact of drug solubility and membrane permeability on the drug absorption has been done by the framework of the biopharmaceutics classification system (BCS) (1, 2). Different physicochemical and physiological properties determine the reasons for poor drug absorption which are poor water solubility, low membrane permeability, carrier mediated drug efflux, drug metabolism, and pharmacological interactions. The most important cause for low permeability is the ability of the molecule itself to cross a biological barrier by passive diffusion. Several physicochemical properties are influencing the ability to cross biological barriers, which are lipophilicity, molecular weight, hydrogen bonding capacity, and charge (3-6).

An increasing number of drugs has been identified to be subject of carrier mediated efflux, which is limiting the trans-membrane permeability and finally the oral bioavailability. Carrier mediated efflux is caused by proteins located in the apical cell membrane by pumping back drug molecules from the cellular compartment to the intestinal lumen. These efflux pumps have a broad substrate spectrum which is a powerful mechanism to prevent the body from the uptake of toxic alimentary ingredients and, unfortunately, from the oral absorption of many drugs (8). Most important efflux transporters for drugs belong to the ATP-binding cassette (ABC) family, e.g. P-glycoprotein (Pgp), breast cancer resistance protein (BCRP) and MRP2 (9-13).

A successful strategy to improve the oral bioavailability of poorly water soluble drugs is the use of lipid containing dosage forms in vivo. Lipid formulation can reduce the inherent limitation of slow and incomplete dissolution of poorly water soluble drugs by facilitating the formation of solubilized phases from which absorption may occur (105). Oral administered lipid containing dosage forms generally consist of a drug dissolved in a mixture of two or more excipients like triglycerides, partial glycerides, surfactants and cosolvents (107). Some partially successful attempts have been done for the oral administration of liposomes, most in the field of protein and peptide delivery like vaccine or insulin delivery, only few in the field of poorly water soluble drugs (108). Of special commercial interest are soft gelatine capsules filled with concentrates of lipid phases, that form fine oil in water emulsions or microemulsions when they are diluted by aqueous solutions under mild agitation (106). Few commercially available products on this basis have been approved so far, e.g. Neoral[®] (cyclosporine), Norvir[®] (ritonavir), Fortovase[®] (saquinavir), and Agenerase[®] (amprenavir) (22-28, 104). Reasons for this small amount of approved products may be limited knowledge about formulation parameters that are responsible for good in vivo performance based on limited knowledge about the underlying mechanisms. It is generally agreed so far that improved dissolution compared to an aqueous suspension of lipophilic drug increases the absorption because the drug is already solubilized in a lipid containing dosage form (102-104). The formation of lipoproteins in the intestinal tract of highly lipophilic drugs formulated with suitable vehicles promotes intestinal lymphatic transport (106). The presence of digestion products and bile salts may facilitate diffusion through diffusion boundary layer and alter intrinsic permeability of the intestinal membrane via paracellular and transcellular permeation (105). Ingredients like surfactants are known to have an inhibitory potential on efflux (92-100, 118).

There is little information in the literature dealing with the effect of lipid containing dosage forms on the passive permeation, which is considered to be the main pathway of drug absorption of poorly water soluble drugs. It was observed that drug solubilization may decrease the free fraction of poorly soluble drugs (105). This could potentially lead to a decrease in absorption, if no other beneficial mechanisms are involved (4, 59, 88, 115). There is little information in literature describing a mechanism for lipophilic drugs that contributes to the transmembranal permeability based on mass transfer from lipid particles to membrane surfaces originating from membrane biochemistry studies with liposomes as model membranes. Two models have been proposed to explain the inter-membrane transfer of lipophilic molecules between two lipid domains. The first model proposes molecule transfer through water phase as postulated by cholesterol transfer (109). This transfer is mathematically described as first order model, suggesting that the transfer is independent from donor and acceptor vesicle concentration (110). The second model proposes a transfer of lipophilic molecules from lipid domain to lipid domain by collision of lipid vesicles in addition to transfer through the aqueous phase. This collision-model is mathematically described as a second order model (111). Lipophilic drugs may be subject of the same underlying mechanism (112). The role of these models for drug transport from lipid vesicles to cellular membranes is rarely known.

In vitro cell models are useful tools to investigate the influence of lipid containing formulations on passive permeation and efflux of poorly water soluble drugs, because none of the in vivo described possible beneficial mechanisms, such as lymphatic transport and lipid digestion, may take place. One of the most frequently used and best characterized cell models for mechanistical studies on drug absorption is the human colon adenocarcinoma cell line Caco-2. These cells spontaneously differentiate into enterocyte like cells and form a cell monolayer when cultivated on a semipermeable filter support. The characteristics of Caco-2 cells have been well described and nicely reviewed elsewhere (32-39, 43, 70, 77-80). Few attempts have been undertaken to investigate complex drug formulations with the Caco-2 model, most of them by testing physiologically more relevant media for their suitability as transport media. Most of these experiments were focusing on cell viability and qualitative effects of the tested formulation on model drugs (44-53, 115, 117). Little systematical work on the quantitative interactions of lipids on cellular drug permeation has been done so far. Previous work of our group showed the possibility to use liposomes as tool to increase solubility of poorly water soluble compounds saquinavir and indinavir (115).

Aim of the study: One of the major objectives of this work was to refine the previously published mathematical model for the kinetics of cellular transport, because this model predicted intracellular concentrations systematically too low (115). On the basis of cell permeation experiments a new biophysical model was developed describing the interactions between lipid containing drug formulation, the drugs, and the cell monolayer for a better understanding of the absorption process through the epithelial barrier. We focused on the influence of the formulations on passive permeability. Additionally we investigated the influence of microemulsions and emulsions on the carrier mediated efflux, because an inhibition of Pgp was observed for saquinavir liposomes in previous work of our group. As model formulations we chose liposomes, an emulsion, and a microemulsion. All components of the formulations, the liposomes, and the microemulsion were tested already for their compatibility with the Caco-2 cell model in previous work of our group regarding cell toxicity (115,

117). Since it is known that several formulation components may work as permeation enhancers by tight junction modulation and we wanted to study the influence of formulations on the intact monolayer, it was very important to use formulations with small influence on the cell monolayer integrity. In this context Cremophor EL was chosen as surfactant in emulsion and microemulsion for this study because it shows no cell damage up to high concentrations (up to 10%) and shows additionally an inhibiting effect on active efflux (94). To determine the influence of the different formulations, we used different model drugs, which had lipophilic properties in common. Propranolol was chosen as model compound for high water solubility and high permeability and belongs to the BCS class I (2). Propranolol is a widely used marker compound for transcellular transport in the Caco-2 assay with a log P of 2.53 (42). Progesterone was chosen as model compound for low water solubility and high permeability and belongs to the BCS class II. Progesterone is very slightly soluble in water exhibiting a log P of 3.8-3.87, no carrier mediated transport is known (42, 113). Triclabendazole was chosen as a model compound for BCS class IV. It is practically insoluble in water and exhibits a calculated log P of 5.969 (calculated using Advanced Chemistry Development Software V8.14 for Solaris [1994-2008 ACD/Labs]). The permeability classification is inconclusive and is described in literature as high or low (1, 114). No carrier mediated apical drug efflux has been reported. As complement saquinavir was chosen as model compound of BCS class IV, possessing low solubility, exhibiting a log P of 4.1, low permeability, and it is subject of carrier mediated transport (1, 115, 116).

4.1.3 Material and Methods

4.1.3.1 Material

The human colon adenocarcinoma cell line Caco-2 was a kindly provided by Prof. H P Hauri, Biocenter, University of Basel, and originated from the American Type Culture Collection (ATCC, Rockville, MD, USA). Dulbecco's Modified Eagle's Medium (DMEM) (with l-glutamine, 4500 mg/l D-glucose, without sodium pyruvate), l-glutamine 200 mM (100x), MEM non essential amino acids solution (100x, without l-glutamine), foetal bovine serum (FBS), Trypsin EDTA (10x) liquid, and Dulbecco's Phosphate Buffered Saline (without Ca^{2+} , Mg^{2+}) were all purchased from Gibco (Gaithersburg, MD, USA). The cell culture medium was composed of DMEM supplemented with 10% (V/V) FBS, 2 mM l-glutamine, and 1% (V/V) MEM.

Transport media used for the permeation studies and the equilibrium dialysis experiments were prepared with Dulbecco's Modified Eagle's Medium (DMEM) base powder (without glucose, l-glutamine, phenol red, sodium pyruvate and sodium bicarbonate, purchased from SIGMA-Aldrich, Fluka Chemie GmbH, Buchs, Switzerland). DMEM base powder was dissolved in bi-distilled and autoclaved water and supplemented with glucose (4.5 g/l), HEPES (4.76 g/l), NaCl (1.987 g/l), and l-glutamine (0.876 g/l). The pH was adjusted to 7.4 and the final medium was filtered through a sterile filter (Supor-200, 0.2 μm pore size, Pall Corporation, Michigan, USA) under aseptic conditions. Glucose, HEPES, NaCl, and l-glutamine were purchased from SIGMA-Aldrich (Fluka Chemie GmbH, Buchs, Switzerland). Dulbecco's Phosphate Buffered Saline (D-PBS) (with Ca^{2+} , Mg^{2+}) was purchased from SIGMA-Aldrich (Fluka Chemie GmbH, Buchs, Switzerland).

Petri dishes (56.7 cm²) were purchased from Nunc (Roskilde, Denmark) and 6-well Polycarbonate Membrane Transwell Plates with an insert area of 4.7 cm² and 0.4 µm pore size were ordered from Costar (Corning Incorporated, Corning, NY, USA).

Captex 8000 was purchased from SIGMA-Aldrich (Fluka Chemie GmbH, Buchs, Switzerland), Capmul MCM was purchased from Abitec Corporation (Janesville, USA). Cremophor EL was ordered from Fluka (Fluka Chemie GmbH, Buchs, Switzerland). Lipoid S 100 and Lipoid EPG were kindly provided by Lipoid GMBH (Ludwigshafen, Germany). Saquinavir was kindly provided by Roche Pharmaceuticals (Basel, Switzerland). Progesterone and propranolol were purchased from Fluka (SIGMA-Aldrich, Fluka Chemie GmbH, Buchs, Switzerland). Triclabendazole was kindly provided by Phares Drug Delivery (Muttens, Switzerland). All other chemicals were of analytical grade.

4.1.3.2 Cell Culture Procedures

Caco-2 cells were cultivated in Petri dishes using culture medium at 37°C in a water saturated atmosphere of 8% CO₂. The cells were passaged by treatment with a solution of 0.25% trypsin and 2.65 mM EDTA with a splitting ratio of 1:12 when the cell monolayer reached 90% confluence on the Petri dishes. Transwell were seeded at a density of 1.14*10⁵ cells/cm² into 6-well Transwell plates. The culture medium was changed every alternating day.

4.1.3.3 Drug Quantification

Drug quantification of all drugs was performed by HPLC-UV (Agilent series 1100, Agilent Technologies USA, equipped with a G1312A binary pump, an auto sampler G1367B and a variable wavelength detector G1314B) using a C-18 reversed phase column (CC 125/2 Lichrospher 100 RP 18 ec, Macherey Nagel, Oensingen, Switzerland). Isocratic methods with a flow rate of 0.25 ml/min were used. The samples were stored at 4°C. Quantification was performed against a set of external standard solutions within the linear response concentration range.

The drug concentration of progesterone was determined with the following mobile phase: distilled water (bi-distilled and filtered through 0.45 µm)/methanol/tetrahydrofuran 40/45/15 (V/V). Ammonium acetate with a concentration of 0.55 g/l was added to the mobile phase. The pH-value at 25°C was 6.9. An injection volume of 100 µl and a runtime of 7.5 min were used to detect progesterone at 239 nm in UV. Using this method, retention time of progesterone was approximately 5 min.

The drug concentration of propranolol was determined with the following mobile phase: distilled water (bi-distilled and filtered through 0.45 µm)/methanol/tetrahydrofuran 55/20/25 (V/V). Ammonium acetate with a concentration of 0.55 g/l was added to the mobile phase. The pH- value at 25°C was 7.0. An injection volume of 100 µl and a runtime of 8 min were used to detect propranolol at 295 nm in UV. Using this method retention time of propranolol was approximately 3.5 min.

The drug concentration of saquinavir was determined with the following mobile phase: distilled water (bi-distilled and filtered through 0.45 µm)/methanol/tetrahydrofuran 40/45/15 (V/V). Ammonium acetate with a concentration of 0.55 g/l was added to the mobile phase. The pH- value at 25°C was 6.7. An injection volume of 100 µl and a runtime of 8 min were used to detect saquinavir at 239 nm in UV. Using this method retention time of saquinavir was approximately 5 min.

The drug concentration of triclabendazole was determined with the following mobile phase: distilled water (bi-distilled and filtered through 0.45 μm)/methanol/tetrahydrofuran 35/40/25 (V/V). Ammonium acetate with a concentration of 0.55 g/l was added to the mobile phase. The pH- value at 25°C was 6.7. An injection volume of 100 μl and a runtime of 8 min were used to detect triclabendazole at 305 nm in UV. Using this method retention time of triclabendazole was approximately 5.6 min. Quantification of triclabendazole was performed against a set of external standard solutions within the linear response concentration range. To maintain the sample stability over time and reproducibility of the method, the standard solutions of triclabendazole contained the same amount of lipids as the samples. Samples were stored at 4°C.

4.1.3.4 TEER Measurements

The integrity of the Caco-2 cell monolayer in the Transwell plates was ensured with the measurement of the trans-epithelial electrical resistance (TEER) before and after every drug permeation study.

After washing the cell monolayer with 37°C tempered D-PBS (with Ca^{2+} , Mg^{2+}), 1600 μl transport medium was added into the apical and 2800 μl transport medium was added into the basal compartment. The Transwell plate was equilibrated 60 min in the cell culture incubator before the pre-experimental measurement. The TEER was measured with an EVOM-G-Meter (EVOM-G-Meter Modell -24, World Precision Instruments, Berlin, Germany) equipped with an Endohm™ tissue resistance measurement chamber containing 4.6 ml tempered transport media (World Precision Instruments, Berlin, Germany). The measurement chamber was tempered to 37°C with transport medium before the measurement. For the post-experimental TEER measurement, the withdrawn volume in the apical compartment was replaced with transport medium before TEER was measured. Caco-2 monolayer with TEER values exceeding 250 Ωcm^2 were used for transport experiments.

4.1.3.5 Drug Permeation Across Caco-2 Cell Monolayers

Cells between culture days 19-23 at passage numbers 60-65 were used for the permeation studies. After the pre-experimental TEER measurement, the transport medium was removed and the formulations, tempered to 37°C, were added. In the apical to basal direction, 1600 μl of the drug formulation was added to the apical compartment and 2800 μl of the placebo formulation was added to the basal compartment. In the basal to apical direction, 1600 μl of the placebo formulation was added to the apical compartment and 2800 μl of the drug formulation was added to the basal compartment. At least three wells were used for each direction. The Transwell plate was shaken at 37°C in a water saturated atmosphere under an incubator hood (KS15, Edmund Bühler GmbH, Tübingen & Hechingen, Germany) with a stirring rate of 75 rpm on an orbital shaker (KS15, Edmund Bühler GmbH, Tübingen & Hechingen, Germany). Permeation of drug across the cell monolayer was monitored by sampling the solutions of both compartments at predefined points of time during 5 h, except for the microemulsion experiments with 5 mg/ml lipid phase, where the permeation was monitored during 3 h only.

Samples were drawn after 15, 30, 60, 90, 120, 180, and 300 min for the 5 h experiments and after 15, 30, 45, 60, 90, 120, and 180 min for the 3 h experiments. The sample volume was 50 μl . The withdrawn volume was not replaced. The samples were diluted 1:10 with transport medium and

collected in glass vials (Schmidlin Labor& Service AG, Sarbach, Switzerland) and stored at 4 °C until the HPLC analysis was performed.

4.1.3.6 Cell Monolayer Drug Extraction

Following the post-experimental TEER measurement, the 6-well Transwell plate was washed apical with 3 ml and basal with 4 ml of 4 °C D-PBS (without Ca²⁺ and Mg²⁺). The inserts were transferred to Petri dishes and 0.3 ml trypsin solution (0.25% trypsin and 2.65 mM EDTA) was added to each insert. The inserts were incubated in the cell culture incubator for 15 min. After neutralizing the trypsin solution with 1 ml of cell culture medium, the cells were scraped off the polycarbonate membrane using a cell scraper (BD Falcon, BD Biosciences Discovery Labware, Bedford, USA), transferred into centrifuge tubes (BD Falcon blue max 15 ml, BD Biosciences Discovery Labware, Bedford, USA), and spun 5 min with 1000 rpm (Sigma 302K, Sigma Laborzentrifugen GmbH, Germany). The pellets were suspended in 750 µl bi-distilled water and transferred to microtubes (Treff AG, Degersheim, Switzerland). The microtubes were frozen at -80 °C over night and thawed at 37 °C under shaking with 1400 rpm (Thermomixer comfort, Eppendorf, Hechingen, Germany) then 750 µl methanol was added to the samples. The samples were put on ice for 20 min, shaken at 37 °C for 10 min, and spun on an Eppendorf centrifuge for 3 min at 14000 rpm (5415C, Eppendorf / Dr. Vaudaux AG, Schönenbuch, Switzerland). The supernatants of the first extraction were transferred into microtubes and stored at 4 °C. After adding 750 µl methanol, the cell pellets were disintegrated with 6 pulses of an ultrasonic disintegrator (Branson Sonifier 250, Model 101-063-197, SKAN AG, Basel, Switzerland, Instrument settings were: output control: 2, duty cycle: 30%), followed by 5 min on the thermomixer (37 °C and 1400 rpm) and centrifugation with the Eppendorf centrifuge at 14000 rpm for 3 min. After an additional extraction with 750 µl methanol, 5 min shaking on the thermomixer at 37 °C, and centrifugation for 3 min at 14000 rpm, the methanolic supernatant of the second extraction was united with its supernatant of the third extraction. Then, the methanol was evaporated under nitrogen flow. Each residue was merged with its supernatant of the first methanol- water extraction step on the thermomixer at 37 °C for 3 min. Before the HPLC-analysis, the cell extracts were spun with the Eppendorf centrifuge for 25 min at 14000 rpm.

4.1.3.7 Drug Extraction out of Transwell Plates

After removal of the Caco-2 cells, the 6-well Transwell plates and the filter inserts were extracted with methanol to determine the surface bound amount of drug. To the apical compartment 1600 µl methanol was added, 2800 µl to the basal. The plate was sealed with four layers of Parafilm to avoid methanol evaporation and incubated at 37 °C for 45 min under the incubator hood with a stirring rate of 75 rpm. Samples of 500 µl were taken and diluted 1:1 with distilled water before drug quantification by HPLC.

4.1.3.8 Production and Characterization of Lipid Containing Drug Dosage Forms

4.1.3.8.1 Preparation of Liposomes

The liposomes were composed of Lipoid S 100 (soy lecithin, >94% phosphatidylcholine) and Lipoid EPG (EPG) (egg phosphatidylglycerin-sodium >98%). To prepare drug loaded liposomes, the film method was used. Lipoid S 100 concentrations were corresponding to the lipid concentrations. Additionally, the indicated amount of drug and EPG corresponding to 10% (m/m) of the drug mass were added. Lipoid S100, EPG, and drug were dissolved in ethanol 96% in a round bottomed flask. The solvent was evaporated to dryness at 40°C and the lipid film was kept under vacuum for 30 min to eliminate solvent traces. The lipid film was suspended with 20 ml of tempered transport medium. The suspension was extruded under nitrogen pressure with a filter candle through polycarbonate filters (Nucleopore track edge membrane filters, Whatman plc, Kent, UK) with descending pore sizes in the following scheme: 2 x 0.4 µm, 5 x 0.2 µm, and 20 x 0.1 µm. The addition of the drugs and the variable EPG concentrations had no measurable effect on the size of the liposomes.

4.1.3.8.2 Preparation of Emulsions and Microemulsions

The lipid phase was prepared by mixing the components at 37°C as following: 35.05% (m/m) triglyceride (Captex 8000), 17.58% (m/m) of a mixture of mono- and diglycerides (Capmul MCM), 36.84% (m/m) surfactant (Cremophor EL), and 10% (m/m) ethanol for the microemulsion and 67% (m/m) Captex 8000, 5% (m/m) Capmul MCM, 18% (m/m) Cremophor EL, and 10% (m/m) ethanol for the emulsion. The lipid phases were stored at 4°C. The lipid phase was warmed to 37°C before use and the according amount was balanced and mixed with two thirds of the final transport medium volume. The formulation was homogenized for 5 min at 15000 rpm with a Polytron homogenizer (Polytron PT 3000, Kinematica AG, Littau, Switzerland) and preheated transport medium was added to the final volume.

4.1.3.8.3 Particle Size Measurement

Particle size of the formulations was measured by dynamic light scattering. The z-average diameter of the liposomes was determined in disposable cuvettes (2 ml sample volume, Greiner Labortechnik, Kremsmünster, Austria) with a Zetasizer 1000 HSA (Malvern Instruments Ltd, Worcestershire, England), equipped with a 100 nm lens, at 25°C and a wavelength of 633 nm. A detector angle of 90° was used. Samples were diluted with sterile filtered transport media (filter pore size 0.2 µm) until counting rates between 100 and 300 KCts/s were reached. The resulting z-average diameter was the average out of 5 runs, consisting of 10 measurements each.

The z-average particle size of the emulsions and the microemulsions were measured with a Zetasizer Nano ZS ZEN 3600 (Malvern Instruments Ltd, Worcestershire, England) in disposable cuvettes (2.5 ml sample volume, Brand GmbH & Co, Wertheim, Germany) at 37°C. The resulting z-average diameter was the average out of 3 runs, consisting of 10 measurements each.

4.1.3.9 Equilibrium Dialysis for Free Fraction Determination

The formulations were dialyzed with glass made horizontal diffusion cells with a chamber volume of 10 ml and a membrane surface of approximately 2 cm². The chambers were separated by a SpectraPor® 7 regenerated cellulose membrane with a molecular weight cutoff of 50000 D (Spectrum Labs, DG Breda, Netherlands). To maintain a temperature of 37°C, a water bath was used. The solutions in the cells were stirred at 1000 rpm with Teflon-paddles driven by a stirring device (Janke & Kunkel RE162, IKA Labortechnik, Staufen, Germany). The formulations were dialyzed for at least 34-48 h until equilibrium was reached. At least 5 samples were taken during the experiment. The samples were analyzed with HPLC. To avoid microbial contamination, resulting in a possible degradation of the drug or the formulation, 0.5% (m/V) sodium azide was added to the transport media and the formulations.

4.1.3.10 Theoretical Modeling

4.1.3.10.1 Mathematical Model for the Determination of Drug Absorption Parameters in Caco-2 Cell Monolayers Including a Term Describing Drug Partition between Donor, Acceptor, and Cell Compartment

Our group has introduced previously a mathematical model to describe the transport of drug between the apical, the basal, and the cellular compartment (115). This model enables a direct estimation of transport parameters from concentration-time profiles. The model takes into account passive permeation, described by the permeability coefficient P , and carrier mediated efflux described by the kinetic parameters v_{max} and K .

An extension of this model including a partition coefficient from formulation to cell is derived in this section. The model was based on the following assumptions:

- 1) Three different compartments are considered in which drug concentration varies with time, the apical, the cellular, and the basal compartment.
- 2) Drug may move between the apical and the cellular and the basal compartment in both directions by passive diffusion. Permeation through the apical and the basal cell membrane may not be symmetrical and is characterized in both cases by a permeability coefficient, where P_a denotes permeability coefficient of the apical and P_b the permeability coefficient of the basal membrane. No effect of electrical membrane potential on the transport is considered.
- 3) Because of their properties, lipophilic compounds may partition from an aqueous solution into lipophilic structures such as cell membranes.
- 4) Drug may be subject to carrier mediated efflux from the cellular to the apical compartment. This follows saturable kinetics that may be characterized by one global parameter v_k , the carrier mediated efflux rate.
- 5) No two different orientations or conformations of the carrier at the two faces of the membrane are explicitly involved, the drug concentration in the apical compartment does not influence efflux transport and the entire mass of drug present in the cellular compartment is substrate of the transporter.
- 6) The total mass of drug in the three compartments is preserved.

The substance flux J of a drug from the apical compartment to the cellular compartment through the apical cell membrane in apical to basal direction can be described as

$$J = -D \frac{dc}{dx} = -D \frac{c_{m2} - c_{m1}}{h} = D \frac{c_{m1} - c_{m2}}{h}$$

Equation 10

where D is the diffusion coefficient of the compound in the membrane, c_{m1} the concentration of the compound at the outer membrane surface [μM], c_{m2} the concentration of the compound at the inner

membrane surface and h the membrane thickness. The partition coefficient between cell membrane and apical compartment ($K_{m/a}$) of a drug is defined as

$$\frac{c_{m1}}{c_a} = K_{m/a}$$

Equation 11

where c_a denotes apical total concentration. The partition coefficient between apical cell membrane and cell lumen ($K_{m/c}$) of a drug is defined as

$$\frac{c_{m2}}{c_c} = K_{m/c}$$

Equation 12

where c_c denotes the cellular concentration of the drug, which is homogeneous in the cellular compartment. Equation 11 and Equation 12 were solved after c_{m1} and c_{m2} and were inserted in Equation 10:

$$J = D \frac{K_{m/a}c_a - K_{m/c}c_c}{h} = \frac{DK_{m/a}}{h} \left(c_a - \frac{K_{m/c}}{K_{m/a}}c_c \right) = P_a \left(c_a - \frac{K_{m/c}}{K_{m/a}}c_c \right)$$

Equation 13

In Equation 13, P_a denotes the apparent permeability coefficient of the apical membrane. If the apical compartment is identical with the cellular compartment it follows out of Equation 13 that the ratio of the partition coefficient between cell membrane and apical compartment and partition coefficient between apical cell membrane and cell lumen is 1. It follows:

$$J = P_a(c_a - c_c)$$

Equation 14

If apical compartment and cellular compartment are not identical it follows out of Equation 13 that the partition coefficient between cell membrane and apical compartment and the partition coefficient between apical cell membrane and cell lumen are different. Because the membrane is the same for both partition coefficients, formulation-to-cell partition coefficient $K_{a/c}$ is defined as

$$\frac{K_{m/c}}{K_{m/a}} = K_{a/c}$$

Equation 15

It follows, out of Equation 13, that the flux of a compound from apical to cellular compartment is:

$$J = P_a(c_a - K_{a/c}c_c)$$

Equation 16

The substance flux of a drug from the cellular compartment to the basal compartment through the basal cell membrane in apical to basal direction can be described as:

$$J = -D \frac{c_{m4} - c_{m3}}{h}$$

Equation 17

In Equation 17, D is the diffusion coefficient of the compound, c_{m3} the concentration of the compound at the inner cellular surface of the basal membrane [μM], c_{m4} the concentration of the compound at the outer membrane surface of basal membrane and h the membrane thickness. The partition coefficient of a drug between cell lumen and basal membrane ($K_{m/c}$) is defined as

$$\frac{c_{m3}}{c_c} = K_{m/c}$$

Equation 18

whereas partition of a drug between basal membrane and basal compartment ($K_{m/b}$) is defined as

$$\frac{c_{m4}}{c_b} = K_{m/b}$$

Equation 19

Equation 18 and Equation 19 were solved after c_{m3} and c_{m4} and were inserted in Equation 17

$$J = D \frac{K_{m/c} c_c - K_{m/b} c_b}{h} = \frac{D \cdot K_{m/b}}{h} \left(\frac{K_{m/c}}{K_{m/b}} c_c - c_b \right) = P_b \left(\frac{K_{m/c}}{K_{m/b}} c_c - c_b \right) = P_b (K_{b/c} c_c - c_b)$$

Equation 20

In Equation 20, P_b denotes the apparent permeability coefficient of the basal membrane for non-identical cellular and basal compartment. Since the apical and the basal compartment are always identically composed regarding lipid formulation, it follows:

$$K_{m/c} = K_{b/c}$$

Equation 21

In Equation 16 and Equation 20, the partition coefficient $K_{a/c}$ is not related to the permeability coefficient but depends on the composition of the media in apical and basal compartment. P_a describes the entire passive transport process between apical compartment and cellular compartment and P_b the entire passive transport process between cellular and basal compartment. These parameters are independent of the direction of the permeation according to the formal definition. Because of different membrane composition (expressed in different partition coefficients between cell membrane and compartment), different thickness of the cellular membranes, and different thickness of diffusion boundary layer, P_a and P_b may be different. The derivation in the basal to apical direction is analogous.

Equation 16 and Equation 20 were implemented into the mathematical model to describe the transport of drug between the apical, the basal, and the cellular compartment. The resulting extended model allows a direct estimation of relevant transport parameters out of concentration-time profiles. These parameters are apparent passive permeation over the apical and basal membrane denoted by the

permeation coefficients P_a and P_b , carrier mediated apical efflux rate expressed by the simplified zero order parameter v_k , and formulation-to-cell partition coefficient $K_{a/c}$. The apical and the basal compartment were containing the same formulation, except for the drug which was added only to the donor compartment according to the transport direction, resulting in the same drug partition between apical and cellular compartment and between basal and cellular compartment denoted both by the formulation-to-cell partition coefficient $K_{a/c}$.

The model encompasses the following equations:

apical to basal direction

$$\frac{dc_{aAB}}{dt} = -P_a * (c_{aAB} - K_{a/c} \cdot c_{cAB}) * \frac{S_m}{V_a} + v_k * \frac{S_m}{V_a}$$

Equation 22 Change of concentration in apical compartment

$$\frac{dc_{bAB}}{dt} = P_b * (K_{a/c} \cdot c_{cAB} - c_{bAB}) * \frac{S_m}{V_b}$$

Equation 23 Change of concentration in basal compartment

$$\frac{dm_{cAB}}{dt} = P_a * (c_{aAB} - K_{a/c} \cdot c_{cAB}) * S_m - v_k * S_m - P_b * (K_{a/c} \cdot c_{cAB} - c_{bAB}) * S_m$$

Equation 24 Change of mass in cellular compartment

basal to apical direction

$$\frac{dc_{aBA}}{dt} = P_a * (K_{a/c} \cdot c_{cBA} - c_{aBA}) * \frac{S_m}{V_a} + v_k * \frac{S_m}{V_a}$$

Equation 25 Change of concentration in apical compartment

$$\frac{dc_{bBA}}{dt} = -P_b * (c_{bBA} - K_{a/c} \cdot c_{cBA}) * \frac{S_m}{V_b}$$

Equation 26 Change of concentration in basal compartment

$$\frac{dm_{cBA}}{dt} = P_b * (c_{bBA} - K_{a/c} \cdot c_{cBA}) * S_m - P_a * (K_{a/c} \cdot c_{cBA} - c_{aBA}) * S_m - v_k * S_m$$

Equation 27 Change of mass in cellular compartment

The molar concentration [μM] in Equation 22 to Equation 27 is denoted by c . The indices a , b , and c denote the apical, basal, and cellular compartment. Indices AB and BA denote the transport direction apical to basal and basal to apical, respectively. P_a is the apparent permeability coefficient [$\text{cm} \cdot \text{min}^{-1}$] of the apical membrane, P_b the apparent permeability coefficient [$\text{cm} \cdot \text{min}^{-1}$] of the basal membrane. These permeation coefficients were apparent because they summarize permeation through diffusion boundary layer and through the cellular membrane. S_m denotes the cell monolayer surface area [cm^2],

V the compartment volume [ml], $K_{a/C}$ the partition coefficient of a compound between formulation and cell compartment, and v_k [nmol*cm⁻²*min⁻¹] carrier mediated apical efflux rate.

$$v_k = \frac{v_{\max} * m_{cAB}}{K + m_{cAB}}$$

Equation 28

The carrier mediated apical efflux rate is described by the kinetic parameters v_{\max} and K and depends on the molar amount of drug in the cellular compartment, which is denoted as m_{cAB} or m_{cBA} [nmol]. A cell monolayer volume of 0.00094 ml was used based on a monolayer thickness of 20 μ m to calculate cellular drug concentrations.

The reduction of the solution volume in the apical and the basal compartment due to sampling as a function of time was accounted for by the following relations that were determined empirically using regression analysis.

$$V = V_{(0)} - 0.0029681 \cdot t + 9.8457 \cdot 10^{-6} \cdot t^2 - 1.247 \cdot 10^{-8} \cdot t^3$$

Equation 29

$$V = V_{(0)} - 0.0042 \cdot t + 1.63953 \cdot 10^{-5} \cdot t^2 - 2.0985 \cdot 10^{-8} \cdot t^3$$

Equation 30

Where $V_{(0)}$ is volume of the respective compartment at time zero and t the time [min]. Equation 29 applies to both compartments to a sampling volume of 50 μ l over 5 h, Equation 30 applies to both compartments to a sampling volume of 50 μ l over 3 h.

4.1.3.10.2 Delineating the Components of Apparent Permeability Coefficient Based on a Biophysical Model

For understanding the mechanism that considers contribution of individual processes to drug permeation influenced by lipid containing drug formulations, contributions were expressed quantitatively by permeability coefficients. The relationship between individual permeability coefficients and measured apparent permeability coefficients was established based on a developed biophysical model that describes the overall process. A schematic overview of the model is given in Figure 4.

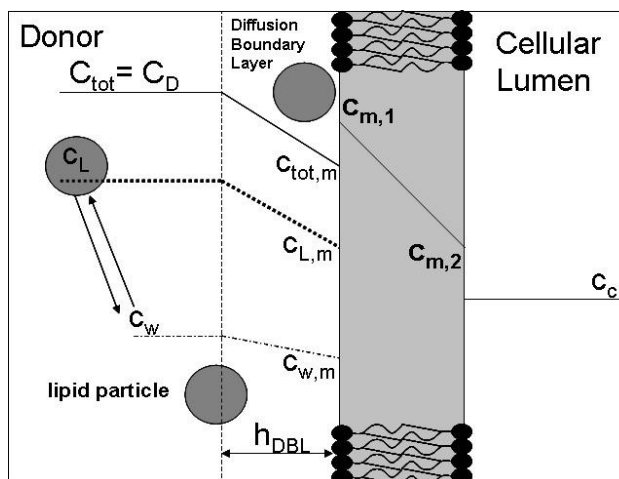


Figure 4 Biophysical model of a drug flux over a Caco-2 cell membrane from donor compartment containing lipid particles to cellular lumen.

This model is based on the following assumptions:

- 1) Diffusional transport of free drug molecules and lipid particles takes place in solution adjacent to cell membrane. Kinetics of this transport is expressed by permeability coefficient of diffusion boundary layer.
- 2) Unbound drug molecules permeate through the cell monolayer.
- 3) Lipid particles do not permeate through the cell monolayer.
- 4) If lipid particles collide with the cell membrane, direct drug transfer from lipid particles to the cell membrane may take place.
- 5) The free fraction of a drug is dependent on lipid concentration and is independent of drug concentration except concentrations reaching saturation.

Substance fluxes are defined by flux through cell membrane J_m (Equation 31) and flux through diffusion boundary layer J_{DBL} (Equation 32):

$$J_m = \frac{D_m}{h_m} (c_{m,1} - c_{m,2})$$

Equation 31

where h_m denotes thickness of cell membrane, D_m diffusion coefficient of drug in cell membrane, $c_{m,1}$ drug concentration at outer cell membrane surface inside of the membrane, $c_{m,2}$ drug concentration at inner membrane surface inside of the membrane.

$$J_{DBL} = \frac{D_{w,d}}{h_{DBL}} \cdot (c_w - c_{w,m}) + \frac{D_{w,L}}{h_{DBL}} (c_L - c_{L,m})$$

Equation 32

The flux through diffusion boundary layer is composed of the flux of the free drug molecules and the flux of the lipid particles, where $c_{w,m}$ denotes drug concentration of the water phase at membrane surface, c_L drug concentration associated with lipid phase referring to total volume, $c_{L,m}$ drug concentration associated with lipid phase referring to total volume at membrane surface, c_w drug concentration in water phase, h_{DBL} thickness of diffusion boundary layer, $D_{w,d}$ the diffusion coefficient of drug in water phase, and $D_{w,L}$ diffusion coefficient of lipid particle in water phase.

The free fraction (z) of a drug is defined as ratio of drug concentration in the water phase (c_w) of the formulation to the total drug concentration in the formulation denoted by c_{tot} :

$$\frac{c_w}{c_{tot}} = z$$

Equation 33

Substitutions that were used to replace unknown parameters are shown in Equation 34 to Equation 37:

$$q = \frac{D_{w,d}}{D_{w,L}}$$

Equation 34

q is defined as ratio of diffusion coefficient of drug in water phase ($D_{w,d}$) to diffusion coefficient of lipid particle in water phase ($D_{w,L}$).

$$VF = \frac{V_w}{V_{tot}}$$

Equation 35

The volume fraction VF is defined as ratio of the volume of the water phase (V_w) to the volume of the formulation (V_{tot}). Because lipid phase concentrations were low in performed cell permeation experiments, $1-VF$ was assumed to be the ratio of the amount of lipid phase [g] to the volume of aqueous phase [ml].

The mass of drug in lipid phase (m_L) was assumed to be the total mass of drug (m_{tot}) minus the mass of drug in water phase (m_w). This was used to express c_L with c_{tot} and c_w .

$$c_L = \frac{m_L}{V_{tot}} = \frac{m_{tot} - m_w}{V_{tot}} = \frac{c_{tot}V_{tot} - c_wV_w}{V_{tot}} = c_{tot} - c_w \frac{V_w}{V_{tot}} = c_{tot} - c_w VF$$

Equation 36

Equation 36 applies to bulk, and with indices m (e.g. $c_{w,m}$) at cell membrane surface.

The unknown drug concentration at cell membrane surface inside the membrane ($c_{m,1}$) was substituted by the following equation:

$$c_{m,1} = c_{w,m} \cdot K_{m/w} + c_{L,m} \cdot K_{m/L}$$

Equation 37

where $K_{m/w}$ denotes the partition coefficient of the free drug between aqueous phase and membrane and $K_{m/L}$ denotes the partition coefficient between lipid associated drug in solution and cell membrane.

Inserting Equation 37 into Equation 31 and rearranging yields:

$$\begin{aligned} J_m &= \frac{D_m}{h_m} (c_{m,1} - c_{m,2}) = \frac{D_m}{h_m} (c_{w,m} \cdot K_{m/w} + c_{L,m} \cdot K_{m/L} - c_{m,2}) \\ &= \frac{D_m \cdot K_{m/w}}{h_m} c_{w,m} + \frac{D_m \cdot K_{m/L}}{h_m} c_{L,m} - \frac{D_m}{h_m} c_{m,2} = P_{m,d} \cdot c_{w,m} + P_{m,L} \cdot c_{L,m} - \frac{D_m}{h_m} K_{m/c} \cdot c_c \end{aligned}$$

Equation 38

In Equation 38 denotes $P_{m,d}$ the permeability coefficient of the free drug through cell monolayer, $P_{m,L}$ the permeability coefficient of the drug because of direct drug transfer from lipid particle to the cell membrane, c_c cellular drug concentration and $K_{m/c}$ the partition coefficient between cellular drug concentration and cell membrane.

Inserting Equation 33 and Equation 36 into Equation 38 and rearranging yields:

$$J_m = c_{w,m} \left(P_{m,d} + \frac{P_{m,L}}{z} - P_{m,L} \cdot VF \right) - \frac{D_m}{h_m} K_{m/c} \cdot c_c$$

Equation 39

Inserting Equation 34 into Equation 32 and rearranging yields:

$$J_{DBL} = \frac{P_{dbl,d}}{q} \cdot (qc_w - qc_{w,m} + c_L - c_{L,m})$$

Equation 40

where $P_{dbl,d}$ denotes the permeability coefficient of the free drug through diffusion boundary layer.

At steady state fluxes are set equal ($J_m = J_{DBL}$), Equation 33 and Equation 36 were inserted and the resulting equation was rearranged and solved for the unknown concentration $c_{w,m}$.

$$\frac{P_{dbl,d}}{q} \cdot [(qzc_{tot} - qc_{w,m} + c_{tot} - c_w \cdot VF) - (c_{tot,m} - c_{w,m} \cdot VF)] = P_{m,d} \cdot c_{w,m} + P_{m,L} \cdot (c_{tot,m} - c_{w,m} \cdot VF) - \frac{D_m}{h_m} K_{m/c} \cdot c_c$$

Equation 41

$$c_{w,m} = \frac{\frac{P_{dbl,d}}{q} \cdot c_{tot} (qz + 1 - z \cdot VF) + \frac{D_m}{h_m} K_{m/c} \cdot c_c}{P_{m,d} + \frac{P_{m,L}}{z} - P_{m,L} \cdot VF + \frac{P_{dbl,d}}{q} \left(q + \frac{1}{z} - VF \right)}$$

Equation 42

Equation 42 was inserted into Equation 39. Transformation of this equation after insertion resulted in:

$$J_m = \frac{\frac{P_{dbl,d}}{q} \left(q + \frac{1}{z} - VF \right) \cdot \left[c_{tot} \cdot z \left(P_{m,d} + \frac{P_{m,L}}{z} - P_{m,L} \cdot VF \right) - \frac{D_m}{h_m} K_{m/c} \cdot c_c \right]}{\left(P_{m,d} + \frac{P_{m,L}}{z} - P_{m,L} \cdot VF \right) + \frac{P_{dbl,d}}{q} \left(q + \frac{1}{z} - VF \right)}$$

Equation 43

Assuming for the sake of simplicity sink conditions on the receiver (cell) side and setting c_c to zero and dividing Equation 43 by c_{tot} , it follows:

$$P = \frac{\frac{P_{dbl,d}}{q} z \left(q + \frac{1}{z} - VF \right) \cdot \left(P_{m,d} + \frac{P_{m,L}}{z} - P_{m,L} \cdot VF \right)}{\left(P_{m,d} + \frac{P_{m,L}}{z} - P_{m,L} \cdot VF \right) + \frac{P_{dbl,d}}{q} \left(q + \frac{1}{z} - VF \right)}$$

Equation 44

Conversion of this formula leads to the following equation:

$$\frac{1}{P} = \frac{1}{\frac{P_{dbl,d}}{q} \cdot (q \cdot z + 1 - z \cdot VF)} + \frac{1}{z \left(P_{m,d} + \frac{P_{m,L}}{z} - P_{m,L} \cdot VF \right)}$$

Equation 45

In Equation 32 was assumed that thickness of diffusion boundary layer (h_{DBL}) is the same for free drug molecules and lipid particles. However, based on hydrodynamics of lipid particles and the aqueous solubilized drug, h_{DBL} is proportional to $D^{1/3}$ (119). Therefore, it follows for the ratio of diffusion boundary layer thicknesses:

$$\frac{h_{DBL,d}}{h_{DBL,L}} = \left(\frac{D_{w,d}}{D_{w,L}} \right)^{1/3} = q^{1/3}$$

Equation 46

Where $h_{DBL,d}$ is the thickness of diffusion boundary layer of the unbound drug and $h_{DBL,L}$ the thickness of diffusion boundary layer of the lipid particles in water phase.

Accordingly, for the ratio of diffusion coefficient of the lipid particle in water phase to thickness of diffusion boundary layer of the lipid particles holds:

$$\frac{D_{w,L}}{h_{DBL,L}} = \frac{D_{w,d}}{q} \frac{1}{\frac{h_{DBL,d}}{q^{1/3}}} = \frac{D_{w,d}}{h_{DBL,d}} \frac{q^{1/3}}{q} = \frac{D_{w,d}}{h_{DBL,d} q^{2/3}}$$

Equation 47

Since it holds that

$$P_{abl,d} = \frac{D_{w,d}}{h_{DBL,d}}$$

Equation 48

$q^{2/3}$ instead of q must be used as conversion term in Equation 40 through Equation 45. The parameter q was calculated by experimentally determined diffusivity coefficients. The diffusivity coefficients of the lipid particles of the formulations were determined by PCS during particle size measurements and were $1.37 \cdot 10^{-7} \text{ cm}^2 \cdot \text{s}^{-1}$ for microemulsion, $0.27 \cdot 10^{-7} \text{ cm}^2 \cdot \text{s}^{-1}$ for emulsion, and $0.42 \cdot 10^{-7} \text{ cm}^2 \cdot \text{s}^{-1}$ for liposomes. A representative diffusivity coefficient for all drugs, $7.8 \cdot 10^{-6} \text{ cm}^2 \cdot \text{s}^{-1}$ deduced for testosterone (molecular weight 288.42 g/mol) at 37°C in aqueous solution was used (119). The different molecular weights of the compounds were not taken into account, because the molecule radius corresponds to the molecular weight with the cube root causing a small effect on the diffusivity coefficient D and the effect of the molecular weight is additionally minimized by the conversion of q .

Because of the dependence of the permeability coefficient through diffusion boundary layer on different particle diffusivities, q was converted by squaring and taking the cube root before inserting the parameter into the model. In Equation 45 $q^{2/3}$ instead of q was used as conversion term. Finally inserted values into the model (Equation 45) were 14.79 for the microemulsions, 43.70 for the emulsions, and 32.55 for the emulsions.

The resulting Equation 45 was applied to delineate the components of the estimated apparent permeability coefficients P_a and P_b out of the transport studies. Either P_a or P_b were inserted for P , depending on which of them is representing the rate determining apparent permeability coefficient.

4.1.3.10.3 Analysis of the Permeation Data

The system of differential equations, Equation 22 to Equation 27, was fitted to the experimental data with Easy Fit® to deduce optimal values for the kinetic parameters P_a , P_b , v_k , and $K_{a/C}$. A two step fitting procedure was performed. In the first step, the data was fitted to the model and the results were analyzed: For the substances where we expected no apical carrier mediated efflux and a very low value for v_k was estimated by EasyFit® too, v_k was set zero for a second fitting. The P_a and P_b values were compared and if they were for a drug over all experiments equal, they were set equal for a second fitting.

The regression analysis of the transport experiments with Easy Fit® was performed generally with the model type ODE, the numerical method DFNLP, a scaling of 1, an initial stepsize of 0.0001 to

0.000001, a final accuracy (absolute and relative) of 0.000001 and a termination tolerance of $1 \cdot 10^{-18}$. The transport parameters were determined for every single transport experiment, taking into account the mentioned volume reduction.

Equation 45 was fitted with Easy Fit[®] to data of apparent permeability coefficients versus free fractions for different volume fractions to deduce optimal values for $P_{m,d}$, $P_{m,L}$, and $P_{dbl,d}$. Using “explicit” model, the numerical method DFNLP, a scaling of 1, an initial stepsize of 0.0001 to 0.000001, a final accuracy (absolute and relative) of 0.000001 and a termination tolerance of $1 \cdot 10^{-18}$ were used.

4.1.4 Results

4.1.4.1 Formulation Characterization

The optical aspect of the milky liposomes and emulsions differed strongly from the microemulsions that were optically clear, exhibiting a weak opalescence. The obtained formulations were insensitive for phase separation and coalescence for at least 48 h in all used dilutions and with all used drugs, indicating physical stability during experimental procedures. The z-average particle sizes of the formulations are shown in Table 1.

Table 1 Determined z-average particle sizes of the formulations, measured with PCS

Formulation	Particle Size \pm Standard Deviation [nm] (number of measurements)
Liposomes	128.5 \pm 14.7 (n=95)
Microemulsion	53.8 \pm 12.7 (n=51)
Emulsion	176.2 \pm 34.4 (n=66)

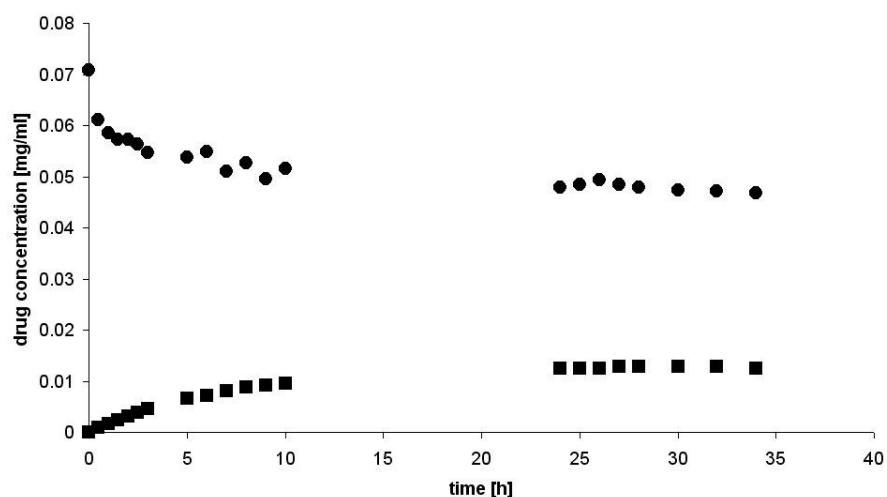


Figure 5 Equilibrium dialysis of progesterone liposome formulation containing 0.5 mg/ml lipids and 159 μ M (corresponding to 0.05 mg/ml) progesterone. Legend: donor compartment (●), acceptor compartment (■)

Free fractions of the formulations were determined by equilibrium dialysis. A representing example of an obtained time dependent concentration curve is shown in Figure 5. Owing a molecular weight of 2515 D, Cremophor EL was theoretically able to pass the dialysis membrane (120). In a preliminary experiment a microemulsion was dialyzed with a dialysis membrane with a molecular weight cut of 2000 D, which does not allow Cremophor EL to pass. No difference in free fraction (z) was found when this experiment was compared with the free fraction obtained by an equilibrium dialysis using a 50000 D membrane (data not shown/see Chapter 4.5).

No influence of the drug concentration on the free fraction was observed with the liposome formulations of all drugs within the same lipid concentration (see Table 2, Table 3, and Table 5). This was true for a wide range of lipid and drug concentrations. For this reason, one dialysis per lipid concentration for emulsions and microemulsions was considered to be appropriate to determine the influence of the lipid concentration on the free fraction. Generally, the free fraction decreased with increasing lipid concentration. When the lipid concentration was plotted versus the inverse of z , a linear relationship resulted for all drugs and all formulations. Figure 6 shows a typical, representative example. If no experimental data for a certain lipid concentration was available, this linear relationship was used to calculate singular free fractions of progesterone liposomes (0.1 mg/ml and 1 mg/ml lipid phase) by applying linear regression analysis.

The obtained free fractions by equilibrium dialysis are enclosed in Table 2 to Table 5. No decrease was observed with propranolol emulsions and microemulsions.

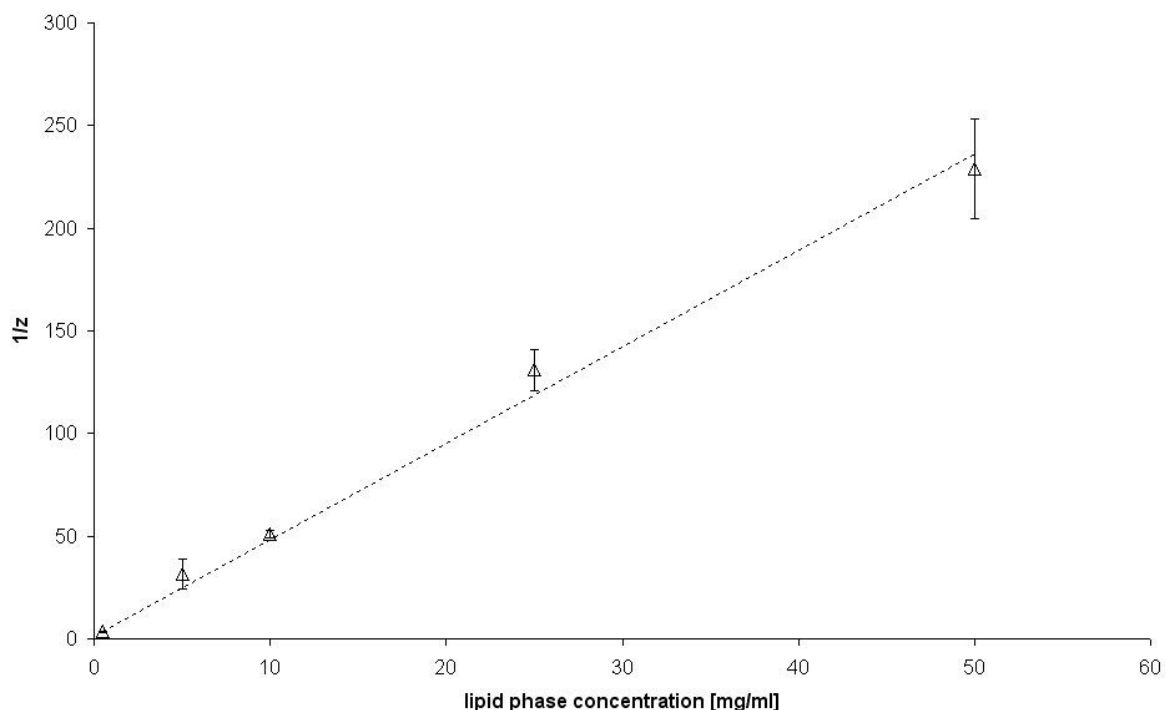


Figure 6 Plot of lipid concentration versus $1/z$ for progesterone liposomes. Linear regression analysis resulted in the following equation: $y=4.7059x+1$ ($r^2=0.9921$).

4.1.4.2 Cell Permeation of Drugs from Aqueous Solutions and Formulations

Measurement of drug permeation in the Caco-2 model was possible with purely aqueous solutions of all drugs except triclobandazole, where a strong adsorption to the Transwell surfaces was observed (data not shown). Tested liposome and emulsion formulations were well tolerated by the cell monolayer. Microemulsions were well tolerated up to 5 mg/ml lipid phase and 3 h of incubation as monitored by TEER measurements. Higher microemulsion lipid phase concentrations as well as longer incubation times were resulting in a damage of the cell monolayer expressed as decrease of TEER below 200 Ohm*cm².

Permeation data were analyzed using the mathematical model for the determination of drug absorption parameters in Caco-2 cell monolayers presented in the method section (Section 4.1.3.10.1). The concentration variables defined by the system of differential equations, Equation 22 to Equation 27, were fitted to the experimental concentration data and cell monolayer drug extraction data and optimal values for P_a , P_b , v_k , and $K_{a/C}$ were deduced using Easy Fit[®]. Initial concentration values, c_{0aAB} and c_{0bBA} corresponding to $t=0$ for both transport directions were treated as adjustable parameters in the regression analysis. Concentration data of both compartments and cell extraction data obtained from apical to basal and basal to apical direction of permeation of three wells each were used simultaneously in the fitting, resulting in a more stable regression analysis compared to the separate calculation of each permeation direction as shown in previous work (115). A subset of the resulting plots of simultaneously data fitting is shown in Figure 7 to Figure 12. These plots were typical for all formulations and drugs.

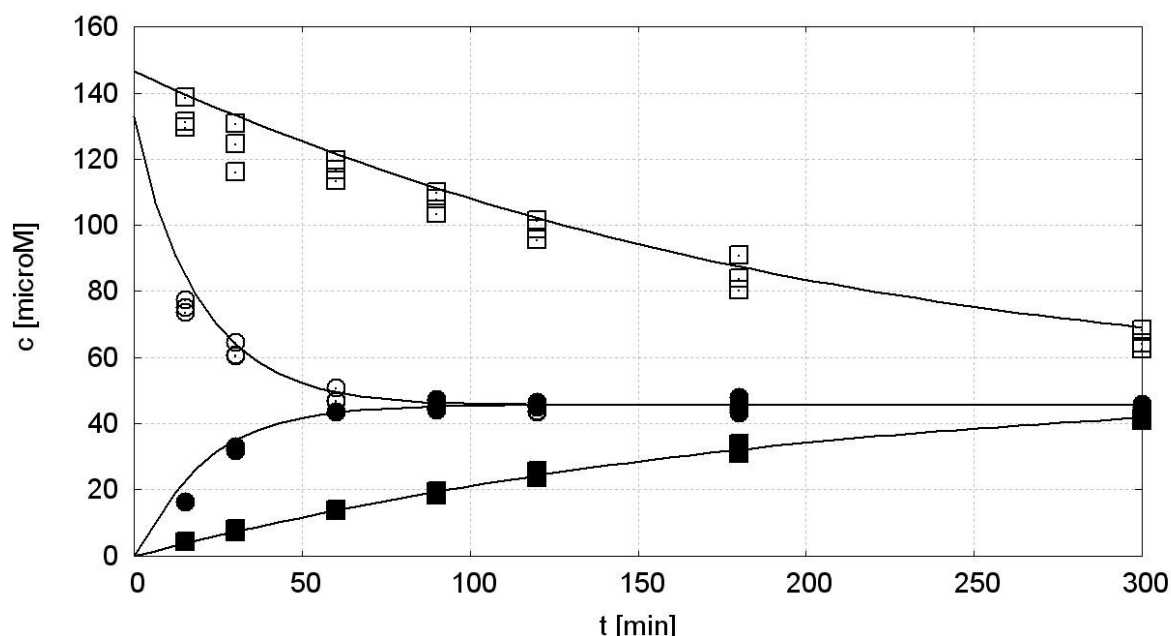


Figure 7 Apical to basal drug permeation of liposome formulations containing 159 μ M progesterone and 0.1 mg/ml and 10 mg/ml phospholipids. The solid line represents the best obtained fit. Legend: apical (\circ) and basal (\bullet) compartment containing 0.1 mg/ml phospholipids, apical (\square) and basal (\blacksquare) compartment containing 10 mg/ml phospholipids.

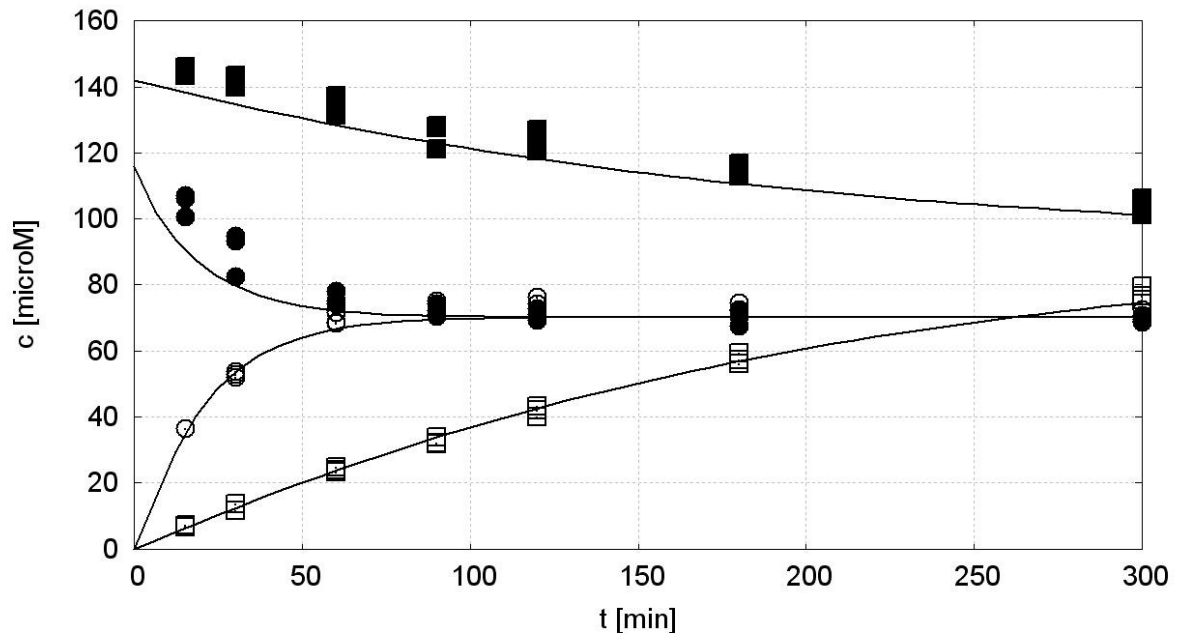


Figure 8 Basal to apical drug permeation of liposome formulations containing $159 \mu\text{M}$ progesterone and 0.1 mg/ml and 10 mg/ml phospholipids. The solid line represents the best obtained fit. Legend: apical (\circ) and basal (\bullet) compartment containing 0.1 mg/ml phospholipids, apical (\square) and basal (\blacksquare) compartment containing 10 mg/ml phospholipids.

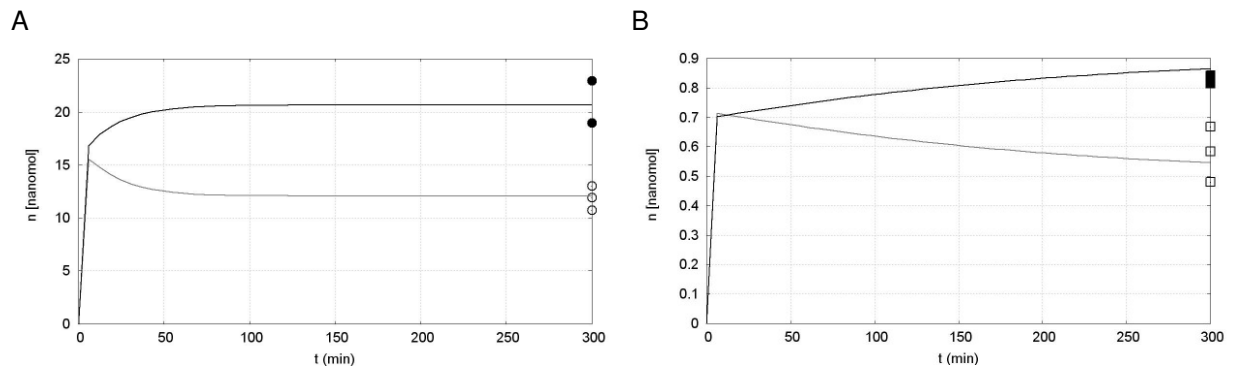


Figure 9 Time dependent drug mass in cellular compartment during cell permeation experiments of liposomes containing $159 \mu\text{M}$ progesterone. Panel A shows liposome formulations containing 0.1 mg/ml phospholipids for apical to basal direction (\circ) and basal to apical direction (\bullet). Panel B shows liposome formulations containing 10 mg/ml phospholipids for apical to basal direction (\square) and basal to apical direction (\blacksquare). The solid line represents fitted curve and points represent experimental data.

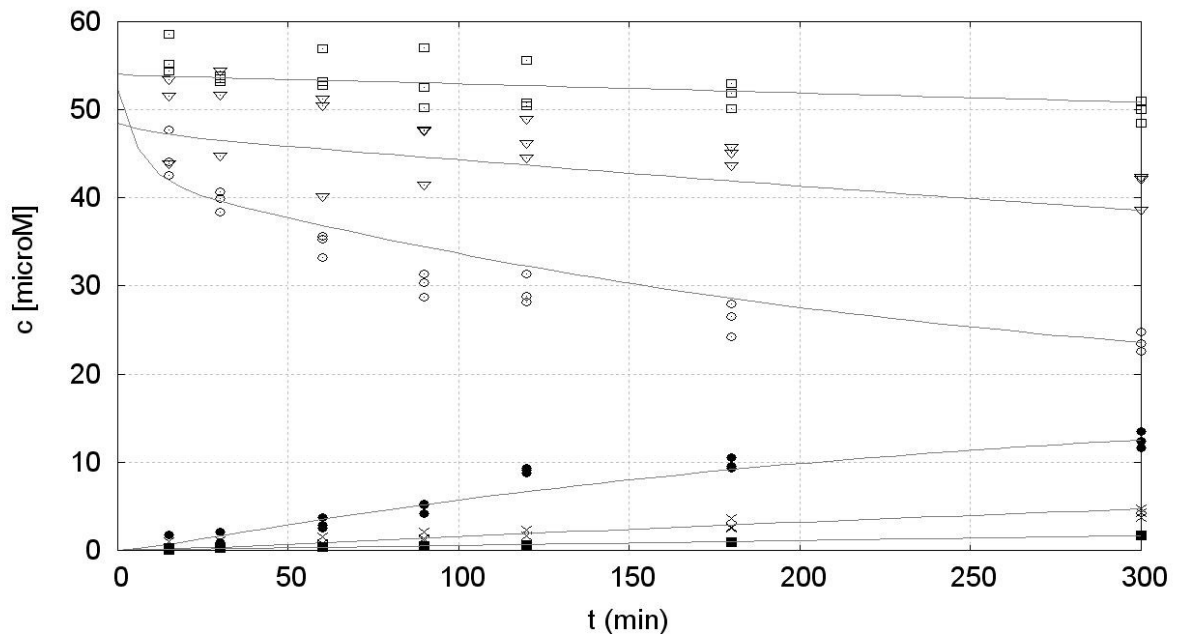


Figure 10 Apical to basal drug permeation of liposome formulations containing $63 \mu\text{M}$ triclabendazole and 0.1 mg/ml , 1 mg/ml , and 10 mg/ml phospholipids. The solid line represents the best obtained fit. Legend: apical (\circ) and basal (\bullet) compartment containing 0.1 mg/ml phospholipids, apical (∇) and basal (\times) compartment containing 1 mg/ml phospholipids apical (\square) and basal (\blacksquare) compartment containing 10 mg/ml phospholipids.

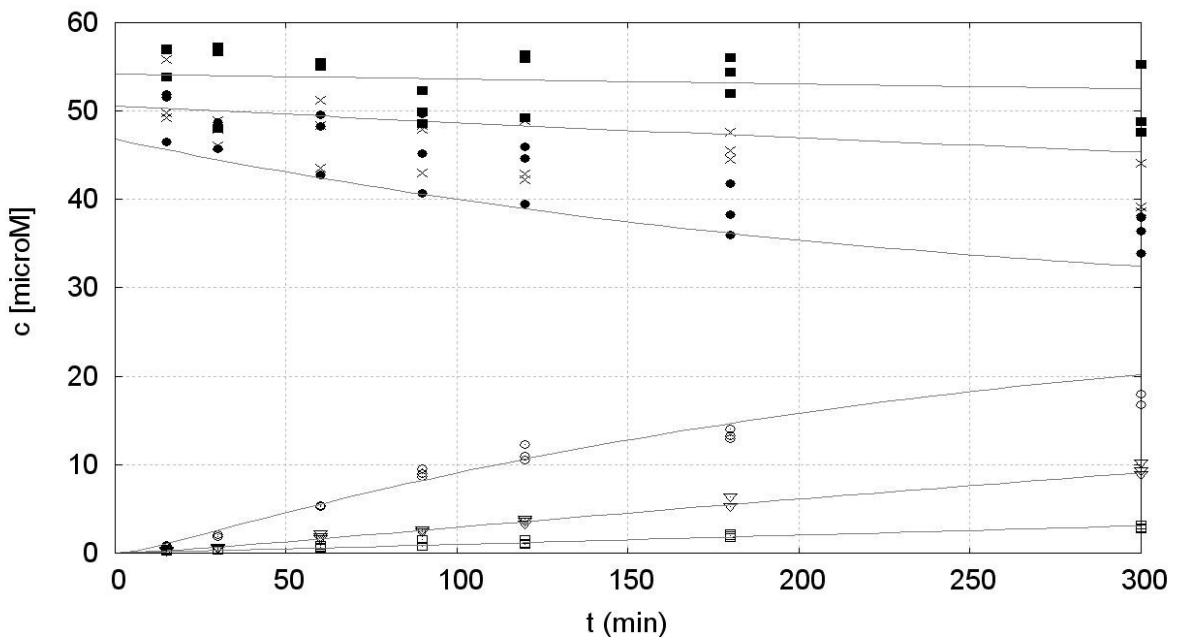


Figure 11 Basal to apical drug permeation of liposome formulations containing $63 \mu\text{M}$ triclabendazole and 0.1 mg/ml , 1 mg/ml , and 10 mg/ml phospholipids. The solid line represents the best obtained fit. Legend: apical (\circ) and basal (\bullet) compartment containing 0.1 mg/ml phospholipids, apical (∇) and basal (\times) compartment containing 1 mg/ml phospholipids apical (\square) and basal (\blacksquare) compartment containing 10 mg/ml phospholipids

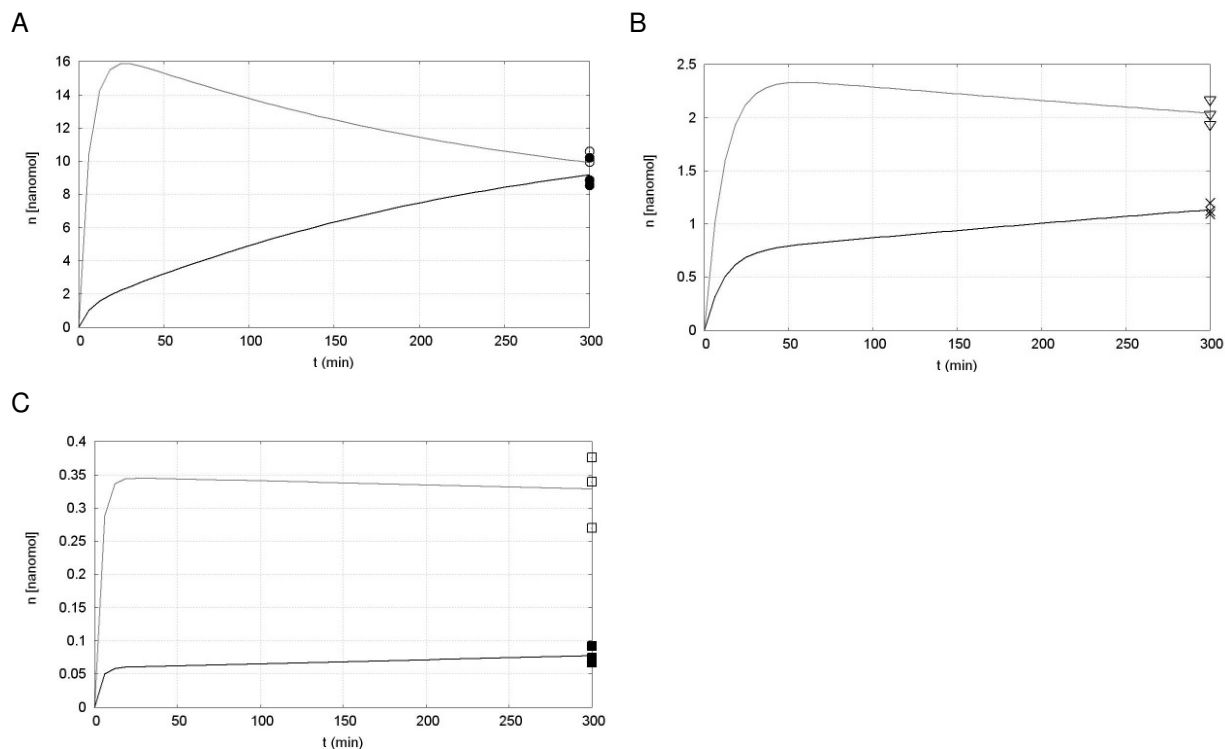


Figure 12 Time dependent drug mass in cellular compartment of liposome formulations containing 63 μM triclabendazole. Panel A shows liposome formulations containing 0.1 mg/ml phospholipids for apical to basal direction (\circ) and basal to apical direction (\bullet). Panel B shows liposome formulations containing 1 mg/ml phospholipids for apical to basal direction (∇) and basal to apical direction (\times), and panel C shows liposome formulations containing 10 mg/ml phospholipids for apical to basal direction (\square) and basal to apical direction (\blacksquare). Solid line represents fitted curve and points represent experimental data.

The estimated transport parameters are displayed in Table 2 to Table 5. The model provides values of permeability coefficients of the apical membrane P_a and of the basal membrane P_b of the cell monolayer. Consistent values of the passive apical and basal permeability coefficients were always obtained. For all drugs, except triclabendazole, estimated P_a and P_b , representing the best fit, were equal. All transport studies with triclabendazole showed that P_b was smaller than P_a . For further calculations the rate limiting parameter P_b was taken. With increased lipid concentrations, the passive permeability coefficient decreased generally. Within one lipid concentration no influence of the drug concentration was observed.

The simplified parameter v_k , describing carrier mediated efflux rate, was introduced to eliminate the correlation between parameters in the regression analysis, as observed in previous work (115). Using this parameter, the model was still able to differentiate between compounds that are subject to carrier mediated efflux and compounds that are not subject of carrier mediated efflux. Deduced v_k parameters of compounds that are not subject to carrier mediated efflux were localized at the lower bound defined for fitting procedure. Additionally, these very low v_k values were independent of drug and lipid phase concentration. No effect on fitting quality and the other estimated parameters was obtained if v_k was set to zero in these cases. Contrary to these findings, the compounds that have been subject to carrier mediated efflux showed a deduced value for v_k that was dependent on drug and lipid concentration. Carrier mediated efflux was found for saquinavir and propranolol. Propranolol showed exiguous carrier

mediated efflux rate only, whereas high carrier mediated efflux rate was found for saquinavir. Figure 13 shows the influence of the lipid concentration on the carrier mediated efflux rate of saquinavir in microemulsion and emulsion formulations. The same qualitative effect for both of the formulations was observed. The carrier mediated efflux decreased with increasing lipid concentration but within the same lipid concentration a drug concentration dependent increase of the carrier mediated efflux was observed, indicating first order kinetics and drug concentrations below saturation of the involved transporter.

The impact of the microemulsion on the carrier mediated efflux appears also if the permeated fractions of saquinavir microemulsion experiments are compared. Permeated fraction is the molar amount of drug at endpoint of the cell permeation experiment in acceptor compartment divided by initial molar amount of drug in apical to basal direction. Permeated fraction of saquinavir microemulsion containing 0.5 mg/ml lipid phase and 14.5 μM saquinavir was 1.88% and increased to 7.43% when lipid phase concentration was increased to 5 mg/ml and contains the same drug concentration.

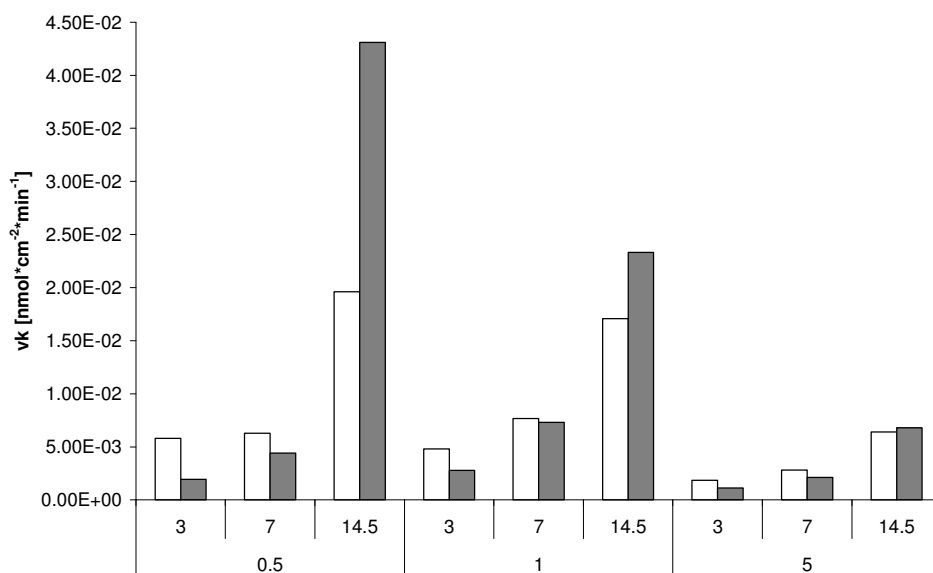


Figure 13 Influence of lipid phase concentration on the carrier mediated efflux rate v_k of saquinavir. Open columns represent the saquinavir emulsions, closed columns saquinavir microemulsions. Upper row numbers on x-axis indicate used drug concentration [μM]; lower row numbers indicate used lipid phase concentration [mg/ml].

The initial drug concentrations, C_{0aAB} and C_{0bBA} , obtained from the best fit were generally lower than the theoretical concentration of the prepared aqueous solutions and the formulations. This was because some loss of drug firstly during preparation, which was confirmed by measuring the drug concentration of the formulations before their use, and secondly at the onset of the transport experiment possibly because of an initial adsorption of the drug to the plastic made surface of the Transwell plates. Time dependent mass balance demonstrates, that total drug mass was constant after the first sampling point. Therefore, the estimation of the kinetic parameters was not affected by this initial decrease of drug content of the drug formulations. Furthermore the adsorption decreased with increasing lipid phase concentration.

Estimated drug mass in the cellular compartment obtained from model simulation was the same at the endpoint of the experiment as the drug mass determined by cell extraction. The introduction of $K_{a/C}$, the formulation-to-cell partition coefficient, improved the fitting quality. Without this coefficient, the drug mass in cellular compartment obtained from model simulation was systematically much lower than the drug mass measured by cell extraction. Simultaneous increase of $K_{a/C}$ with increasing lipid phase concentration was observed indicating that the lipophilic drugs remain in the formulation rather than diffusing out of the lipid particles to cross the cell monolayer. No systematic effect of the drug concentration on $K_{a/C}$ was observed.

Table 2 Kinetic parameters of transport of progesterone as solution and diverse drug formulations across Caco-2 cell monolayer

Formulation	Lipid Content [mg/ml]	Drug [μM]	Conc.	Px10 ⁵ [cm/s]	Free Fraction	V _k [nmol*cm ⁻² *min ⁻¹]	K _a /C	C _{0a} AB [μM]	C _{0b} BA [μM]
Solution	0	4.45	30.3	1	1	0	0.0626	2.59	2.59
		14.63	26.2	1	1	0	0.126	9.57	9.71
		31.80	38.0	1	1	0	0.0655	20.80	22.94
		63.60	29.1	1	1	0	0.0255	53.38	49.13
Liposomes	0.1	31.80	29.6	0.680 [#]	0	0.0717	25.11	23.80	
		63.60	34.6	0.680 [#]	0	0.0289	64.87	58.70	
		159.00	35.8	0.680 [#]	0	0.398	115.75	132.82	
	0.5	31.80	14.3	0.297	0	0.0670	24.93	25.04	
		63.60	18.5	0.305	0	0.0748	45.88	47.36	
		159.00	15.7	0.271	0	0.0923	125.73	130.99	
	1	31.80	15.4	0.175 [#]	0	0.117	27.50	29.71	
		63.60	16.3	0.175 [#]	0	0.151	59.35	54.96	
		159.00	15.0	0.175 [#]	0	0.0752	131.36	143.74	
	5	159.00	4.59	0.0356	0	0.120	151.87	151.44	
		318.00	6.35	0.0364	0	0.170	318.83	346.18	
		794.99	4.50	0.0231	0	0.223	750.41	743.60	
	10	63.60	2.69	0.0195	0	2.84	63.00	63.00	
		159.00	3.56	0.0197 ^A	0	0.955	142.06	146.51	
		318.00	3.58	0.0189	0	0.739	276.05	297.68	
		794.99	3.62	0.0197 ^A	0	0.673	846.42	846.42	
		1589.98	3.04	0.0207	0	0.991	1547.34	1591.60	
	25	63.60	2.35	0.00847	0	8.40	58.01	56.08	
		159.00	2.37	0.00764 ^A	0	0.900	144.65	145.74	
		318.00	1.81	0.00702	0	4.15	304.54	304.54	
		794.99	1.68	0.00742	0	2.18	762.61	762.61	
		1589.98	1.91	0.00764 ^A	0	1.68	1344.85	1343.93	
		3307.15	1.64	0.00764 ^A	0	1.42	3137.28	3233.73	
		6709.70	0.92	0.00437 ^A	0	1.91	6126.27	6249.31	
50	63.60	2.04	0.00437 ^A	0	0.627	68.19	88.88		
	159.00	1.35	0.00455	0	3.69	146.00	154.84		
	318.00	1.05	0.00437 ^A	0	4.19	283.57	288.83		
	794.99	1.00	0.00437 ^A	0	4.56	802.35	732.85		
	1589.98	1.27	0.00377	0	1.83	1394.30	1490.86		
	3307.15	0.94	0.00437 ^A	0	2.22	4312.91	4337.57		
	6709.70	0.92	0.00437 ^A	0	1.91	6126.27	6249.31		
	11193.44	0.85	0.00479	0	2.67	11011.91	11745.82		
	Emulsion	0.5	3	25.6	0.436	0	0.560	2.30	2.54
14.5			19.5	0.436	0	0.115	10.44	10.43	
31.8			20.0	0.436	0	0.108	23.48	23.91	
1		3	14.0	0.266	0	1.07	2.42	2.16	
		14.5	11.4	0.266	0	0.498	14.98	14.05	
		31.8	10.3	0.266	0	0.410	20.77	21.30	
5		63.6	3.71	0.0672	0	3.23	53.96	53.29	
		14.5	4.33	0.0672	0	4.28	13.77	13.62	
		31.8	5.01	0.0672	0	2.19	38.32	34.02	
Micro-emulsion	0.5	3	36.1	0.396	0	0.0468	3.92	7.41	
		14.5	19.1	0.396	0	0.0782	7.18	5.99	
		31.8	29.1	0.396	0	0.0153	26.58	28.35	
	1	14.5	14.6	0.195	0	0.0748	9.76	9.59	
		31.8	13.7	0.195	0	0.0281	30.84	25.84	
		63.6	14.0	0.195	0	0.167	32.98	31.38	
	5	14.5	4.47	0.0656	0	0.277	11.35	11.76	
		31.8	7.14	0.0656	0	0.266	38.33	41.66	
		63.6	4.55	0.0656	0	0.256	58.07	54.93	

[#] Calculated value by using linear regression analysis

^A Calculated value by taking the average out of the measured free fractions inside this particular lipid concentration

Table 3 Kinetic parameters of transport of propranolol as solution and diverse drug formulations across Caco-2 cell monolayer

Formulation	Lipid Content [mg/ml]	Drug Conc. [μM]	Px10 ⁵ [cm/s]	Free Fraction	V _k [nmol*cm ⁻² *min ⁻¹]	K _a /C	C _{0a} AB [μM]	C _{0b} BA [μM]
Solution	0	4.10	35.8	1	4.13*10 ⁻³	0.0791	3.64	3.98
	0	13.75	33.1	1	2.26*10 ⁻²	0.0791	11.82	11.41
	0	30.63	27.1	1	3.13*10 ⁻²	0.0791	27.15	26.13
	0	60.71	32.9	1	6.95*10 ⁻¹	0.0742	50.06	52.66
Liposomes	0.1	31.8	45.8	0.8061	1.00*10 ⁻¹⁰	0.0674	25.44	28.51
	0.1	63.6	35.7	1	3.21*10 ⁻²	0.0669	53.84	55.46
	0.1	159	31.7	0.9416	1.00*10 ⁻¹⁰	0.1876	127.86	139.71
	1	31.8	20.9	0.5723	2.36*10 ⁻³	0.1805	25.57	25.94
	1	63.6	21.2	0.6211	1.00*10 ⁻¹⁰	0.0617	42.55	46.72
	1	159	24.6	0.6746	1.00*10 ⁻¹⁰	0.1244	111.85	123.65
	10	63.6	6.11	0.1158	5.75*10 ⁻³	0.2921	40.20	46.81
	10	159	6.64	0.1356	1.08*10 ⁻²	0.3643	90.15	97.00
	10	794	7.08	0.1644	1.47*10 ⁻¹	0.2985	655.02	669.08
Emulsion	0.5	14.5	44.0	0.9152	5.81*10 ⁻³	0.0422	18.03	19.62
		31.8	52.8	0.9152	2.48*10 ⁻²	0.0444	33.32	39.43
		63.6	32.8	0.9152	8.77*10 ⁻³	0.0653	66.78	66.89
	1	14.5	42.1	1	9.39*10 ⁻³	0.0141	13.91	15.80
		31.8	39.4	1	1.00*10 ⁻¹⁰	0.0318	28.23	32.89
		63.6	34.6	1	1.94*10 ⁻²	0.1597	56.62	60.01
	5	14.5	46.8	0.7829	1.00*10 ⁻¹⁰	0.1116	16.95	20.37
		31.8	34.4	0.7829	1.00*10 ⁻¹⁰	0.0756	32.01	33.83
		63.6	32.2	0.7829	1.00*10 ⁻¹⁰	0.1313	59.82	66.58
Micro-emulsion	0.5	14.5	50.2	0.8568	1.81*10 ⁻³	0.0601	11.72	14.16
		31.8	25.0	0.8568	2.65*10 ⁻³	0.0595	40.78	35.00
		63.6	30.9	0.8568	1.00*10 ⁻¹⁰	0.0590	58.68	60.16
	1	14.5	36.0	0.9056	1.00*10 ⁻¹⁰	0.0560	13.74	14.20
		31.8	20.5	0.9056	1.64*10 ⁻²	0.0621	60.34	50.00
		63.6	33.5	0.9056	1.00*10 ⁻¹⁰	0.0682	55.97	64.69
	5	14.5	37.8	0.8090	6.90*10 ⁻³	0.1051	15.20	18.18
		31.8	30.1	0.8090	8.90*10 ⁻³	0.1264	26.07	27.86
		63.6	30.1	0.8090	2.02*10 ⁻²	0.1477	65.26	64.23

Table 4 Kinetic parameters of transport of saquinavir as solution and diverse drug formulations across Caco-2 cell monolayer

Formulation	Lipid Content [mg/ml]	Drug Conc. [μM]	$P \times 10^5$ [cm/s]	Free Fraction	V_k [$\text{nmol} \cdot \text{cm}^{-2} \cdot \text{min}^{-1}$]	$K_{a/C}$	C_{0aAB} [μM]	C_{0bBA} [μM]
Solution	0	4.5	8.790	1	-	-	-	-
		5	16.3	1	-	-	-	-
		10.4	8.83	1	-	-	-	-
		14.5	14.3	1	-	-	-	-
Emulsion	0.5	3	5.32	0.2718	$5.82 \cdot 10^{-3}$	0.2792	1.85	2.03
		7	3.90	0.2718	$6.28 \cdot 10^{-3}$	0.8385	2.84	2.95
		14.5	4.30	0.2718	$1.96 \cdot 10^{-2}$	0.2331	7.78	8.24
	1	3	3.27	0.1534	$4.82 \cdot 10^{-3}$	0.9034	2.68	2.73
		7	3.86	0.1534	$7.67 \cdot 10^{-3}$	0.5403	3.59	3.60
		14.5	2.74	0.1534	$1.71 \cdot 10^{-2}$	0.3612	10.68	11.24
	5	3	1.44	0.0524	$1.85 \cdot 10^{-3}$	1.8330	2.77	2.76
		7	1.16	0.0524	$2.81 \cdot 10^{-3}$	2.3992	5.36	5.54
		14.5	0.901	0.0524	$6.39 \cdot 10^{-3}$	1.9203	13.56	13.70
Micro-emulsion	0.5	3	3.28	0.1770	$1.95 \cdot 10^{-3}$	0.1793	1.00	1.08
		7	2.74	0.1770	$4.41 \cdot 10^{-3}$	0.1607	2.66	2.93
		14.5	3.72	0.1770	$4.31 \cdot 10^{-2}$	0.1700	19.51	19.62
	1	3	2.15	0.0963	$2.79 \cdot 10^{-3}$	0.5671	2.27	2.29
		7	2.25	0.0963	$7.31 \cdot 10^{-3}$	0.9196	5.98	5.80
		14.5	1.91	0.0963	$2.33 \cdot 10^{-2}$	0.7434	20.01	20.81
	5	3	1.51	0.0205	$1.14 \cdot 10^{-3}$	0.8794	3.44	3.56
		7	1.05	0.0205	$2.12 \cdot 10^{-3}$	1.1951	5.82	5.97
		14.5	0.967	0.0205	$6.79 \cdot 10^{-3}$	1.0373	20.54	19.95

Table 5 Deduced kinetic parameters of transport of triclo bendazole of diverse drug formulations across Caco-2 cell monolayer

Formulation	Lipid Content [mg/ml]	Drug Conc. [μM]	$P_a \times 10^5$ [cm/s]	$P_b \times 10^5$ [cm/s]	Free Fraction $\times 10^3$	V_k [$\text{nmol} \cdot \text{cm}^{-2} \cdot \text{min}^{-1}$]	$K_{a/C}$	C_{0aAB} [μM]	C_{0bBA} [μM]
Liposomes	0.1	14.5	8.45	2.02	39.4	0	0.0086	7.35	6.83
		31.8	14.6	1.46	52.7	0	0.0194	17.33	18.85
		63.6	18.2	1.81	56.7	0	0.0216	52.40	46.82
	0.5	31.8	4.28	0.593	13.4	0	0.0741	31.83	32.43
		63.6	4.46	0.585	7.13	0	0.0523	42.68	43.96
		159	3.33	0.581	5.66	0	0.0753	112.12	119.64
	1	31.8	2.38	0.438	2.68	0	0.1849	30.67	30.84
		63.6	1.58	0.472	2.49	0	0.1426	48.54	50.64
		159	1.53	0.478	2.08	0	0.1742	127.30	127.61
	10	63.6	0.665	0.115	0.338	0	1.2493	54.14	54.20
		159	0.410	0.211	0.161	0	1.3079	156.11	149.69
		794	0.777	0.165	0.201	0	0.7244	633.92	665.68
Emulsion	0.5	14.5	3.04	0.703	2.38	0	0.1166	15.47	19.21
		31.8	1.68	0.777	2.38	0	0.0917	23.54	26.95
		63.6	3.63	0.676	2.38	0	0.0716	37.62	41.82
	1	14.5	1.63	0.697	1.80	0	0.1499	13.74	14.62
		31.8	1.08	0.471	1.80	0	0.1368	28.12	30.65
		63.6	1.96	0.608	1.80	0	0.1917	54.30	59.41
	5	14.5	0.339	0.264	0.160	0	0.3644	18.00	18.00
		31.8	0.685	0.367	0.160	0	0.4752	32.61	35.69
		63.6	1.10	0.519	0.160	0	0.5816	70.13	69.84
Micro-emulsion	0.5	14.5	4.02	0.924	1.95	0	0.0671	12.24	13.27
		31.8	3.39	0.925	1.95	0	0.0597	28.74	32.98
		63.6	6.34	0.884	1.95	0	0.0524	42.81	45.96
	1	14.5	2.73	0.936	1.55	0	1.3090	13.91	14.53
		31.8	1.59	1.12	1.55	0	1.2777	51.70	54.57
		63.6	3.45	0.840	1.55	0	1.2464	56.43	59.17
	5	14.5	1.41	0.609	0.178	0	0.3929	21.35	21.18
		31.8	1.23	0.577	0.178	0	0.7228	41.08	42.30
		63.6	1.43	0.544	0.178	0	0.3549	69.15	70.45

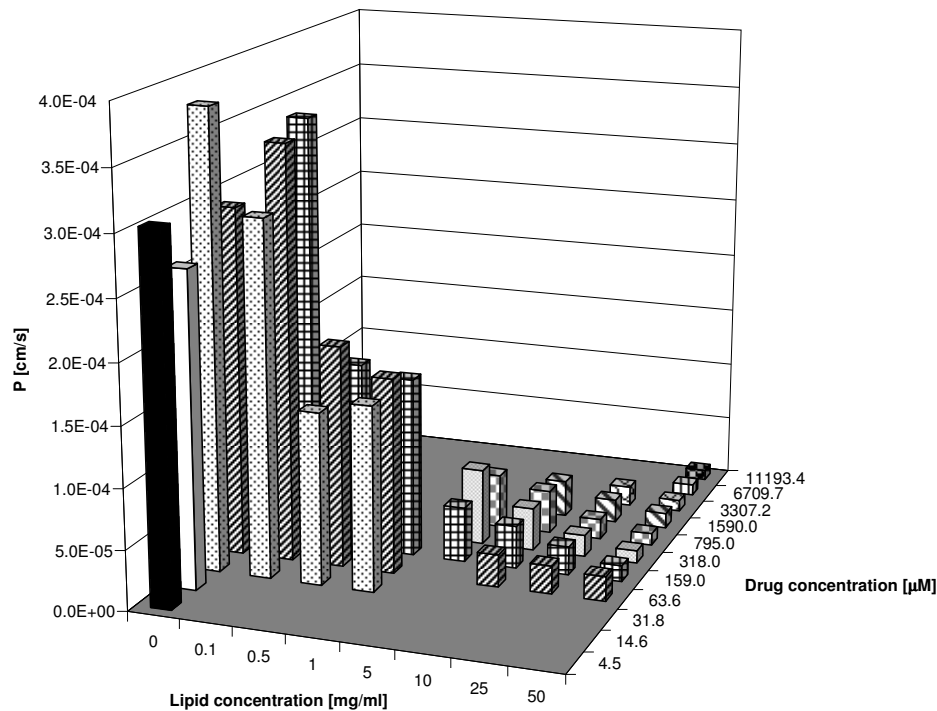
No relevant metabolism of the drugs was found in the Caco-2 cells. It is known from previous work of our group that saquinavir undergoes phase I metabolism in Caco-2 cells by hydroxylation. The main metabolite was detectable by HPLC-MS but contributed less than 2% to the mass balance and was therefore neglected in this study (115). Propranolol is known to be subject of phase I metabolism by ring hydroxylation, mainly by Cyp 450 2D6 and N-desisopropylation by Cyp 450 1A2, as well as phase II metabolism by glucuronidation (121). No evidence for metabolism, expected to be found in an additional peak in HPLC analysis, was observed in our experiments. No reports have been found concerning progesterone metabolism in Caco-2 cells as well as no evidence for progesterone metabolism has been found in our experiments. Triclabendazole is known to be subject of phase I and II metabolism. In sheep, the flavin monooxygenase system is the main metabolic pathway (122). Phase II metabolism to sulpho-metabolites by metabolism over glutathione-S-transferase is reported in literature (123). Nevertheless, no evidence of triclabendazole metabolism by the Caco-2 cells was found in our experiments.

4.1.4.3 Qualitative Influence of Lipid Phase Concentration on Apparent Permeability Coefficient

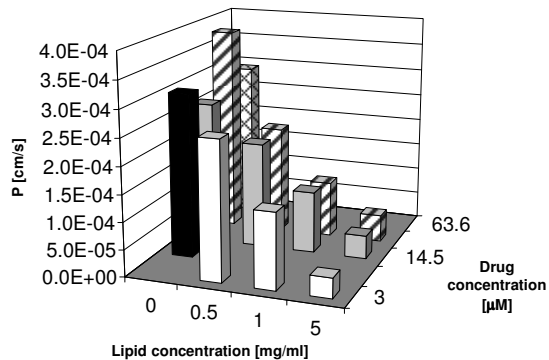
A strong influence of the lipid phase concentration on the permeability coefficient was observed, where the passive apparent permeability coefficient decreased with increasing lipid concentrations. Within the same lipid concentration no influence of the drug concentration on apparent permeability coefficient was observed, since the free fraction is determined by the lipid phase concentration and apparent permeability coefficient depends on free fraction. An example is given in Figure 14 that shows the influence of lipid phase concentration and drug concentration of the different progesterone formulations. Shown results were typical for the other used drugs and formulations too, except for propranolol emulsion and microemulsion. These exceptions showed no effect of the lipid concentration on the permeability coefficient and on free fraction.

Thus, formulation of the drugs with a lipid containing system appears to profoundly influence their permeation behavior through Caco-2 cell monolayer when an interaction of the drug with the vehicle was present.

A Progesterone Liposomes



B Progesterone Emulsion



C Progesterone Microemulsion

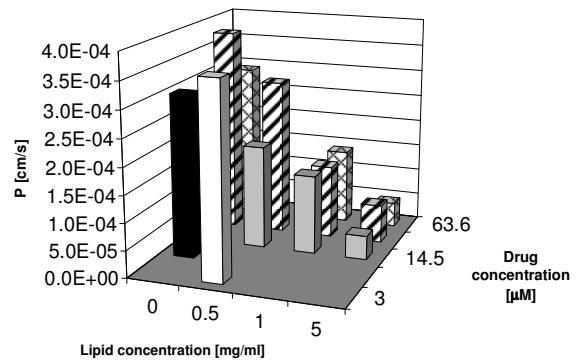


Figure 14 Qualitative influence of the lipid concentration and the drug concentration on apparent permeability coefficient of progesterone formulations. Panel A shows the liposome formulations, panel B shows the emulsion formulations, and panel C shows the microemulsion formulations. Each column represents the determined apparent permeability coefficient out of one transport experiment. Same pattern or color indicates same drug concentration.

4.1.4.4 Quantitative Influence of Free Fraction on Apparent Permeability Coefficient

Both, the determined free fractions and the deduced apparent permeability coefficients are dependent individually on the lipid concentration. The apparent permeability coefficient may be seen as function of the free fraction because it is generally agreed that the unbound drug concentration permeates

through the cell membrane and determines drug permeation. Equation 45 that was derived from the biophysical model expresses the apparent permeability coefficient as a function of free fraction. In this equation, the effect of the diffusion boundary layer and the contribution of firstly of permeation of free drug through the membrane and secondly of permeation of lipid bound drug through the membrane following direct transfer of drug upon collision of lipid particles with the membrane are taken into account. These processes are expressed as permeability coefficients. This equation was used to analyze the measured permeability coefficients. This equation was at first fitted to apparent permeability coefficient versus free fraction data for different volume fraction (VF) values of each drug with each formulation. Although, similar values of permeability coefficient of the free drug through the membrane ($P_{m,d}$) and permeability coefficient delineating transport through diffusion boundary layer ($P_{dbl,d}$) for all formulations of the same drug were generally deduced. From the fit, individual values of these parameters showed rather strong deviation. This was either because of the experimental variability of the data or because of the domination of one parameter over the process. Therefore, in order to alleviate these deviations and to obtain more universally valid values of the deduced parameters, data of each drug with all formulations were simultaneously used in the fitting. In this, the same $P_{m,d}$ and $P_{dbl,d}$ were used for all formulations. A different $P_{m,L}$ for each formulation was used. This fitting procedure improved the quality of the resulting fit compared to above first option. Figure 15 to Figure 25 show plots of apparent permeability coefficient as function of the free fraction. The array of curves in Figure 15 to Figure 25 represents the best fits corresponding to the different VF values. For a better clarity no z-axis was used. The model explained the data satisfactorily.

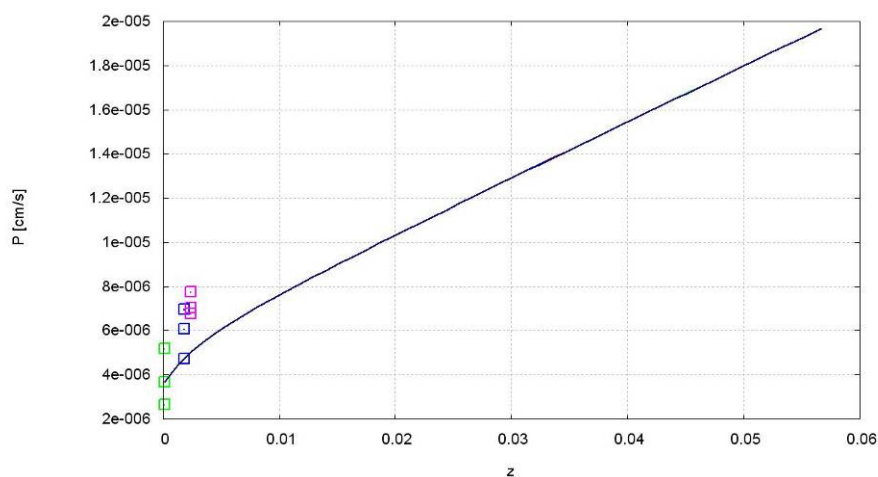


Figure 15 Plot of the apparent permeability coefficient as function of the free fraction of tricloabendazole emulsion including best obtained fit

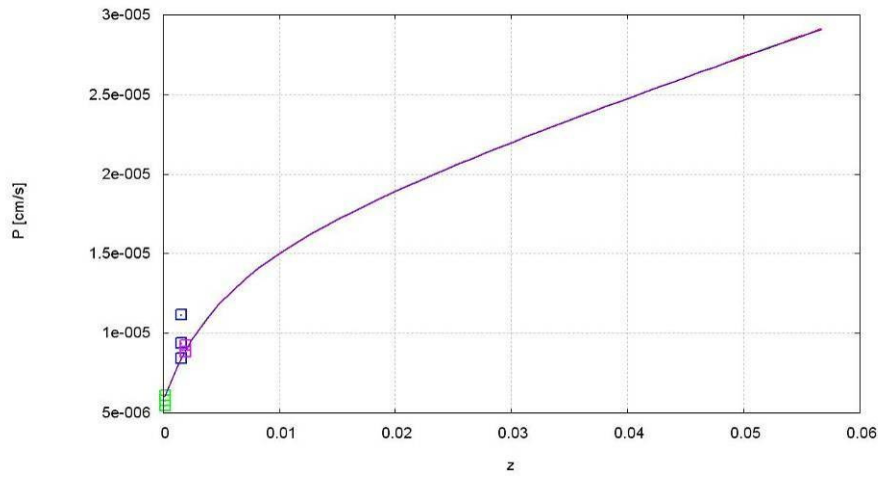


Figure 16 Plot of the apparent permeability coefficient as function of the free fraction of triclabendazole microemulsion including best obtained fit.

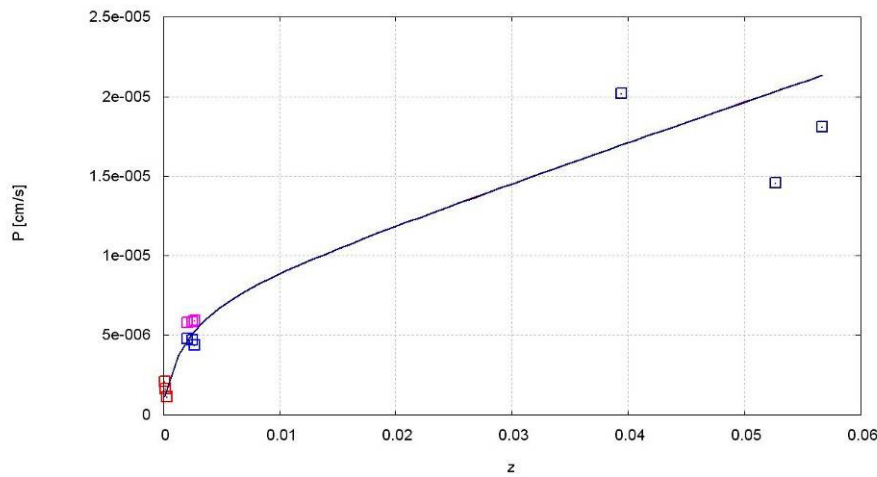


Figure 17 Plot of the apparent permeability coefficient as function of the free fraction of triclabendazole liposomes including best obtained fit.

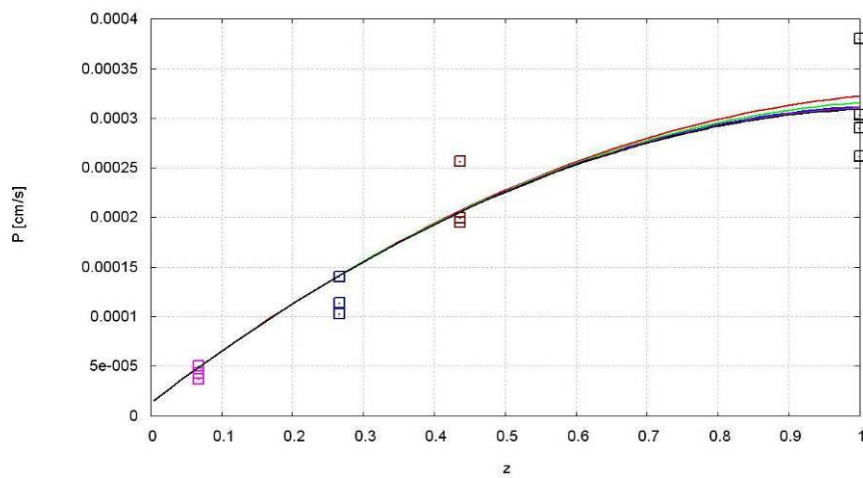


Figure 18 Plot of the apparent permeability coefficient as function of the free fraction of progesterone emulsion including best obtained fit.

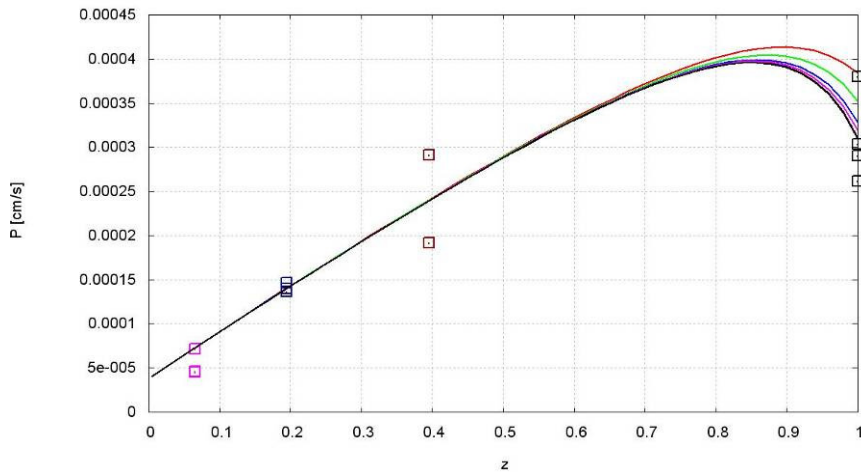


Figure 19 Plot of the apparent permeability coefficient as function of the free fraction of progesterone microemulsion including best obtained fit.

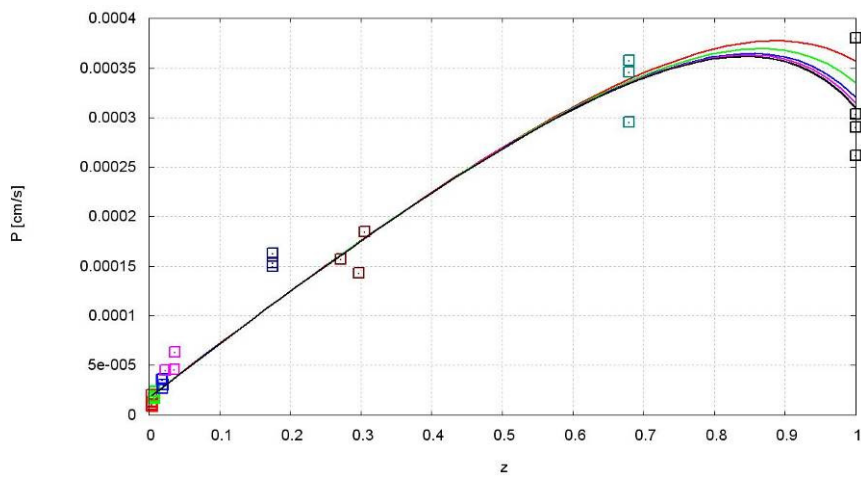


Figure 20 Plot of the apparent permeability coefficient as function of the free fraction of progesterone liposomes including best obtained fit.

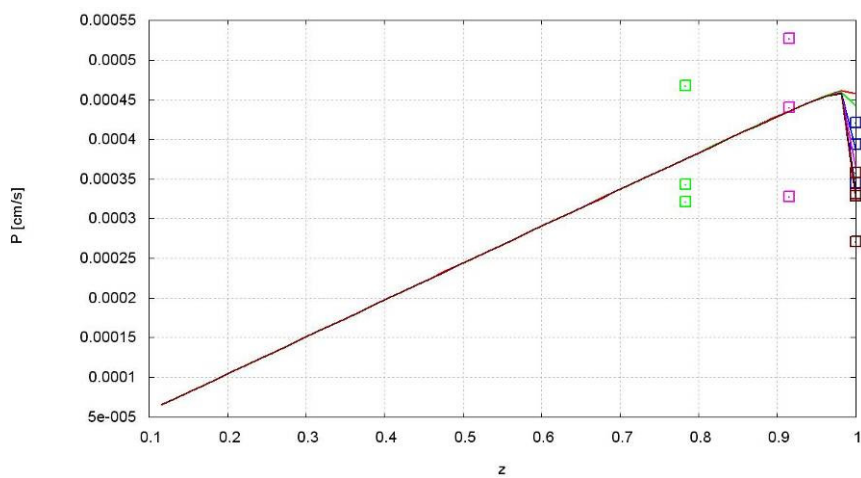


Figure 21 Plot of the apparent permeability coefficient as function of the free fraction of propranolol emulsion including best obtained fit.

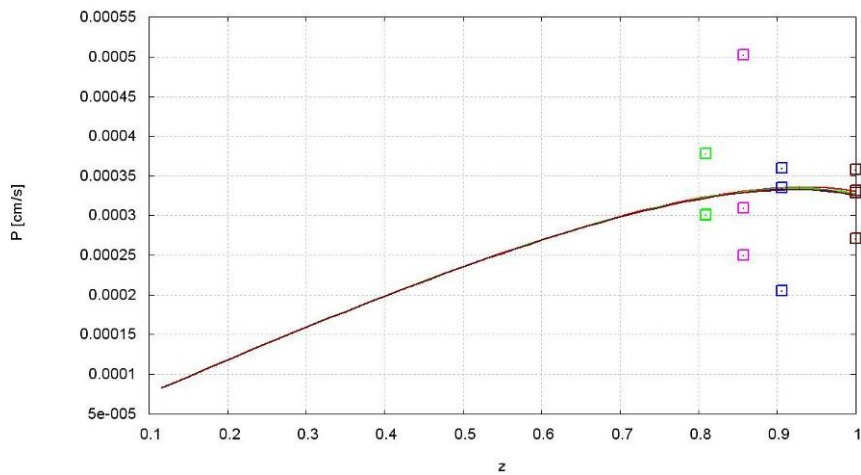


Figure 22 Plot of the apparent permeability coefficient as function of the free fraction of propranolol microemulsion including best obtained fit.

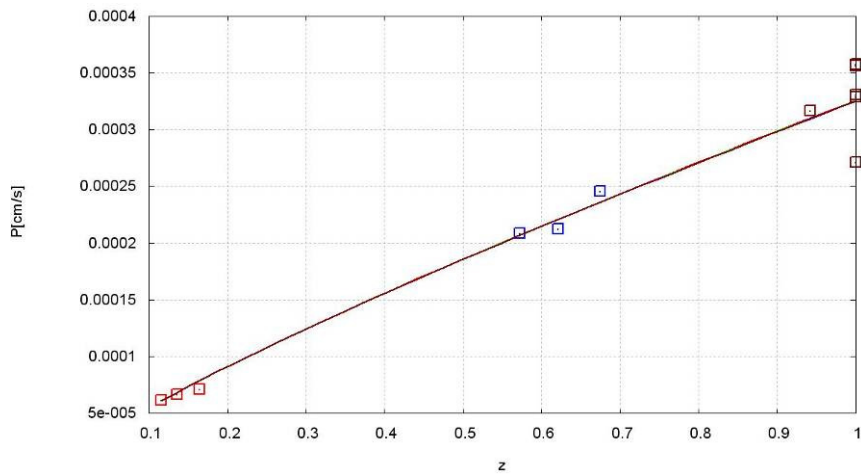


Figure 23 Plot of the apparent permeability coefficient as function of the free fraction of propranolol liposomes including best obtained fit.

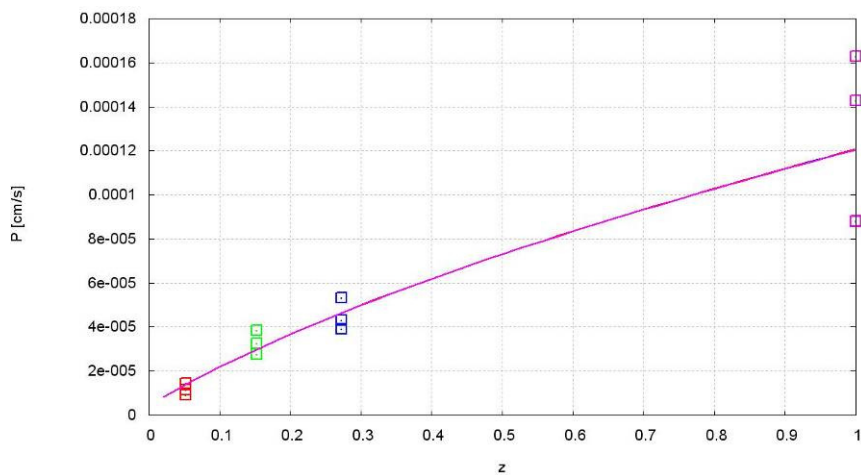


Figure 24 Plot of the apparent permeability coefficient as function of the free fraction of saquinavir emulsion including best obtained fit.

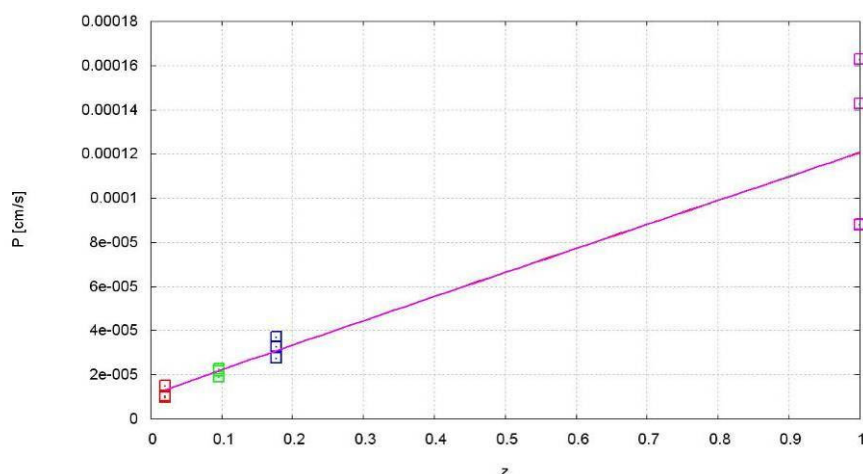


Figure 25 Plot of the apparent permeability coefficient as function of the free fraction of saquinavir microemulsion including best obtained fit.

The estimated parameters of all drugs and formulations by fitting the model to the experimental determined apparent permeability coefficients and determined free fractions are given in Table 6.

Table 6 Estimated parameters of all drugs and formulations by fitting Equation 45 to the experimental determined apparent permeability coefficients and free fractions.

Drug	Type of Formulation	$P_{m,d}$ [cm*s ⁻¹]	$P_{m,L}$ [cm*s ⁻¹]	$P_{dbl,d}$ [cm*s ⁻¹]
Triclabendazole ^A	Emulsion		$8.16 \pm 3.38 \cdot 10^{-6}$	
	Microemulsion	$4.48 \pm 1.54 \cdot 10^{-3}$	$8.19 \pm 1.73 \cdot 10^{-6}$	$2.72 \pm 0.40 \cdot 10^{-4}$
	Liposomes		$6.07 \pm 4.50 \cdot 10^{-7}$	
Progesterone	Emulsion		$1.31 \pm 0.90 \cdot 10^{-3}$	
	Microemulsion	$6.74 \pm 0.83 \cdot 10^{-4}$	$9.80 \pm 33.0 \cdot 10^{-3}$	$5.71 \pm 0.52 \cdot 10^{-4}$
	Liposomes		$5.49 \pm 4.40 \cdot 10^{-3}$	
Propranolol	Emulsion		$1.01 \pm 1.12^{\#}$	
	Microemulsion	$1.02 \pm 0.20 \cdot 10^{-3}$	$5.10 \pm 3.84 \cdot 10^{-3\#}$	$4.77 \pm 0.31 \cdot 10^{-4}$
	Liposomes		$4.90 \pm 9.20 \cdot 10^{-4}$	
Saquinavir	Emulsion		$2.01 \pm 12.9 \cdot 10^{-4}$	$2.02 \pm 2.50 \cdot 10^{-4}$
	Microemulsion	$3.00 \pm 5.17 \cdot 10^{-4}$	$4.54 \pm 9.24 \cdot 10^{-5}$	

[#] no interaction between formulation and drug, values not meaningful

^A to improve fitting quality, a scaling of -1 instead of 1 was used

Similar values for all drugs were obtained for the permeability coefficient of the diffusion boundary layer. Big differences between $P_{m,d}$ and $P_{m,L}$ depending on the drug and the formulation were found. For example triclobandazole showed a $P_{m,d}$ that is much larger than the $P_{m,L}$. In contrast to that, for progesterone, the $P_{m,L}$ was larger than the $P_{m,d}$.

To verify that lipid particles contribute to the total membrane permeability coefficient, as proposed in this work, depending on the drug and the formulation, a simplified model was fitted, where $P_{m,L}$ was not taken into account to the same datasets. The resulting estimations for the $P_{dbl,d}$ are in the same order of magnitude as the values obtained by the full equation. Except for the triclobandazole formulations, however, very poor fitting quality was obtained resulting in unrealistically high values for $P_{m,d}$ (data not shown/detailed results can be found in appendix, section 6.6.2.1). This confirms the importance to introduce the contribution of permeability caused by direct mass transfer from lipid particle to the cell membrane.

4.1.4.5 Effect of Lipid Containing Drug Formulations on Drug Fluxes

Drug flux is defined as product of apparent permeability coefficient and drug concentration. Flux is relevant for drug amount delivered and hence bioavailability. Whereas apparent permeability coefficient correlates directly with the free fraction (see Equation 45), flux correlates with the absolute free drug concentration in water phase. By calculating fluxes of all cell permeation experiments we observed that within one lipid concentration the drug flux increases with increasing drug concentration, because permeability coefficient remains constant. Within the same drug concentration drug flux decreases with increasing lipid concentration because the permeability coefficient decreases with increasing lipid concentration. The above is demonstrated in the example of progesterone liposomes (see Figure 26) and is considered to apply also to the other formulations and drugs.

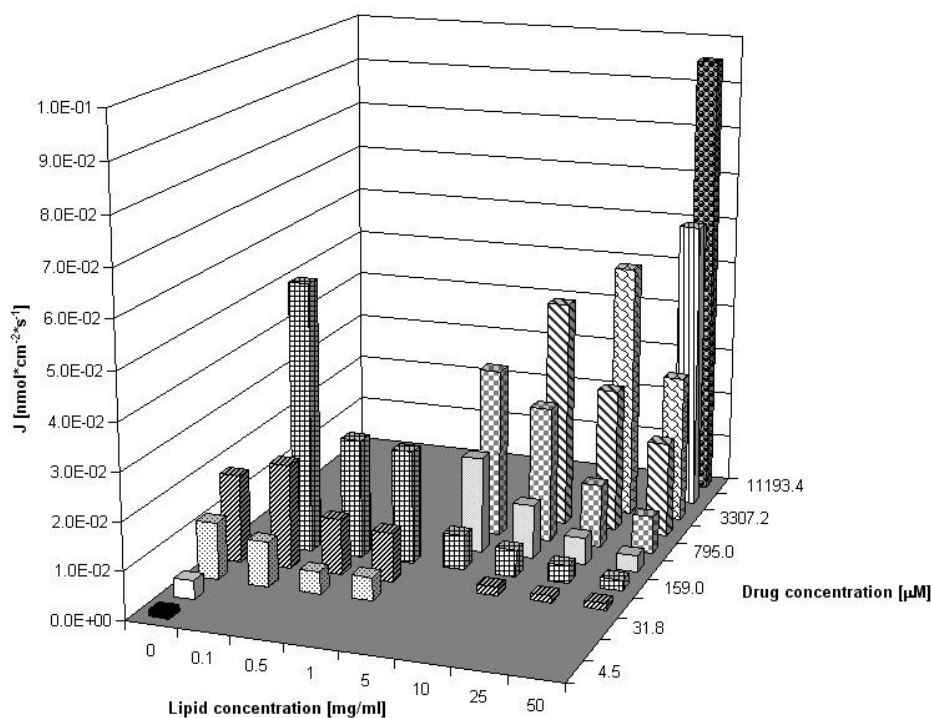


Figure 26 Qualitative influence of lipid concentration and drug concentration of progesterone liposomes on drug flux through Caco-2 cell monolayer. Each column represents the calculated flux of apparent permeability coefficient and total drug concentration of one transport experiment. Same pattern or color indicates same drug concentration and is the same as in Figure 14 panel A.

Because of the wide drug and lipid phase concentrations tested, progesterone liposome series offered the possibility to compare experiments exhibiting the same free drug concentration. If experiments exhibiting the same free drug concentration were considered, an increase of total drug concentration is needed to maintain same free drug concentration with higher lipid concentration. Figure 27, Panel A demonstrates a linear relationship of total drug concentration as a function of lipid concentration of formulations having the same free drug concentration in water phase. Since drug flux correlates with absolute free concentration, it follows that the flux should be constant for these formulations if free drug alone is responsible for membrane permeation. Calculated drug fluxes of the experiments with equal unbound drug concentration, however, showed an increased drug flux with increasing lipid and drug concentration, using total drug concentration and apparent permeability coefficients for the calculation. The resulting increasing relationship is shown in Figure 27, Panel B. In this plot the apparent permeability is the slope.

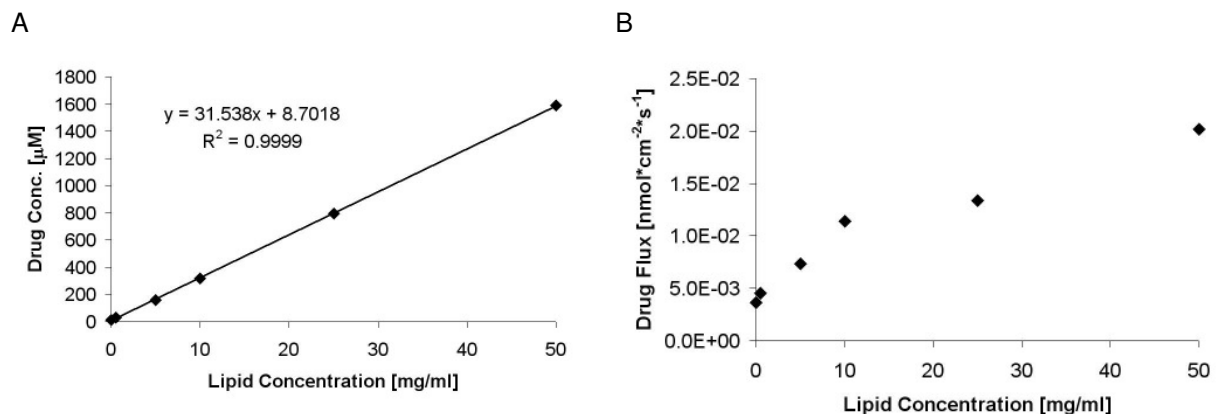


Figure 27 Resulting plots if experiments of progesterone liposomes in which the drug concentration in the water phase (free drug concentration) were equal are compared. Panel A shows the resulting linear relation of experiments with the same drug concentration in the water phase, if the total drug concentration of these formulations is plotted against the lipid concentration. Panel B shows the influence of the lipid concentration on the drug flux of the same experiments, resulting in a non-linear relationship with decreasing slope.

4.1.5 Discussion

4.1.5.1 Cell Permeation Kinetics

The model based evaluation of the experimental results of this study shows that the developed mathematical model for the determination of drug absorption parameters in Caco-2 cell monolayers distinguishes in a quantitative fashion between the permeability coefficients of the apical and the basal membrane. The model allows calculating a formulation-to-cell partition coefficient, which enables to gain information about cellular retention and accumulation of a drug. Additionally the model enables to quantify the contributions of passive permeation and carrier mediated efflux. Carrier mediated efflux was determined for propranolol and saquinavir which was in agreement with the literature (21, 115, 124).

The used drugs were classified by the model as expected based on literature, taking aqueous solutions (or low lipid concentrations in the case of triclobandazole) as reference. Obtained permeability coefficients of all drugs were not dependent on the used drug concentrations within one lipid concentration, which is in agreement with the diffusion theory.

The definition of different apparent permeability coefficients for the apical and the basal membrane permits to differentiate between the two sides of polarized cells and allows concluding on the possible effect of different membrane properties on cellular permeation of drugs.

Progesterone showed no differences of apparent permeability coefficient of the apical membrane and the basal membrane. If no difference between apical and basal membrane permeability coefficient exists, it may be sensible to replace the two different parameters by a common apparent permeability coefficient (P) to lower the numbers of parameters estimated by data fitting to optimize the estimation

of all other parameters. This approach makes sense especially if a carrier mediated transport is involved.

Concerning propranolol and saquinavir, a high correlation level ($\sim 0.95-1$) of P_a and P_b in the regression analysis of most of the data sets was obtained. There were some data sets showing no correlation, but P_a and P_b were estimated equal in these cases, indicating no difference of P_a and P_b . For these reasons a common apparent permeability coefficient was used.

All tested triclabendazole formulations showed a distinct difference between P_a and P_b , whereas P_b was always smaller. Lower apparent permeability coefficient of the basal membrane may be a consequence of different interactions of triclabendazole with the apical and the basal membrane caused by different membrane composition. It is known that the basolateral membrane is composed different, e.g. enriched in sphingomyelin and phosphatidylcholine (64, 65).

The deduced permeability coefficients of aqueous solutions in this work were systematically higher compared to apparent permeability coefficients from literature. Several parameters like hydrodynamics inside the Transwell inserts, caused by different oscillation and stirring rate of the shaker, or cell culture conditions may be responsible for this, but the different calculation method for apparent permeability coefficients in the literature compared to the proposed model in this work mainly causes this effect. The standard literature model for the calculation of the transcellular apparent permeability coefficient takes into account the whole cell monolayer as barrier (34). In contrast to the standard approach, the model proposed in this study takes into account two permeability coefficients to describe the transcellular permeability, where P_a describes drug permeation through the apical membrane between formulation and cellular compartment in both directions, and P_b describes the same for the basal membrane. This different definition of permeability coefficients mainly causes the obtained differences compared to literature.

The introduction of the formulation-to-cell partition coefficient $K_{a/C}$ is very useful for a better understanding of the mechanism responsible for the impact of a drug formulation on drug permeation. Misinterpretation of the data is diminished because $K_{a/C}$ is important for a precise assessment of the time dependent concentration change in the cellular compartment. The partition coefficient additionally explains, in addition to independent prediction of P_a and P_b , cellular accumulation of a compound that could otherwise be interpreted wrongly as adsorption to the Transwell device, not detectable metabolism, or substance loss because of degradation.

4.1.5.2 Influence of Lipid Containing Formulations on Carrier Mediated Efflux

A low carrier mediated apical efflux rate was estimated for propranolol, which is consistent with the literature where a slightly higher permeability coefficient from basal to apical transport direction is reported (21, 124). Saquinavir showed an extensive carrier mediated apical efflux, which was expected and consistent with previous work of our group. The qualitative effect on the carrier mediated efflux of saquinavir of microemulsions and emulsions, shown in Figure 13, indicates a common underlying mechanism. The decrease of the carrier mediated efflux with increasing lipid concentration

may be explained by the decreasing amount of free drug able to cross the cellular membrane. This is expressed as well in the increase of the formulation-to-cell partition coefficient, indicating a lower intracellular concentration compared to the donor and the acceptor with increasing lipid concentration. Furthermore, the concentration dependence of the carrier mediated efflux within one lipid concentration may be evidence that the amount of drug crossing the cellular membrane is below that required for saturation of the involved carrier. Hence, a first order kinetics of apical efflux is implied. Inhibition of the apical efflux rate by Cremophor EL is described in literature (94, 95, 125). While containing the double amount of Cremophor EL in the lipid phase, no additional inhibition of the efflux by the microemulsion compared to the emulsion was determined in the experiments of this work. Maybe the difference in Cremophor EL content was too low or the influence of the surfactant is low in the used experimental setting. However, significant effect of the used concentration range of Cremophor EL (0.005%-0.1% (m/V)) on drug transport by inhibiting active efflux has been reported (94, 125). It is assumed that the amount of Cremophor EL available to inhibit active efflux was very low, because of the evidence, provided by equilibrium dialysis experiments, that Cremophor EL is strongly associated with the lipid particles. No differences could be found in free fraction, caused by free Cremophor EL molecules available to solubilize drug in the acceptor compartment, when experiments using a dialysis membrane that was not permeable for Cremophor EL, were compared with experiments using a dialysis membrane that was permeable for Cremophor EL. Therefore, a very small concentration of monomeric Cremophor EL can be assumed in tested lipid formulations.

4.1.5.3 Influence of Formulation and Free Fraction on Apparent Permeability Coefficient

The results of the study showed that free fraction generally determines apparent permeability. High free fractions of drugs in a lipid containing dosage form results in similar permeability coefficients as aqueous solutions, whereas low free fractions have low apparent permeability coefficients as a consequence. All drugs showed strong interaction with lipid formulation regardless of structure of the formulation. This was because of the lipophilicity of the used drugs. In contrast to all other drugs, propranolol showed no interaction with the microemulsion and the emulsion causing apparent permeability coefficients equal to the aqueous solutions which can be explained by its low solubility in the lipid phase of the emulsion and the microemulsion, which is caused by its moderate lipophilicity and its occurrence as mainly charged ion at pH 7.4. Propranolol is known to interact with cellular membranes and model membrane systems. The naphthalene moiety of propranolol partitions into the hydrocarbon core of the lipid bilayer and the charged amine side chain is most likely positioned in the aqueous phospholipid head group region which may explain strong interaction of propranolol with the liposomes and the cells (126). This may explain the observed strong interaction of propranolol with the liposomes.

Besides the influence of the free fraction, the need of an additional mechanism to describe trans-membranal drug permeability was evident, because a model taking into account only permeation of free drug molecules did not adequately explain the data. Excluding paracellular permeation by monitoring TEER and excluding phagocytotic activity of Caco-2 cells, it was obvious to assume a

beneficial effect caused by the lipid containing drug formulations to the passive permeation. Considering this effect, permeation caused by direct drug transfer from lipid particle to the cell membrane was taken into account additionally to the permeability coefficient of the free drug through the cell membrane, because direct drug transfer from lipid domain to lipid domain has been described in literature.

The resulting model, proposed in this work, described the data satisfactorily. Standard error was relatively large, because of experimental variation and depending on drug, cases of extremely high or low free fractions making fitting difficult. Big differences were found regarding the $P_{m,L}$ depending on the drug and the formulation. Depending on the drug, mass transfer caused by direct drug transfer from lipid particle to cellular membrane has high or low contributions to substance flux over the cellular membrane.

Generally high $P_{m,L}$ were found for all progesterone formulations indicating an important contribution of the “lipid pathway” to the trans-membranal permeability. Progesterone is a physiologically occurring compound and has the same scaffold and similar physicochemical properties as cholesterol that occurs physiologically in the cellular membranes. This physicochemical similarity and even more the physiological relevance for progesterone to cross membranes easily, because of the intracellular localization of the steroid hormone receptor, may explain why progesterone may easily be transferred between lipid particles and membrane. While progesterone is possessing a low free fraction, the resulting apparent permeability coefficient is high compared to other drugs, because high $P_{m,L}$ partially compensates the effect of low permeability on drug permeation.

The lowest $P_{m,L}$ was resulting for triclobandazole for all formulations, indicating a small contribution of the lipid particles to the trans-membrane transport of the drug. Compared to progesterone and saquinavir, which had both similar free fractions, the free fractions of triclobandazole were more than one order of magnitude lower, indicating a strong interaction of the formulations with the drug. This implies a low tendency of triclobandazole to leave the lipid phase of the formulations. The interaction of the drug with the formulation seems to be stronger than the interaction of the drug with the cell, causing low contribution of the “lipid pathway” to the trans-membranal permeability resulting in a low apparent permeability.

Regarding the dataset used for this work, too little data were collected with only four drugs to conclude on concrete molecular properties important to direct lipid-lipid transfer. Nevertheless, several general points may be important for a contribution of lipid-lipid transfer to transcellular permeation. For liposomes, the localization of the drug inside the bilayer may be important for lipid-lipid transfer from liposomes to cell membrane. Less lipid-lipid drug transfer would be expected if a drug is located in the core region of the bilayer compared to the localization of a drug in the surface region. Very high drug solubility in the used lipid phase combined with a high lipophilicity may be disadvantageous, because the drug is then trapped inside the lipid particles causing a low free fraction and a high affinity of the drug to the lipid phase, which impedes together transcellular permeation.

The obtained permeability coefficients of the free drug through cell monolayer ($P_{m,d}$) were independent of the formulations for all drugs. A classification of the used drugs results in the following order from

highest to lowest $P_{m,d}$: triclabendazole > propranolol > progesterone > saquinavir. Surprisingly, triclabendazole was found to be the compound with the highest $P_{m,d}$, indicating a high permeability coefficient out of an aqueous solution. In vivo data of triclabendazole showed an increase of bioavailability after oral triclabendazole administration together with a fatty meal (127). This is a typical BCS class II substance behavior by which the permeability coefficient is high but the flux through the epithelial barrier is limited because of low solubility. With an increase of the solubility an increase of the flux is obtained. Additional indication of high membrane permeability of triclabendazole is a high apparent permeability coefficient determined in our lab for albendazole, a structurally very similar compound (unpublished results). Due to unspecific adsorption to the Transwell surfaces it was not possible to measure the permeability of a purely aqueous triclabendazole solution as reference. If triclabendazole is formulated with small amounts of lipids the permeability coefficient decreases rapidly because of a very low free fraction caused by high lipophilicity.

All obtained $P_{dbi,d}$ are in the same order of magnitude, but the resulting differences are bigger than expected. It was expected that saquinavir resulted in the lowest $P_{dbi,d}$, because of its size. It was expected further to find similar $P_{dbi,d}$ for all other drugs because of nearly equal molecular weights. There is very recently published work dealing with drug transport of bile micelle containing drug formulations through diffusion boundary layer that shows, that the assumptions made in the present work describes drug transport through diffusion boundary layer most appropriately (128).

Unspecific adsorption to the filter insert may contribute to determined differences because $P_{dbi,d}$ of triclabendazole and saquinavir were similar, but different from the other drugs. Both drugs undergo unspecific adsorption to the Transwell device. It may be possible that triclabendazole and saquinavir would be slightly retarded during diffusion through the polycarbonate filter caused by the tendency of these drugs to adsorb to surfaces. The unspecific adsorption of triclabendazole was more distinctive than the absorption of saquinavir and could explain the slow permeation through the basal diffusion boundary layer.

It is often encountered in literature that for most lipophilic compounds that exceed log D 2-3 cell membrane permeation is very rapid. Therefore, permeation through diffusion boundary layer would be the rate limiting step for lipophilic compounds (85, 128-132). If aqueous solutions of the model drugs tested in this work were regarded, this is confirmed for all compounds (see Table 6). If lipid containing formulations of the tested model compounds are considered, one has to take into account, that the resulting permeability coefficients are also dependent on the free fraction. Out of this follows that a low free fraction decisively influences the apparent permeability coefficient of a drug through the membrane. Depending on free fraction, lipid concentration, and the drug, the diffusion boundary layer or the membrane may be rate determining. This is also expressed in the shape of apparent permeability versus free fraction plots.

Taken together, lipid containing drug formulations influence transcellular drug permeation with different mechanisms. Lipid containing formulations decrease the free fraction of a lipophilic drug and decrease the apparent permeability coefficient. Depending on the drug, contribution of drug

permeation because of direct drug transfer from lipid particle to cell membrane may compensate the decrease of apparent permeability coefficient partially, as observed for progesterone. On the other hand, very low apparent permeability coefficients may result if a highly lipophilic and highly membrane permeable compound does not permeate by direct drug transfer from lipid particle to cell membrane. In this case, the extremely low free fraction determines the permeation totally, such as observed for tricloabendazole.

4.1.5.4 Drug Flux: Consequences for In-Vivo Drug Delivery?

Drug flux depends on total drug concentration and apparent permeability coefficient and correlates directly with the absolute free drug concentration. If a single drug concentration is considered with different lipid concentrations, drug flux decreases with increasing lipid concentration because decreasing apparent permeability coefficient with increasing lipid concentration. If free drug concentration alone is responsible for membrane permeation, the flux of a drug of different lipid containing formulations with the same absolute free concentration should be constant and independent of lipid concentration. As displayed in Figure 27, Panel B, flux of progesterone increases with increasing lipid concentration if experiments with the same absolute unbound drug concentration were regarded. The fact that this plot, where the apparent permeability is the slope, does not show a constant flux but an increase with increasing lipid concentration shows indirectly the contribution of the lipid particles to the transmembranal drug permeation. This is consistent with the high $P_{m,L}$ compared to $P_{m,d}$ obtained for progesterone. Drug fluxes of experiments with equal unbound drug concentration showed an increased flux with increasing drug and lipid concentration, but the benefit for drug flux leveled off at high lipid concentrations. Because apparent permeability coefficient remains constant within one lipid concentration, the drug flux may be increased by augmenting the total drug concentration to compensate the decrease of apparent permeability coefficient, if drug solubility in that formulation is high enough. It is a precondition that the lipid containing formulation allows a large drug solubility enhancement. This may lead to absorption enhancement in vivo. Since drug flux is time dependent, a time independent parameter to characterize the influence on drug transport is the situation in equilibrium. Regarding cell permeation experiments with different progesterone formulations, the extent of drug permeation was always the same in equilibrium in apical to basal direction, but time to reach equilibrium was prolonged with increasing lipid concentrations. If no active efflux, degradation, and metabolism are involved, even formulations with high lipid concentrations would equilibrate, but it is a question of time. Regarding a given amount of drug, this would result in vivo in same area under the curve (AUC), but prolonged time to attain the maximal plasma concentration. The maximal plasma concentration would be lowered because drug flux and permeability were decreased with increasing lipid concentration resulting in slower drug invasion. Lipid systems offer the possibility to compensate lower maximal plasma concentration by increasing drug concentration in the formulation, which is not affecting the permeability coefficient of the drug and would entail, assuming same permeated fraction, to increased AUC and maximal plasma concentration. That again may cause longer time period exceeding the minimal effective drug concentration.

After peroral administration, the lipid formulations are altered by lipid digestion, presence of bile salts, and phospholipids, but drug solubilization in colloidal systems may still take place in the intestine. Because similar effects of structurally different formulations on drug permeation have been shown, similar effects of the digested product were expected, if the particles are able to interact physically with the cellular membrane.

There is a mucus layer present, which is first of all an additional hydrophilic diffusion barrier for drug permeation itself. It was shown that mainly the lipid components of the mucus lower the diffusion of lipophilic compounds (133). Additionally, the mucus layer is a barrier with unknown influence on the mass transfer caused by direct drug transport from lipid particle to the cell membrane upon collision. Few data are available dealing with small particles diffusing through mucus. These data indicate that, depending on particle properties, diffusion of particles through mucus is possible (106, 134-136). Alternatively, a drug transfer from lipid particles to lipophilic mucus components may be thinkable since human intestinal mucus is containing glycolipids, lipids, and phospholipoidal constituents 0.5-5%[w/w] overall (58).

There is evidence, that lipid containing formulations have the ability to affect the pharmacokinetics of an orally administered drug. Particularly for highly lipophilic molecules, lipid containing dosage forms provide a good possibility to improve bioavailability. In vivo, different mechanisms like uptake of lipid vesicles by the lymphatic tissue are involved and may contribute additionally to the absorption enhancement which makes it difficult to estimate the importance of the drug permeation because of direct drug transfer from lipid particle to the cell membrane out of the in vitro data of this work. It would be challenging to assess the in vivo quantification of this transfer because other involved mechanisms have to be excluded somehow. Another possibility to investigate on this open question would be to use a suitable in vitro model e.g. to put a layer of mucus or artificial mucus on Caco-2 cell monolayer or to use a mucus producing cell model.

4.1.6 Conclusions

The refined mathematical model, which is proposed in this study for the determination of drug absorption parameters in Caco-2 cell monolayers, is able to differentiate between active and passive transported compounds. The model is able to divide trans-monomer permeability into independent permeability coefficients of the apical membrane and the basal membrane. It allows deducing formulation-to-cell partition coefficient, intracellular time dependent concentration, and quantification of carrier mediated efflux rate directly out of time dependent experimental concentration data. The analysis of the transcellular permeation experiments with this model indicated a decrease of apparent permeability with increasing lipid concentration, if an interaction of a drug and a lipid containing formulation is given.

A biophysical model for delineating contribution of different transport steps to the apparent permeability coefficient was developed taking into account transport of lipid particles and free drug molecules through diffusion boundary layer, permeation of free drug molecules through cell membrane, and drug permeation because of direct drug transfer from lipid particles to the cell membrane. This evaluation of the apparent permeability coefficient confirmed that the free fraction of a

drug is the major determinant of intestinal cell permeation. Additionally, the direct transfer of lipophilic drugs from lipid phase of the formulation to cell membrane can also make an essential contribution to drug permeation. The relative significance of these two processes may depend on the drug and the formulation. These observations apply to structurally different lipid containing drug formulations.

Since drug flux is relevant for the amount delivered and hence bioavailability, simultaneous increase of drug and lipid concentration provides an undiminished flux which may improve bioavailability by prolonged intestinal absorption at a sustained rate. The results of this study may be used for the development of efficient oral dosage forms to improve bioavailability of poorly water soluble drugs.

4.1.7 Acknowledgements

We would like to thank Lipoid GmbH for the generous supply with Lipoid S 100 and Lipoid EPG. We would like to thank Roche Pharmaceuticals for the kind gift of saquinavir and Phares Drug Delivery for the kind gift of triclabendazole.

4.2 Screening of Several Lipophilic Compounds to Find a Poorly Soluble Compound with Low Membrane Permeability and No Carrier Mediated Efflux

To investigate the influence of lipid containing dosage forms on drugs with different properties, a drug exhibiting poor water solubility and low membrane permeability had to be chosen. Furthermore the drug should be no subject of carrier mediated efflux. Ideally, the compound should have been used in Caco-2 permeation studies already and drug metabolism should be known.

In a log D range from 0 to 5 and a molecular weight up to 500 D, high lipophilicity and good membrane permeability are usually connected properties if the compound is no subject of carrier mediated efflux (5). If log D exceeds 5 or the molecular weight exceeds 500 D membrane permeability decreases (7).

After extensive literature study, some compounds were chosen to test their suitability with the Caco-2 model: Carbamazepine was chosen because of its poor solubility and high lipophilicity (log D 2.6), a known moderate to low Caco-2 permeability, and no reported carrier mediated transport in the Caco-2 model (33, 84, 137).

The moderately lipophilic triamterene (log D 1.26) was chosen because of its poor solubility and because it was one order of magnitude less permeable than propranolol in the mdr1-mdck cell model (138).

A permeability coefficient in the Caco-2 model of $1.3 \cdot 10^{-6} \text{ cm}^2/\text{s}$ indicated that the poor soluble and moderately lipophilic bendroflumethiazide (log D 1.91) may have the desired properties (33).

Poorly soluble proscillaridine was chosen because of its molecular weight of 531 D, a log D of 2.48, and a reported permeability of $0.63 \cdot 10^{-6} \text{ cm}^2/\text{s}$ in the Caco-2 cell model (60).

Albendazole and triclabendazole were chosen because of their low solubility and their high lipophilicity (log D of 3.01 and of 5.9, respectively). Both compounds achieve a low bioavailability if orally administered in vivo (1).

4.2.1 Material and Methods

4.2.1.1 Material

Carbamazepine, triamterene, bendroflumethiazide, and albendazole were purchased from SIGMA-Aldrich, Fluka Chemie GmbH, Buchs, Switzerland and were of analytical grade. Proscillaridine (minimum 80%) was purchased from SIGMA-Aldrich, Fluka Chemie GmbH, Buchs, Switzerland. Triclabendazole was kindly provided by Phares Drug Delivery, Muttens, Switzerland. Transport media used for the permeation studies were prepared with Dulbecco's Modified Eagle's Medium (DMEM) base powder (without glucose, l-glutamine, phenol red, sodium pyruvate and sodium bicarbonate, purchased from SIGMA-Aldrich, Fluka Chemie GmbH, Buchs, Switzerland). DMEM base powder was dissolved in bi-distilled and autoclaved water and supplemented with glucose (4.5 g/l), HEPES (4.76 g/l), NaCl (1.987 g/l), and l-glutamine (0.876 g/l). The pH was adjusted to 7.4 and the final medium was filtered through a sterile filter (Supor-200, 0.2 μm pore size, Pall Corporation, Michigan,

USA) under aseptic conditions. Glucose, HEPES, NaCl, and L-glutamine were purchased from SIGMA-Aldrich (Fluka Chemie GmbH, Buchs, Switzerland). Dulbecco's Phosphate Buffered Saline (D-PBS) (with Ca²⁺, Mg²⁺) was purchased from SIGMA-Aldrich (Fluka Chemie GmbH, Buchs, Switzerland).

4.2.1.2 Drug Quantification

The drug quantification of cell permeation experiments with aqueous solutions of the drugs was performed with HPLC-UV (Agilent series 1100, Agilent Technologies USA, equipped with a capillary pump G1376A, an auto sampler G1377AµWPS and a variable wavelength detector G1314a). A C-18 reversed phase column was used (CC 125/2 Lichrospher 100 RP 18 ec, Macherey Nagel, Oensingen, Switzerland).

The drug concentration of albendazole was determined using the following mobile phase: distilled water (bi-distilled and filtered through 0.45 µm)/methanol/tetrahydrofuran 40/45/15 (V/V). Ammonium acetate with a concentration of 0.55 g/l was added to the mobile phase. pH-value at 25 °C was 7.30. An isocratic method was used for quantification with a flow of 0.2 ml/min, an injection volume of 40 µl and a runtime of 7 min. Albendazole was detected at 254 nm in UV. Quantification was performed against a set of external standard solutions within the linear response concentration range. Samples were stored at 4 °C.

The drug concentration of bendroflumethazide was determined with the following mobile phase: distilled water (bi-distilled and filtered through 0.45 µm)/methanol/tetrahydrofuran 50/35/15 (V/V). Ammonium acetate with a concentration of 0.55 g/l was added to the mobile phase. pH-value at 25 °C was 6.95. An isocratic method was used for quantification with a flow of 0.2 ml/min, an injection volume of 40 µl and a runtime of 8 min. Bendroflumethazide was detected at 254 nm in UV. Using this method, retention of bendroflumethazide was approximately 4.7 min. Quantification was performed against a set of external standard solutions within the linear response concentration range. Samples were stored at 4 °C.

The drug concentration of carbamazepine was determined with the following mobile phase: distilled water (bi-distilled and filtered through 0.45 µm)/methanol/tetrahydrofuran 55/35/10 (V/V). Ammonium acetate with a concentration of 0.55 g/l was added to the mobile phase. pH-value at 25 °C was 6.9. An isocratic method was used for quantification with a flow of 0.2 ml/min, an injection volume of 40 µl and a runtime of 6 min. Carbamazepine was detected at 284 nm in UV. Using this method, retention of carbamazepine was approximately 3.7 min. Quantification was performed against a set of external standard solutions within the linear response concentration range. Samples were stored at 4 °C.

The drug concentration of proscillaridine was determined with the following mobile phase: distilled water (bi-distilled and filtered through 0.45 µm)/methanol/tetrahydrofuran 45/45/10 (V/V). Ammonium acetate with a concentration of 0.55 g/l was added to the mobile phase. pH-value at 25 °C was 7.21. An isocratic method was used for quantification with a flow of 0.2 ml/min, an injection volume of 40 µl and a runtime of 7 min. Proscillaridine was detected at 300 nm in UV. Using this method, retention of

proscillaridine was approximately 4.7 min. Quantification was performed against a set of external standard solutions within the linear response concentration range. Samples were stored at 4°C.

The drug concentration of triamterene was determined by HPLC-UV with the following mobile phase: distilled water (bi-distilled and filtered through 0.45 µm)/methanol/tetrahydrofuran 60/35/5 (V/V). Ammonium acetate with a concentration of 0.55 g/l was added to the mobile phase. pH-value at 25°C was 6.81. An isocratic method was used for quantification with a flow of 0.2 ml/min, an injection volume of 40 µl and a runtime of 8 min. Triamterene was detected at 233 nm in UV. Using this method, retention of triamterene was approximately 5.5 min. Quantification was performed against a set of external standard solutions within the linear response concentration range. Samples were stored at 4°C.

The drug concentration of triclabendazole was determined with the following mobile phase: distilled water (bi distilled and filtered through 0.45 µm)/methanol/tetrahydrofuran 35/40/25 (V/V). Ammonium acetate with a concentration of 0.55 g/l was added to the mobile phase. pH-value at 25°C was 6.7. An isocratic method was used for quantification with a flow of 0.25 ml/min, an injection volume of 40 µl and a runtime of 8 min. Triclabendazole was detected at a wavelength of 305 nm. Using this method retention of triclabendazole was approximately 5.6 min. Quantification was performed against a set of external standard solutions within the linear response concentration range. To maintain the stability and reproducibility, the standard solutions contained the same amount of lipids as the samples. Lipid containing samples were diluted 1:10 with transport media before injection. Samples were stored at 4°C.

4.2.1.3 TEER Measurements

The integrity of the Caco-2 cell monolayer in the Transwell plates was ensured with the measurement of the trans-epithelial electrical resistance (TEER) before and after every transport study.

After washing the cell monolayer with 37°C tempered D- PBS (with Ca²⁺, Mg²⁺), 1600 µl transport medium was added into the apical and 2800 µl transport medium was added into the basal compartment. The Transwell plate was equilibrated for 60 min in the cell culture incubator before the pre-experimental measurement. The TEER was measured with an EVOM-G-Meter (EVOM-G-Meter Modell -24, World Precision Instruments, Berlin, Germany) equipped with an Endohm™ tissue resistance measurement chamber containing 4.6 ml tempered transport media (World Precision Instruments, Berlin, Germany). The measurement chamber was tempered to 37°C with transport medium before the measurement. For the post-experimental TEER measurement, the withdrawn volume in the apical compartment was replaced with transport medium before TEER was measured. Caco-2 monolayer exceeding TEER values of 250 Ωcm² were used for transport experiments.

4.2.1.4 Drug Permeation Across Caco-2 Cell Monolayers

Cells between culture days 19-23 at passage numbers 60-65 were used for the permeation studies. After the pre-experimental TEER measurement, the transport medium was removed from the donor compartment and replaced by the tempered (37°C) drug solutions. In the apical to basal direction,

1600 μl of the drug solution was added to the apical compartment whereas the basal compartment contained 2800 μl of transport media. In the basal to apical direction, the apical compartment contained 1600 μl transport media and 2800 μl of the drug formulation was added to the basal compartment. Triclabendazole was tested additionally as liposomal formulation. After the pre-experimental TEER measurement, transport medium was completely removed. In the apical to basal direction, 1600 μl drug formulation was added to the apical compartment and 2800 μl placebo formulation (same lipid concentration as donor) was added to the basal compartment. In the basal to apical direction, 1600 μl placebo formulation was added to the apical compartment and 2800 μl drug formulation was added to the basal compartment.

At least three wells were used for each direction. The Transwell plate was shaken at 37°C in a water saturated atmosphere under an incubator hood (KS15, Edmund Bühler GmbH, Tübingen & Hechingen, Germany) with a stirring rate of 75 rpm on an orbital shaker (KS15, Edmund Bühler GmbH, Tübingen & Hechingen, Germany). Permeation of drug across the cell monolayer was monitored by sampling the solutions in both compartments at predefined points of time during 5 h, which were 15, 30, 60, 90, 120, 180, and 300 min. The sample volume was 50 μl . The withdrawn volume was not replaced. The samples were collected in glass vials (Schmidlin Labor & Service AG, Sarbach, Switzerland) and stored at 4°C until the HPLC analysis was performed.

4.2.1.5 Data Analysis

The kinetic model describing cell permeation described by Kapitza et al. (115) was fitted to the time dependent concentration data with the software Easy Fit[®] to deduce parameters describing cell permeation. Easy Fit[®] deduced apparent permeability coefficient (P), carrier mediated efflux parameter (v_k), initial concentration in apical compartment in apical to basal direction (c_{0a_ab}), and initial concentration in basal compartment in basal to apical direction (c_{0b_ba}).

4.2.2 Results and Discussion

Table 7 gives an overview of the determined transport parameters out of the concentration versus time curves fitted by Easy Fit® using the kinetic model describing cell permeation described by Kapitza et al. (115). Albendazole showed high apparent permeability coefficients, equilibrium was reached after 90 min independent of drug concentrations and transport direction. No carrier mediated efflux was observed. Similar observations were made with carbamazepine. Albendazole and carbamazepine were not suitable as model compound because their membrane permeability was similar to progesterone and propranolol, which were model compounds for high membrane permeability.

Table 7 Kinetic parameters by fitting the concentration versus time profiles to the diffusion model with Easy Fit®. Abbreviations: P indicates apparent permeability coefficient, v_k carrier mediated efflux rate, C_{0a_AB} fitted apical concentration in apical to basal direction at $t=0$, C_{0b_BA} fitted basal concentration at $t=0$ in basal to apical direction.

Drug	Drug concentration [μM]	$P \cdot 10^5$ [cm/s]	v_k [nmol*cm ⁻² *min ⁻¹]	C_{0a_AB} [μM]	C_{0b_BA} [μM]
Albendazole	0.45	34.0	0.00027	0.61	0.52
	3.18	44.1	$1 \cdot 10^{-10}$	3.55	3.24
Bendroflumethiazide	4.6	8.33	0.01353	3.25	3.28
	31.8	5.31	0.06749	23.82	24.43
Carbamazepine	4.6	30.3	0.00512	30.58	29.88
	31.8	33.4	$1 \cdot 10^{-10}$	4.15	4.36
Proscillaridine	4.6	8.49	0.01847	4.27	4.1421
	31.8	8.03	0.13066	30.15	28.39
Triamterene	4.6	8.30	0.01073	4.79	4.41
	31.8	5.52	0.04651	32.14	30.59
Triclabendazole#	4.6	5.27	$1 \cdot 10^{-10}$	0.23600	0.61
	14.9	4.1	$1 \cdot 10^{-10}$	1.13	2.33
Triclabendazole liposomes (0.1 mg/ml lipid)	63	2.84	$1 \cdot 10^{-10}$	45.363	43.17
Triclabendazole liposomes (10 mg/ml lipid)	63	0.298	$1 \cdot 10^{-10}$	97.220	95.25

poor fitting quality due to high adsorption of triclabendazole to the Transwell surfaces.

For bendroflumethiazide, proscillaridine, and triamterene moderate to low passive permeability coefficients were obtained. These drugs showed asymmetric cell permeation because they were subject to carrier mediated apical efflux. For that reason they were not suitable as model drug. Triclabendazole permeation data suggested an apparent permeability coefficient that was one order of magnitude lower than the apparent permeability coefficients of chosen highly membrane permeable model drugs progesterone and propranolol, which attained an apparent permeability coefficient exceeding $1 \cdot 10^{-4}$ cm/s. No active carrier mediated efflux was observed. Cell permeation experiments

with aqueous solutions of triclabendazole showed a poor recovery because of extensive unspecific drug adsorption to the Transwell surface. In an additional experiment, where liposomes with low lipid phase concentrations were used, the unspecific adsorption of triclabendazole disappeared. Because of the disappearance of adsorption to the surfaces in presence of lipids, triclabendazole could be used to determine the influence of lipid containing drug formulations on passive permeation.

4.2.3 Conclusion

Despite the lack of reliable permeation data because of unspecific adsorption of aqueous triclabendazole to Transwell surface, triclabendazole was the most suitable drug inside the tested drugs. Triclabendazole exhibits poor water solubility, low cell membrane permeability, and no carrier mediated efflux. Because unspecific adsorption to Transwell surfaces disappears if transport media is supplemented with small amounts of phospholipids, triclabendazole is a suitable model drug to study the influence of different lipid formulations on the passive permeation of poorly water soluble drugs.

4.3 Screening of Different Emulsions and Microemulsions for their Suitability as Model Formulation

To determine the influence of lipid containing drug formulations on the permeability of lipophilic drugs, three structurally different formulations should be tested, which obtain ideally different microscopic structures. Besides of liposomes, which had been characterized already regarding cell toxicity and used for permeation studies through Caco-2 cell monolayer, and a microemulsion, that was characterized regarding cell toxicity on Caco-2 cells in previous work of our group, a third, structurally different lipid containing drug formulation had to be developed (115, 117). This formulation should consist of well characterized excipients regarding compatibility with the Caco-2 cell model. Cytotoxicity and influence on cell membrane of Caco-2 cell monolayer of Capmul MCM, Captex 8000, Cremophor EL, and ethanol had been determined in previous work. Cytotoxic effects of Capmul MCM had been shown exceeding concentrations of 0.02% (m/V) if used alone (117). Cremophor EL is known to inhibit unspecifically Pgp, the main efflux transporter in Caco-2 cells achieving carrier mediated efflux (94, 95, 120, 125, 139).

It was the aim of the following section to develop an emulsion consisting of these well characterized components, which is well tolerated by the Caco-2 cells. Because Capmul MCM and Cremophor EL are known to increase paracellular transport by tight junction modulation, cell permeation experiments were performed observing TEER and paracellular permeability using the paracellular marker compound fluoresceine.

4.3.1 Material

Fluoresceine sodium was purchased from SIGMA-Aldrich (Fluka Chemie GmbH, Buchs, Switzerland) and was of analytical grade. Captex 8000 was purchased from SIGMA-Aldrich (Fluka Chemie GmbH, Buchs, Switzerland). Capmul MCM was purchased from Abitec Corporation (Janesville, USA). Cremophor was ordered from Fluka (Fluka Chemie GmbH, Buchs, Switzerland). Transport media used for the permeation studies and the equilibrium dialysis experiments were prepared with Dulbecco's Modified Eagle's Medium (DMEM) base powder (without glucose, l-glutamine, phenol red, sodium pyruvate and sodium bicarbonate, purchased from SIGMA-Aldrich, Fluka Chemie GmbH, Buchs, Switzerland). DMEM base powder was dissolved in bi-distilled and autoclaved water and supplemented with glucose (4.5 g/l), HEPES (4.76 g/l), NaCl (1.987 g/l), and l-glutamine (0.876 g/l). The pH was adjusted to 7.4 and the final medium was filtered through a sterile filter (Supor-200, 0.2 µm pore size, Pall Corporation, Michigan, USA) under aseptic conditions. Glucose, HEPES, NaCl, and l-glutamine were purchased from SIGMA-Aldrich (Fluka Chemie GmbH, Buchs, Switzerland). Dulbecco's Phosphate Buffered Saline (D-PBS) (with Ca²⁺, Mg²⁺) was purchased from SIGMA-Aldrich (Fluka Chemie GmbH, Buchs, Switzerland).

4.3.2 Methods

4.3.2.1 Preparation of the Formulations

Lipid phases were prepared by melting the components at 37°C and mixing the components together. Lipid phase was warmed to 37°C before use and the according amount for the final formulation was balanced and mixed with two thirds of the final transport medium volume. The formulation was homogenized for 5 min at 15000 rpm with a Polytron homogenizer (Polytron PT 3000, Kinematica AG, Littau, Switzerland) then preheated transport medium was added to the final volume. The manufactured formulations were analyzed for physical stability over 24 h by examining the optical aspect and measuring particle size by PCS. No tendency for phase separation should be found after 24 h.

4.3.2.2 Particle Size Measurement

The particle size of the formulations was determined by dynamic light scattering. The z-average particle size of the emulsions and the microemulsions were measured with a Zetasizer Nano ZS ZEN 3600 (Malvern Instruments Ltd, Worcestershire, England) in disposable cuvettes (2.5 ml sample volume, Brand GmbH & Co, Wertheim, Germany) at 37°C. The resulting z-average diameter was the average out of 3 runs, consisting of 10 measurements each.

4.3.2.3 TEER Measurements

The integrity of the Caco-2 cell monolayer in the Transwell plates was ensured with the measurement of the trans-epithelial electrical resistance (TEER) before and after every transport study.

After washing the cell monolayer with 37°C tempered D- PBS (with Ca^{2+} , Mg^{2+}), 1600 μl transport medium was added into the apical and 2800 μl transport medium was added into the basal compartment. The Transwell plate was equilibrated 60 min in the cell culture incubator before the pre-experimental measurement. The TEER was measured with an EVOM-G-Meter (EVOM-G-Meter Modell -24, World Precision Instruments, Berlin, Germany) equipped with an Endohm™ tissue resistance measurement chamber containing 4.6 ml tempered transport media (World Precision Instruments, Berlin, Germany). The measurement chamber was tempered to 37°C with transport medium before the measurement. For the post-experimental TEER measurement, the withdrawn volume in the apical compartment was replaced with transport medium before TEER was measured. Caco-2 monolayer exceeding TEER values of $250 \Omega\text{cm}^2$ were used for transport experiments.

4.3.2.4 Determination of Transcellular Drug Permeation

Since it is known that nonionic surfactants like Cremophor EL were interacting with tight junctions of a cell monolayer, physically stable formulations were tested in transport experiments, where the cell monolayer integrity was indirectly determined by measuring the change of fluoresceine sodium permeability coefficient caused by the formulations compared to the permeability coefficient of aqueous fluoresceine solutions as reference. Fluoresceine is a hydrophilic marker compound for paracellular transport (98, 140). Additionally, TEER was measured before and after the experiment.

Decreased integrity of the cell monolayer is expressed as increased fluoresceine permeability coefficient and a decreased post- experimental TEER compared to aqueous transport media.

Cells between culture days 19-23 at passage numbers 60-65 were used for the permeation studies. After the pre-experimental TEER measurement, the transport medium was removed from the donor compartment and replaced by the tempered (37°C) drug solutions for the determination of cell permeation kinetics of the aqueous fluoresceine solutions. To determine the influence of the formulations, placebo formulations were pipetted after pre-experimental TEER measurement into Transwell, 1600 µl into the apical, 2800 µl to the basal compartment. Then, 30.1 µl ethanolic fluoresceine sodium stock solution (concentration 2 mg/ml) was added into apical compartment (apical to basal direction) and 52.6 µl to basal compartment (basal to apical direction). The resulting Fluoresceine concentration in the donor compartment was 100 µM. At least three wells were used for each direction. The Transwell plate was shaken at 37°C in a water saturated atmosphere under an incubator hood (KS15, Edmund Bühler GmbH, Tübingen& Hechingen, Germany) with a stirring rate of 75 rpm on an orbital shaker (KS15, Edmund Bühler GmbH, Tübingen& Hechingen, Germany). Permeation of drug across the cell monolayer was monitored by sampling the solutions in both compartments at predefined points of time during 5 h, which were 15, 30, 60, 90, 120, 180, and 300 min. The sample volume was 50 µl. The withdrawn volume was not replaced. Lipid containing samples were diluted 1:10 with transport medium. The samples were collected in glass vials (Schmidlin Labor& Service AG, Sarbach, Switzerland) and stored at 4°C until the HPLC analysis was performed.

4.3.2.5 Fluoresceine Quantification

The drug concentration of sodium fluoresceine was determined by HPLC-UV (Agilent series 1100, Agilent Technologies USA, equipped with a capillary pump G1376A, an auto sampler G1377AµWPS and a variable wavelength detector G1314a). A C-18 reversed phase column was used (CC 125/2 Lichrospher 100 RP 18 ec, Macherey Nagel, Oensingen, Switzerland) with the following mobile phase: distilled water (bi-distilled and filtered through 0.45 µm)/methanol 60/40 (V/V). Ammonium acetate with a concentration of 0.55 g/l was added to the mobile phase. pH-value at 25°C was 6.85. An isocratic method was used for quantification with a flow of 0.2 ml/min, an injection volume of 40 µl and a runtime of 6 min. Sodium fluoresceine was detected at 475 nm in UV. Using this method, retention of sodium fluoresceine was approximately 4.5 min. Quantification was performed against a set of external standard solutions within the linear response concentration range. Samples were stored at 4°C.

4.3.2.6 Data Analysis

The kinetic model describing cell permeation described by Kapitza et al. (115) was fitted to the time dependent concentration data with the software Easy Fit[®] to deduce parameters describing cell permeation. Easy Fit[®] deduced apparent permeability coefficient (P), carrier mediated efflux parameter (v_k), initial concentration in apical compartment in apical to basal direction (C_{0a_AB}), and initial concentration in basal compartment in basal to apical direction (C_{0b_BA}).

4.3.3 Results and Discussion

Table 8 shows the composition of the tested lipid phases and the results of the stability examinations of the tested formulations.

Table 8 Lipid phase composition of screened formulations and the stability of the resulting formulations with transport media over 24 h. All formulations were manufactured containing 10 mg/ml lipid phase with transport media as aqueous phase.

Composition of the lipid phase				Mean		
Capmul MCM	Captex 8000	Cremophor EL	Ethanol	particle	t=0	
[%m/m]	[%m/m]	[%m/m]	[%m/m]	size		Optical aspect after 24h
				[nm]		
5.0	49	36	10	181		opalescent, homogenous
8.5	45.5	36.0	10	121		opalescent, homogenous
0.0	52.63	36.84	10.53	n.d.		milky, phase separation
0.0	80.0	15.0	5.0	n.d.		turbid, phase separation
15.0	50.0	35.0	0.0	n.d.		opalescent, homogenous
10.0	80.0	10.0	0.0	n.d.		turbid, phase separation
8.5	63.5	18.0	10.0	189		turbid, homogenous
5.0	67.0	18.0	10.0	172		turbid, homogenous
0.0	70.0	20.0	10.0	323		turbid, phase separation
5.0	65.0	20.0	10.0	173		turbid, homogenous
3.0	72.0	15.0	10.0	282		turbid, homogenous

Since it is known that mono- and diglycerides such as Capmul MCM and nonionic surfactants such as Cremophor EL interact with the tight junctions of a cell monolayer, formulations that were physically stable for at least 24 h and contain as low Capmul MCM and Cremophor EL concentrations as possible were tested in transport experiments. Cell monolayer integrity was tested with the hydrophilic paracellular transport marker fluoresceine sodium and by monitoring the TEER. Table 9 gives an overview of the results.

Table 9 Test of physically stable formulations on their influence on Caco-2 cell monolayer integrity. The formulations contained 100 μ M fluoresceine sodium.

Lipid phase composition [% ^m / _m]	Lipid phase concentration [mg/ml]	TEER before experiment [Ohm*cm ⁻²]	TEER after 300 min [Ohm*cm ⁻²]	Decrease of TEER over 300 min [%]	Fluoresceine P _{app} [*10 ⁻⁶ cm ² /s]
Fluoresceine in Transport Media	0	644.36	535.80	16.85	2.0
Capmul MCM 5%, Captex 8000 67%, Cremophor EL 18%, Ethanol 10%	0.5 1 5	427.70 436.32 432.40	310.20 223.25 209.93	27.47 48.83 51.45	1.10 2.60 2.80
Capmul MCM 8.5%, Captex 8000 45.5%, Cremophor EL 36%, Ethanol 10%	0.5 1 5	472.35 484.10 488.80	263.20 169.20 195.05	44.28 65.05 60.10	2.39 3.25# 5.19#
Capmul MCM 5%, Captex 8000 49%, Cremophor EL 36%, Ethanol 10%	0.5 1 5	481.75 460.60 470.00	274.95 180.95 162.15	42.93 60.71 65.50	1.34 5.05# 6.73#
Capmul MCM 3%, Captex 8000 72%, Cremophor EL 15%, Ethanol 10%	0.5 1 5	462.95 439.45 427.70	249.10 272.60 251.45	46.19 37.97 41.21	1.95* 3.58* 1.31*

Cell monolayer detached from the filter of the Transwell insert, * Phase separation after 5 h

The results of the fluoresceine permeation studies indicated the suitability of a lipid phase consisting of 5%^(m/m) Capmul, 67%^(m/m) Captex, 18%^(m/m) Cremophor, and 10%^(m/m) ethanol to act as a model formulation. Different concentrations of this lipid phase were mixed with transport media resulting in an emulsion that was physically stable for at least 24 h and had a low influence on the integrity of the Caco-2 cell monolayer. The permeability coefficient of fluoresceine in this formulation was in the same range as for the reference fluoresceine solution. The decrease of TEER value was bigger than the decrease induced by the lipid phase consisting of 3%^(m/m) Capmul, 72%^(m/m) Captex, 15%^(m/m) Cremophor, and 10%^(m/m) ethanol, but the formulations of this lipid phase showed phase separation after 5 h. All other lipid phases were not compatible with the Caco-2 cell monolayer, which was indicated by detached cell monolayer after 300 min incubation. This progressive damage of the cell monolayer was additionally shown as increased fluoresceine permeation.

4.3.4 Conclusions

A lipid phase consisting of 5%^(m/m) Capmul, 67%^(m/m) Captex, 18%^(m/m) Cremophor, and 10%^(m/m) ethanol, resulting in a stable emulsion with a mean droplet size of around 170 nm in transport media,

does increase fluoresceine permeability only slightly. It lowers the TEER dose dependent but in all cases not below the limit of $200 \text{ Ohm} \cdot \text{cm}^{-2}$ over 5 h. This emulsion is the most suitable emulsion-like formulation for the determination of the influence of structurally different formulations on the permeation of lipophilic drugs. An additional validation of the influence of the emulsion and the microemulsion on time and lipid phase concentration dependent decrease of the monolayer integrity was necessary to ensure optimal experimental conditions (see next chapter).

4.4 Maintaining TEER over Time of the Chosen Formulations: Determination of Duration of Transport Experiments

It was observed that different lipid containing drug formulations containing Captex 8000, Capmul MCM, Cremophor EL, and ethanol, decrease the cell monolayer integrity. An optimal experimental procedure had to be found to use these formulations for cell permeation experiments. Observations during formulation screening experiments indicated that the cells tolerated lipid phase concentrations up to 5 mg/ml for up to 3 h well. But after 5 h, depending on the formulation, detached cell monolayer were observed. To assure the cell monolayer integrity during incubation of the cell monolayer with the chosen formulations, TEER was observed over 5 h. This procedure was not necessary for the liposomes, because no effect of the liposomes on the cell monolayer integrity was observed up to 50 mg/ml phospholipids in previous work (115).

4.4.1 Material and Methods

4.4.1.1 Material

Captex 8000 was purchased from SIGMA-Aldrich (Fluka Chemie GmbH, Buchs, Switzerland). Capmul MCM was purchased from Abitec Corporation (Janesville, USA). Cremophor was ordered from Fluka (Fluka Chemie GmbH, Buchs, Switzerland). Transport media used for the permeation studies and the equilibrium dialysis experiments were prepared with Dulbecco's Modified Eagle's Medium (DMEM) base powder (without glucose, l-glutamine, phenol red, sodium pyruvate and sodium bicarbonate, purchased from SIGMA-Aldrich, Fluka Chemie GmbH, Buchs, Switzerland). DMEM base powder was dissolved in bi-distilled and autoclaved water and supplemented with glucose (4.5 g/l), HEPES (4.76 g/l), NaCl (1.987 g/l), and l-glutamine (0.876 g/l). The pH was adjusted to 7.4 and the final medium was filtered through a sterile filter (Supor-200, 0.2 µm pore size, Pall Corporation, Michigan, USA) under aseptic conditions. Glucose, HEPES, NaCl, and l-glutamine were purchased from SIGMA-Aldrich (Fluka Chemie GmbH, Buchs, Switzerland). Dulbecco's Phosphate Buffered Saline (D-PBS) (with Ca²⁺, Mg²⁺) was purchased from SIGMA-Aldrich (Fluka Chemie GmbH, Buchs, Switzerland).

4.4.1.2 Preparation of Emulsions and Microemulsions

Microemulsions containing 1 mg/ml and 5 mg/ml lipid phase (lipid phase consisting of 17.58%^[m/m], Capmul, 35.05%^[m/m] Captex, 36.84%^[m/m] Cremophor, and 10%^[m/m] ethanol) and emulsions containing 1 mg/ml and 5 mg/ml lipid phase (lipid phase consisting of 5%^[m/m] Capmul, 67%^[m/m] Captex, 18%^[m/m] Cremophor, and 10%^[m/m] ethanol) were tested. The lipid phases were prepared by mixing the components at 37°C. The lipid phases were stored at 4°C. Lipid phase was warmed up to 37°C before use and the according amount was balanced and mixed with two thirds of the final transport medium volume. This crude formulation was homogenized for 5 min at 15000 rpm with a Polytron homogenizer (Polytron PT 3000, Kinematica AG, Littau, Switzerland) then preheated transport medium was added to the final volume.

4.4.1.3 TEER Measurements

The time dependent integrity of the Caco-2 cell monolayer in the Transwell plates was ensured with the measurement of the trans-epithelial electrical resistance (TEER). After washing the cell monolayer with 37°C tempered D-PBS (with Ca^{2+} , Mg^{2+}), 1600 μl transport medium was added into the apical and 2800 μl transport medium was added into the basal compartment. The Transwell plate was equilibrated 60 min in the cell culture incubator before the pre-experimental measurement. The TEER was measured with an EVOM-G-Meter (EVOM-G-Meter Modell -24, World Precision Instruments, Berlin, Germany) equipped with an Endohm™ tissue resistance measurement chamber (World Precision Instruments, Berlin, Germany) containing 4.6 ml tempered transport media. The measurement chamber was tempered to 37°C with transport medium before the measurement. After the pre experimental TEER measurement transport media was removed and the formulations were pipetted into the Transwell plates (3 well each). The Transwell plates were put on an orbital shaker (KS15, Edmund Bühler GmbH, Tübingen & Hechingen, Germany) with a stirring rate of 75 rpm under water saturated atmosphere at 37°C using an incubator hood (KS15, Edmund Bühler GmbH, Tübingen & Hechingen, Germany). TEER was monitored in intervals of 30 min during 300 min.

4.4.2 Results

TEER measurements during 300 min of the emulsion showed an initial decrease of the TEER. After 60 min TEER was stabilized and remained constant, which is shown in Figure 28. No difference between the different lipid phase concentrations was observed. The TEER obtained after 300 min incubation indicates for both of the tested lipid concentrations an intact cell monolayer.

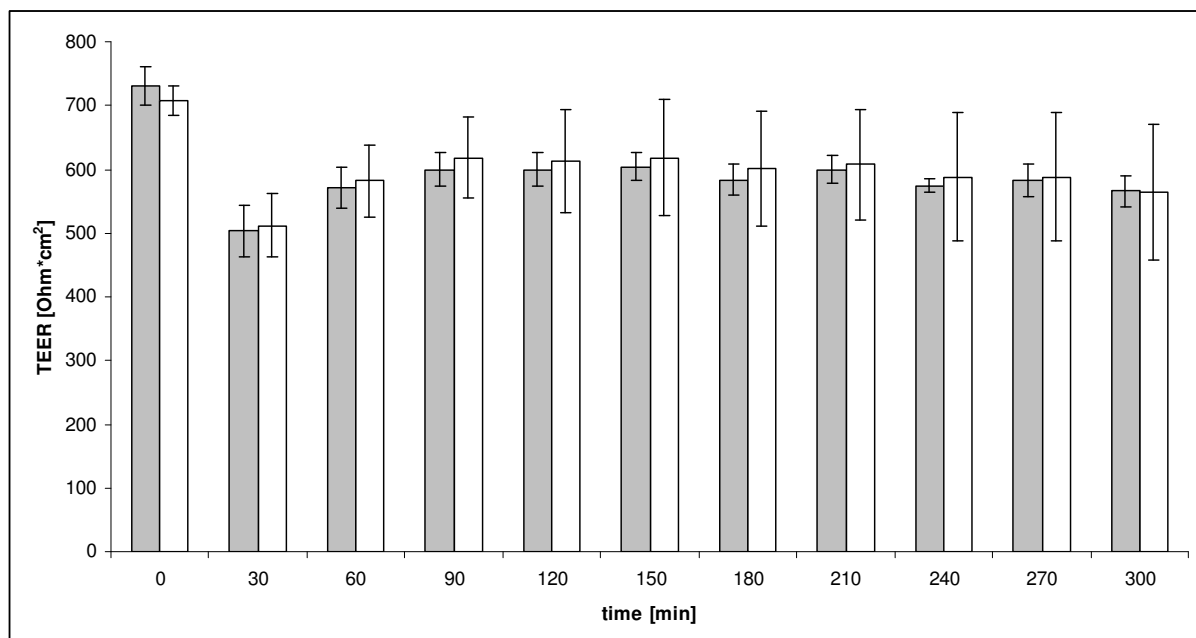


Figure 28 Influence of two different lipid phase concentrations of the emulsion formulation on TEER over 300 min. Legend: closed bars: 1 mg/ml lipid phase, open bars: 5 mg/ml lipid phase.

The observed behavior of the microemulsion containing 1 mg/ml lipid phase was comparable to the TEER progression of the emulsions. In contrast to that, the microemulsion containing 5 mg/ml lipid phase causes a continuous TEER decrease over time (see Figure 29). This indicates progressive and

time dependent damage of the cell monolayer. In this experiment, the initial TEER was $681.1 \pm 4.7 \text{ Ohm} \cdot \text{cm}^2$ and the TEER after 300 min was $306.7 \pm 46.6 \text{ Ohm} \cdot \text{cm}^2$, which corresponds to a TEER decrease of 55%. In this particular experiment, cell monolayer integrity after 300 min was still ensured, since a limit of $200 \text{ Ohm} \cdot \text{cm}^2$ is defined in literature for an intact Caco-2 cell monolayer (141). Taking into account that in this particular experiment initial TEER was slightly higher than the average initial TEER in our lab (see Appendix), cell monolayer integrity during transport experiments would be compromised under average or slightly lower initial TEER. A moderate TEER decrease down to 60% of the initial value was determined after 180 min, which would assure intact cell monolayer with average or slightly lower initial TEER during cell permeation experiment if cell permeation experiments are shortened to 180 min by the use of microemulsions containing 5 mg/ml lipid phase.

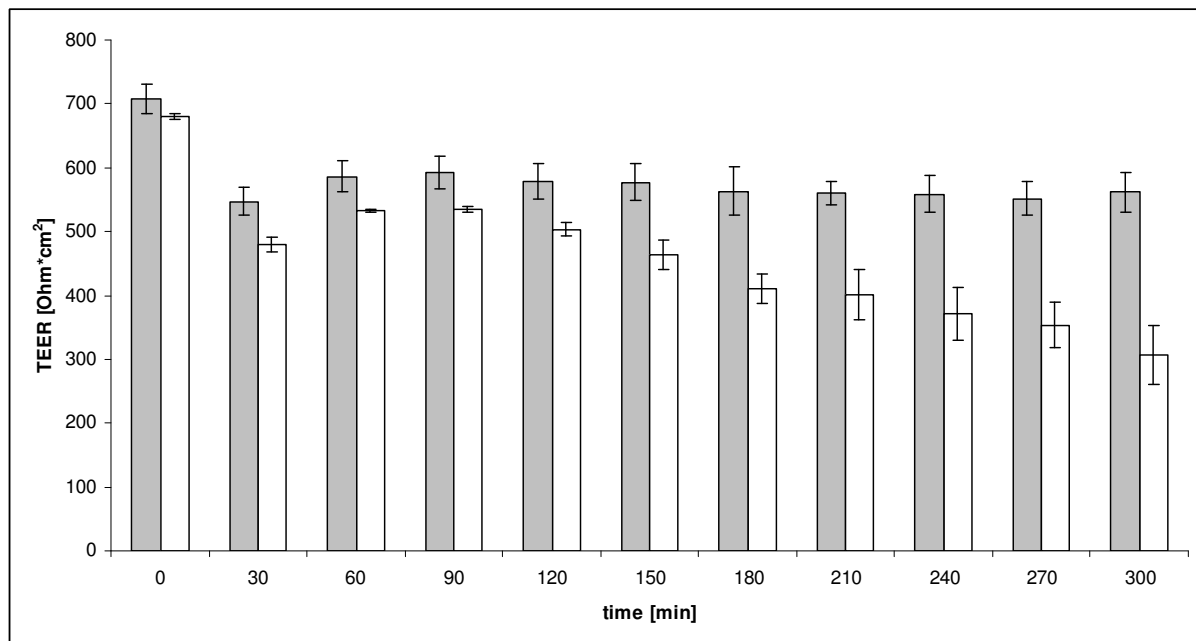


Figure 29 Influence of two different lipid phase concentrations of the microemulsion formulation on TEER over 300 min. Legend: closed bars: 1 mg/ml lipid phase, open bars: 5 mg/ml lipid phase.

4.4.3 Conclusions

The cell monolayer integrity is ensured during 300 min of cell monolayer incubation with emulsions containing 1 mg/ml and 5 mg/ml lipid phase and a microemulsion containing 1 mg/ml lipid phase. In a singular experiment, it was shown that the monolayer integrity of the microemulsion containing 5 mg/ml lipid phase was still maintained after 300 min incubation. But TEER decrease of 55% was indicating a strong interference of the formulation with the barrier function of the cell monolayer. To assure monolayer integrity during transport experiments the transport experiments of microemulsions with 5 mg/ml lipid phase were shortened to 180 min.

4.5 Development of a Method to Determine the Free Fraction of a Drug Formulation Containing Lipids

It was essential to have knowledge about the free fraction of the drug in the different formulations for a deeper understanding of the results of the transport experiments. The development of a method to determine the free amount of drug in lipid containing dosage forms like liposomes, microemulsions and emulsions is described in this chapter. Three different approaches for the determination of unbound drug concentration were evaluated. Ultrafiltration using centrifugal filter devices was evaluated as fast technique for the separation of lipid particles and aqueous phase. As second method, ultracentrifugation was evaluated, which allows fast separation of constituents with different densities and is used for the phase separation of semisolid dosage forms. This method would allow direct measurement of unbound drug concentration in the aqueous phase too. The third method, which was evaluated, was equilibrium dialysis. This time consuming method allows indirectly calculation of the drug concentration in the water phase of a formulation via the determination of the lipid water partition coefficient. It allows the calculation of the free fraction of a drug in a formulation.

4.5.1 Material and Methods

4.5.1.1 Material

Lipoid S 100 and Lipoid EPG were kindly provided by Lipoid GmbH (Ludwigshafen, Germany). Saquinavir was a kindly provided by Roche (Roche Pharmaceuticals, Basel, Switzerland). Progesterone, Captex 8000, and Cremophor EL were purchased from Fluka (SIGMA-Aldrich, Fluka Chemie GmbH, Buchs, Switzerland). Capmul MCM was purchased from Abitec (Abitec Corp., Janesville, WI, USA). Transport media used as buffer were made with Dulbecco's modified Eagle's medium (DMEM) base (without glucose, l-glutamine, phenol red, sodium pyruvate and sodium bicarbonate) (SIGMA-Aldrich, Fluka Chemie GmbH, Buchs, Switzerland). This was dissolved in bi-distilled and autoclaved water and supplemented with glucose (4.5 g/l), HEPES (4.76 g/l), NaCl (1.987 g/l) and l-glutamine (0.876 g/l), the pH was adjusted to 7.40 and the final medium was subjected to sterile filtration and 0.5%(m/V) sodium azide was added as antimicrobial preservative. Glucose, HEPES, NaCl, sodium azide, and l-glutamine were all obtained from SIGMA-Aldrich (Fluka Chemie GmbH, Buchs, Switzerland). All other reagents were of analytical grade.

4.5.1.2 Preparation of Liposomes

Lipoid S100, EPG and the drug were dissolved in ethanol in a round bottomed flask. The solvent was evaporated to dryness and the lipid film was kept under vacuum for 30 min to eliminate solvent traces. The lipid film was suspended with 20 ml of tempered transport medium. The suspension was extruded under nitrogen pressure with a filter candle through polycarbonate filters (Nucleopore track edge membrane filters, Whatman plc, Kent, UK) with descending pore sizes in the following scheme:

2 x 0.4 μm , 5 x 0.2 μm 20 x 0.1 μm . The liposomes were analyzed with dynamic light scattering for particle size (see below).

4.5.1.3 Preparation of Microemulsions

The components of the lipid phase (Captex 8000 35.05% [m/m], Capmul MCM 17.58% [m/m], Cremophor EL 36.84% [m/m], and ethanol 10% [m/m]) were mixed at 37°C. The lipid phase was stored at 4°C. Before use, the lipid phase was warmed to 37°C and the according amount was balanced and mixed with transport medium. The formulation was homogenized for 5 min at 15000 rpm with a Polytron homogenizer (Polytron PT 3000, Kinematica AG, Littau, Switzerland). The formulations were analyzed with dynamic light scattering for particle size.

4.5.1.4 Particle Size

The particle size of the formulations was measured by dynamic light scattering. The z-average diameter of the formulations were determined with a Zetasizer 1000HSA (Malvern Instruments Ltd, Worcestershire, England) equipped with a 100 nm lens in disposable cuvettes (2 ml size, Greiner Labortechnik, Kremsmünster, Austria) at 25°C. Samples were diluted with sterile filtered transport media (0.2 μm) until counting rates between 100 and 300 KCts/s were reached. The resulting z-average diameter was the average out of 5 runs, consisting of 10 measurements each.

4.5.1.5 Ultrafiltration

Centrifugal filter devices with a molecular weight cut off of 3000 D, 100000 D (Microcon YM3, Millipore, Bedford, MA, USA), and 30000 D (Ultrafree- 0.5 centrifugal filter NMWL Membrane, Tube Biomax, Millipore, Bedford, MA, USA) were used. After pipetting 1 ml of the formulation, the filter devices were spun for 30 min at 14000 rpm with an Eppendorf centrifuge (5415C, Eppendorf / Dr. Vaudaux AG, Schönenbuch, Switzerland). This method allows a direct measurement of the free drug. Therefore, the filtrate was injected into the HPLC for determination of drug content.

4.5.1.6 Ultracentrifugation

The formulations were fractionated by ultracentrifugation using an ultracentrifuge type Centricon T-1075 and a rotor TFT 7013 (Kontron Instruments, Mailand, Italy). Quick-Seal centrifuge tubes, 5/8X3 (Beckman Instruments, Palo Alto, USA) were used. The formulations were centrifuged at 37°C for 2 and 4 h at 450000 g. The clear water phase was carefully removed by a syringe and analyzed with HPLC for determination of drug concentration. This drug concentration represents the free drug concentration.

4.5.1.7 Equilibrium Dialysis

The formulations were dialyzed with horizontal diffusion cells consisting of glass with a chamber volume of 10 ml and a membrane surface of approximately 2 cm². The chambers were separated by the following membranes: SpectraPor® 7 regenerated cellulose membranes with a molecular weight cut off of 50000 D, 2000 D (Spectrum Labs, DG Breda, Netherlands), and Membracell MD 34-14 (Amersham, Uppsala, Sweden) with a molecular weight cut off of 34000 D. To maintain a temperature

of 37°C, a water bath was used. The solutions in the cells were stirred at 1000 rpm with Teflon-paddles driven by a stirring device (Janke & Kunkel RE162, IKA Labortechnik, Staufen, Germany). The formulations were dialyzed for at least 34-48 h until equilibrium was reached. The samples were analyzed with HPLC. To avoid microbial contamination, resulting in a potential degradation of the drug or the formulation, 0.5% (^m/_v) sodium azide was added to the transport media and the formulations. The method does not allow measuring directly the unbound amount of drug, because the total volume of the water phase changes. The partition between the lipid particles and the water phase was calculated using Equation 49.

$$z = \frac{c_w}{c_{tot}}$$

Equation 49

Free fraction of drug is denoted by z , c_w indicates equilibrium concentration of drug in water phase (acceptor concentration) [mg/ml], and c_{tot} indicates total equilibrium concentration of drug (donor concentration) [mg/ml]

4.5.1.8 Drug Quantification

The drug concentration of progesterone and saquinavir was determined by HPLC-UV (Agilent series 1100, Agilent Technologies USA, equipped with a G1312A binary pump, an auto sampler G1367B and a variable wavelength detector G1314B). A C-18 reversed phase column was used (CC 125/2 Lichrospher 100 RP 18 ec, Macherey Nagel, Oensingen, Switzerland) with the following mobile phase for progesterone: distilled water (bi-distilled and filtered through 0.45 μ m)/methanol/tetrahydrofuran 40/45/15 (^V/_v). Ammonium acetate with a concentration of 0.55 g/l was added to the mobile phase. The pH-value at 25°C was 6.9. For saquinavir the following mobile phase was used: distilled water (bi-distilled and filtered through 0.45 μ m)/methanol/tetrahydrofuran 35/50/15 (^V/_v). Ammonium acetate with a concentration of 0.55 g/l was added to the mobile phase. The pH-value at 25°C was 7.0. An isocratic method was used for quantification with a flow of 0.25 ml/min, an injection volume of 100 μ l and a runtime of 8 min. Progesterone and saquinavir were detected at 239 nm in UV. Using this methods, retention of progesterone was approximately 5 min, retention of saquinavir was approximately 7 min. Quantification was performed against a set of external standard solutions within the linear response concentration range. Lipid containing samples were diluted 1:10 with transport media before injection.

4.5.2 Results and Discussion

4.5.2.1 Ultrafiltration

After the centrifugation of liposomes, containing saquinavir (2.2 mg/ml), Lipoid S100 (50 mg/ml), and Lipoid EPG (0.22 mg/ml), the centrifugate was clear and no particles were detected with dynamic light scattering, whereas liposomes had a particle size of approximately 140 nm. As control, a solution containing saquinavir (10 μ g/ml) was ultrafiltrated. The drug concentration of the clear filtrates and the control solution was determined by HPLC (Table 10).

Table 10 Saquinavir concentrations after ultrafiltration of liposomes (containing saquinavir [2.2 mg/ml], Lipoid S100 [50 mg/ml], and Lipoid EPG [0.22 mg/ml]) and a control solution (containing 10 µg/ml saquinavir). Supernatant is denoted by s, filtrate by f, and recovery by rec.

	Saquinavir concentration [mg/ml] before ultrafiltration			Saquinavir concentration after ultrafiltration with Microcon YM3, Cut off 3000			Saquinavir concentration after ultrafiltration with Ultrafree Membrane, Cut off 30000 [mg/ml]			
	s	f	rec	s	f	rec	s	f	rec	
Liposomes	2.2	1.44	#	65%	1.44	#	65%	1.8	#	85%
Solution	0.01	n.d.	#	-	n.d.	#	-	n.d.	#	-

#: below detection limit, n.d. not determined

None of the filtrates contained a measurable amount of saquinavir. While the cut off of the membranes was 50 to 500 times higher than the molecular weight, saquinavir was not able to pass the membranes. Due to the low recovery of the formulations, we assume that the lipophilic saquinavir adsorbed to the filter membranes or the filtration devices. For the determination of free drug concentration of highly lipophilic molecules, ultrafiltration is not suitable.

4.5.2.2 Ultracentrifugation

After 2 h of centrifugation of saquinavir liposomes, a gradient over the whole tube was visible but there was no clear phase separation. Centrifugation for 4 h resulted in two separated phases containing of a clear water phase on the top and a liposome pellet on the bottom of the centrifugation tube. No particles were detected with PCS in the clear water phase. The results of the saquinavir quantification of the clear water phase by HPLC are displayed in Table 11.

Table 11 Saquinavir quantification in the clear water phase after ultracentrifugation of liposomes (containing saquinavir [concentrations listed in table], Lipoid S100 [50 mg/ml], and Lipoid EPG [0.22 mg/ml]) for 4 h at 450000 g.

Total saquinavir concentration [mg/ml]	Saquinavir concentration in the water phase [µg/ml]	Number of measurements
2.2	19.3 ± 13.1	5
4.5	23.7 ± 20.7	7
7.5	12.8 ± 8.8	5

The results were in the expected order of magnitude but the expected correlation of the lowest to the highest saquinavir concentration was not found. Together with the poor reproducibility, expressed in the high standard deviation, it was concluded that the used ultracentrifugation method is not a suitable method to determine the amount of a highly lipophilic drug in the water phase.

4.5.2.3 Equilibrium Dialysis

We evaluated three different membranes on the permeation of saquinavir dissolved in transport media. Saquinavir was taken for this evaluation because it achieves the highest molecular mass out of the model compounds, which was expected to be responsible for slowest permeation through dialysis membrane. Three different dialysis membranes were compared, all of them consisting of hydrophilic material (regenerated cellulose in the case of 34000 D and 50000 D and of cellulose ester in the case of 2000 D) to avoid adsorption of lipophilic drug molecules. Dialysis was performed during 30-50 h. Figure 30 shows the resulting concentration versus time profiles. It indicates that the 2000 D membrane is not applicable for the chosen conditions. For further experiments, the Spectra/por 50000 D membrane was preferred because it showed a higher drug permeation resulting in shorter time for equilibration.

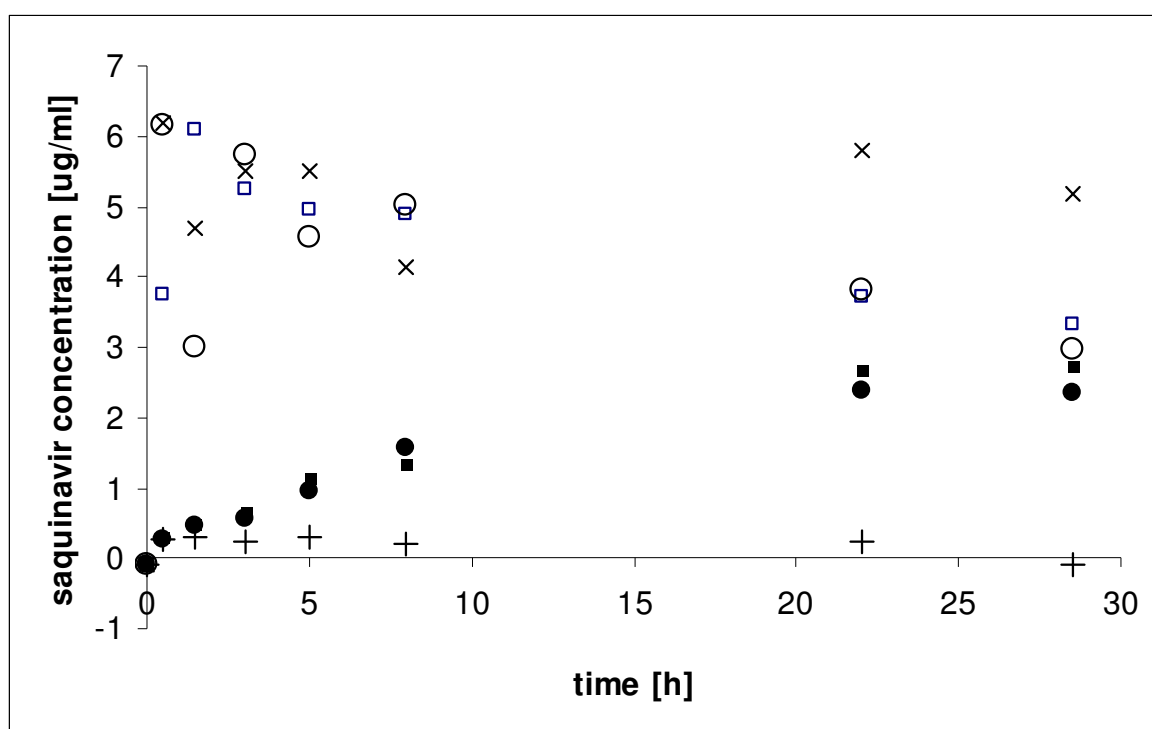


Figure 30 Dialysis of a saquinavir solution containing saquinavir (7.5 $\mu\text{g/ml}$) in transport media at 37°C. Comparison of three different dialysis membranes. Legend: donor compartment with the MembraCell membrane (○), acceptor compartment with the MembraCell membrane (●), donor compartment with the 50000 D membrane (□), acceptor compartment with the 50000 D membrane (■), donor compartment with the 2000 D membrane (x), acceptor compartment with the 2000 D membrane (+).

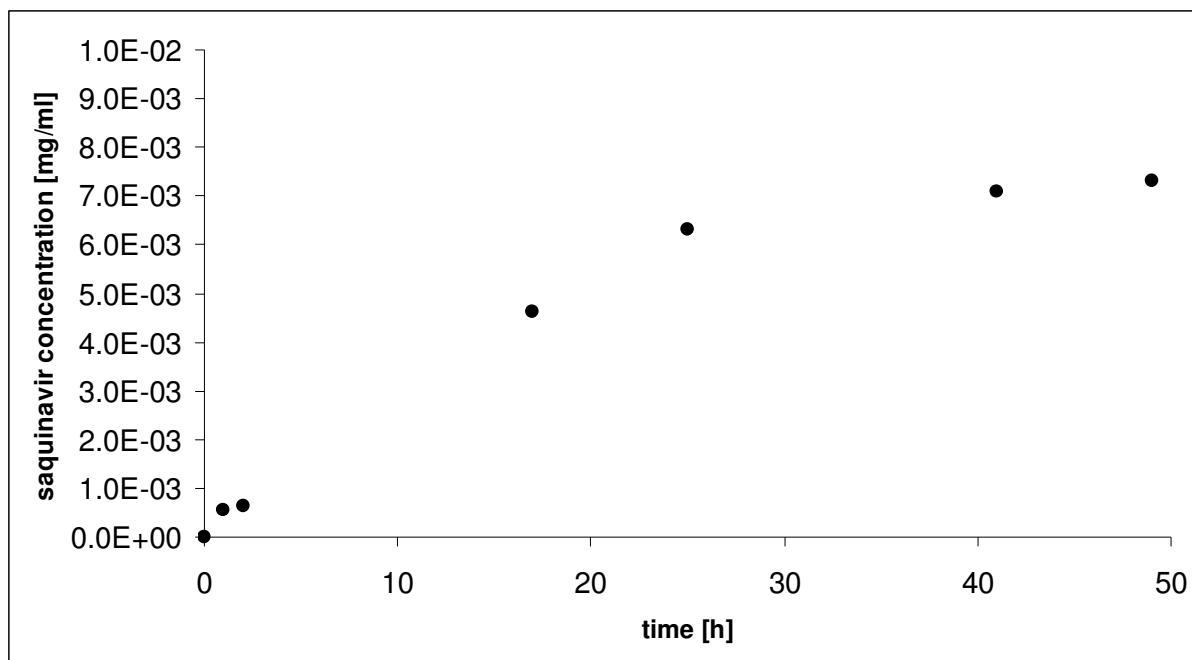


Figure 31 Concentration curve of the acceptor compartment of an equilibrium dialysis of liposomes, containing saquinavir (7.5 mg/ml), Lipoid S100 (50 mg/ml), and Lipoid EPG (0.22 mg/ml). A SpectraPor® 7 regenerated cellulose membrane with a cutoff of 50000 D was used.

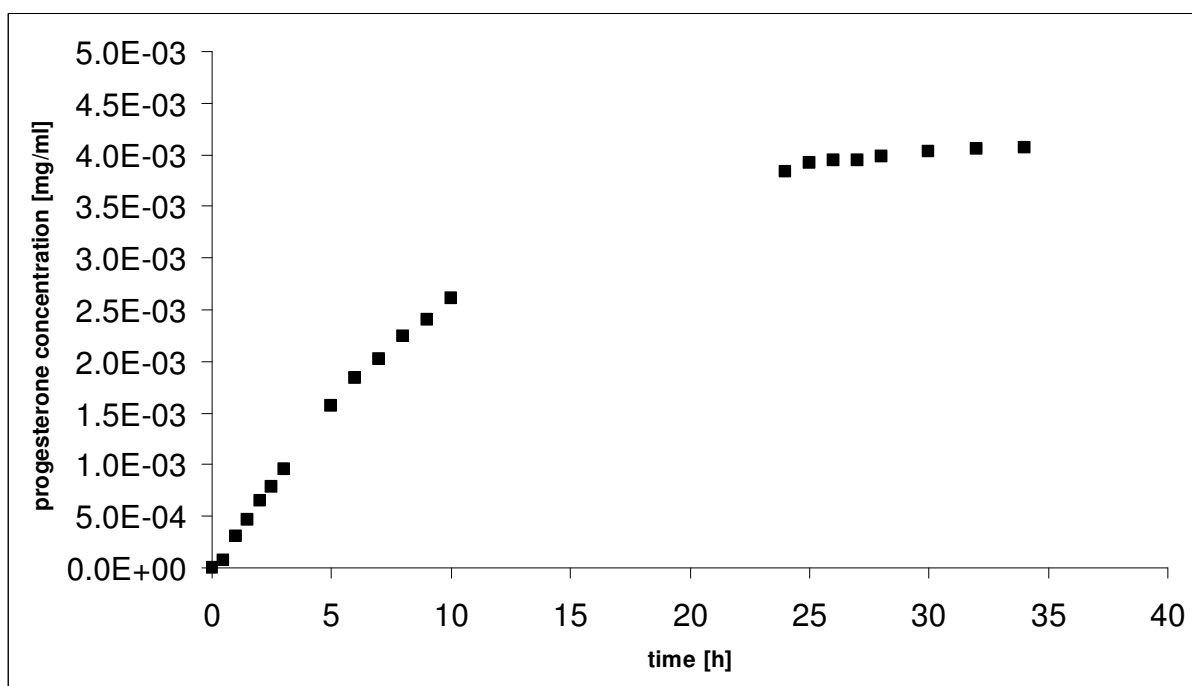


Figure 32 Concentration curve of the acceptor compartment of an equilibrium dialysis of liposomes, containing progesterone (0.5 mg/ml), Lipoid S100 (50 mg/ml), and Lipoid EPG (0.05 mg/ml). A SpectraPor® 7 regenerated cellulose membrane with a cutoff of 50000 D was used.

The method was tested with saquinavir liposomes, containing saquinavir (7.5 mg/ml), Lipoid S100 (50 mg/ml), and Lipoid EPG (0.22 mg/ml) and proven with progesterone liposomes, containing progesterone (0.5 mg/ml), Lipoid S100 (50 mg/ml), and Lipoid EPG (0.05 mg/ml). After 48 h the saquinavir formulation was nearly in equilibrium. The resulting time concentration curve of the

acceptor compartment is shown in Figure 31. The resulting time concentration curve of the acceptor compartment of the progesterone formulation dialysis is displayed in Figure 32. Equilibrium conditions of the progesterone formulation dialysis were reached faster than of the saquinavir formulation. Because of the smaller molecular weight of progesterone, faster membrane permeation was expected. The equilibrium dialysis of lipophilic drugs in liposomes is a suitable method to characterize these drug delivery systems.

Phospholipids are insoluble in aqueous media, no unbound phospholipids are available to pass the dialysis membrane. Compared to liposomes, in emulsions and microemulsions free surfactant molecules were expected in solution and therefore able to cross the dialysis membrane. Cremophor EL (Molecular weight 2515 D, from ref. (120)) is able to cross a 50000 D dialysis membrane, but not a dialysis membrane with a cut off of 2000 D. Therefore, we dialyzed a progesterone microemulsion containing progesterone (0.01 mg/ml) and 5 mg/ml lipid phase with a 2000 D and a 50000 D membrane. Progesterone was chosen because of its small molecular weight and because saquinavir showed no reproducible data when a saquinavir solution was dialyzed with the 2000 D membrane (see Figure 30).

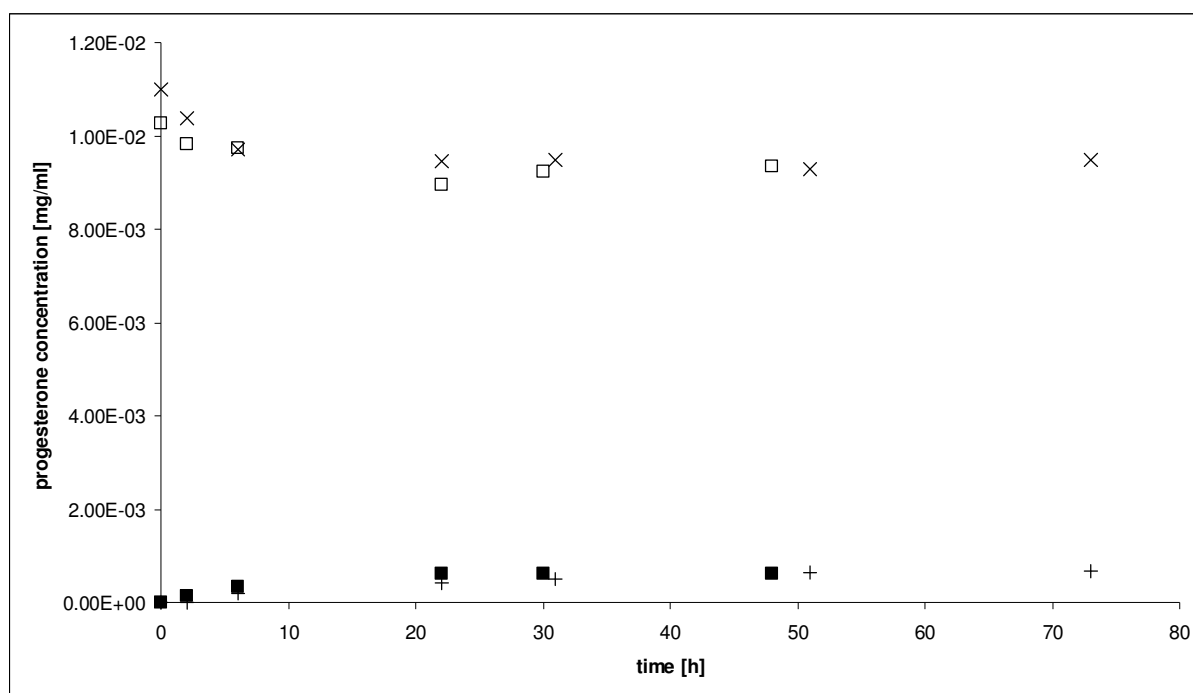


Figure 33 Comparison of two different dialysis membranes on the dialysis of progesterone microemulsion containing progesterone (0.01 mg/ml) and 5 mg/ml lipid phase (Captex 8000 35.05% [m/m], Capmul MCM 17.58% [m/m] Cremophor EL 36.84% [m/m], and ethanol 10% [m/m]) at 37°C. Legend: donor compartment with the 50000 D membrane (□), acceptor compartment with the 50000 D membrane (■), donor compartment with the 2000 D membrane (x), acceptor compartment with the 2000 D membrane (+).

The overlay of the resulting concentration versus time profiles is displayed in Figure 33. Time needed for the system to equilibrate was different, 30 h with the 50000 D membrane and 50 h with the 2000 D membrane. The measured unbound drug concentration in equilibrium was the same, which indicates that there were no Cremophor EL molecules present in the acceptor or at least that the amount was too small to have a measurable effect on the solubility of the drug in the water phase. This suggestion

is supported by recently published findings of Mahler et al. where a polysorbate 20 containing protein formulation was dialyzed. It was concluded that polysorbate 20, that has similar properties as Cremophor EL, could not be significantly reduced by dialysis (142).

Table 12 displays the calculated free fractions of progesterone and saquinavir formulations. The resulting free fractions were consistent with the theory, where one expects a lower free fraction for a higher amount of lipid phase and for a higher lipophilicity of a drug. Saquinavir, representing the more lipophilic drug, has the lower free fraction than progesterone.

Table 12 Calculated free fractions of different drugs and formulations

Formulation	Drug	Lipid phase [mg/ml]	Free fraction (*10 ⁴)
Liposomes	saquinavir	50	6.73
	progesterone	50	47.9
Microemulsion	progesterone	5	696.4

4.5.3 Conclusions

Equilibrium dialysis was found to be a reliable method to determine the free fraction of a lipophilic drug in liposomes and microemulsions. It was shown that the surfactant Cremophor EL had no influence on the free fraction of progesterone in a microemulsion.

4.6 Calculation of the Free Fraction of Progesterone Liposome Formulations

For the progesterone liposomes containing 0.1 mg/ml and 1 mg/ml lipids, no equilibrium dialysis to determine the free fraction was performed. Therefore, two different approaches for the calculation of free fraction of a drug between lipid phase and transport media were developed and compared to each other, which were a graphical approach to estimate directly the free fraction and a mathematical approach to calculate the free fraction out of a partition coefficient K .

4.6.1 Derivation of an Equation for the Calculation of a Partition Coefficient of a Drug Between Lipid Phase and Water Phase out of Equilibrium Dialysis Experiments

This chapter describes the derivation of an equation for the calculation of a partition coefficient of a drug between lipid phase and water phase out of equilibrium dialysis experiments that can be applied for the calculation of free fractions of formulations if no equilibrium dialysis data are available for singular lipid phase concentrations. Figure 34 shows the equilibrium situation in dialysis cells.

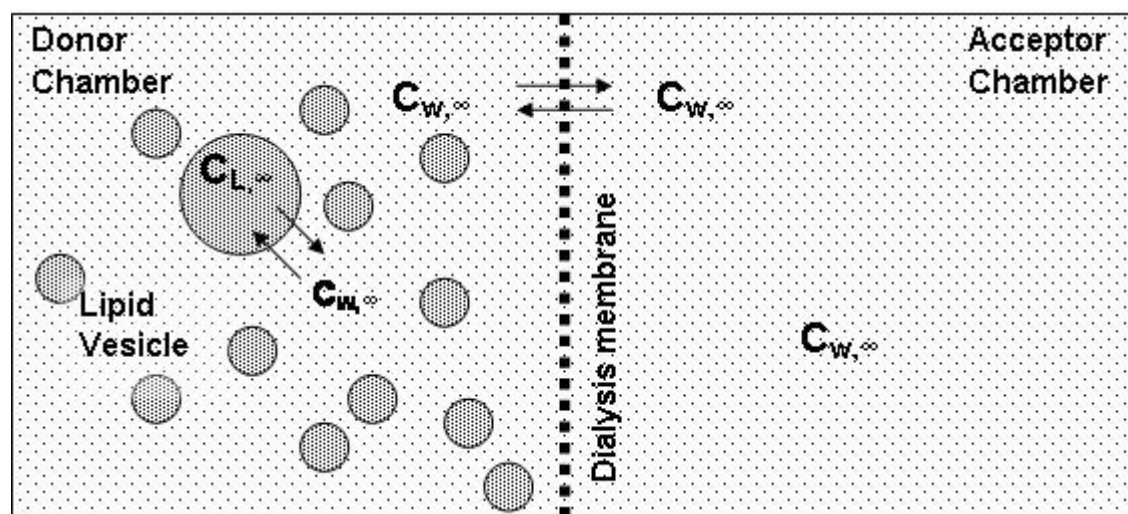


Figure 34 The equilibrium situation in dialysis cells.

Definition of lipid/water partition coefficient (K) referring to the total molar mass (“mole Fraction”) is shown in Equation 50, where n_{dL} are the moles of drug associated with lipid phase, n_{dw} are the moles of unbound drug in water phase, n_L moles of lipids in the system, and n_w the moles of water in the system.

$$K = \frac{\frac{n_{dL}}{n_L + n_{dL}}}{\frac{n_{dw}}{n_w + n_{dw}}}$$

Equation 50

Mass balance considerations:

$$n_{tot,w} = n_w + n_{dw}$$

Equation 51

The water phase, expressed as $n_{tot,w}$ is composed of the moles of water in the system and the moles of free drug in the water phase. The total amount of drug is the sum of drug in the lipid phase (n_{dL}) and the free drug in the water phase and is equal to the total drug concentration in equilibrium ($c_{tot,\infty}$) in the formulation, expressed as total mass (m_{tot}) divided by density of the formulation (ρ_{tot}):

$$n_{dL} + n_{dw} = \frac{c_{tot,\infty}}{\rho_{tot}} \cdot m_{tot}$$

Equation 52

$$m_{tot} = n_{dL} \cdot MW_d + n_L \cdot MW_L + n_{dw} \cdot MW_d + n_w \cdot MW_w$$

Equation 53

There is MW_d the molecular weight of drug, MW_L molecular weight of Lipid, MW_w the molecular weight of water assumed to be 18 g/mol. Equation 53 was inserted into Equation 52:

$$n_{dL} + n_{dw} = \frac{c_{tot,\infty}}{\rho_{tot}} n_{dL} \cdot MW_d + \frac{c_{tot,\infty}}{\rho_{tot}} n_L \cdot MW_L + \frac{c_{tot,\infty}}{\rho_{tot}} n_{dw} \cdot MW_d + \frac{c_{tot,\infty}}{\rho_{tot}} n_w \cdot 18$$

Equation 54

$$0 = n_{dL} \left(\frac{c_{tot,\infty}}{\rho_{tot}} \cdot MW_d - 1 \right) + \frac{c_{tot,\infty}}{\rho_{tot}} n_L \cdot MW_L + n_{dw} \left(\frac{c_{tot,\infty}}{\rho_{tot}} \cdot MW_d - 1 \right) + \frac{c_{tot,\infty}}{\rho_{tot}} n_w \cdot 18$$

Equation 55

$$0 = \left(\frac{c_{tot,\infty}}{\rho_{tot}} \cdot MW_d - 1 \right) \cdot (n_{dL} + n_{dw}) + \frac{c_{tot,\infty}}{\rho_{tot}} (n_L \cdot MW_L + n_w \cdot 18)$$

Equation 56

Replacement of unknown parameters n_{dL} and n_{dw} in Equation 56 by Equation 50 solved after n_{dL}

$$K = \frac{\frac{n_{dL}}{n_L + n_{dL}}}{\frac{n_{dw}}{n_w + n_{dw}}} \Rightarrow n_{dL} = \frac{K \cdot n_{dw} \cdot n_L}{n_w + n_{dw} - K \cdot n_{dw}}$$

and the following equation solved after n_{dw} :

$$\frac{c_{w,\infty}}{\rho_w} = \frac{n_{dw}}{n_{dw} \cdot MW_d + n_w \cdot 18} \Rightarrow n_{dw} = \frac{c_{w,\infty} \cdot n_w \cdot 18}{\rho_w - c_{w,\infty} \cdot MW_d}$$

Equation 57

where $c_{w,\infty}$ delineates the concentration of unbound drug in water in equilibrium and ρ_w the density of water phase.

$$n_{dL} + n_{dw} = \frac{K \cdot n_{dw} n_L}{n_w + n_{dw} - K \cdot n_{dw}} + n_{dw} = n_{dw} \left(1 + \frac{K \cdot n_L}{n_w + n_{dw}(1-K)} \right) = \frac{c_{w,\infty} \cdot n_w \cdot 18}{\rho_w - c_{w,\infty} \cdot MW_d} \left(1 + \frac{K \cdot n_L}{n_w + n_{dw}(1-K)} \right)$$

Equation 58

Insertion of Equation 58 in Equation 56:

$$0 = \left(\frac{c_{tot,\infty} \cdot MW_d}{\rho_{tot}} - 1 \right) \cdot \frac{c_{w,\infty} \cdot n_w \cdot 18}{\rho_w - c_{w,\infty} \cdot MW_d} \left(1 + \frac{K \cdot n_L}{n_w + \frac{c_{w,\infty} \cdot n_w \cdot 18}{\rho_w - c_{w,\infty} \cdot MW_d} (1-K)} \right) + \frac{c_{tot,\infty}}{\rho_{tot}} (n_L \cdot MW_L + n_w \cdot 18)$$

$$0 = \left(\frac{c_{tot,\infty} \cdot MW_d}{\rho_{tot}} - 1 \right) \cdot \frac{c_{w,\infty}}{\rho_w - c_{w,\infty} \cdot MW_d} \left(1 + \frac{K \cdot n_L}{n_w + \frac{c_{w,\infty} \cdot n_w \cdot 18}{\rho_w - c_{w,\infty} \cdot MW_d} (1-K)} \right) + \frac{c_{tot,\infty}}{\rho_{tot}} \left(\frac{n_L \cdot MW_L}{n_w \cdot 18} + 1 \right)$$

$$= \left(\frac{c_{tot,\infty} \cdot MW_d}{\rho_{tot}} - 1 \right) \cdot \frac{c_{w,\infty}}{\rho_w - c_{w,\infty} \cdot MW_d} \left(1 + \frac{K \cdot n_L}{n_w + \frac{c_{w,\infty} \cdot n_w \cdot 18}{\rho_w - c_{w,\infty} \cdot MW_d} (1-K)} \right) + \frac{c_{tot,\infty}}{\rho_{tot}} \left(\frac{n_L \cdot MW_L}{n_w \cdot 18} + 1 \right)$$

$$0 = \left(\frac{c_{tot,\infty} \cdot MW_d}{\rho_{tot}} - 1 \right) \cdot \frac{c_{w,\infty}}{\rho_w - c_{w,\infty} \cdot MW_d} \left(1 + \frac{K \cdot \frac{n_L}{n_w}}{1 + \frac{c_{w,\infty} \cdot 18}{\rho_w - c_{w,\infty} \cdot MW_d} (1-K)} \right) + \frac{c_{tot,\infty}}{\rho_{tot}} \left(\frac{n_L \cdot MW_L}{n_w \cdot 18} + 1 \right)$$

Equation 59

In Equation 59 all parameters except K were known. Parameters were inserted and the equation was solved after K.

To calculate the free fraction z out of lipid/water partition coefficient K, the following mathematical coherence was used, where K' indicates a lipid/water partition referring the drug concentration in the lipid particles (c'_L) to the concentration of the drug in the water phase (c_w):

$$K' = \frac{c'_L}{c_w} = \frac{\frac{n_{d,L}}{V_{tot} - V_w}}{\frac{n_{dw}}{V_w}} = \frac{n_{d,L} V_w}{n_{dw} (V_{tot} - V_w)} = K \frac{n_L}{n_w} \frac{1}{VF} - 1$$

Equation 60

It follows out of mass balance considerations:

$$V_{tot}c_{tot} = V_w c_w + V_L c'_L = V_w c_w + K' c_w (V_{tot} - V_w)$$

Equation 61

If Equation 61 is divided by $V_{tot}c_w$ and is transformed, Equation 62 results.

$$1 = zVF + K'z(1 - VF)$$

Equation 62

where VF denotes the volume fraction, which is the ratio of V_w to V_{tot} . When Equation 62 is solved after z, the following mathematical relation results:

$$z = \frac{1}{VF + K'(1 - VF)} - \frac{1}{K' + VF(1 - K')}$$

Equation 63

Equation 63 was used to calculate the free fraction if no experimental data was available.

4.6.1.1 Results of the Calculated Partition Coefficients

Lipid/water partitions referring to the total molar mass (K) of dialyzed progesterone liposomes were calculated using Equation 59. Table 13 gives an overview of the results.

Table 13 Lipid/water partition coefficients referring to the total molar mass (K) of dialyzed progesterone liposomes. The density of transport media (1.0 g/ml) and lipid particles (1.0 g/ml) was inserted into Equation 59. For the molar amount of lipids, the molecular weight of the phospholipid phosphatidylcholine of 761 g/mol was used.

lipid concentration [mg/ml]	$c_{tot} (*10^6)$ [mol/ml]	$c_w (*10^8)$ [mol/ml]	$n_L (*10^5)$ [mol]	n_w [mol]	K	K'
50	9.44	4.52	6.57	0.56	$9.71*10^5$	$2.18*10^3$
50	3.42	1.29	6.57	0.56	$2.49*10^6$	$5.59*10^3$
50	0.33	0.15	6.57	0.56	$4.30*10^6$	$9.67*10^3$
25	1.53	1.14	3.29	0.56	$2.23*10^6$	$5.16*10^3$
25	0.74	0.52	3.29	0.56	$3.09*10^6$	$7.13*10^3$
25	0.12	0.10	3.29	0.56	$3.38*10^6$	$7.80*10^3$
10	3.03	6.26	1.31	0.56	$6.66*10^5$	$1.56*10^3$
10	0.79	1.49	1.31	0.56	$1.64*10^6$	$3.84*10^3$
10	0.13	0.25	1.31	0.56	$2.50*10^6$	$5.87*10^3$
5	1.98	4.56	0.66	0.56	$9.43*10^5$	$2.22*10^3$
5	0.65	2.36	0.66	0.56	$1.24*10^6$	$2.92*10^3$
5	0.33	1.16	0.66	0.56	$1.72*10^6$	$4.04*10^3$
0.5	0.15	4.06	0.066	0.56	$8.60*10^5$	$2.04*10^3$
0.5	0.09	2.89	0.066	0.56	$9.73*10^5$	$2.30*10^3$
0.5	0.04	1.30	0.066	0.56	$1.38*10^6$	$3.27*10^3$
Average K					$1.89*10^6$	

The average K of $1.89 \cdot 10^6$, representing the lipid/water partition referring to the total molar mass of the used formulation, was used to calculate the free fraction of the progesterone liposomes, where no experimental data was available. Table 14 displays the results. The obtained free fractions of progesterone liposomes containing 0.1 and 1 mg/ml phospholipids were in the expected order of magnitude.

Table 14 Calculated free fractions for the progesterone liposomes containing 0.1 mg/ml and 1 mg/ml phospholipids. For the calculation of the lipid/water partition referring the drug concentration in the lipid particles to the concentration of the drug in the water phase K' , the displayed volume fraction VF was used and inserted into Equation 63 for the calculation of the free fraction. Molar mass of the lipids is denoted by n_L , molar mass of the water phase is denoted by n_w .

Lipid concentration [mg/ml]	n_L [mol]	n_w [mol]	K	K'	VF	Calculated free fraction z
1	$1.31 \cdot 10^{-6}$	0.555	$1.89 \cdot 10^6$	4474.25	0.999	0.18
0.1	$1.31 \cdot 10^{-7}$	0.555	$1.89 \cdot 10^6$	4478.29	0.9999	0.69

4.6.2 Graphical Approach to Assess the Free Fraction of Liposome Formulations

If the lipid phase concentration is plotted against $1/z$, a linear relationship results for all drugs and all formulations. Figure 35 displays the resulting plot of the progesterone liposomes.

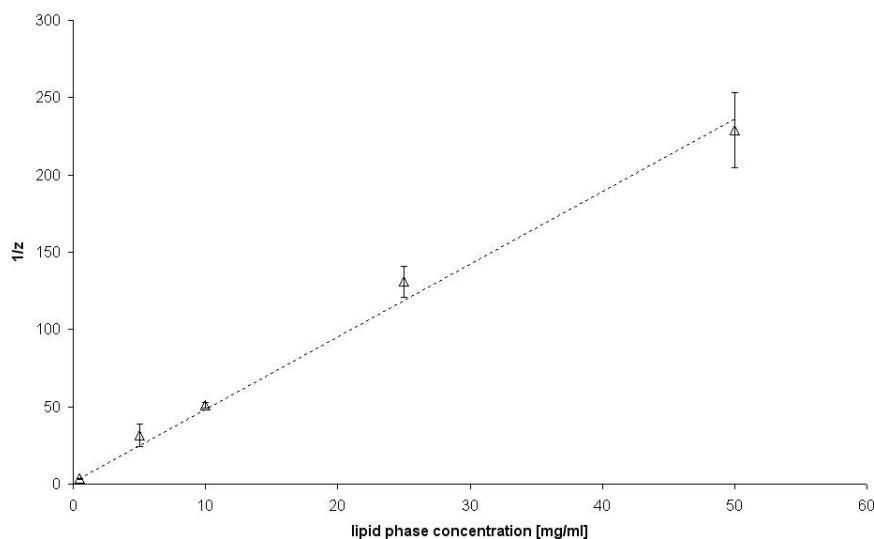


Figure 35 Plot of lipid concentration versus $1/z$ for progesterone liposomes. Linear regression analysis resulted in the following equation: $y=4.7059x+1$ ($r^2=0.9921$).

The equation resulting out of linear regression analysis of the plot, $y=4.7059x+1$ ($r^2=0.9921$), was used to calculate the free fraction of progesterone liposomes containing 0.1 mg/ml ($z= 0.18$) and 1 mg/ml ($z=0.68$) lipid phase.

4.6.3 Conclusions

The two methods to calculate the free fractions of lipid containing drug formulations were equal for the two free fractions where no equilibrium dialysis data was available. The mathematical approach is a general solution to calculate free fractions of lipid containing dosage forms, if lipid/water partition is known or can be calculated as shown in this section. For the calculation of the free fraction of progesterone liposomes in this work, the easier and less error-prone approach to assess the missing free fractions without experimental data was used. A free fraction of 0.18 for 1 mg/ml lipids and of 0.68 for 0.1 mg/ml lipids was used for further calculations.

4.7 Measurements of Cellular Drug Uptake

The filter of the Transwell insert is a possible additional diffusion barrier for both, the drug and the lipid particles. This additional barrier may hinder the drug permeation across the cell monolayer on the basolateral side of the Caco-2 cell monolayer. If this happens, different apparent permeability coefficients from the apical to cellular compartment compared to basal to cellular compartment result. Additionally, if the lipid particles are not able to diffuse through the filter pores, drug permeation because of direct transfer from lipid particle to cell membrane will not take place on the basolateral membrane.

Usually, drug uptake experiments were performed using a cell monolayer grown on a Petri dish after adding a drug containing solution into the Petri dish by determination of the disappearance of drug from this solution. Correlating this method with cell permeation experiments in Transwell plates may lead to inconclusive data, because of different hydrodynamics, different monolayer density, different cell differentiation, and a different surface area. Taking into consideration that the cell uptake of highly permeable compounds may be diffusion boundary layer controlled, it is of importance to use Transwell inserts for the evaluation of the uptake to ensure hydrodynamics. A procedure to estimate the permeation of a compound between basal and cellular compartment using Transwell plates was described by Ho et. al already for drug efflux (59). For the determination of the drug permeation from apical to basal compartment, sealed Transwell inserts instead of Petri dishes were used (see method section below).

Using this method, an experimental evaluation of uptake of lipophilic drugs is difficult, because the intracellular concentration is calculated indirectly by the decrease of the donor concentration. Permeation of a lipophilic drug could be overestimated easily because of possible unspecific drug adsorption to the plastic made surface of the Transwell plates which could be wrongly interpreted as drug permeation into the cell. For this reason drug uptake was performed for progesterone only, because propranolol showed low interaction with the formulations and unspecific adsorption was observed for saquinavir and triclobandazole. Assuming that the particle size of the formulation affects drug permeation through the Transwell filter, the emulsion was taken as model formulation expecting the highest influence on drug permeation because of its particle size that was bigger than particle sizes of the other formulations.

4.7.1 Material and Methods

4.7.1.1 Material

Transport media used for the permeation studies and the equilibrium dialysis experiments were prepared with Dulbecco's Modified Eagle's Medium (DMEM) base powder (without glucose, l-glutamine, phenol red, sodium pyruvate and sodium bicarbonate, purchased from SIGMA-Aldrich, Fluka Chemie GmbH, Buchs, Switzerland). DMEM base powder was dissolved in bi-distilled and autoclaved water and supplemented with glucose (4.5 g/l), HEPES (4.76 g/l), NaCl (1.987 g/l), and l-glutamine (0.876 g/l). The pH was adjusted to 7.4 and the final medium was filtered through a sterile filter (Supor-200, 0.2 µm pore size, Pall Corporation, Michigan, USA) under aseptic conditions.

Glucose, HEPES, NaCl, and L-glutamine were purchased from SIGMA-Aldrich (Fluka Chemie GmbH, Buchs, Switzerland). Dulbecco's Phosphate Buffered Saline (D-PBS) (with Ca^{2+} , Mg^{2+}) was purchased from SIGMA-Aldrich (Fluka Chemie GmbH, Buchs, Switzerland). 6-well Polycarbonate Membrane Transwell Plates with an insert area of 4.7 cm^2 and $0.4 \mu\text{m}$ pore size were ordered from Costar (Corning Incorporated, Corning, NY, USA). Captex 8000 was purchased from SIGMA-Aldrich (Fluka Chemie GmbH, Buchs, Switzerland), Capmul MCM was purchased from Abitec Corporation (Janesville, USA). Cremophor EL was ordered from Fluka (Fluka Chemie GmbH, Buchs, Switzerland). Progesterone was purchased from Fluka (SIGMA-Aldrich, Fluka Chemie GmbH, Buchs, Switzerland).

4.7.1.2 Preparation of the Emulsions

Emulsions containing $14.5 \mu\text{M}$ progesterone and 0.5 mg/ml or 5 mg/ml of the emulsion lipid phase (lipid phase consisting of 5%^[m/m] Capmul MCM, 67%^[m/m] Captex 8000, 18%^[m/m] Cremophor EL, and 10%^[m/m] ethanol) were tested. The lipid phase was prepared by mixing the components at 37°C . The lipid phase was warmed up to 37°C before use and the according amount was balanced and mixed with two thirds of the final transport medium volume. The formulation was homogenized for 5 min at 15000 rpm with a Polytron homogenizer (Polytron PT 3000, Kinematica AG, Littau, Switzerland) and preheated transport medium was added to the final volume.

4.7.1.3 Measuring the Cellular Uptake to the Cellular Compartment

Caco-2 cells cultured during 21 days were used. Both compartments of the wells were rinsed with tempered D-PBS (with magnesium and calcium). For determination of drug uptake from apical compartment to cellular compartment, the Transwell inserts were sealed on the basal side using aluminum foil, cut to the size of the filter insert. PTFE Thread seal tape was wrapped three times around the insert to seal it completely. Then $1600 \mu\text{l}$ of the drug formulation was added into the apical compartment.

For the drug uptake from the basal to the cellular compartment, $200 \mu\text{l}$ transport media was added to the apical compartment to avoid desiccation of the cells and then $2800 \mu\text{l}$ of the drug formulation was added into the basal compartment. The plate was shaken on an orbital shaker (KS15, Edmund Bühler GmbH, Tübingen & Hechingen, Germany) with 75 rpm under water saturated atmosphere with 75 rpm at 37°C . Samples of $100 \mu\text{l}$ were taken after 0, 2.5, 5, 7.5, 10, 15, 20, and 30 min. Drug quantification was performed by HPLC.

4.7.1.4 Drug Quantification

Drug quantification of progesterone was performed by HPLC-UV (Agilent series 1100, Agilent Technologies USA, equipped with a G1312A binary pump, an auto sampler G1367B and a variable wavelength detector G1314B) using a C-18 reversed phase column (CC 125/2 Lichrospher 100 RP 18 ec, Macherey Nagel, Oensingen, Switzerland). An Isocratic method with a flow rate of 0.25 ml/min was used with the following mobile phase: distilled water (bi-distilled and filtered through $0.45 \mu\text{m}$)/methanol/tetrahydrofuran 40/45/15 (V/V). Ammonium acetate with a concentration of 0.55 g/l was added to the mobile phase. The pH-value at 25°C was 6.9. An injection volume of $40 \mu\text{l}$ and a runtime of 7.5 min were used to detect progesterone at 239 nm in UV. Using this method, retention

time of progesterone was approximately 5 min. The samples were stored at 4°C. Quantification was performed against a set of external standard solutions within the linear response concentration range.

4.7.1.5 Calculation of the Permeability Coefficients

The time dependent change of mass in apical to basal direction of the cellular compartment (m_{cAB}) is described for progesterone by the following equation

$$\frac{dm_{cAB}}{dt} = P_a * (c_{aAB} - K_{a/c} \cdot c_{cAB}) * S_m$$

Equation 64

where P_a denotes apparent permeability coefficient, c_{aAB} concentration in apical compartment, $K_{a/c}$ formulation-to-cell partition coefficient, c_{cAB} drug concentration in cellular compartment and S_m cell monolayer surface area. If sink conditions are assumed, c_{cAB} is assumed to be 0 and the apparent permeability coefficients were calculated after Equation 2 (as described in the theoretical section) for the time interval 0 to 2.5 min. For that reason the intracellular concentrations were calculated assuming that the disappeared drug amount permeated into the cell. This amount was divided by the cell monolayer volume resulting in the intracellular concentration which was inserted into the equation. The volume of the cell monolayer as receiver volume was inserted as 0.0094 cm^3 .

4.7.2 Results and Discussion

It was possible to measure drug uptake from basal compartment to cellular compartment and from apical compartment to cellular compartment using Transwell plates for both directions. The sealing with aluminum foil and PTFE seal tape worked well, no leakage was observed. The results clearly indicate an influence of the lipid concentration on drug uptake by the cells. Initially, the drug uptake is higher from the 0.5 mg/ml lipid phase than from the 5 mg/ml lipid phase formulation, expressed in a higher apparent permeability for the time interval from 0 to 2.5 min as displayed in Table 15. The results of these uptake experiments show a decrease of drug uptake with increasing lipid concentration, which is the same tendency as observed in cell permeation experiments.

Table 15: Quantitative results of progesterone uptake from an emulsion containing 0.5 mg/ml and 5 mg/ml lipid phase, respectively. The apparent permeability coefficients were calculated for the time interval from 0 to 2.5 min.

Lipid phase concentration [mg/ml]	Apical-cell uptake permeability coefficient [cm/s]	Basal-cell uptake permeability coefficient [cm/s]	Drug fraction remaining in donor after apical to cell uptake	Drug fraction remaining in donor after basal to cell uptake
0.5	$3.45 \pm 0.23 * 10^{-4}$	$5.31 \pm 0.18 * 10^{-4}$	0.72 ± 0.014	0.76 ± 0.015
5	$1.76 \pm 0.16 * 10^{-4}$	$1.42 \pm 0.06 * 10^{-4}$	0.91 ± 0.0079	0.91 ± 0.0069

Over time, a higher fraction of the 0.5 mg/ml formulation is taken up, which is consistent with the estimated formulation-to-cell partition coefficient of the transport experiments. $K_{a/c}$ was smaller for the

0.5 mg/ml formulation and indicates a higher drug concentration in the cell after the equilibrium was reached. The normalized uptake profiles are shown in Figure 36 and Figure 37.

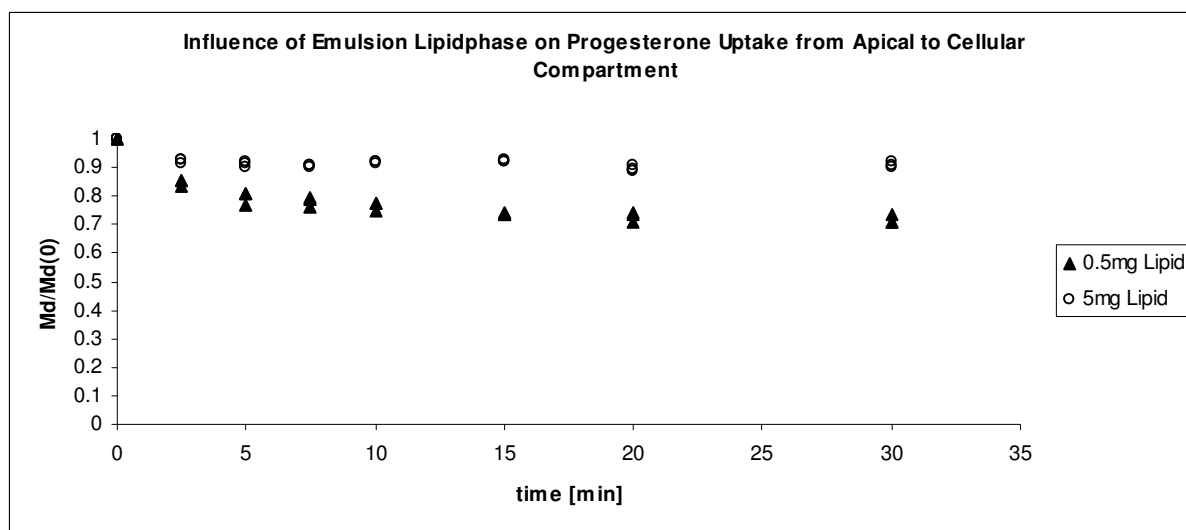


Figure 36 Transport of progesterone from apical to cellular compartment is influenced by the lipid concentration. The y-axis describes the amount of drug divided by the initial amount.

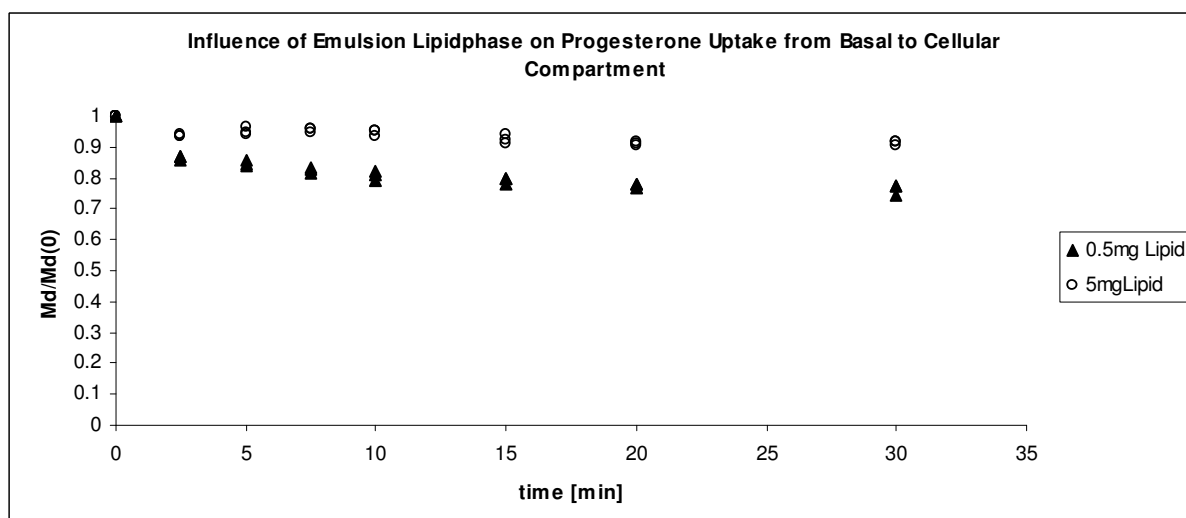


Figure 37 Transport of progesterone from basal to cellular compartment is influenced by the lipid concentration. The y-axis describes the amount of drug divided by the initial amount.

No difference between apical to cell and basal to cell uptake was observed. The result of the drug uptake experiments implicates that the drug uptake of the chosen formulation and drug is direction independent. This indicates a negligible influence of the filter insert on the permeation of progesterone out of emulsions. Taking into account that no systematic influence on cellular uptake was measured with the chosen experimental setting, no influence of the filter insert is expected on other formulations and drug uptake of the other model drugs.

4.7.3 Conclusions

The drug uptake of progesterone out of emulsions is influenced by the lipid concentration. Increased lipid concentrations decrease the apparent permeability delineating drug uptake. The analogy of the effects of the lipid phase to the cell permeation experiments is obvious. The filter insert did not influence drug uptake with the chosen experimental setting. No influence of the filter insert is expected on other formulations and drug uptake of the other model drugs either.

4.8 Measurements of Passive Cellular Efflux

Similar to cell uptake experiments, drug permeation from cell monolayer to the apical or basal compartment can be determined (59). Fundamental understanding of drug uptake and drug efflux by the cells may help to understand the transcellular drug permeation. Passive drug efflux may be influenced by lipophilicity of the drug, type and concentration of lipid particles, presence of carrier mediated efflux, and presence of a filter on basolateral side. If the process is diffusion boundary layer controlled, hydrodynamics may have a contribution to the permeation. Therefore all experiments were performed into Transwell plates.

The aim of these experiments was the determination of the passive drug efflux from the cell monolayer to the basal compartment. Progesterone and triclobandazole were used as model drugs to estimate the influence of passive drug efflux from cellular to basal compartment. Using these drugs, drug permeation on the basolateral side is not interfered by carrier mediated apical efflux. The different lipophilicity of these two compounds may allow a conclusion on a possible influence of lipophilicity on drug permeation from cell monolayer to basal compartment. We compared microemulsions and emulsions of both drugs representing the formulations with the most different particle sizes. This may allow conclusion on a possible effect of the particle size on drug permeation from cell monolayer to basal compartment.

4.8.1 Material and Methods

4.8.1.1 Material

Transport media used for the permeation studies and the equilibrium dialysis experiments were prepared with Dulbecco's Modified Eagle's Medium (DMEM) base powder (without glucose, l-glutamine, phenol red, sodium pyruvate and sodium bicarbonate, purchased from SIGMA-Aldrich, Fluka Chemie GmbH, Buchs, Switzerland). DMEM base powder was dissolved in bi-distilled and autoclaved water and supplemented with glucose (4.5 g/l), HEPES (4.76 g/l), NaCl (1.987 g/l), and l-glutamine (0.876 g/l). The pH was adjusted to 7.4 and the final medium was filtered through a sterile filter (Supor-200, 0.2 μm pore size, Pall Corporation, Michigan, USA) under aseptic conditions. Glucose, HEPES, NaCl, and l-glutamine were purchased from SIGMA-Aldrich (Fluka Chemie GmbH, Buchs, Switzerland). Dulbecco's Phosphate Buffered Saline (D-PBS) (with Ca^{2+} , Mg^{2+}) was purchased from SIGMA-Aldrich (Fluka Chemie GmbH, Buchs, Switzerland). 6-well Polycarbonate Membrane Transwell Plates with an insert area of 4.7 cm^2 and 0.4 μm pore size were ordered from Costar (Corning Incorporated, Corning, NY, USA). Captex 8000 was purchased from SIGMA-Aldrich (Fluka Chemie GmbH, Buchs, Switzerland), Capmul MCM was purchased from Abitec Corporation (Janesville, USA). Cremophor EL was ordered from Fluka (Fluka Chemie GmbH, Buchs, Switzerland). Triclobandazole was provided by Phares Drug Delivery (Muttens, Switzerland). Progesterone was purchased from Fluka (SIGMA-Aldrich, Fluka Chemie GmbH, Buchs, Switzerland).

4.8.1.2 Preparation of the Formulations

Emulsions containing 63 μM progesterone or 63 μM tricloabendazole combined with 0.5 mg/ml or 5 mg/ml of the emulsion lipid phase (lipid phase consisting of 5%^[m/m] Capmul MCM, 67%^[m/m] Captex 8000, 18%^[m/m] Cremophor EL, and 10%^[m/m] ethanol) and microemulsions containing 63 μM progesterone or 63 μM tricloabendazole and 0.5 mg/ml or 5 mg/ml of the microemulsion lipid phase (lipid phase consisting of Captex 8000 35.05%^[m/m], Capmul MCM 17.58%^[m/m], Cremophor EL 36.84%^[m/m], and ethanol 10%^[m/m]) were tested. The lipid phase was prepared by mixing the components at 37°C. The lipid phase was warmed to 37°C before use and the according amount was balanced and mixed with two thirds of the final transport medium volume. The formulation was homogenized for 5 min at 15000 rpm with a Polytron homogenizer (Polytron PT 3000, Kinematica AG, Littau, Switzerland) and preheated transport medium was added to the final volume.

4.8.1.3 Determination of Passive Drug Efflux

The Transwell plates, cultured for 19-21 days, were rinsed with D-PBS (with magnesium and calcium). The drug formulation was added to the apical compartment. Placebo formulation, containing the same lipid concentration, was added to the basal compartment and the plates were incubated at 37°C under water saturated atmosphere at a stirring rate of 75 rpm for 180 min on an orbital shaker (KS15, Edmund Bühler GmbH, Tübingen& Hechingen, Germany). Before the formulations were removed and the plates rinsed twice with transport media, samples were taken in apical and basal compartment. Fresh placebo formulation was added to the basal compartment and to avoid dryness, 200 μl transport media was added to the apical compartment. Samples of 100 μl were taken and quantified with HPLC at predefined points of time after 0, 15, 30, 45, 60, 90, and 120 min.

4.8.1.4 Drug Quantification

Drug quantification of all drugs was performed by HPLC-UV (Agilent series 1100, Agilent Technologies USA, equipped with a G1312A binary pump, an auto sampler G1367B and a variable wavelength detector G1314B) using a C-18 reversed phase column (CC 125/2 Lichrospher 100 RP 18 ec, Macherey Nagel, Oensingen, Switzerland). Isocratic methods with a flow rate of 0.25 ml/min were used. The drug concentration of progesterone was determined with the following mobile phase: distilled water (bi-distilled and filtered through 0.45 μm)/methanol/tetrahydrofuran 40/45/15 (V/V). Ammonium acetate with a concentration of 0.55 g/l was added to the mobile phase. The pH-value at 25°C was 6.9. An injection volume of 40 μl and a runtime of 7.5 min were used to detect progesterone at 239 nm in UV. Using this method, retention time of progesterone was approximately 5 min. The samples were stored at 4°C. Quantification was performed against a set of external standard solutions within the linear response concentration range.

The drug concentration of tricloabendazole was determined with the following mobile phase: distilled water (bi-distilled and filtered through 0.45 μm)/methanol/tetrahydrofuran 35/40/25 (V/V). Ammonium acetate with a concentration of 0.55 g/l was added to the mobile phase. The pH- value at 25°C was 6.7. An injection volume of 40 μl and a runtime of 8 min were used to detect tricloabendazole at 305 nm in UV. Using this method retention time of tricloabendazole was approximately 5.6 min. Quantification of tricloabendazole was performed against a set of external standard solutions within the linear

response concentration range. To maintain the sample stability and reproducibility, the standard solutions of triclabendazole contained the same amount of lipids as the samples. Samples were stored at 4 °C.

4.8.1.5 Calculation of Permeability Coefficient Delineating Drug Efflux

The time dependent change of concentration in apical to basal direction of the basal compartment (c_{bAB}) is described for drugs, which were no subject to carrier mediated apical efflux, by the following equation

$$\frac{dc_{bAB}}{dt} = P_b * (K_{\%} \cdot c_{cAB} - c_{bAB}) * \frac{S_m}{V_b}$$

Equation 65

where P_b denotes apparent permeability coefficient, c_{bAB} concentration in basal compartment, $K_{a/c}$ formulation-to-cell partition coefficient, c_{cAB} drug concentration in cellular compartment and S_m cell monolayer surface area and V_b volume of basal compartment. If sink conditions are assumed c_{bAB} is 0. Consequently, apparent permeability coefficient delineating passive drug efflux from cellular to basal compartment was calculated after Equation 66 for the time interval 0 to 15 min.

$$P_b = \frac{dc_{bAB}}{dt} \cdot \frac{V_b}{S_m \cdot K_{\%} \cdot c_{cAB0}}$$

Equation 66

For that reason the initial intracellular concentration (c_{cAB0}) was calculated out of pre-experimental mass balance, assuming that the disappeared drug amount had permeated into the cell. The disappeared amount was calculated by comparing the initial drug amount of the formulation with the sum of drug amounts of basal and apical compartment after 180 min of incubation. This amount was divided by the cell monolayer volume resulting in the initial intracellular concentration which was used for the calculation. The cell monolayer volume was assumed to be 0.0094 cm³.

4.8.2 Results and Discussion

It was possible to measure passive drug efflux from cell compartment to basal compartment for both drugs with the described method. The results displayed in Table 16 indicate decreasing apparent permeability coefficient with increased lipid concentration for both drugs. The obtained apparent permeability coefficients of the passive efflux experiments were one order of magnitude lower than the apparent permeability coefficients deduced by data fitting of cell permeation experiments.

Because of the initially small amount of drug inside of the cell monolayer and the high permeability coefficient of progesterone, an initial time interval of 15 min was obviously too long to maintain sink conditions which is a limitation of the used equation. This may explain the lower apparent permeability coefficients compared to apparent permeability coefficients deduced from cell permeation experiments.

The passive efflux of triclabendazole from the cellular to the basal compartment delineated by the apparent permeability coefficient was lower than the passive efflux of progesterone. The permeation of

triclabendazole from cell monolayer to the emulsions and to the microemulsion containing 0.5 mg/ml lipid was not finished after 120 min (see Figure 38).

Qualitatively, these results correspond to the deduced apparent permeability coefficients of the cell permeation experiments, where a decrease of the permeability coefficients was observed if the lipid concentration was increased.

Table 16 Quantification of passive drug efflux from cellular to basal compartment. All formulations used for incubation contained a drug concentration of 63 μ M. The apparent permeability coefficient delineating passive drug efflux from cellular to basal compartment was calculated for the time interval 0-15 min.

Formulation	Lipid phase concentration [mg/ml]	Apparent permeability coefficient cell-basal efflux [cm/s]	Drug fraction effluxed to acceptor after cell to basal efflux after 120 min
Progesterone emulsion	0.5	$9.25 \pm 0.7 \cdot 10^{-6}$	0.25
	5	$7.62 \pm 1.0 \cdot 10^{-7}$	0.32
Progesterone microemulsion	0.5	$2.57 \pm 0.66 \cdot 10^{-5}$	0.47
	5	$4.71 \pm 0.83 \cdot 10^{-6}$	0.49
Triclabendazole emulsion	0.5	$6.19 \pm 0.37 \cdot 10^{-6}$	0.20
	5	$9.83 \pm 0.33 \cdot 10^{-7}$	0.21
Triclabendazole microemulsion	0.5	$3.11 \pm 0.22 \cdot 10^{-6}$	0.52
	5	$2.13 \pm 0.09 \cdot 10^{-6}$	0.67

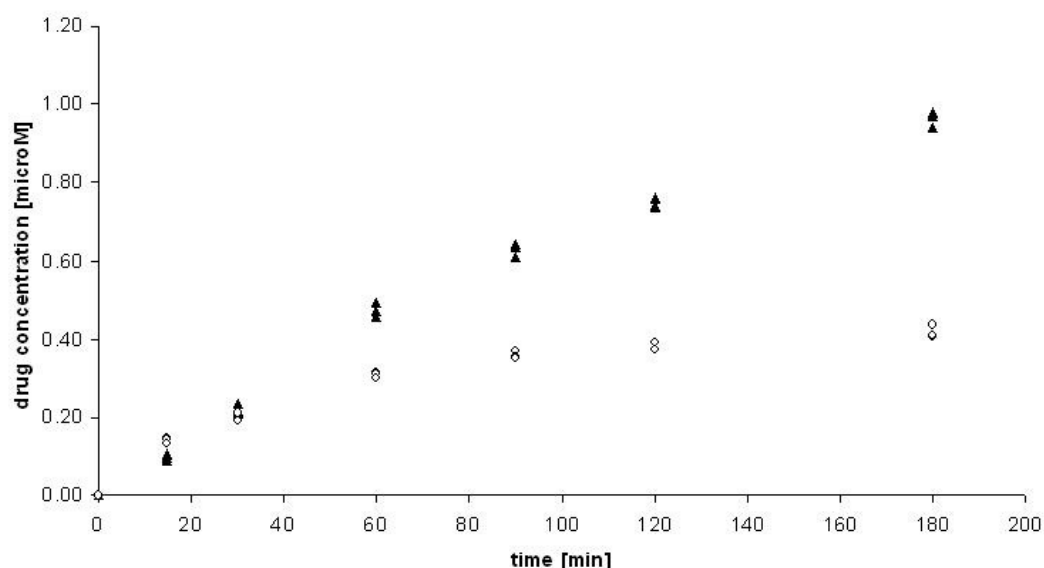


Figure 38 Transport of triclabendazole from the cellular to the basal compartment (containing a microemulsion with 0.5 mg/ml (▲) and 5 mg/ml (○) lipid phase) is influenced by the lipid concentration.

4.8.3 Conclusions

Apparent permeability coefficients delineating passive drug efflux from cell monolayer to basal compartment show that the lipid concentration of a lipid containing formulation influences drug permeation from cellular compartment to the acceptor. The observed decrease of apparent permeability coefficients corresponds to observations made by cell permeation experiments. The obtained permeabilities were much lower than the apparent trans-monolayer permeabilities caused by violation of sink conditions. Therefore no quantitatively relevant statement can be made.

5 CONCLUSIONS AND OUTLOOK

5.1 Conclusions

It was shown in this work, that it is possible to test the effect of lipid containing drug formulations on drug permeation using the Caco-2 model, if the formulations are tolerated by the cell monolayer. Therefore, much attention had to be paid on the maintenance of the cell monolayer integrity during the cell permeation experiments which resulted in determination of the maximal applicable lipid phase concentrations and additionally a limitation of duration of cell permeation experiment.

A methodology to determine unbiased parameters describing the in vitro absorption of lipid containing formulations of poorly water soluble drugs was developed and evaluated in this work. This methodology comprises the description of transcellular drug permeation through Caco-2 cell monolayers and the analysis of the obtained data with a biophysical model for a mechanistic understanding of the influence of lipid containing drug formulations on drug absorption.

For the determination of drug absorption parameters in Caco-2 cell monolayer, a refined mathematical model based on previous work of our group was used. In earlier work, this model was derived for a mechanistic description of transcellular drug permeation including passive permeation and carrier mediated efflux. This model showed difficulties in prediction of intracellular drug concentration during cell permeation experiment of highly lipophilic compounds. To improve prediction of intracellular drug concentrations during cell permeation experiments, experimental cell monolayer extractions were taken into account for data fitting. A formulation-to-cell partition coefficient and independent permeability coefficients for the apical and the basal cell membrane were introduced into the model. This refined mathematical model, which is proposed in this study for the determination of drug absorption parameters in Caco-2 cell monolayers, is still able to detect carrier mediated transport. It further divides trans-monolayer permeability into independent permeability coefficients of the apical membrane and the basal membrane and allows deducing formulation-to-cell partition coefficient, intracellular time dependent concentration, and quantification of carrier mediated efflux directly out of time dependent experimental concentration data. If a compound undergoes carrier mediated efflux, the differentiation of P_a and P_b is limited because of mathematical correlation of these parameters.

The analysis of the transcellular permeation experiments with this model indicates a decrease of apparent permeability coefficient with increasing lipid concentration, if an interaction of a drug with a lipid containing formulation is given. For a better understanding of this formulation effect, a reliable method for the determination of the free fraction of drug was developed, based on equilibrium dialysis that allows precise measurement of the free fraction. It was shown in this thesis, that this method is applicable to the used lipid containing drug formulations.

A biophysical model for delineating contribution of different transport steps to the apparent permeability coefficient was developed taking into account transport of lipid particles and free molecules through diffusion boundary layer, permeation of free drug molecules through the cell membrane, and the drug permeation caused by direct drug transfer from lipid particles to the cell membrane. It was shown that the permeability coefficient that delineates the contribution of drug transport in the diffusion boundary layer is in the same order of magnitude for all tested drugs and

formulations and is the rate limiting step for an aqueous solution of the lipophilic model drugs. The permeability coefficient of the free drug through the cell membrane was independent of the formulation and dependent on the drug. This evaluation of the apparent permeability coefficient has confirmed that the free fraction of a drug is the major determinant of intestinal cell permeation. High free fraction indicates apparent permeability coefficients similar to aqueous solution; low free fraction indicates lower apparent permeability coefficients. Additionally, the direct transfer of lipophilic drugs from lipid phase of the formulation to cell membrane can also make an essential contribution to drug permeation. The relative significance of these two processes depends on the drug and the formulation. In this work drug transfer from the lipid particles to the membrane upon collision was relevant for progesterone only. These observations apply to structurally different lipid containing drug formulations.

It was shown that permeability coefficient that delineates drug uptake of progesterone formulations and permeability coefficient that delineates passive drug efflux of progesterone and triclofenadazole formulations are influenced by the lipid concentration similar as observed in cell permeation experiments. It was shown further that drug uptake of progesterone was independent of transport direction. Based on these results we assume that the microporous Transwell filter support was not rate limiting.

Summarized, the effects of lipid containing drug formulations on the absorption of lipophilic drugs are:

- 1) The use of lipid containing drug formulations lowers apparent permeability coefficient by lowering the drug uptake from donor compartment to cellular compartment. The extent is dependent on free fraction. Increased lipid phase concentration increases formulation-to-cell partition coefficient.
- 2) The qualitative effect on apparent permeability coefficient is independent of the formulation if the used drug interacts with the formulation.
- 3) Depending on formulation and drug, direct mass transfer from lipid particle to cellular membrane may contribute to transcellular permeation.

Apparent drug permeability coefficient depends on free fraction, whereas drug flux depends on absolute amount of free drug in water phase. Therefore simultaneous increase of drug and lipid concentration provides an undiminished drug flux, which may improve bioavailability by prolonged intestinal absorption at a sustained rate. These findings are independent of the composition and the structure of the lipid formulation. In addition flux can be further increased by direct drug transfer from lipid particle to cellular membrane. This was observed for only one drug in the present work. Possible necessary structure activity relationship of drugs for this to take place should be investigated in the future. The results of this work shed light into the mechanism of drug absorption from lipid formulations and demonstrate potential beneficial effects of these formulations on absorption of lipophilic drugs in vivo. They may be used for the development of efficient oral dosage forms to improve bioavailability for these drugs.

5.2 Outlook

The proposed mathematical model for the determination of drug absorption parameters in Caco-2 cell monolayer is a useful tool for a better understanding of the mechanisms taking place during cell monolayer permeation. To increase the knowledge about rate determining processes and partial steps of the absorption process it may be of great interest to implement measurements of partial processes into the model such as cellular uptake and cellular efflux from apical and basal side systematically, since few uptake and passive efflux data have been used in this work.

The proposed biophysical model for the subdivision of the apparent permeability coefficient showed that besides of the free fraction, a mass transfer caused by direct drug transport from lipid particles to the cell membrane may take place. The data of this work are based on few model drugs and three structurally different lipid containing drug formulations. To proof the proposed concept, one should take into consideration additional drugs and formulations. Since we did not observe for all tested drugs a mass transfer caused by direct drug transport from lipid particles to the cell membrane, it would be essential to have a more profoundly understanding about possible systematical relationship between drug molecular structure or physicochemical properties responsible for the ability of drugs to undergo mass transfer caused by direct drug transfer. Ideally, the outcome may be used predictively for the improvement of oral drug absorption of poorly water soluble compounds.

It is considered to be difficult to proof the observed mass transfer caused by direct drug transport from lipid particles to the cell membrane by additional measurements and alternative methods. It is considered to be easier to exclude the effects of direct mass transfer by comparing the results of this thesis with a different experimental setting that does not allow any interaction of lipid vesicles with the cellular membrane. This could be done by the introduction of an additional physical barrier, which is on one hand not rate determining for the used drugs but does not allow permeation of any lipid particles on the other hand. The use of particles with much larger particle sizes may help to separate the particles from the cell surfaces without affecting drug permeation, if these large particles show similar effects on drug permeation with the experimental setup used in this thesis. For the investigation of this particular case, liposomes may be a useful model, because it is possible to produce large and homogenous particles.

Another open question is the relevance of the described mechanism *in vivo*, because the situation in the small intestine is different from the experimental setting used in this study. Most important difference and possibly affecting mass transfer from lipid particle to cellular membrane is the presence of a mucus layer in the intestine, which is described as an additional barrier for drug transport. The mucus layer may allow particles to diffuse, but will surely influence the velocity of diffusion of these particles because of an increased viscosity compared to buffer media. The investigation of permeation of lipid particles through mucus, use of an artificial mucus layer on the Caco-2 cells, use of a cell model producing a mucus layer, or use of animal intestinal tissue may be valuable tools for the investigation of this interesting question.

Oral administered drug formulations undergo dilution, degradation, and lipid digestion in vivo. The products of this mechanisms and the presence of bile salts results in physically different formulations, such as mixed micelles. Since methods for in vitro lipid digestion have been developed in recent years it may be interesting to study the influence of digested products on drug absorption with a suitable model. Because of the known sensitivity of the Caco-2 cell monolayers to surfactants, bile salts, mono-, and di-glycerides one would have to proof the model suitability for this kind of investigation or maybe to use a different model, e.g. excised tissue.

6 APPENDIX

6.1 Determined TEER Values

6.1.1 Screening Experiments

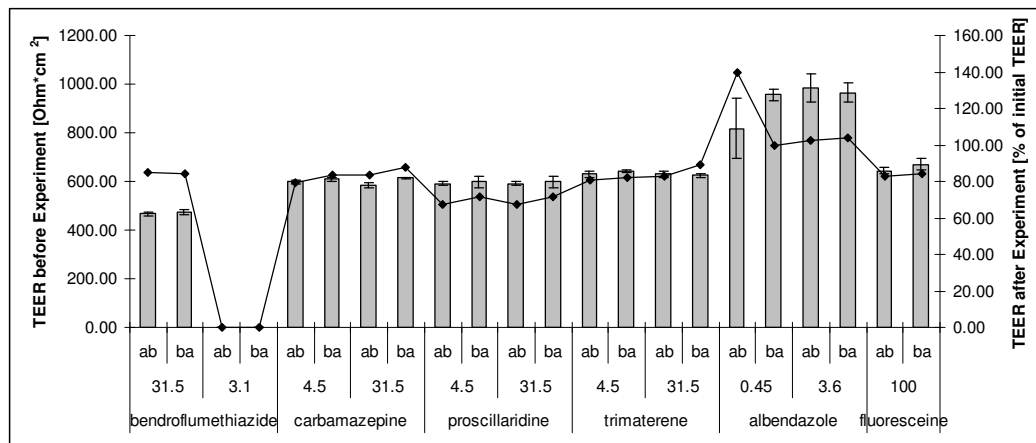


Figure 39 TEER values of Caco-2 cell monolayer used in drug screening experiments. The columns display the absolute values measured before the experiments and the connected points the TEER values after the experiment in % of the initial values. At least 3 wells were used per group. Meaning of the x-axis labels: ab apical to basal transport, ba basal to apical transport; numbers in the middle row: used drug concentration [μM].

6.1.2 Microemulsions

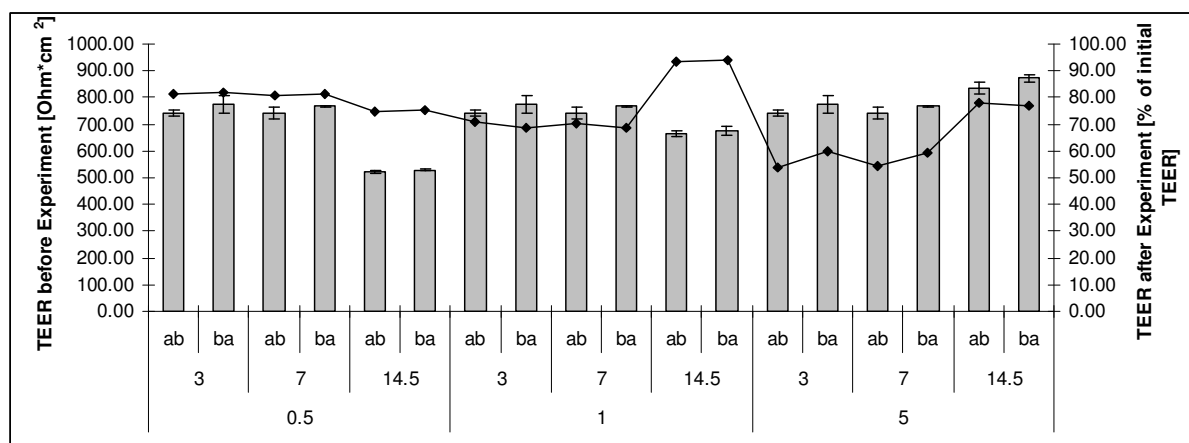


Figure 40 TEER values of Caco-2 cell monolayer used in the experiments with saquinavir microemulsions. The columns display the absolute values measured before the experiments and the connected points the TEER values after the experiment in % of the initial values. At least 3 wells were used per group. Meaning of the x-axis labels: ab apical to basal transport, ba basal to apical transport; numbers in the middle row: used drug concentration [μM]; numbers in the bottom row: used lipid concentrations [mg/ml].

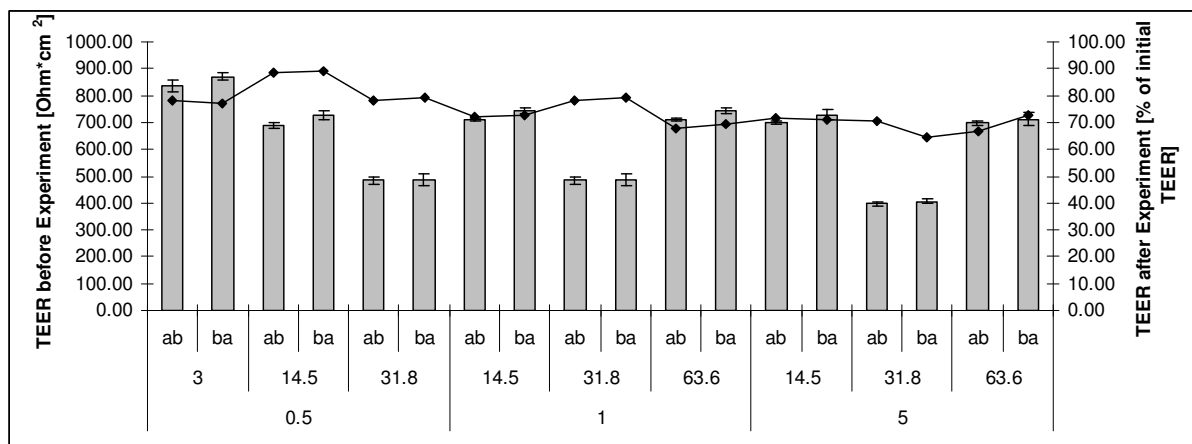


Figure 41 TEER values of Caco-2 cell monolayer used in the experiments with progesterone microemulsions. The columns display the absolute values measured before the experiments and the connected points the TEER values after the experiment in % of the initial values. At least 3 wells were used per group. Meaning of the x-axis labels: ab apical to basal transport, ba basal to apical transport; numbers in the middle row: used drug concentration [μM]; numbers in the bottom row: used lipid concentrations [mg/ml].

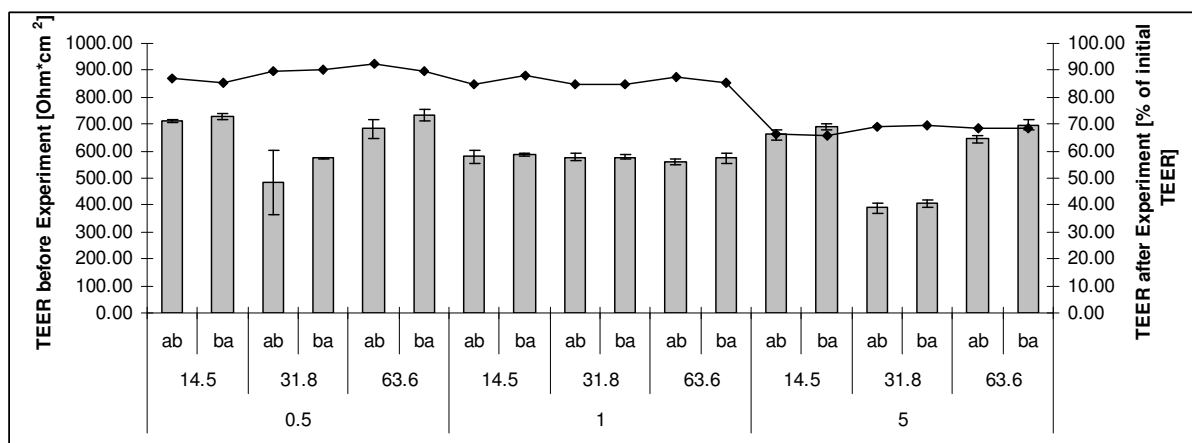


Figure 42 TEER values of Caco-2 cell monolayer used in the experiments with triclabendazole microemulsions. The columns display the absolute values measured before the experiments and the connected points the TEER values after the experiment in % of the initial values. At least 3 wells were used per group. Meaning of the x-axis labels: ab apical to basal transport, ba basal to apical transport; numbers in the middle row: used drug concentration [μM]; numbers in the bottom row: used lipid concentrations [mg/ml].

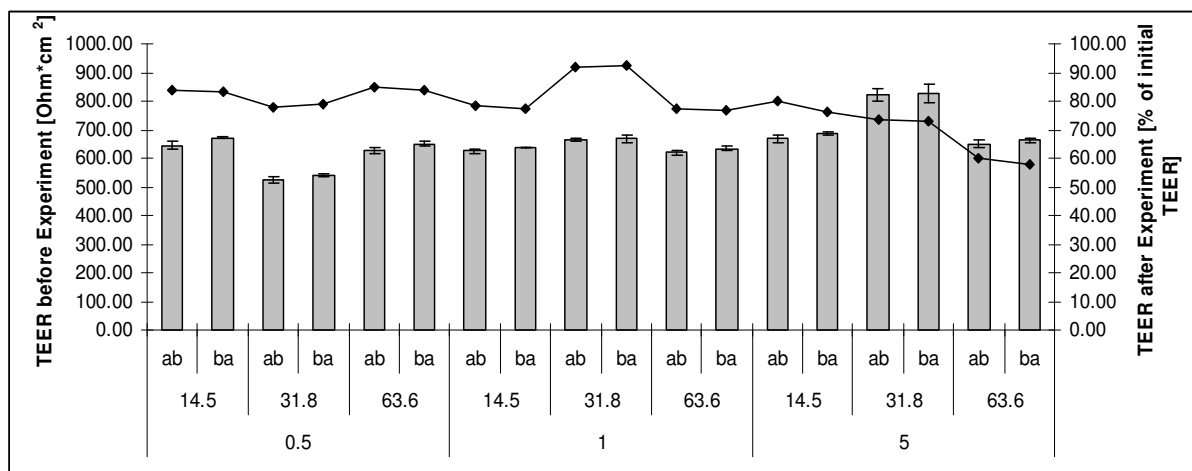


Figure 43 TEER values of Caco-2 cell monolayer used in the experiments with propranolol microemulsions. The columns display the absolute values measured before the experiments and the connected points the TEER values after the experiment in % of the initial values. At least 3 wells were used per group. Meaning of the x-axis labels: ab apical to basal transport, ba basal to apical transport; numbers in the middle row: used drug concentration [μM]; numbers in the bottom row: used lipid concentrations [mg/ml].

6.1.3 Emulsions

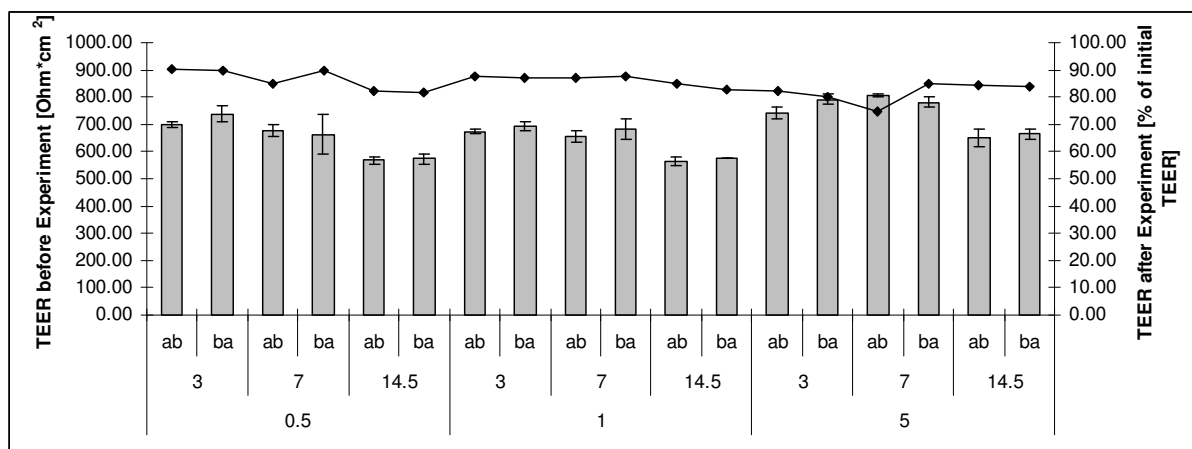


Figure 44 TEER values of Caco-2 cell monolayer used in the experiments with saquinavir emulsions. The columns display the absolute values measured before the experiments and the connected points the TEER values after the experiment in % of the initial values. At least 3 wells were used per group. Meaning of the x-axis labels: ab apical to basal transport, ba basal to apical transport; numbers in the middle row: used drug concentration [μM]; numbers in the bottom row: used lipid concentrations [mg/ml].

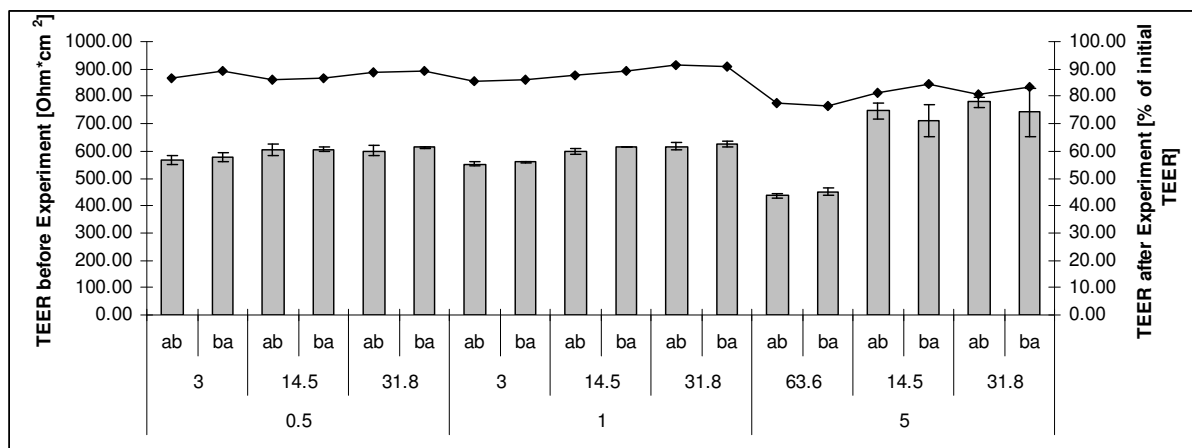


Figure 45 TEER values of Caco-2 cell monolayer used in the experiments with progesterone emulsions. The columns display the absolute values measured before the experiments and the connected points the TEER values after the experiment in % of the initial values. At least 3 wells were used per group. Meaning of the x-axis labels: ab apical to basal transport, ba basal to apical transport; numbers in the middle row: used drug concentration [μM]; numbers in the bottom row: used lipid concentrations [mg/ml].

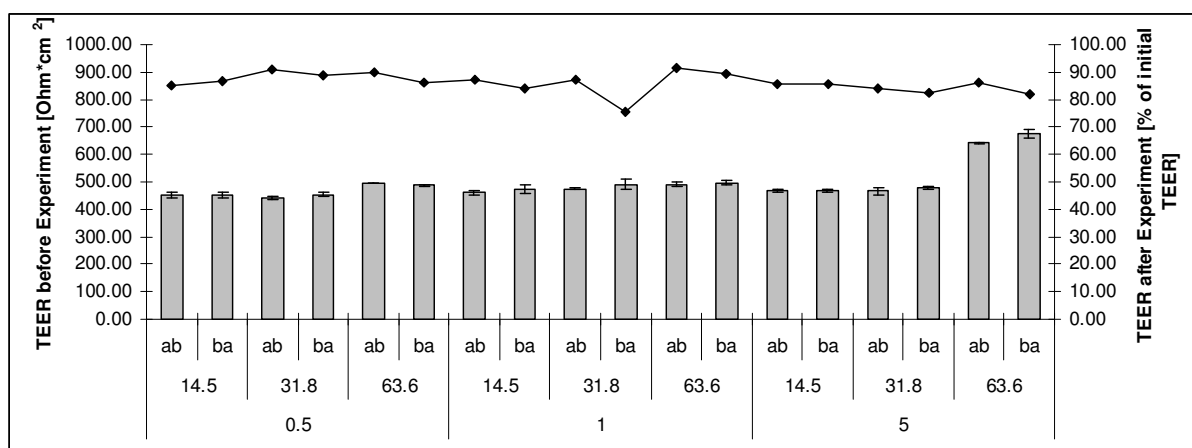


Figure 46 TEER values of Caco-2 cell monolayer used in the experiments with triclabendazole emulsions. The columns display the absolute values measured before the experiments and the connected points the TEER values after the experiment in % of the initial values. At least 3 wells were used per group. Meaning of the x-axis labels: ab apical to basal transport, ba basal to apical transport; numbers in the middle row: used drug concentration [μM]; numbers in the bottom row: used lipid concentrations [mg/ml].

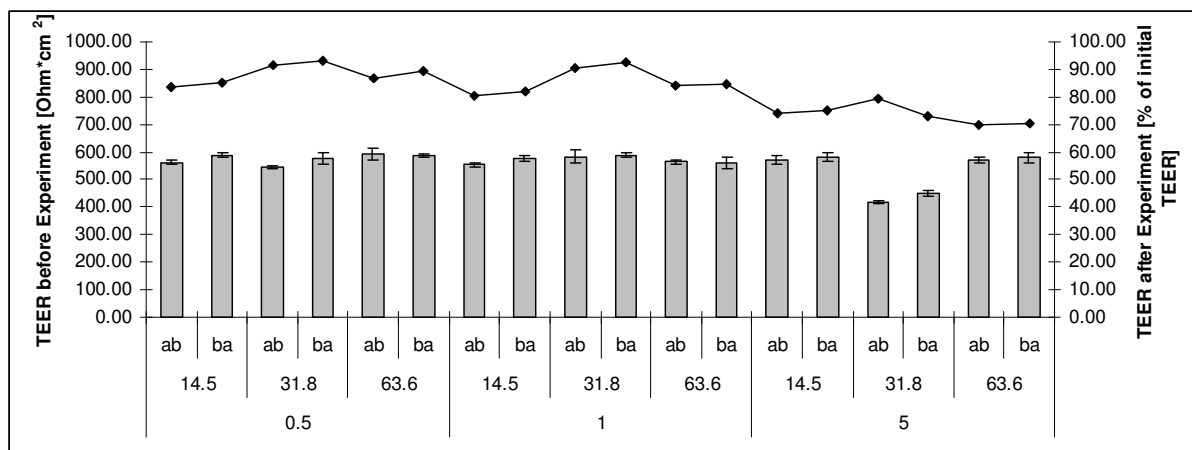


Figure 47 TEER values of Caco-2 cell monolayer used in the experiments with propranolol emulsions. The columns display the absolute values measured before the experiments and the connected points the TEER values after the experiment in % of the initial values. At least 3 wells were used per group. Meaning of the x-axis labels: ab apical to basal transport, ba basal to apical transport; numbers in the middle row: used drug concentration [μM]; numbers in the bottom row: used lipid concentrations [mg/ml].

6.1.4 Liposomes

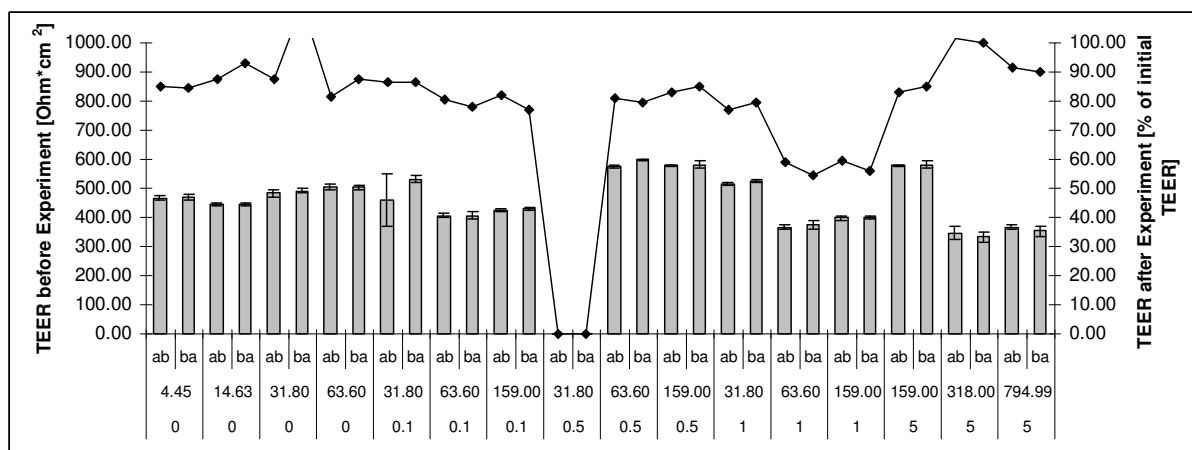


Figure 48 TEER values of Caco-2 cell monolayer used in the experiments with progesterone liposomes (lipid concentrations from 0-5 mg/ml). The columns display the absolute values measured before the experiments and the connected points the TEER values after the experiment in % of the initial values. At least 3 wells were used per group. Meaning of the x-axis labels: ab apical to basal transport, ba basal to apical transport; numbers in the middle row: used drug concentration [μM]; numbers in the bottom row: used lipid concentrations [mg/ml].

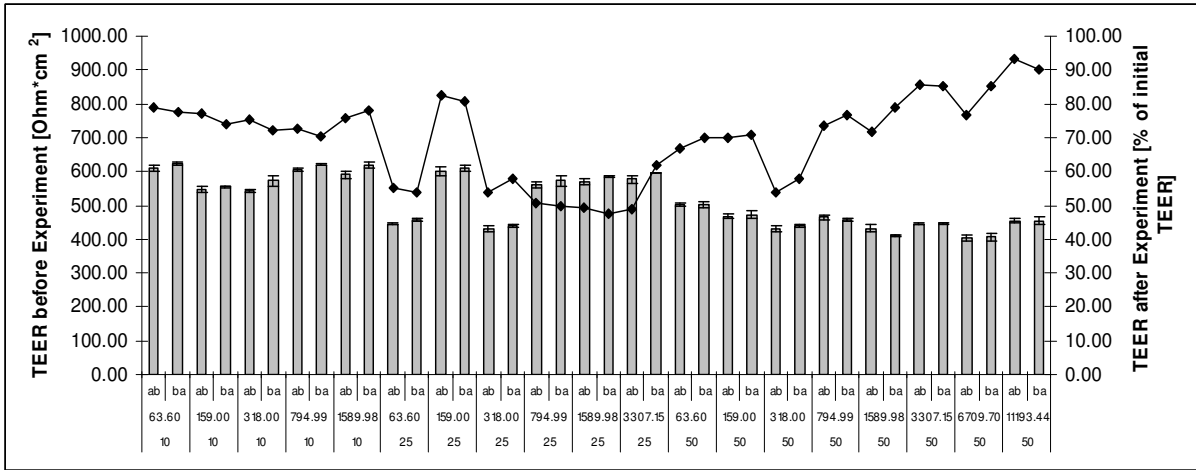


Figure 49 TEER values of Caco-2 cell monolayer used in the experiments with progesterone liposomes (lipid concentrations from 10-50 mg/ml). The columns display the absolute values measured before the experiments and the connected points the TEER values after the experiment in % of the initial values. At least 3 wells were used per group. Meaning of the x-axis labels: ab apical to basal transport, ba basal to apical transport; numbers in the middle row: used drug concentration [µM]; numbers in the bottom row: used lipid concentrations [mg/ml].

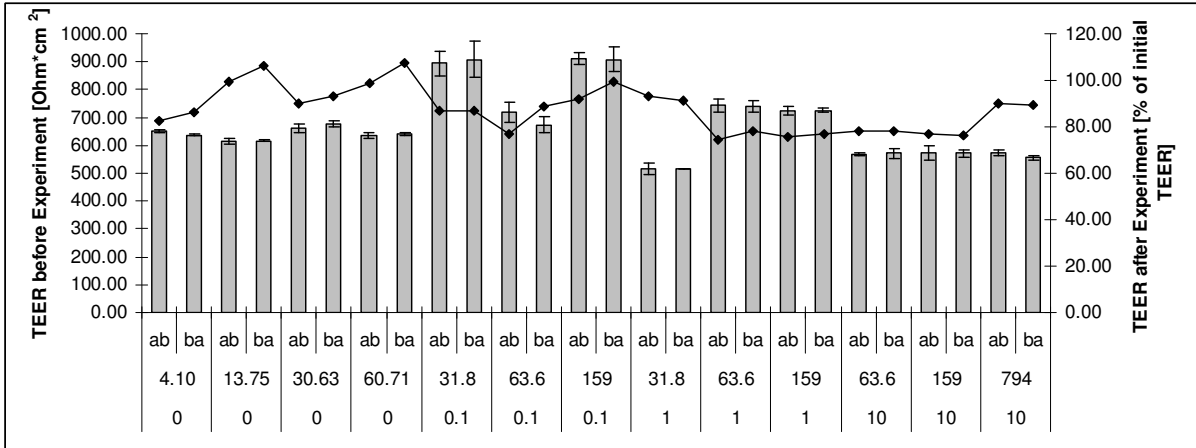


Figure 50 TEER values of Caco-2 cell monolayer used in the experiments with propranolol liposomes. The columns display the absolute values measured before the experiments and the connected points the TEER values after the experiment in % of the initial values. At least 3 wells were used per group. Meaning of the x-axis labels: ab apical to basal transport, ba basal to apical transport; numbers in the middle row: used drug concentration [µM]; numbers in the bottom row: used lipid concentrations [mg/ml].

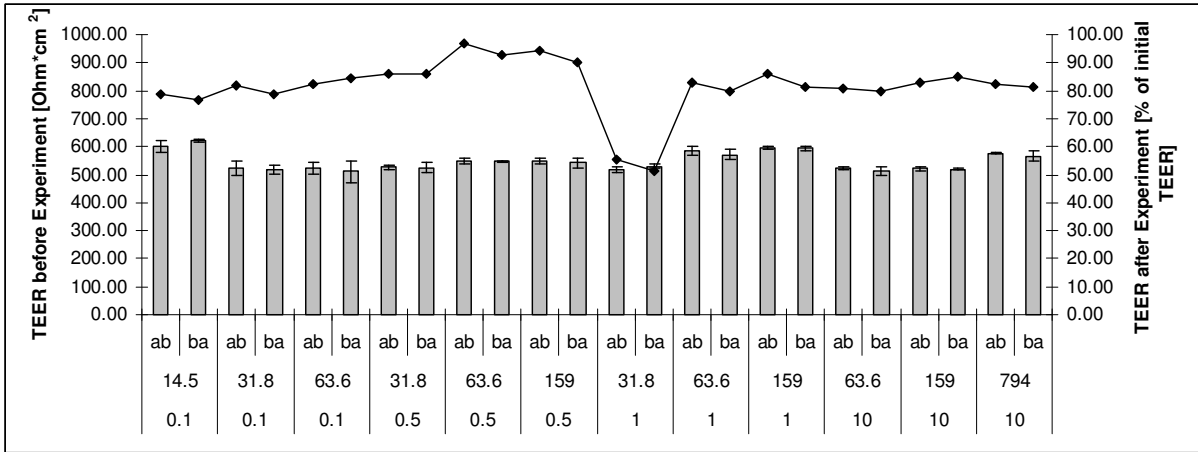


Figure 51 TEER values of Caco-2 cell monolayer used in the experiments with triclabendazole liposomes. The columns display the absolute values measured before the experiments and the connected points the TEER values after the experiment in % of the initial values. At least 3 wells were used per group. Meaning of the x-axis labels: ab apical to basal transport, ba basal to apical transport; numbers in the middle row: used drug concentration [μM]; numbers in the bottom row: used lipid concentrations [mg/ml].

6.2 Drug Extraction from Caco-2 Cell Monolayer at the Endpoint of the Transport Experiments

Table 17 to Table 20 show the obtained intracellular concentrations obtained of cell monolayer extraction at the endpoint of the transport studies. Formulation-to-cell partition coefficients were calculated out of the different concentrations in the compartments at the endpoint of the experiments. These are in apical to basal direction the apical to cell and the basal to cell partition coefficient, in basal to apical direction the basal to cell and the apical to cell partition coefficient, respectively. The average of these four partition coefficients are shown in the tables as $K_{a/C}$ and were very similar to the $K_{a/C}$ obtained by data fitting.

Table 17 Cell extractions and calculated $K_{a/C}$ values of liposome permeation experiments of progesterone (PG) formulations.

Drug	Lipid content [mg/ml]	Drug Conc. [μ M]	Cellular Drug Conc a_b [μ M]	Cellular Drug Conc b_a [μ M]	C_a end a-b [μ M]	C_b end ab [μ M]	C_a end b-a [μ M]	C_b end b-a [μ M]	Average $K_{a/C}$
PG	0	4.45	0.00	28.40	0.73	0.77	1.53	1.56	0.0545
	0	14.63	34.89	40.14	2.93	5.94	3.07	6.09	0.1206
	0	31.80	154.63	171.13	7.17	7.30	13.08	13.73	0.0626
	0	63.60	659.14	1202.80	16.19	16.30	31.56	31.53	0.0254
	0.1	31.80	120.48	210.75	8.25	7.62	14.84	14.89	0.0682
	0.1	63.60	655.13	1401.48	18.51	19.00	36.00	34.46	0.0269
	0.1	159.00	1265.95	1595.05	43.07	44.69	71.01	69.51	0.0394
	0.5	31.80	137.29	220.20	9.74	5.24	13.85	17.07	0.0624
	0.5	63.60	230.18	368.87	17.04	15.74	26.69	29.41	0.0736
	0.5	159.00	538.60	800.13	47.36	42.50	73.22	85.49	0.0913
	1	31.80	95.92	140.50	10.02	10.46	17.05	17.80	0.1154
	1	63.60	120.34	267.28	19.09	21.14	36.47	34.24	0.1497
	1	159.00	695.45	1049.61	51.52	46.67	80.61	83.16	0.0743
	5	159.00	465.23	775.51	61.64	46.78	86.23	102.01	0.1189
	5	318.00	766.21	1130.61	135.32	113.63	196.75	217.46	0.1728
	5	794.99	1234.39	2077.54	311.00	223.86	428.03	511.03	0.2213
	10	63.60	20.22	11.38	28.98	19.26	28.67	43.95	2.1919
	10	159.00	61.49	87.79	65.10	41.32	77.25	104.04	0.9489
	10	318.00	158.53	223.20	148.86	90.46	144.80	205.20	0.7694
	10	794.99	548.91	704.78	372.37	242.50	437.40	583.10	0.6420
	10	1589.98	666.88	899.45	734.56	412.87	801.05	1133.16	0.9678
	25	63.60	1.61	4.63	38.16	14.63	23.22	48.90	12.1086
	25	159.00	86.48	82.82	93.64	35.25	62.63	115.00	0.9088
	25	318.00	35.22	38.87	192.49	62.34	108.33	242.79	4.0674
	25	794.99	185.05	178.08	507.55	152.88	276.51	632.48	2.1684
	25	1589.98	304.93	333.71	1033.54	271.25	528.66	1292.86	2.4343
	25	3307.15	1241.57	1106.94	2044.42	608.99	1042.78	2538.78	1.3432
	50	63.60	62.65	60.29	47.30	12.28	17.22	61.62	0.5647
	50	159.00	23.55	19.89	110.45	24.32	42.83	129.46	3.5962
	50	318.00	46.72	32.68	215.48	37.30	66.91	252.34	3.7949
	50	794.99	63.97	114.37	596.49	102.28	183.26	679.98	4.6177
	50	1589.98	495.75	363.80	1101.94	240.24	359.43	1262.80	1.7916
	50	3307.15	1506.21	910.71	3427.77	512.65	931.84	3953.98	1.9952
	50	6709.70	1954.92	1505.31	3603.25	736.25	1319.70	5410.18	1.6726
	50	11193.44	8069.20	2107.93	9923.23	1315.14	2179.33	8534.93	1.6189

Table 18 Cell extractions and calculated $K_{a/C}$ values of liposome permeation experiments of tricloabendazole (TBZ) and propranolol (PPL) formulations.

Drug	Lipid content [mg/ml]	Drug Conc. [μ M]	Cellular Drug Conc a_b [μ M]	Cellular Drug Conc b_a [μ M]	C_a end a-b [μ M]	C_b end ab [μ M]	C_a end b-a [μ M]	C_b end b-a [μ M]	Average $K_{a/C}$
PPL	0	60.71	252.33	376.64	19.44	15.83	36.22	29.48	0.0786
	0	30.63	n.d.	n.d.	10.13	7.90	18.82	14.60	n.d.
	0	13.75	n.d.	88.30	5.04	3.13	8.26	6.10	0.0813
	0	4.10	n.d.	n.d.	1.56	1.29	2.59	1.93	n.d.
	0.1	31.8	141.94	246.37	10.16	10.29	15.15	15.37	0.0670
	0.1	63.6	294.14	472.63	17.56	14.64	30.65	25.55	0.0571
	0.1	159	299.52	394.31	46.24	47.23	81.71	87.93	0.1856
	1	31.8	53.37	85.52	7.16	6.88	15.06	13.88	0.1504
	1	63.6	283.91	402.54	16.52	14.06	25.84	26.22	0.0593
	1	159	382.88	528.89	43.94	42.01	73.95	75.33	0.1267
	10	63.6	63.35	77.70	17.81	14.78	25.76	28.83	0.3043
	10	159	99.29	146.16	38.76	31.23	62.22	60.55	0.3862
	10	794	741.33	1388.24	271.28	214.28	399.55	452.47	0.3172
TBZ	0.1	14.5	311.67	303.71	2.59	1.36	2.34	4.19	0.0085
	0.1	31.8	421.76	384.65	8.25	3.48	6.62	12.21	0.0192
	0.1	63.6	1042.52	978.04	23.60	12.47	17.61	36.11	0.0224
	0.5	31.8	279.46	132.46	22.78	3.99	7.90	28.72	0.0931
	0.5	63.6	522.38	246.24	29.53	4.89	9.91	34.97	0.0620
	0.5	159	960.73	494.59	80.36	13.39	27.84	98.51	0.0883
	1	31.8	114.23	48.75	23.60	3.04	5.75	27.79	0.2303
	1	63.6	217.46	120.93	41.01	4.22	9.46	40.63	0.1555
	1	159	309.45	255.17	104.03	12.18	22.50	111.84	0.2255
	10	63.6	34.94	8.27	49.83	1.66	2.89	50.58	1.9857
10	159	74.18	43.20	143.92	5.93	11.24	140.37	1.3824	
10	794	669.20	212.06	642.85	24.02	51.60	572.38	0.9847	

n.d.: not determined

Table 19 Cell extractions and calculated $K_{a/C}$ values of all microemulsion permeation experiments. Abbreviations: Progesterone (PG), triclobandazole (TBZ), propranolol (PPL), saquinavir (SQV)

Drug	Lipid Content [mg/ml]	Drug Conc. [μ M]	Cellular Drug Conc a_b [μ M]	Cellular Drug Conc b_a [μ M]	C_a end a-b [μ M]	C_b end ab [μ M]	C_a end b-a [μ M]	C_b end b-a [μ M]	Average $K_{a/C}$
PG	0	4.45	0.00	28.40	0.73	0.77	1.53	1.56	0.0545
	0	14.63	34.89	40.14	2.93	5.94	3.07	6.09	0.1206
	0	31.80	154.63	171.13	7.17	7.30	13.08	13.73	0.0626
	0	63.60	659.14	1202.80	16.19	16.30	31.56	31.53	0.0254
	0.5	14.5	26.27	58.46	1.81	1.68	5.05	3.83	0.0712
	0.5	31.8	782.33	938.45	9.11	9.32	14.91	13.84	0.0135
	0.5	63.6	139.94	163.04	10.06	11.44	16.96	16.43	0.0896
	1	14.5	57.01	77.42	3.27	2.82	6.18	6.81	0.0686
	1	31.8	267.29	821.54	8.58	9.58	15.97	18.26	0.0274
	1	63.6	61.68	136.74	10.64	12.69	19.66	13.94	0.1560
	5	14.5	16.94	24.21	6.50	2.91	5.26	9.02	0.2864
	5	31.8	n.d.	n.d.	20.89	12.54	20.25	29.16	n.d.
	5	63.6	79.71	144.59	30.37	14.36	26.07	42.70	0.2592
PPL	0	60.71	252.33	376.64	19.44	15.83	36.22	29.48	0.0786
	0	30.63	n.d.	n.d.	10.13	7.90	18.82	14.60	n.d.
	0	13.75	n.d.	88.30	5.04	3.13	8.26	6.10	0.0813
	0	4.10	n.d.	n.d.	1.56	1.29	2.59	1.93	n.d.
	0.5	14.5	81.47	120.70	5.63	5.08	8.19	6.76	0.0639
	0.5	31.8	n.d.	n.d.	14.11	12.16	27.82	24.14	n.d.
	0.5	63.6	359.70	607.11	22.92	20.53	39.36	35.03	0.0608
	1	14.5	90.63	147.65	5.74	4.96	9.87	8.15	0.0600
	1	31.8	n.d.	n.d.	23.65	15.28	44.50	35.28	n.d.
	1	63.6	393.03	455.59	23.25	21.38	40.46	36.17	0.0704
	5	14.5	68.62	82.17	7.01	6.16	11.47	9.64	0.1122
	5	31.8	n.d.	n.d.	10.34	9.17	19.12	15.18	n.d.
	5	63.6	149.51	280.15	27.13	22.62	46.51	38.67	0.1592
TBZ	0.5	14.5	102.97	77.80	8.02	1.90	4.26	9.92	0.0697
	0.5	31.8	n.d.	n.d.	16.24	4.76	9.87	32.86	n.d.
	0.5	63.6	476.17	316.87	30.55	6.90	14.93	33.31	0.0577
	1	14.5	5.88	4.93	9.05	2.43	4.65	11.99	1.3319
	1	31.8	n.d.	n.d.	28.56	8.58	15.96	43.90	n.d.
	1	63.6	26.67	19.39	38.91	9.39	18.68	48.54	1.3196
	5	14.5	33.79	20.05	18.57	1.48	2.84	19.26	0.4239
	5	31.8	34.87	22.41	31.49	2.30	4.36	31.80	0.6457
	5	63.6	125.91	68.68	57.86	4.50	8.58	65.12	0.3921
SQV	0	14	n.d.	n.d.	n.d.	n.d.	n.d.	n.d.	n.d.
	0	5	n.d.	n.d.	n.d.	n.d.	n.d.	n.d.	n.d.
	0	4.5	n.d.	n.d.	n.d.	n.d.	n.d.	n.d.	n.d.
	0	10.4	n.d.	n.d.	n.d.	n.d.	n.d.	n.d.	n.d.
	0.5	3	1.00	1.62	1.08	0.02	1.24	0.41	0.5314
	0.5	7	1.70	2.53	2.58	0.08	2.76	1.07	0.7701
	0.5	14.5	n.d.	n.d.	18.62	0.09	23.12	5.50	n.d.
	1	3	1.98	1.31	2.19	0.02	1.88	1.13	0.8525
	1	7	1.74	1.46	5.68	0.08	5.29	3.18	2.2763
	1	14.5	n.d.	n.d.	22.12	0.10	16.47	11.32	n.d.
	5	3	2.08	1.71	3.23	0.18	1.02	2.87	0.9800
	5	7	1.63	1.41	5.66	0.18	1.56	5.08	2.0707
	5	14.5	n.d.	n.d.	19.40	0.65	5.53	18.04	n.d.

n.d.: not determined

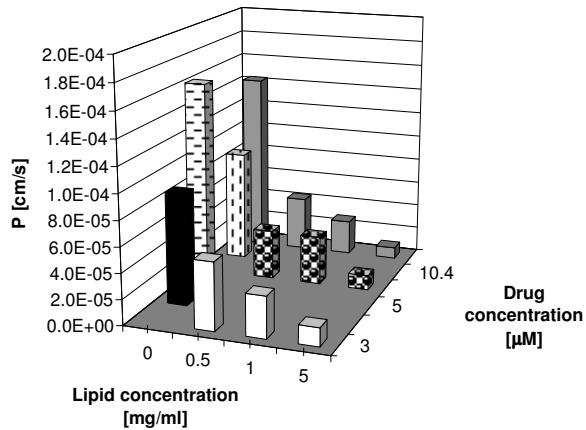
Table 20 Cell extractions and calculated $K_{a/c}$ values of all emulsion permeation experiments. Abbreviations: Progesterone (PG), triclabendazole (TBZ), propranolol (PPL), saquinavir (SQV)

Drug	Lipid content [mg/ml]	Drug conc. [μ M]	Cellular drug conc a_b [μ M]	Cellular drug conc b_a [μ M]	C_a end a-b [μ M]	C_b end ab [μ M]	C_a end b-a [μ M]	C_b end b-a [μ M]	Average $K_{a/c}$
PG	0	4.45	0.00	28.40	0.73	0.77	1.53	1.56	0.0545
	0	14.63	34.89	40.14	2.93	5.94	3.07	6.09	0.1206
	0	31.80	154.63	171.13	7.17	7.30	13.08	13.73	0.0626
	0	63.60	659.14	1202.80	16.19	16.30	31.56	31.53	0.0254
	0.5	3	0.79	2.67	0.68	0.72	1.24	1.08	0.6625
	0.5	14.5	31.96	57.26	3.70	3.31	6.30	5.95	0.1084
	0.5	31.8	84.57	128.56	8.43	8.14	15.85	14.36	0.1077
	1	3	0.64	1.70	0.49	0.70	1.27	1.14	0.8167
	1	14.5	9.70	35.80	4.94	4.82	9.34	8.43	0.3757
	1	31.8	19.66	30.62	7.80	7.20	13.78	12.87	0.4083
	5	14.5	2.51	2.08	5.39	4.05	6.59	9.27	2.8439
	5	31.8	5.12	12.55	14.67	11.56	21.99	23.84	2.1936
	5	63.6	151.77	241.63	20.90	14.45	27.07	36.36	0.1239
PPL	0	60.71	252.33	376.64	19.44	15.83	36.22	29.48	0.0786
	0	30.63	n.d.	n.d.	10.13	7.90	18.82	14.60	n.d.
	0	13.75	n.d.	88.30	5.04	3.13	8.26	6.10	0.0813
	0	4.10	n.d.	n.d.	1.56	1.29	2.59	1.93	n.d.
	0.5	14.5	151.50	272.31	7.78	7.00	11.76	9.81	0.0442
	0.5	31.8	313.11	434.55	14.67	12.91	23.37	18.59	0.0462
	0.5	63.6	350.24	640.52	25.71	22.34	44.80	38.04	0.0666
	1	14.5	374.60	504.37	5.25	4.23	8.86	6.98	0.0142
	1	31.8	403.35	482.99	11.42	10.11	19.69	16.60	0.0321
	1	63.6	133.04	219.57	22.84	19.84	39.06	32.72	0.1619
	5	14.5	63.71	96.93	7.83	7.32	11.21	10.38	0.1151
	5	31.8	161.34	256.88	12.75	11.06	20.94	19.63	0.0764
	5	63.6	187.65	276.19	24.31	23.77	40.55	38.47	0.1356
TBZ	0.5	14.5	81.13	59.74	9.52	2.02	5.84	12.58	0.1126
	0.5	31.8	139.62	125.60	15.69	2.78	6.89	17.16	0.0809
	0.5	63.6	326.65	196.38	24.74	4.69	11.20	27.19	0.0714
	1	14.5	51.75	40.62	8.46	1.70	3.27	10.92	0.1364
	1	31.8	122.66	85.44	19.63	2.54	9.33	20.77	0.1333
	1	63.6	179.51	128.57	40.76	6.23	14.09	44.39	0.1792
	5	14.5	26.18	22.66	14.92	0.70	2.34	16.32	0.3550
	5	31.8	40.36	30.47	27.85	2.19	4.89	30.24	0.4743
	5	63.6	70.51	49.40	59.14	6.42	12.34	59.87	0.5978
SQV	0	14	n.d.	n.d.	n.d.	n.d.	n.d.	n.d.	n.d.
	0	5	n.d.	n.d.	n.d.	n.d.	n.d.	n.d.	n.d.
	0	4.5	n.d.	n.d.	n.d.	n.d.	n.d.	n.d.	n.d.
	0	10.4	n.d.	n.d.	n.d.	n.d.	n.d.	n.d.	n.d.
	0.5	3	0.36	1.65	1.75	0.07	2.65	0.41	1.7413
	0.5	7	0.12	1.94	2.89	0.07	3.32	1.02	6.8533
	0.5	14.5	2.11	6.90	7.89	0.21	10.92	1.85	1.4228
	1	3	0.09	1.04	2.77	0.07	3.14	1.11	8.7227
	1	7	0.21	2.75	3.55	0.07	4.29	1.22	4.8349
	1	14.5	2.37	5.97	11.80	0.19	11.40	5.07	1.9555
	5	3	0.18	0.33	2.68	0.09	1.67	1.89	6.5866
	5	7	0.26	0.56	5.08	0.21	2.72	3.90	8.0184
	5	14.5	0.38	1.52	13.56	0.20	6.08	10.38	11.6663

n.d.: not determined

6.3 Additional Figures of Qualitative Influence of Lipid Phase Concentration on Apparent Permeability Coefficient

A Saquinavir Emulsion



B Saquinavir Microemulsion

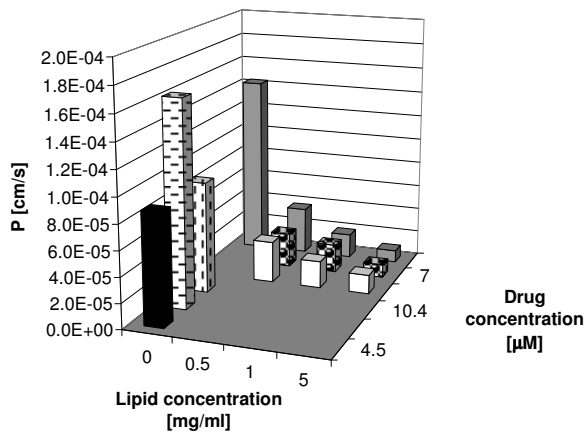
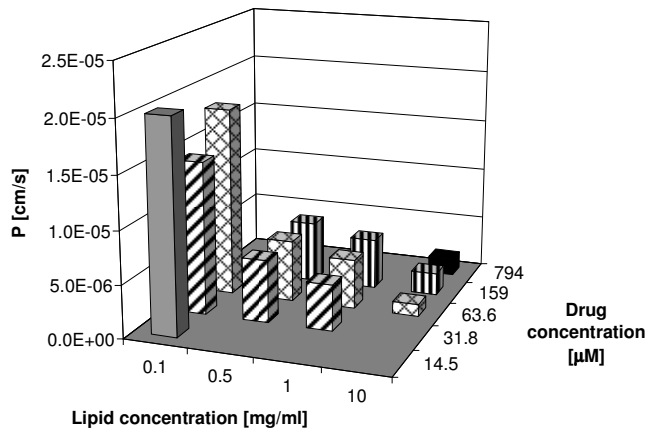
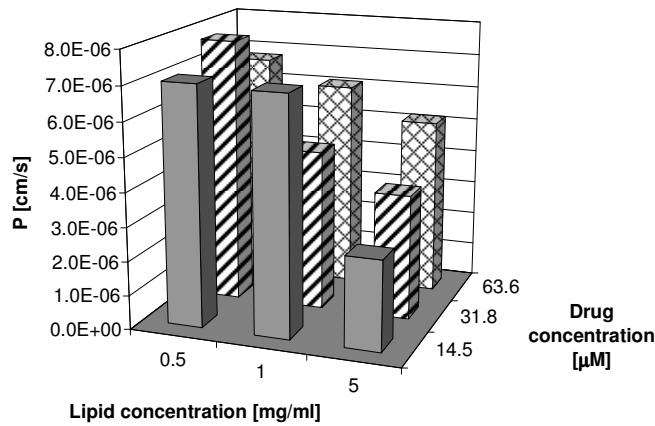


Figure 52 Qualitative influence of the lipid concentration on apparent permeability coefficient of the tested saquinavir formulations: Panel A shows the influence of lipid phase concentrations of the emulsion, and panel B shows the influence of the lipid phase of the microemulsion on the apparent permeability coefficient. Same pattern or color indicates same drug concentration. Each column represents the deduced apparent permeability coefficient out of one transport experiment (n=3).

A Triclabendazole Liposomes



B Triclabendazole Emulsion



C Triclabendazole Microemulsion

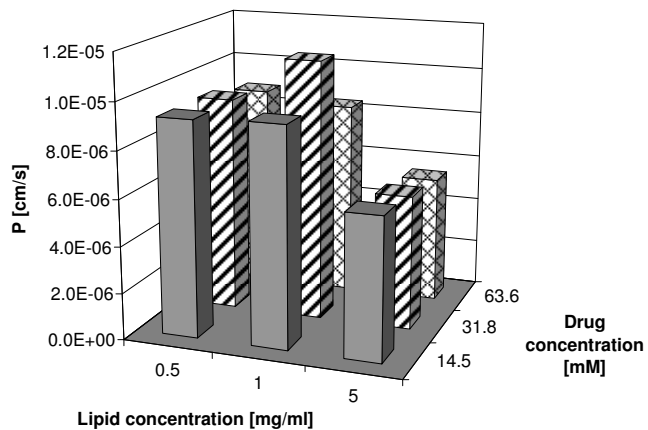
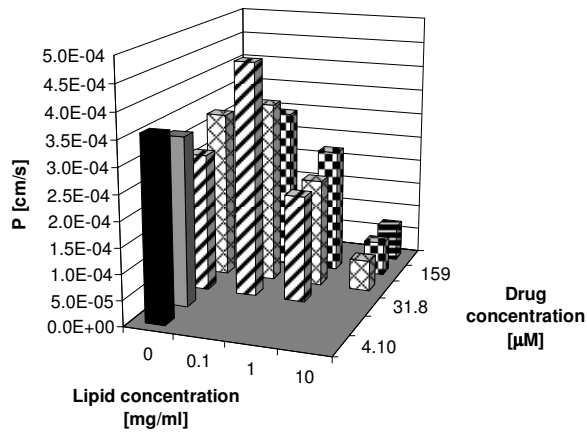
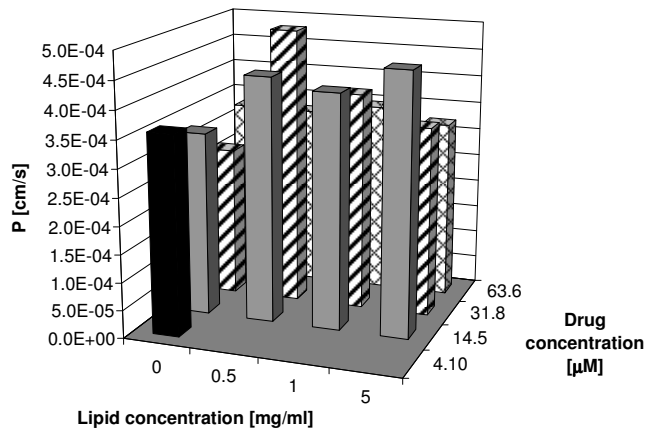


Figure 53 Qualitative influence of the lipid concentration on apparent permeability coefficient of the tested triclabendazole formulations: Panel A shows the influence of the liposomes, panel B shows the influence of lipid phase concentrations of the emulsion, and panel C shows the influence of the lipid phase of the microemulsion on the apparent permeability coefficient. Same pattern or color indicates same drug concentration. Each column represents the deduced apparent permeability coefficient out of one transport experiment (n=3).

A Propranolol Liposomes



B Propranolol Emulsion



C Propranolol Microemulsion

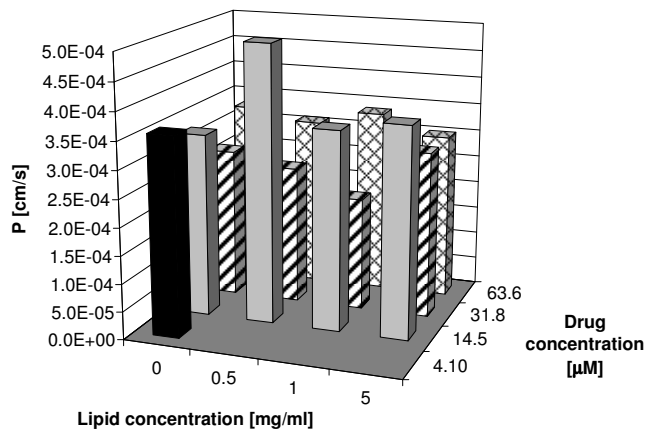


Figure 54 Qualitative influence of the lipid concentration on apparent permeability coefficient of the tested propranolol formulations: Panel A shows the influence of the liposomes, panel B shows the influence of lipid phase concentrations of the emulsion, and panel C shows the influence of the lipid phase of the microemulsion on the apparent permeability coefficient. Same pattern or color indicates same drug concentration. Each column represents the deduced apparent permeability coefficient out of one transport experiment (n=3).

6.4 Determination of Maximal Drug Solubility in Formulation Lipid Phases and Calculation of Theoretical Maximal Fluxes

For a prediction of the maximal drug load in transport experiments and to avoid oversaturated conditions using emulsions and microemulsions, the maximal drug solubility in the lipid phase was determined for each drug.

6.4.1 Methods

To determine the saturation solubility of the used drugs in transport media and the lipid phases of the microemulsion and the emulsion, 0.5 ml of transport media or lipid phase, all tempered to 37°C, were pipetted into a microtube. The drug was added to the samples in exceeding the solubility. The microtubes were sealed with two layers of Parafilm additionally and shaken at 37°C and 1000 rpm. After 12 h the tubes were checked and if all drug was dissolved, more drug was added. After equilibration for at least 48 h, the microtubes were spun for 3 min at 14000 rpm on an Eppendorf centrifuge. Samples of 50 µl of clear supernatant were taken and diluted 1:10'000 with transport media before analyzing them by HPLC.

6.4.2 Results

The results of the maximal solubility in the lipid phases (c_{ss}) are shown in Table 21. Besides of the maximal solubility, this table contains additional information. It displays the theoretical maximal possible drug load of a formulation containing the maximal lipid concentration. Out of permeability coefficient within the maximal lipid concentration, a theoretical maximal flux was calculated.

Table 21 Maximal drug solubility in the lipid phase (c_{ss}) and theoretical maximal flux

Formulation	lipid content [mg/ml]	c_{ss} in Transport Media [µM], 37°C	c_{ss} in lipid phase [µM] 37°C	drug conc. [µM]	P_{app} [cm/s]	maximal flux $J=P \cdot C_{ss}$ [µmol/(cm ² s)]
Progesterone solution	0	n.d	-	63.60	$2.9 \cdot 10^{-4}$	$1.85 \cdot 10^{-2}$
Progesterone liposomes	50	-	n.d.	11193.44	$8.5 \cdot 10^{-6}$	$9.54 \cdot 10^{-2}$
Progesterone emulsion	5	-	106800	534	$4.3 \cdot 10^{-5}$	$2.32 \cdot 10^{-2}$
Progesterone microemulsion	5	-	53066	260	$5.4 \cdot 10^{-5}$	$1.40 \cdot 10^{-2}$
Saquinavir solution	0	1.5	-	1.5	$1.2 \cdot 10^{-4}$	$1.81 \cdot 10^{-4}$
Saquinavir emulsion	5	-	6490	32.4	$1.2 \cdot 10^{-5}$	$3.78 \cdot 10^{-4}$
Saquinavir microemulsion	5	-	29056	145	$1.2 \cdot 10^{-5}$	$1.70 \cdot 10^{-3}$
Propranolol solution	0	1243	-	1243	$3.2 \cdot 10^{-4}$	$4.01 \cdot 10^{-1}$
Propranolol liposomes	10	-	n.d.	794	$6.6 \cdot 10^{-5}$	$5.25 \cdot 10^{-2}$
Propranolol emulsion	5	-	n.d.	63.6	$3.8 \cdot 10^{-4}$	$2.40 \cdot 10^{-2}$
Propranolol microemulsion	5	-	53700	269	$3.3 \cdot 10^{-4}$	$8.79 \cdot 10^{-2}$
Triclabendazole solution	0	0.39	-	0.39	$2.3 \cdot 10^{-4}$	$8.79 \cdot 10^{-5}$
Triclabendazole liposomes	10	-	n.d.	794	$1.6 \cdot 10^{-6}$	$1.30 \cdot 10^{-3}$
Triclabendazole emulsion	5	-	36757	183	$3.8 \cdot 10^{-6}$	$7.02 \cdot 10^{-4}$
Triclabendazole microemulsion	5	-	158974	791	$5.8 \cdot 10^{-6}$	$4.56 \cdot 10^{-3}$

6.5 Determination of Inorganic and Organic Phosphate of the Acceptor Compartment after Equilibrium Dialysis of a Liposome Formulation

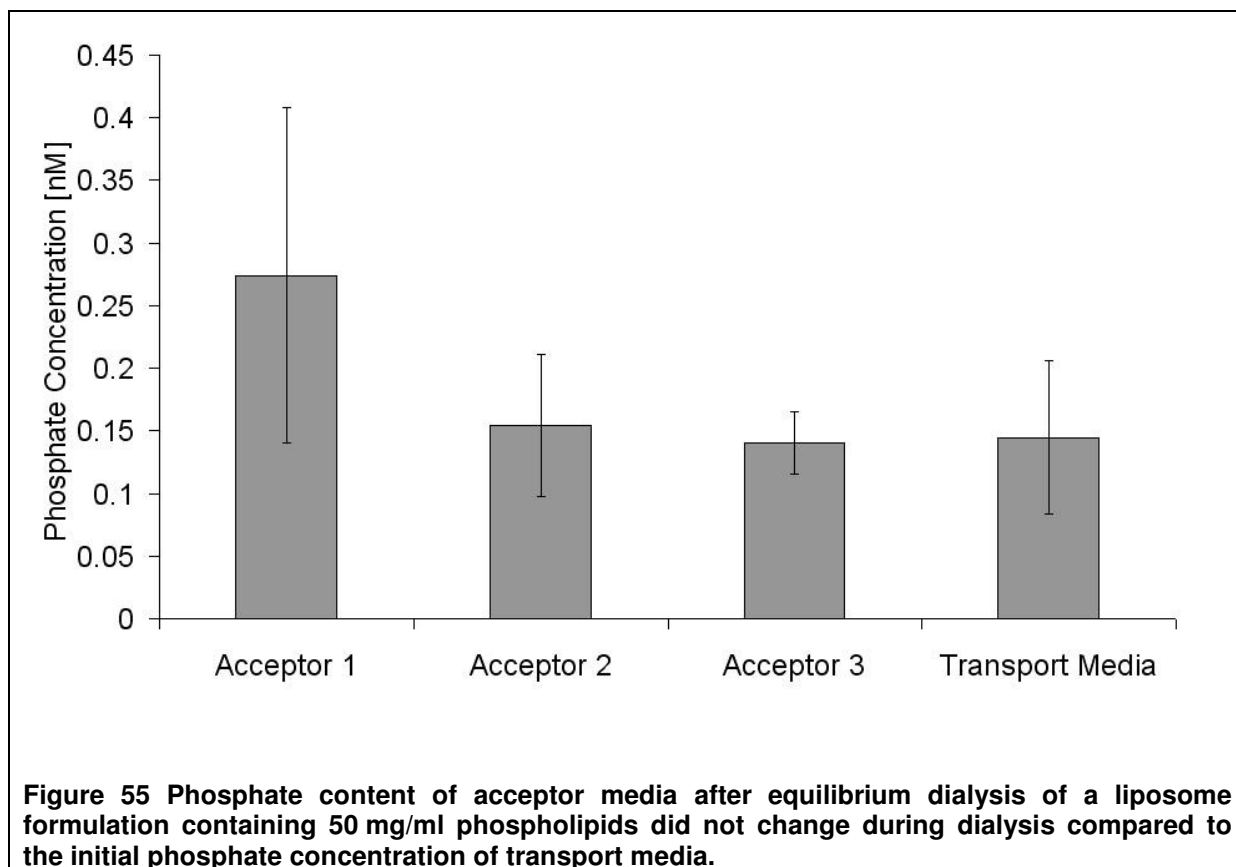
If phosphatidylcholine is in contact with an aqueous environment, a degradation product, lyso-phosphatidylcholine, may occur. This degradation product has surfactant like properties and may influence the solubility of a poor soluble drug in transport media. Because of its mass of approximately 500 D it may pass the dialysis membrane and therefore alter drug partition between lipid- and water phase. Diffusion of lyso-phosphatidylcholine through the dialysis membrane can be determined by measuring the change of (anorganic and organic) phosphate content in acceptor compartment.

6.5.1 Material and Methods

Liposomes containing 50 mg/ml phospholipids were dialyzed as described and after 40 h of dialysis phosphate content of the acceptor compartment was determined and compared with transport media that contains a phosphate buffer. A method where phosphor in organic molecules is converted by sulfuric acid to anorganic phosphate was used to determine the organic and the anorganic phosphate (143). The phosphate forms a complex with ammonium molybdat and malachite green that can be detected by extinction measurement at 610 nm. Quantification was performed against a set of external standard solutions out of potassium hydrogenphosphat within the linear response concentration range (0-12 nM). Samples of 10 µl were pipetted into test tubes and amended with 990 µl distilled water. Three aliquots of the standard solutions (100 µl each) and of the diluted samples (50 µl each) were pipetted into test tubes and 700 µl of a reagent containing 5%(V/V) sulfuric acid and 7%(V/V) of perchloric acid solution (20%) in distilled water. The samples were incubated 1 h at 150 °C and dried 2 h at 230 °C. After cooling down, 1000 µl distilled water was added to the tubes. Samples of 100 µl were transferred into 96-well plates (Nunc, Roskilde, Denmark) and mixed with 20 µl of a solution containing 1.25% (m/V) ammonium heptamolybdat in distilled water. After 20 min incubation at room temperature, 20 µl of a reagent, containing 0.35 g polyvinyl alcohol and 0.035 g malachite green in 100 ml reagent, was added and after an incubation of 10 min the samples were measured with a plate reader (Versamax Tunable Multiplate Reader, No. SIN/B 02553, Molecular Devices Corporation, Sunnyville, USA). All reagents were of analytical grade and purchased from SIGMA-Aldrich (Fluka Chemie, Buchs, Switzerland).

6.5.2 Results

The result of the equilibrium dialysis of a liposome formulation is shown in Figure 55. Phosphate content of acceptor transport media after equilibrium dialysis of a liposome formulation containing 50 mg/ml phospholipids did not change during dialysis compared to the initial phosphate concentration of transport media. This indicates that no phospholipids or degradation products cross the dialysis membrane during experimental duration.



6.5.3 Conclusions

No falsifying of the free fraction by phospholipids or degradation products of phospholipids is expected. Therefore, equilibrium dialysis under the chosen conditions is a valuable tool for the investigation of the liposomes used in this thesis.

6.6 Detailed Derivations of Used Models and Additional Calculations

6.6.1 Detailed Derivation of Delineation of Apparent Permeability Coefficient Based on a Biophysical Model

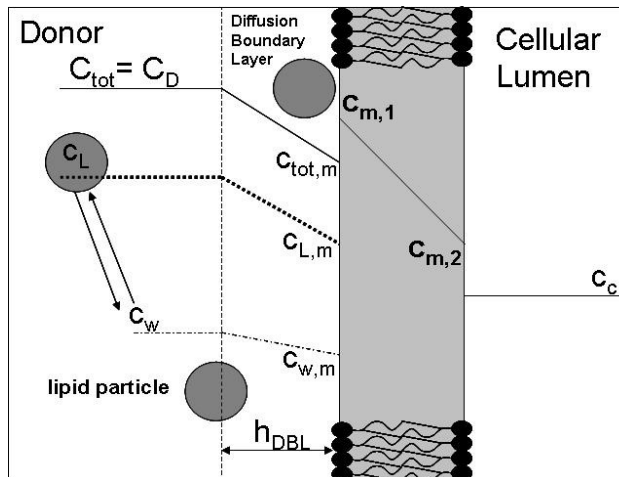


Figure 56 Schematic model of a substance flux over a Caco-2 cell monolayer. Donor and acceptor compartment contain lipid particles of the same formulation.

Substance fluxes are defined as flux through cell membrane J_m (Equation 67) and flux through diffusion boundary layer J_{DBL} (Equation 68):

$$J_m = \frac{D_m}{h_m} (c_{m,1} - c_{m,2})$$

Equation 67

where h_m denotes thickness of cell membrane, D_m diffusion coefficient of drug in cell membrane, $c_{m,1}$ drug concentration at cell membrane surface inside of the membrane, $c_{m,2}$ drug concentration at inner membrane surface inside of the membrane.

$$J_{DBL} = \frac{D_{w,d}}{h_{DBL}} \cdot (c_w - c_{w,m}) + \frac{D_{w,L}}{h_{DBL}} (c_L - c_{L,m})$$

Equation 68

The flux through diffusion boundary layer is composed of the flux of the free drug molecules and the flux of the lipid particles, where $c_{w,m}$ denotes drug concentration of the water phase at membrane surface, c_L drug concentration associated with lipid phase referring to total volume, $c_{L,m}$ drug concentration associated with lipid phase referring to total volume at membrane surface, c_w drug concentration in water phase, h_{DBL} thickness of diffusion boundary layer, $D_{w,d}$ the diffusion coefficient of drug in water phase, and $D_{w,L}$ diffusion coefficient of lipid particle in water phase.

The free fraction (z) of a drug is defined as ratio of drug concentration in the water phase of the formulation to the drug concentration in formulation denoted by c_{tot} :

$$\frac{c_w}{c_{tot}} = z$$

Equation 69

Substitutions that were used to replace unknown parameters were Equation 70 to Equation 75:

$$q = \frac{D_{w,d}}{D_{w,L}}$$

Equation 70

q is defined as ratio of diffusion coefficient of drug in water phase ($D_{w,d}$) to diffusion coefficient of lipid particle in water phase ($D_{w,L}$)

$$VF = \frac{V_w}{V_{tot}}$$

Equation 71

The volume fraction VF is defined as ratio of the volume of the water phase (V_w) to the volume of the formulation V_{tot} . The volume of the water phase was assumed to be

$$V_w = \frac{n_w \cdot 18}{\rho_w}$$

Equation 72

where n_w denotes the moles of water in the formulation, ρ_w the density of the water phase and the molecular weight of water was assumed to be 18 g/mol. The total volume of the formulation was assumed to be the sum of the volume of the water phase and the volume of the lipid phase

$$V_{tot} = \frac{n_w \cdot 18 + n_L \cdot MW_L}{\rho_{tot}}$$

Equation 73

where n_L denotes the moles of lipids in the formulation, MW_L the molecular weight of lipids, and ρ_{tot} the density of the formulation. where n_L denotes the moles of lipids in the formulation, MW_L the molecular weight of lipids, and ρ_{tot} the density of the formulation.

The mass of drug in lipid phase (m_L) was assumed to be the total mass of drug (m_{tot}) minus the mass of drug in water phase (m_w). This was used to express c_L with c_{tot} and c_w :

$$c_L = \frac{m_L}{V_{tot}} = \frac{m_{tot} - m_w}{V_{tot}} = \frac{c_{tot}V_{tot} - c_wV_w}{V_{tot}} = c_{tot} - c_w \frac{V_w}{V_{tot}} = c_{tot} - c_w VF = c_L$$

Equation 74

Equation 74 applies for bulk and with indices m (e.g. $c_{w,m}$) at cell membrane surface.

The unknown drug concentration at cell membrane surface inside of the membrane ($c_{m,1}$) was substituted by the following equation:

$$c_{m,1} = c_{w,m} \cdot K_{m/w} + c_{L,m} \cdot K_{m/L}$$

Equation 75

where $K_{m/w}$ denotes the partition coefficient of the free drug between aqueous phase and cell membrane and $K_{m/L}$ denotes the partition coefficient of the drug between lipid associated drug concentration and cell membrane.

The equation describing the fluxes through the membrane was transformed inserting Equation 75 into Equation 67 and rearranging yields:

$$\begin{aligned} J_m &= \frac{D_m}{h_m}(c_{m,1} - c_{m,2}) = \frac{D_m}{h_m}(c_{w,m} \cdot K_{m/w} + c_{l,m} \cdot K_{m/L} - c_{m,2}) \\ &= \frac{D_m \cdot K_{m/w}}{h_m} c_{w,m} + \frac{D_m \cdot K_{m/L}}{h_m} c_{l,m} - \frac{D_m}{h_m} c_{m,2} = P_{m,d} \cdot c_{w,m} + P_{m,L} \cdot c_{l,m} - \frac{D_m}{h_m} K_{m/c} \cdot c_c \end{aligned}$$

Equation 76

In Equation 76 denotes $P_{m,d}$ the permeability coefficient of the free drug through cell monolayer, $P_{m,L}$ the permeability coefficient of the drug because of direct drug transfer from lipid particle to the cell membrane, c_c cellular drug concentration and $K_{m/c}$ the partition coefficient between cellular drug concentration and cell membrane.

Inserting Equation 69 and Equation 74 into Equation 76 and rearranging yields:

$$J_m = c_{w,m} \left(P_{m,d} + \frac{P_{m,L}}{z} - P_{m,L} \cdot VF \right) - \frac{D_m}{h_m} K_{m/c} \cdot c_c$$

Equation 77

Inserting Equation 70 into Equation 68 and rearranging yields:

$$J_{DBL} = \frac{P_{dbl,d}}{q} \cdot (q c_w - q c_{w,m} + c_L - c_{L,m})$$

Equation 78

Where $P_{dbl,d}$ denotes the permeability coefficient of the free drug through diffusion boundary layer.

At steady state fluxes are set equal ($J_m = J_{DBL}$), Equation 69 and Equation 74 were inserted and the resulting equation was solved for the unknown concentration $c_{w,m}$.

$$\frac{P_{dbl,d}}{q} \cdot [(q z c_{tot} - q c_{w,m} + c_{tot} - c_w \cdot VF) - (c_{tot,m} - c_{w,m} VF)] = P_{m,d} \cdot c_{w,m} + P_{m,L} \cdot (c_{tot,m} - c_{w,m} VF) - \frac{D_m}{h_m} K_{m/c} \cdot c_c$$

Equation 79

$$\frac{P_{dbl,d}}{q} \cdot \left(q z c_{tot} - q c_{w,m} + c_{tot} - c_{tot} z \cdot VF - \frac{c_{w,m}}{z} + c_{w,m} VF \right) = P_{m,d} \cdot c_{w,m} + P_{m,L} \cdot \left(\frac{c_{w,m}}{z} - c_{w,m} VF \right) - \frac{D_m}{h_m} K_{m/c} \cdot c_c$$

Equation 80

$$\frac{P_{dbl,d}}{q} \cdot (q z c_{tot} + c_{tot} - c_{tot} z \cdot VF) + \frac{P_{dbl,d}}{q} \cdot \left(-q c_{w,m} - \frac{c_{w,m}}{z} + c_{w,m} VF \right) = c_{w,m} \left(P_{m,d} + \frac{P_{m,L}}{z} - P_{m,L} \cdot VF \right) - \frac{D_m}{h_m} K_{m/c} \cdot c_c$$

Equation 81

$$\frac{P_{dbl,d}}{q} \cdot (qz c_{tot} + c_{tot} - c_{tot} z \cdot VF) + c_{w,m} \cdot \frac{P_{dbl,d}}{q} \left(-q - \frac{1}{z} + VF \right) = c_{w,m} \left(P_{m,d} + \frac{P_{m,L}}{z} - P_{m,L} \cdot VF \right) - \frac{D_m}{h_m} K_{m/c} \cdot c_c$$

Equation 82

$$\frac{P_{dbl,d}}{q} \cdot (qz c_{tot} + c_{tot} - c_{tot} z \cdot VF) + \frac{D_m}{h_m} K_{m/c} \cdot c_c = c_{w,m} \cdot \left(P_{m,d} + \frac{P_{m,L}}{z} - P_{m,L} \cdot VF + \frac{P_{dbl,d}}{q} \left(q + \frac{1}{z} - VF \right) \right)$$

Equation 83

$$c_{w,m} = \frac{\frac{P_{dbl,d}}{q} \cdot c_{tot} (qz + 1 - z \cdot VF) + \frac{D_m}{h_m} K_{m/c} \cdot c_c}{P_{m,d} + \frac{P_{m,L}}{z} - P_{m,L} \cdot VF + \frac{P_{dbl,d}}{q} \left(q + \frac{1}{z} - VF \right)}$$

Equation 84

Equation 84 was inserted into Equation 77. Transformation of this equation after insertion resulted in:

$$J_m = \frac{\left(\frac{P_{dbl,d}}{q} \cdot c_{tot} (qz + 1 - z \cdot VF) + \frac{D_m}{h_m} K_{m/c} \cdot c_c \right) \cdot \left(P_{m,d} + \frac{P_{m,L}}{z} - P_{m,L} \cdot VF \right) - \frac{D_m}{h_m} K_{m/c} \cdot c_c \cdot \left(P_{m,d} + \frac{P_{m,L}}{z} - P_{m,L} \cdot VF \right) - \frac{D_m}{h_m} K_{m/c} \cdot c_c \cdot \frac{P_{dbl,d}}{q} \left(q + \frac{1}{z} - VF \right)}{\left(P_{m,d} + \frac{P_{m,L}}{z} - P_{m,L} \cdot VF \right) + \frac{P_{dbl,d}}{q} \left(q + \frac{1}{z} - VF \right)}$$

Equation 85

$$J_m = \frac{\frac{P_{dbl,d}}{q} \cdot c_{tot} (qz + 1 - z \cdot VF) \cdot \left(P_{m,d} + \frac{P_{m,L}}{z} - P_{m,L} \cdot VF \right) - \frac{D_m}{h_m} K_{m/c} \cdot c_c \cdot \frac{P_{dbl,d}}{q} \left(q + \frac{1}{z} - VF \right)}{\left(P_{m,d} + \frac{P_{m,L}}{z} - P_{m,L} \cdot VF \right) + \frac{P_{dbl,d}}{q} \left(q + \frac{1}{z} - VF \right)}$$

Equation 86

$$J_m = \frac{\frac{P_{dbl,d}}{q} \left(q + \frac{1}{z} - VF \right) \cdot \left[c_{tot} \cdot z \cdot \left(P_{m,d} + \frac{P_{m,L}}{z} - P_{m,L} \cdot VF \right) - \frac{D_m}{h_m} K_{m/c} \cdot c_c \right]}{\left(P_{m,d} + \frac{P_{m,L}}{z} - P_{m,L} \cdot VF \right) + \frac{P_{dbl,d}}{q} \left(q + \frac{1}{z} - VF \right)}$$

Equation 87

Assuming for the sake of simplicity sink conditions on the receiver (cell) side and setting c_c to zero and dividing Equation 87 by c_{tot} , it follows

$$P = \frac{\frac{P_{dbl,d}}{q} z \left(q + \frac{1}{z} - VF \right) \cdot \left(P_{m,d} + \frac{P_{m,L}}{z} - P_{m,L} \cdot VF \right)}{\left(P_{m,d} + \frac{P_{m,L}}{z} - P_{m,L} \cdot VF \right) + \frac{P_{dbl,d}}{q} \left(q + \frac{1}{z} - VF \right)}$$

Equation 88

Conversion of this formula leads to the following equation:

$$\frac{1}{P} = \frac{1}{\frac{P_{dbl,d}}{q} \cdot (q \cdot z + 1 - z \cdot VF)} + \frac{1}{z \left(P_{m,d} + \frac{P_{m,L}}{z} - P_{m,L} \cdot VF \right)}$$

Equation 89

This equation looks similar to the model equation for the accumulation of permeability coefficients:

$$\frac{1}{P} = \frac{1}{P_{DBL}} + \frac{1}{P_m}$$

Equation 90

The additional terms in Equation 89 can be regarded as model specific exponents containing a term for the lipid/water partitioning of the drug and a term describing the contribution of the lipid particles on the drug transport.

With Easyfit the following equation was used:

$$P_a = \frac{1}{\frac{1}{\frac{P_{dbl,d}}{q} \cdot (q \cdot z + 1 - z \cdot VF)} + \frac{1}{z \left(P_{m,d} + \frac{P_{m,L}}{z} - P_{m,L} \cdot VF \right)}}$$

Equation 91

The resulting Equation 91, was applied for the subdivision of the estimated apparent permeability coefficients P_a and P_b out of the transport studies (because there was no influence of the order of the layers see appendix (Subdivision of the Apparent Permeability Coefficient without Lipid Contribution Including Model Extension for Non-Sink Conditions) for further explanation.)

6.6.2 Subdivision of the Apparent Permeability Coefficient Including Permeation through Diffusion Boundary Layer and through Cellular Membrane Including Model Extension for Non-Sink Conditions.

In this section, a mathematical model is derived to determine the membrane permeability and the permeability through diffusion boundary layer out of permeability data of Caco-2 transport experiments and equilibrium dialysis experiments. This model is based on the following assumptions:

- 1) Sink conditions on acceptor side
- 2) Only unbound drug molecules may diffuse through the cell monolayer
- 3) No drug transfer takes place if lipid particles collide into the cell membrane
- 4) The free fraction (z) of a drug is dependent on lipid concentration and may be independent of drug concentration.

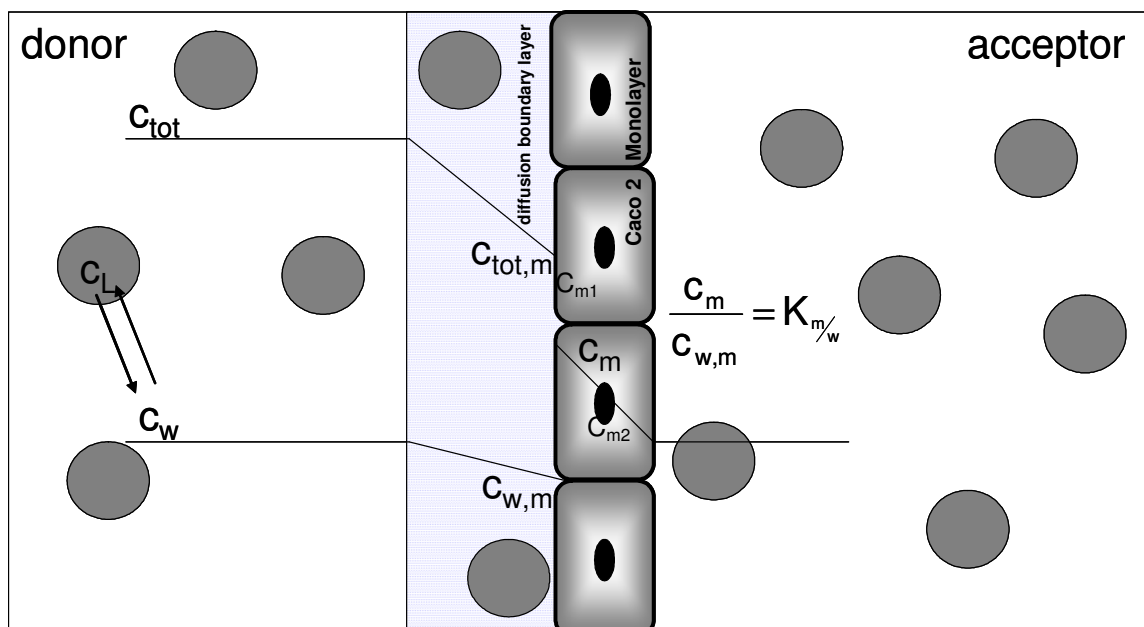


Figure 57 Model for determination of the membrane permeability and the permeability through diffusion boundary layer out of permeability data of Caco-2 transport experiments and equilibrium dialysis experiments.

Abbreviations:

- $C_{w,m}$ drug concentration of the water phase on membrane surface
- $C_{tot, m}$ total drug concentration of the formulation on membrane surface
- $C_{L,m}$ drug concentration of the lipid phase on membrane surface
- C_m drug concentration in cell membrane
- C_L drug concentration in lipid phase, referring to the total volume
- C_W drug concentration in water phase, referring to the water phase
- C_{tot} drug concentration in formulation
- h_m thickness of cell membrane

h_{DBL}	thickness of diffusion boundary layer
J_m	flux through membrane
J_{DBL}	flux through diffusion boundary layer
$D_{w,d}$	diffusion coefficient of drug in water phase
$D_{w,L}$	diffusion coefficient of lipid particle in water phase
D_m	diffusion coefficient of drug in cell membrane
VF	Volume fraction
V_w	Volume of water phase
V_{tot}	Volume of the formulation
n_w	moles of water in the formulation
n_L	moles of Lipids in the formulation
MW_L	molecular weight of lipids
ρ_w	density of water phase
ρ_{tot}	density of the formulation
$K_{m/w}$	membrane/water partition coefficient
m_{tot}	total mass of drug
m_w	mass of drug in water phase
m_L	mass of drug in lipid phase
$P_{DBL,d}$	Permeation coefficient of the Drug through diffusion boundary layer
P_m	Permeation coefficient of the Drug through the cell monolayer

The free fraction of a drug is defined as

$$\frac{C_w}{C_{tot}} = Z$$

Equation 92

Fluxes through cellular membrane and diffusion boundary layer are defined as:

$$J_m = \frac{D_m}{h_m} c_m$$

Equation 93

$$J_{DBL} = \frac{D_{w,d}}{h_{DBL}} \cdot (c_w - c_{w,m}) + \frac{D_{w,L}}{h_{DBL}} (c_L - c_{L,m})$$

Equation 94

$$J_m = J_{DBL}$$

Equation 95

$$\frac{D_m}{h_m} c_m = \frac{D_{w,d}}{h_{DBL}} \cdot (c_w - c_{w,m}) + \frac{D_{w,L}}{h_{DBL}} (c_L - c_{L,m})$$

Equation 96

Some substitutions:

$$q = \frac{D_{w,d}}{D_{w,L}}$$

Equation 97

$$K_{m/w} = \frac{c_m}{c_{w,m}}$$

Equation 98

$$VF = \frac{V_w}{V_{tot}}$$

Equation 99

$$m_{tot} - m_w = m_L$$

Equation 100

$$\frac{m_L}{V_{tot}} = c_L = \frac{m_{tot} - m_w}{V_{tot}} = \frac{c_{tot} V_{tot} - c_w V_w}{V_{tot}} = c_{tot} - c_w \frac{V_w}{V_{tot}} = c_{tot} - c_w VF = c_L$$

Equation 101

where

$$V_w = \frac{n_w \cdot 18}{\rho_w}$$

Equation 102

$$V_{tot} = \frac{n_w \cdot 18 + n_L \cdot MW_L}{\rho_{tot}}$$

Equation 103

Unknown parameters were replaced by the use of some substitutions. The resulting equation was solved for the unknown parameter $c_{w,m}$.

$$\frac{D_m}{h_m} K_{m/w} \cdot c_{w,m} = \frac{D_{w,d}}{h_{DBL}} \cdot (c_w - c_{w,m}) + \frac{D_{w,d}}{q \cdot h_{DBL}} (c_L - c_{L,m})$$

Equation 104

$$P_m \cdot c_{w,m} = \frac{D_{w,d}}{h_{DBL}} \left(c_w - c_{w,m} + \frac{c_L}{q} - \frac{c_{L,m}}{q} \right)$$

Equation 105

$$P_m \cdot c_{w,m} = \frac{D_{w,d}}{h_{DBL} q} (q \cdot c_w - q \cdot c_{w,m} + c_L - c_{L,m})$$

Equation 106

$$P_m \cdot c_{w,m} = \frac{P_{DBL,d}}{q} (q \cdot c_w - q \cdot c_{w,m} + c_L - c_{L,m})$$

Equation 107

$$P_m \cdot c_{w,m} = \frac{P_{DBL,d}}{q} \left(q \cdot z \cdot c_{tot} - q \cdot c_{w,m} + c_{tot} - c_{tot} z VF - \frac{c_{w,m}}{z} + c_{w,m} \cdot VF \right)$$

Equation 108

$$P_m \cdot c_{w,m} = \frac{P_{DBL,d}}{q} c_{tot} (q \cdot z + 1 - z \cdot VF) - \frac{P_{DBL,d}}{q \cdot z} c_{w,m} (q \cdot z + 1 - z \cdot VF)$$

Equation 109

$$P_m \cdot c_{w,m} + \frac{P_{DBL,d}}{q \cdot z} c_{w,m} (q \cdot z + 1 - z \cdot VF) = \frac{P_{DBL,d}}{q} c_{tot} (q \cdot z + 1 - z \cdot VF)$$

Equation 110

$$c_{w,m} = \frac{\frac{P_{DBL,d}}{q} c_{tot} (q \cdot z + 1 - z \cdot VF)}{P_m + \frac{P_{DBL,d}}{q \cdot z} (q \cdot z + 1 - z \cdot VF)}$$

Equation 111

The term for $c_{w,m}$ was inserted into the following equation:

$$J_m = J_{DBL} = J_{tot} = P_m \cdot c_{w,m} = \frac{\frac{P_m \cdot P_{DBL,d}}{q} c_{tot} (q \cdot z + 1 - z \cdot VF)}{P_m + \frac{P_{DBL,d}}{q \cdot z} (q \cdot z + 1 - z \cdot VF)}$$

Equation 112

$$\text{If } J = P \cdot c_{tot} \Rightarrow P = \frac{J}{c_{tot}}$$

Equation 113

then

$$P = \frac{1}{\frac{P_m + \frac{P_{DBL,d}}{q \cdot z} (q \cdot z + 1 - z \cdot VF)}{P_m \cdot \frac{P_{DBL,d}}{q} \cdot (q \cdot z + 1 - z \cdot VF)}}$$

Equation 114

Conversion of this Equation 114 leads to the following equations:

$$P \cdot \frac{P_m + \frac{P_{DBL,d}}{q \cdot z} (q \cdot z + 1 - z \cdot VF)}{P_m \cdot \frac{P_{DBL,d}}{q} \cdot (q \cdot z + 1 - z \cdot VF)} = 1$$

Equation 115

$$\frac{P_m + \frac{P_{DBL,d}}{q \cdot z} (q \cdot z + 1 - z \cdot VF)}{P_m \cdot \frac{P_{DBL,d}}{q} \cdot (q \cdot z + 1 - z \cdot VF)} = \frac{1}{P}$$

Equation 116

$$\frac{P_m}{P_m \cdot \frac{P_{DBL,d}}{q} \cdot (q \cdot z + 1 - z \cdot VF)} + \frac{\frac{P_{DBL,d}}{q \cdot z} (q \cdot z + 1 - z \cdot VF)}{P_m \cdot \frac{P_{DBL,d}}{q} \cdot (q \cdot z + 1 - z \cdot VF)} = \frac{1}{P}$$

Equation 117

$$\frac{1}{P} = \frac{1}{\frac{P_{DBL,d}}{q} \cdot (q \cdot z + 1 - z \cdot VF)} + \frac{1}{P_m \cdot z}$$

Equation 118

Equation 118 looks similar to the model equation for the accumulation of permeability coefficients:

$$\frac{1}{P} = \frac{1}{P_{DBL}} + \frac{1}{P_m}$$

Equation 119

The additional terms (in brackets) in Equation 118 can be regarded as model specific exponents containing a term for the lipid/water partitioning of the drug. With Easyfit the following equation was used:

$$P = \frac{1}{\frac{1}{P_{DBL,d} \cdot \frac{(q \cdot z + 1 - z \cdot VF)}{q}} + \frac{1}{P_m \cdot z}}$$

Equation 120

6.6.2.1 Fitting the Biophysical Model for the Subdivision of Apparent Permeability Coefficient Including Permeation through Diffusion Boundary Layer and through Cellular Membrane to Apparent Permeability Coefficients out of Cell Permeation Experiments

Equation 120 was fitted to the experimental free fractions and apparent permeability coefficients. The results of the best obtained estimation for P_m and P_{DBL} are shown in Table 22.

Table 22 Estimated parameters if the permeability coefficient of the free drug through the cell membrane and the permeability coefficient of the drug because of direct drug transfer from lipid particle to the cell membrane are merged to the permeability coefficient of the drug through the cell membrane, P_m . Except for triclobandazole, very poor description of the data by the model was obtained.

Drug	Type of Formulation	P_m [cm*s ⁻¹]	P_{DBL} [cm*s ⁻¹]
Triclobandazole ^A	Emulsion	0.088	
	Microemulsion	0.041	1.94*10 ⁻⁴
	Liposomes	0.00698	
Progesterone	Emulsion	133.67	
	Microemulsion	294.31	3.49*10 ⁻⁴
	Liposomes	190.6	
Propranolol	Emulsion	276.93	
	Microemulsion	0.0034	3.98*10 ⁻⁴
	Liposomes	0.0021	
Saquinavir	Emulsion	58.9	
	Microemulsion	30.46	1.23*10 ⁻⁴

^A to improve fitting quality, a scaling of -1 instead of 1 was used

6.6.2.2 Model Extension for Non-Sink Conditions of the Subdivision of the Apparent Permeability Coefficient Including Permeation through Diffusion Boundary Layer and through Cellular Membrane

The model described in the last chapter was extended for non sink conditions on the acceptor side, which leads to the following equations ($c_{m2} \neq 0$, see Figure 57):

Step donor compartment to cell lumen

$$J_m = \frac{D_m}{h_m} (c_{m,1} - c_{m,2})$$

Equation 121

$$J_{DBL} = \frac{D_{DBL}}{h_{DBL}} (c_w - c_{w,m}) + \frac{D_{w,L}}{h_{DBL}} (c_L - c_{L,m})$$

Equation 122

it is essential

$$J_m = J_{DBL}$$

Equation 123

$$\frac{D_m}{h_m} K_{m/w} \left(c_{w,m} - \frac{K_{m/c}}{K_{m/w}} c_c \right) = \frac{D_{w,d}}{h_{DBL}} \left(c_w - c_{w,m} + \frac{c_L}{q} - \frac{c_{L,m}}{q} \right)$$

Equation 124

In Equation 124 some unknown variables were substituted and the equation was solved for $c_{w,m}$:

$$P_m c_{w,m} - P_m K_{m/c} c_c = \frac{P_{DBL,d}}{q} (q c_w - q c_{w,m} + c_L - c_{L,m})$$

Equation 125

$$P_m c_{w,m} - P_m K_{m/c} c_c = \frac{P_{DBL,d}}{q} [q z c_{tot} - q c_{w,m} + c_{tot} - c_{tot} z VF - (c_{tot,m} - c_{w,m} VF)]$$

Equation 126

$$P_m c_{w,m} - P_m K_{m/c} c_c = \frac{P_{DBL,d}}{q} (q z c_{tot} + c_{tot} - c_{tot} z VF) + \frac{P_{DBL,d}}{q} \left(-q c_{w,m} - \frac{c_{w,m}}{z} + c_{w,m} VF \right)$$

Equation 127

$$\frac{c_{m,2}}{c_c} = K_{m/c}$$

Equation 128

$$P_m c_{w,m} - \frac{P_{DBL,d}}{q} c_{w,m} \left(-q - \frac{1}{z} + VF \right) = \frac{P_{DBL,d}}{q} c_{tot} (q z + 1 - z VF) + P_m K_{m/c} c_c$$

Equation 129

$$c_{w,m} = \frac{\frac{P_{DBL,d}}{q} c_{tot} (qz + 1 - zVF) + P_m K_{w/c} c_c}{P_m + \frac{P_{DBL,d}}{q} \left(q + \frac{1}{z} - VF \right)}$$

Equation 130

Equation 130 was inserted into Equation 131:

$$J = P_m (c_{w,m} - K_{w/c} c_c)$$

Equation 131

$$= P_m \cdot \frac{\frac{P_{DBL,d}}{q} c_{tot} (qz + 1 - zVF) + P_m K_{w/c} c_c - P_m K_{w/c} c_c - K_{w/c} c_c \frac{P_{DBL,d}}{q} \left(q + \frac{1}{z} - VF \right)}{P_m + \frac{P_{DBL,d}}{q} \left(q + \frac{1}{z} - VF \right)}$$

Equation 132

$$= P_m \cdot \frac{\frac{P_{DBL,d}}{q} \left(q + \frac{1}{z} - VF \right) (c_{tot} z - K_{w/c} c_c)}{P_m + \frac{P_{DBL,d}}{q} \left(q + \frac{1}{z} - VF \right)}$$

Equation 133

$$= \frac{\frac{P_m \cdot P_{DBL,d}}{q} (qz + 1 - zVF) \left(c_{tot} - \frac{K_{w/c} c_c}{z} \right)}{P_m + \frac{P_{DBL,d}}{zq} (zq + 1 - zVF)} = P \cdot \left(c_{tot} - \frac{K_{w/c} c_c}{z} \right)$$

Equation 134

Equation 134 is in fact the same equation as the equation including sink conditions, because

$$K_{w/c} = K_{tot/c} = \frac{K_{w/c}}{z} \Rightarrow P \cdot \left(c_{tot} - K_{w/c} c_c \right)$$

Equation 135

$$P = \frac{\frac{P_m \cdot P_{DBL,d}}{q} (qz + 1 - zVF)}{P_m + \frac{P_{DBL,d}}{qz} (qz + 1 - zVF)}$$

Equation 136

Step from cell lumen to acceptor compartment:

$$J_m = \frac{D_m}{h_m} (c_{m1} - c_{m2})$$

Equation 137

$$J_{DBL} = \frac{D_{DBL}}{h_{DBL}} (c_{w,m} - c_w) + \frac{D_{w,L}}{h_{DBL}} (c_{L,m} - c_L)$$

Equation 138

$$J_m = \frac{D_m}{h_m} (K_{w/c} c_c - K_{w/m} c_{w,m}) = \frac{D_m}{h_m} K_{w/w} \left(\frac{K_{m/c}}{K_{m/w}} c_c - c_{w,m} \right) = P_m (K_{w/c} c_c - c_{w,m})$$

Equation 139

$$J_{DBL} = \frac{D_{w,d}}{h_{DBL}} \left(c_{w,m} - c_w + \frac{c_{L,m}}{q} - \frac{c_L}{q} \right)$$

Equation 140

(it is essential: $J_m = J_{DBL}$)

$$P_m K_{w/c} c_c - P_m c_{w,m} = P_{DBL,d} \left[q c_{w,m} - q z c_{tot} + (c_{tot,m} - c_{w,m} VF) - (c_{tot} - c_{tot} VF) \right]$$

Equation 141

$$P_m K_{w/c} c_c - P_m c_{w,m} = \frac{P_{DBL,d}}{q} \left(q c_{w,m} + \frac{c_{w,m}}{z} - c_{w,m} VF \right) + \frac{P_{DBL,d}}{q} (-q z c_{tot} - c_{tot} + c_{tot} z VF)$$

Equation 142

$$P_m K_{w/c} c_c - \frac{P_{DBL,d}}{q} c_{tot} (-q z - 1 + z VF) = \frac{P_{DBL,d}}{q} c_{w,m} \left(q + \frac{1}{z} - VF \right) + P_m c_{w,m}$$

Equation 143

$$\frac{P_m K_{w/c} c_c - \frac{P_{DBL,d}}{q} c_{tot} (-q z - 1 + z VF)}{\frac{P_{DBL,d}}{q} \left(q + \frac{1}{z} - VF \right) + P_m} = c_{w,m}$$

Equation 144

Equation 144 was inserted to Equation 145:

$$J_m = J_{DBL} = P_m (K_{w/c} c_c - c_{w,m})$$

Equation 145

$$= P_m \frac{K_{w/c} c_c \frac{P_{DBL,d}}{q} \left(q + \frac{1}{z} - VF \right) + P_m K_{w/c} c_c - P_m K_{w/c} c_c + \frac{P_{DBL,d}}{q} c_{tot} (-qz - 1 + zVF)}{\frac{P_{DBL,d}}{q} \left(q + \frac{1}{z} - VF \right) + P_m}$$

Equation 146

$$= P_m \frac{\frac{P_{DBL,d}}{q} \left(q + \frac{1}{z} - VF \right) (K_{w/c} c_c - c_{tot} z)}{\frac{P_{DBL,d}}{q} \left(q + \frac{1}{z} - VF \right) + P_m}$$

Equation 147

Since concentration gradient is directed to the opposite direction, Equation 147 is the same as Equation 133. This derivation leads to the same solution as the derivation with sink conditions. If sink conditions were not warranted, there is no influence on the calculated permeation coefficient. Furthermore the order of the layers does not influence the permeation.

7 REFERENCES

1. Lindenberg M, Kopp S, Dressman JB. Classification of orally administered drugs on the World Health Organization Model list of Essential Medicines according to the biopharmaceutics classification system. *Eur J Pharm Biopharm* 2004;58(2):265-78.
2. Amidon GL, Lennernas H, Shah VP, Crison JR. A theoretical basis for a biopharmaceutic drug classification: the correlation of in vitro drug product dissolution and in vivo bioavailability. *Pharm Res* 1995;12(3):413-20.
3. Camenisch G, Folkers G, van de Waterbeemd H. Review of theoretical passive drug absorption models: historical background, recent developments and limitations. *Pharm Acta Helv* 1996;71(5):309-27.
4. Sawada GA, Barsuhn CL, Lutzke BS, Houghton ME, Padbury GE, Ho NF, et al. Increased lipophilicity and subsequent cell partitioning decrease passive transcellular diffusion of novel, highly lipophilic antioxidants. *J Pharmacol Exp Ther* 1999;288(3):1317-26.
5. Wils P, Warnery A, Phung-Ba V, Legrain S, Scherman D. High lipophilicity decreases drug transport across intestinal epithelial cells. *J Pharmacol Exp Ther* 1994;269(2):654-8.
6. Fischer H, Kansy M, Avdeef A, Senner F. Permeation of permanently positive charged molecules through artificial membranes--influence of physico-chemical properties. *Eur J Pharm Sci* 2007;31(1):32-42.
7. Lipinski CA, Lombardo F, Dominy BW, Feeney PJ. Experimental and computational approaches to estimate solubility and permeability in drug discovery and development settings. *Adv Drug Deliv Rev* 2001;46(1-3):3-26.
8. Hunter J, Hirst BH. Intestinal secretion of drugs. The role of P-glycoprotein and related drug efflux systems in limiting oral drug absorption. *Advanced Drug Delivery Reviews* 1997;25(2-3):129-157.
9. Seithel A, Karlsson J, Hilgendorf C, Bjorquist A, Ungell AL. Variability in mRNA expression of ABC- and SLC-transporters in human intestinal cells: comparison between human segments and Caco-2 cells. *Eur J Pharm Sci* 2006;28(4):291-9.
10. Xia CQ, Liu N, Yang D, Miwa G, Gan LS. Expression, localization, and functional characteristics of breast cancer resistance protein in Caco-2 cells. *Drug Metab Dispos* 2005;33(5):637-43.
11. Gutmann H, Fricker G, Torok M, Michael S, Beglinger C, Drewe J. Evidence for different ABC-transporters in Caco-2 cells modulating drug uptake. *Pharm Res* 1999;16(3):402-7.
12. Ambudkar SV, Kim IW, Sauna ZE. The power of the pump: mechanisms of action of P-glycoprotein (ABCB1). *Eur J Pharm Sci* 2006;27(5):392-400.
13. Ambudkar SV, Dey S, Hrycyna CA, Ramachandra M, Pastan I, Gottesman MM. Biochemical, cellular, and pharmacological aspects of the multidrug transporter. *Annu Rev Pharmacol Toxicol* 1999;39:361-98.
14. Brandon EF, Bosch TM, Deenen MJ, Levink R, van der Wal E, van Meerveld JB, et al. Validation of in vitro cell models used in drug metabolism and transport studies; genotyping of cytochrome P450, phase II enzymes and drug transporter polymorphisms in the human hepatoma

(HepG2), ovarian carcinoma (IGROV-1) and colon carcinoma (CaCo-2, LS180) cell lines. *Toxicol Appl Pharmacol* 2006;211(1):1-10.

15. de Waziers I, Cugnenc PH, Yang CS, Leroux JP, Beaune PH. Cytochrome P 450 isoenzymes, epoxide hydrolase and glutathione transferases in rat and human hepatic and extrahepatic tissues. *J Pharmacol Exp Ther* 1990;253(1):387-94.

16. Kolars JC, Lown KS, Schmiedlin-Ren P, Ghosh M, Fang C, Wrighton SA, et al. CYP3A gene expression in human gut epithelium. *Pharmacogenetics* 1994;4(5):247-59.

17. Lamba JK, Lin YS, Schuetz EG, Thummel KE. Genetic contribution to variable human CYP3A-mediated metabolism. *Adv Drug Deliv Rev* 2002;54(10):1271-94.

18. McKinnon RA, Burgess WM, Hall PM, Roberts-Thomson SJ, Gonzalez FJ, McManus ME. Characterisation of CYP3A gene subfamily expression in human gastrointestinal tissues. *Gut* 1995;36(2):259-67.

19. Meunier V, Bourrie M, Berger Y, Fabre G. The human intestinal epithelial cell line Caco-2; pharmacological and pharmacokinetic applications. *Cell Biol Toxicol* 1995;11(3-4):187-94.

20. Bhattachar SN, Deschenes LA, Wesley JA. Solubility: it's not just for physical chemists. *Drug Discov Today* 2006;11(21-22):1012-8.

21. Pade V, Stavchansky S. Link between drug absorption solubility and permeability measurements in Caco-2 cells. *J Pharm Sci* 1998;87(12):1604-7.

22. Dunn CJ, Wagstaff AJ, Perry CM, Plosker GL, Goa KL. Cyclosporin: an updated review of the pharmacokinetic properties, clinical efficacy and tolerability of a microemulsion-based formulation (neoral)¹ in organ transplantation. *Drugs* 2001;61(13):1957-2016.

23. Figgitt DP, Plosker GL. Saquinavir soft-gel capsule: an updated review of its use in the management of HIV infection. *Drugs* 2000;60(2):481-516.

24. Gill J, Feinberg J. Saquinavir soft gelatin capsule: a comparative safety review. *Drug Saf* 2001;24(3):223-32.

25. Griffin BT, O'Driscoll CM. A comparison of intestinal lymphatic transport and systemic bioavailability of saquinavir from three lipid-based formulations in the anaesthetised rat model. *J Pharm Pharmacol* 2006;58(7):917-25.

26. Huguenin PW, Burger DM, Koopmans PP, Stuart JW, Kroon FP, van Leusen R, et al. Saquinavir soft-gel capsules (Fortovase) give lower exposure than expected, even after a high-fat breakfast. *Pharm World Sci* 2002;24(3):83-6.

27. Perry CM, Noble S. Saquinavir soft-gel capsule formulation. A review of its use in patients with HIV infection. *Drugs* 1998;55(3):461-86.

28. Pereira de Oliveira M, Garcion E, Venisse N, Benoit JP, Couet W, Olivier JC. Tissue distribution of indinavir administered as solid lipid nanocapsule formulation in mdr1a (+/+) and mdr1a (-/-) CF-1 mice. *Pharm Res* 2005;22(11):1898-1905.

29. Sachs-Barrable K, Lee SD, Wasan EK, Thornton SJ, Wasan KM. Enhancing drug absorption using lipids: a case study presenting the development and pharmacological evaluation of a novel lipid-based oral amphotericin B formulation for the treatment of systemic fungal infections. *Adv Drug Deliv Rev* 2008;60(6):692-701.

30. Trevaskis NL, Charman WN, Porter CJ. Lipid-based delivery systems and intestinal lymphatic drug transport: a mechanistic update. *Adv Drug Deliv Rev* 2008;60(6):702-16.
31. Bohets H, Annaert P, Mannens G, Van Beijsterveldt L, Anciaux K, Verboven P, et al. Strategies for absorption screening in drug discovery and development. *Curr Top Med Chem* 2001;1(5):367-83.
32. Hidalgo IJ, Raub TJ, Borchardt RT. Characterization of the human colon carcinoma cell line (Caco-2) as a model system for intestinal epithelial permeability. *Gastroenterology* 1989;96(3):736-49.
33. Skold C, Winiwarter S, Wernevik J, Bergstrom F, Engstrom L, Allen R, et al. Presentation of a structurally diverse and commercially available drug data set for correlation and benchmarking studies. *J Med Chem* 2006;49(23):6660-71.
34. Hubatsch I, Ragnarsson EG, Artursson P. Determination of drug permeability and prediction of drug absorption in Caco-2 monolayers. *Nat Protoc* 2007;2(9):2111-9.
35. Hayeshi R, Hilgendorf C, Artursson P, Augustijns P, Brodin B, Dehertogh P, et al. Comparison of drug transporter gene expression and functionality in Caco-2 cells from 10 different laboratories. *Eur J Pharm Sci* 2008.
36. Braun A, Hammerle S, Suda K, Rothen-Rutishauser B, Gunthert M, Kramer SD, et al. Cell cultures as tools in biopharmacy. *Eur J Pharm Sci* 2000;11 Suppl 2:S51-60.
37. Behrens I, Kissel T. Do cell culture conditions influence the carrier-mediated transport of peptides in Caco-2 cell monolayers? *Eur J Pharm Sci* 2003;19(5):433-42.
38. Volpe DA. Variability in Caco-2 and MDCK cell-based intestinal permeability assays. *J Pharm Sci* 2008;97(2):712-25.
39. Anderle P, Niederer E, Rubas W, Hilgendorf C, Spahn-Langguth H, Wunderli-Allenspach H, et al. P-Glycoprotein (P-gp) mediated efflux in Caco-2 cell monolayers: the influence of culturing conditions and drug exposure on P-gp expression levels. *J Pharm Sci* 1998;87(6):757-62.
40. Lentz KA, Polli JW, Wring SA, Humphreys JE, Polli JE. Influence of passive permeability on apparent P-glycoprotein kinetics. *Pharm Res* 2000;17(12):1456-60.
41. Aungst BJ, Nguyen NH, Bulgarelli JP, Oates-Lenz K. The influence of donor and reservoir additives on Caco-2 permeability and secretory transport of HIV protease inhibitors and other lipophilic compounds. *Pharm Res* 2000;17(10):1175-80.
42. Krishna G, Chen K, Lin C, Nomeir AA. Permeability of lipophilic compounds in drug discovery using in-vitro human absorption model, Caco-2. *Int J Pharm* 2001;222(1):77-89.
43. Yamashita S, Furubayashi T, Kataoka M, Sakane T, Sezaki H, Tokuda H. Optimized conditions for prediction of intestinal drug permeability using Caco-2 cells. *Eur J Pharm Sci* 2000;10(3):195-204.
44. Ingels F, Deferme S, Destexhe E, Oth M, Van den Mooter G, Augustijns P. Simulated intestinal fluid as transport medium in the Caco-2 cell culture model. *Int J Pharm* 2002;232(1-2):183-92.
45. Fossati L, Dechaume R, Hardillier E, Chevillon D, Prevost C, Bolze S, et al. Use of simulated intestinal fluid for Caco-2 permeability assay of lipophilic drugs. *Int J Pharm* 2008;360(1-2):148-55.

46. Ingels FM, Augustijns PF. Biological, pharmaceutical, and analytical considerations with respect to the transport media used in the absorption screening system, Caco-2. *J Pharm Sci* 2003;92(8):1545-58.
47. Ingels F, Beck B, Oth M, Augustijns P. Effect of simulated intestinal fluid on drug permeability estimation across Caco-2 monolayers. *Int J Pharm* 2004;274(1-2):221-32.
48. Sha X, Yan G, Wu Y, Li J, Fang X. Effect of self-microemulsifying drug delivery systems containing Labrasol on tight junctions in Caco-2 cells. *Eur J Pharm Sci* 2005;24(5):477-86.
49. Prabhu S, Ortega M, Ma C. Novel lipid-based formulations enhancing the in vitro dissolution and permeability characteristics of a poorly water-soluble model drug, piroxicam. *Int J Pharm* 2005;301(1-2):209-16.
50. Dahan A, Hoffman A. The effect of different lipid based formulations on the oral absorption of lipophilic drugs: the ability of in vitro lipolysis and consecutive ex vivo intestinal permeability data to predict in vivo bioavailability in rats. *Eur J Pharm Biopharm* 2007;67(1):96-105.
51. Spornath A, Aserin A, Ziserman L, Danino D, Garti N. Phosphatidylcholine embedded microemulsions: physical properties and improved Caco-2 cell permeability. *J Control Release* 2007;119(3):279-90.
52. Brusewitz C, Schendler A, Funke A, Wagner T, Lipp R. Novel poloxamer-based nanoemulsions to enhance the intestinal absorption of active compounds. *Int J Pharm* 2007;329(1-2):173-81.
53. Kataoka M, Masaoka Y, Sakuma S, Yamashita S. Effect of food intake on the oral absorption of poorly water-soluble drugs: in vitro assessment of drug dissolution and permeation assay system. *J Pharm Sci* 2006;95(9):2051-61.
54. Rowland M, Tozer TN. *Clinical Pharmacokinetics: Concepts and Applications*. In. 3rd ed: Lippincott Williams and Wilkins; 1995.
55. Shargel L, A Y. *Applied Biopharmaceutics and Pharmacokinetics*. In. Stamford: Appleton& Lange; 1999.
56. (FDA) FaDA. Waiver of in Vivo Bioavailability and Bioequivalence Studies for Immediate-Release Solid Oral Dosage Forms Based on a Biopharmaceutics Classification System. In: (CDER) CfDEaR, editor. *Guidance for Industry*; 2000.
57. Raaflaub J. *Pharmakokinetik Ein Leitfaden für Autodidakten*. 1999 ed. Basel: Editiones Roche; 1985.
58. Khanvilkar K, Donovan MD, Flanagan DR. Drug transfer through mucus. *Adv Drug Deliv Rev* 2001;48(2-3):173-93.
59. Amidon GL, Lee PI, Topp EM. *Transport Processes in Pharmaceutical Systems*. New York: Marcel Dekker; 2000.
60. Camenisch G, Alsenz J, van de Waterbeemd H, Folkers G. Estimation of permeability by passive diffusion through Caco-2 cell monolayers using the drugs' lipophilicity and molecular weight. *Eur J Pharm Sci* 1998;6(4):317-24.
61. Singer SJ, Nicolson GL. The fluid mosaic model of the structure of cell membranes. *Science* 1972;175(23):720-31.
62. Simons K, Ikonen E. Functional rafts in cell membranes. *Nature* 1997;387(6633):569-72.

63. Shaw AS. Lipid rafts: now you see them, now you don't. *Nat Immunol* 2006;7(11):1139-42.
64. van Meer G, Simons K. Lipid polarity and sorting in epithelial cells. *J Cell Biochem* 1988;36(1):51-8.
65. van 't Hof W, van Meer G. Generation of lipid polarity in intestinal epithelial (Caco-2) cells: sphingolipid synthesis in the Golgi complex and sorting before vesicular traffic to the plasma membrane. *J Cell Biol* 1990;111(3):977-86.
66. Hidalgo IJ. Assessing the absorption of new pharmaceuticals. *Curr Top Med Chem* 2001;1(5):385-401.
67. Shin K, Fogg VC, Margolis B. Tight junctions and cell polarity. *Annu Rev Cell Dev Biol* 2006;22:207-35.
68. Salama NN, Eddington ND, Fasano A. Tight junction modulation and its relationship to drug delivery. *Adv Drug Deliv Rev* 2006;58(1):15-28.
69. Smith DA, van de Waterbeemd H, Walker DK. *Pharmacokinetics and Metabolism in Drug Design, Chapter 3: Absorption*: Wiley-VCH; 2006.
70. Artursson P, Palm K, Luthman K. Caco-2 monolayers in experimental and theoretical predictions of drug transport. *Adv Drug Deliv Rev* 2001;46(1-3):27-43.
71. Swaan PW, Stehouwer MC, Tukker JJ. Molecular mechanism for the relative binding affinity to the intestinal peptide carrier. Comparison of three ACE-inhibitors: enalapril, enalaprilat, and lisinopril. *Biochim Biophys Acta* 1995;1236(1):31-8.
72. Smith P, Mirabelli C, Fondacaro J, Ryan F, Dent J. Intestinal 5-fluorouracil absorption: use of Ussing chambers to assess transport and metabolism. *Pharm Res* 1988;5(9):598-603.
73. Barthe L, Woodley J, Houin G. Gastrointestinal absorption of drugs: methods and studies. *Fundam Clin Pharmacol* 1999;13(2):154-68.
74. Acra SA, Ghishan FK. Methods of investigating intestinal transport. *JPEN J Parenter Enteral Nutr* 1991;15(3):93S-98S.
75. Wikman A, Karlsson J, Carlstedt I, Artursson P. A drug absorption model based on the mucus layer producing human intestinal goblet cell line HT29-H. *Pharm Res* 1993;10(6):843-52.
76. Ward PD, Tippin TK, Thakker DR. Enhancing paracellular permeability by modulating epithelial tight junctions. *Pharm Sci Technol Today* 2000;3(10):346-358.
77. Artursson P, Karlsson J. Correlation between oral drug absorption in humans and apparent drug permeability coefficients in human intestinal epithelial (Caco-2) cells. *Biochem Biophys Res Commun* 1991;175(3):880-5.
78. Hu M, Li Y, Davitt CM, Huang SM, Thummel K, Penman BW, et al. Transport and metabolic characterization of Caco-2 cells expressing CYP3A4 and CYP3A4 plus oxidoreductase. *Pharm Res* 1999;16(9):1352-9.
79. Schmiedlin-Ren P, Thummel KE, Fisher JM, Paine MF, Lown KS, Watkins PB. Expression of enzymatically active CYP3A4 by Caco-2 cells grown on extracellular matrix-coated permeable supports in the presence of 1 α ,25-dihydroxyvitamin D₃. *Mol Pharmacol* 1997;51(5):741-54.
80. Artursson P, Borchardt RT. Intestinal drug absorption and metabolism in cell cultures: Caco-2 and beyond. *Pharm Res* 1997;14(12):1655-8.

81. Yamashita S, Konishi K, Yamazaki Y, Taki Y, Sakane T, Sezaki H, et al. New and better protocols for a short-term Caco-2 cell culture system. *J Pharm Sci* 2002;91(3):669-79.
82. Avdeef A, Artursson P, Neuhoff S, Lazorova L, Grasjo J, Tavelin S. Caco-2 permeability of weakly basic drugs predicted with the double-sink PAMPA pKa(flux) method. *Eur J Pharm Sci* 2005;24(4):333-49.
83. Bermejo M, Avdeef A, Ruiz A, Nalda R, Ruell JA, Tsinman O, et al. PAMPA--a drug absorption in vitro model 7. Comparing rat in situ, Caco-2, and PAMPA permeability of fluoroquinolones. *Eur J Pharm Sci* 2004;21(4):429-41.
84. Kerns EH, Di L, Petusky S, Farris M, Ley R, Jupp P. Combined application of parallel artificial membrane permeability assay and Caco-2 permeability assays in drug discovery. *J Pharm Sci* 2004;93(6):1440-53.
85. Youdim KA, Avdeef A, Abbott NJ. In vitro trans-monolayer permeability calculations: often forgotten assumptions. *Drug Discov Today* 2003;8(21):997-1003.
86. Tran TT, Mittal A, Gales T, Maleeff B, Aldinger T, Polli JW, et al. Exact kinetic analysis of passive transport across a polarized confluent MDCK cell monolayer modeled as a single barrier. *J Pharm Sci* 2004;93(8):2108-23.
87. Sawada G, Ho N, Williams L, Barsuhn C, Raub T. Transcellular permeability of chlorpromazine demonstrating the roles of protein binding and membrane partitioning. *Pharm Res* 1994;11(5):665-73.
88. Raub TJ, Barsuhn CL, Williams LR, Decker DE, Sawada GA, Ho NF. Use of a biophysical-kinetic model to understand the roles of protein binding and membrane partitioning on passive diffusion of highly lipophilic molecules across cellular barriers. *J Drug Target* 1993;1(4):269-86.
89. Charman WN, Porter CJ, Mithani S, Dressman JB. Physicochemical and physiological mechanisms for the effects of food on drug absorption: the role of lipids and pH. *J Pharm Sci* 1997;86(3):269-82.
90. Aungst BJ. Intestinal permeation enhancers. *J Pharm Sci* 2000;89(4):429-42.
91. Sawai T, Drongowski RA, Lampman RW, Coran AG, Harmon CM. The effect of phospholipids and fatty acids on tight-junction permeability and bacterial translocation. *Pediatr Surg Int* 2001;17(4):269-74.
92. Constantinides PP, Wasan KM. Lipid formulation strategies for enhancing intestinal transport and absorption of P-glycoprotein (P-gp) substrate drugs: in vitro/in vivo case studies. *J Pharm Sci* 2007;96(2):235-48.
93. Hugger ED, Audus KL, Borchardt RT. Effects of poly(ethylene glycol) on efflux transporter activity in Caco-2 cell monolayers. *J Pharm Sci* 2002;91(9):1980-90.
94. Nerurkar MM, Burton PS, Borchardt RT. The use of surfactants to enhance the permeability of peptides through Caco-2 cells by inhibition of an apically polarized efflux system. *Pharm Res* 1996;13(4):528-34.
95. Rege BD, Kao JP, Polli JE. Effects of nonionic surfactants on membrane transporters in Caco-2 cell monolayers. *Eur J Pharm Sci* 2002;16(4-5):237-46.

96. Regev R, Assaraf YG, Eytan GD. Membrane fluidization by ether, other anesthetics, and certain agents abolishes P-glycoprotein ATPase activity and modulates efflux from multidrug-resistant cells. *Eur J Biochem* 1999;259(1-2):18-24.
97. Batrakova EV, Li S, Vinogradov SV, Alakhov VY, Miller DW, Kabanov AV. Mechanism of pluronic effect on P-glycoprotein efflux system in blood-brain barrier: contributions of energy depletion and membrane fluidization. *J Pharmacol Exp Ther* 2001;299(2):483-93.
98. Batrakova EV, Li S, Miller DW, Kabanov AV. Pluronic P85 increases permeability of a broad spectrum of drugs in polarized BBMEC and Caco-2 cell monolayers. *Pharm Res* 1999;16(9):1366-72.
99. Bogman K, Zysset Y, Degen L, Hopfgartner G, Gutmann H, Alsenz J, et al. P-glycoprotein and surfactants: effect on intestinal talinolol absorption. *Clin Pharmacol Ther* 2005;77(1):24-32.
100. Dintaman JM, Silverman JA. Inhibition of P-glycoprotein by D-alpha-tocopheryl polyethylene glycol 1000 succinate (TPGS). *Pharm Res* 1999;16(10):1550-6.
101. Werner U, Kissel T, Reers M. Effects of permeation enhancers on the transport of a peptidomimetic thrombin inhibitor (CRC 220) in a human intestinal cell line (Caco-2). *Pharm Res* 1996;13(8):1219-27.
102. Constantinides PP. LIPID MICROEMULSIONS FOR IMPROVING DRUG DISSOLUTION AND ORAL ABSORPTION - PHYSICAL AND BIOPHARMACEUTICAL ASPECTS. *Pharmaceutical Research* 1995;12(11):1561-1572.
103. Shah NH, Carvajal MT, Patel CI, Infeld MH, Malick AW. SELF-EMULSIFYING DRUG-DELIVERY SYSTEMS (SEDDS) WITH POLYGLYCOLYZED GLYCERIDES FOR IMPROVING IN-VITRO DISSOLUTION AND ORAL ABSORPTION OF LIPOPHILIC DRUGS. *International Journal of Pharmaceutics* 1994;106(1):15-23.
104. Porter CJ, Pouton CW, Cuine JF, Charman WN. Enhancing intestinal drug solubilisation using lipid-based delivery systems. *Adv Drug Deliv Rev* 2008;60(6):673-91.
105. Humberstone AJ, Charman WN. Lipid-based vehicles for the oral delivery of poorly water soluble drugs. *Advanced Drug Delivery Reviews* 1997;25(1):103-128.
106. Gershanik T, Benita S. Self-dispersing lipid formulations for improving oral absorption of lipophilic drugs. *European Journal of Pharmaceutics and Biopharmaceutics* 2000;50(1):179-188.
107. Pouton CW. Lipid formulations for oral administration of drugs: non-emulsifying, self-emulsifying and 'self-microemulsifying' drug delivery systems. *Eur J Pharm Sci* 2000;11 Suppl 2:S93-8.
108. Torchilin VP. Recent advances with liposomes as pharmaceutical carriers. *Nat Rev Drug Discov* 2005;4(2):145-60.
109. McLean LR, Phillips MC. Mechanism of cholesterol and phosphatidylcholine exchange or transfer between unilamellar vesicles. *Biochemistry* 1981;20(10):2893-900.
110. Ho MT, Pownall HJ, Hollyfield JG. Spontaneous transfer of retinoic acid, retinyl acetate, and retinyl palmitate between single unilamellar vesicles. *J Biol Chem* 1989;264(30):17759-63.
111. Jones JD, Thompson TE. Spontaneous phosphatidylcholine transfer by collision between vesicles at high lipid concentration. *Biochemistry* 1989;28(1):129-34.

112. Fahr A, van Hoogevest P, May S, Bergstrand N, ML SL. Transfer of lipophilic drugs between liposomal membranes and biological interfaces: consequences for drug delivery. *Eur J Pharm Sci* 2005;26(3-4):251-65.
113. Faassen F, Kelder J, Lenders J, Onderwater R, Vromans H. Physicochemical properties and transport of steroids across Caco-2 cells. *Pharm Res* 2003;20(2):177-86.
114. Brennan GP, Fairweather I, Trudgett A, Hoey E, McCoy, McConville M, et al. Understanding triclabendazole resistance. *Exp Mol Pathol* 2007;82(2):104-9.
115. Kapitza SB, Michel BR, van Hoogevest P, Leigh MLS, Imanidis G. Absorption of poorly water soluble drugs subject to apical efflux using phospholipids as solubilizers in the Caco-2 cell model. *European Journal of Pharmaceutics and Biopharmaceutics* 2007;66(1):146-158.
116. Kim AE, Dintaman JM, Waddell DS, Silverman JA. Saquinavir, an HIV protease inhibitor, is transported by P-glycoprotein. *J Pharmacol Exp Ther* 1998;286(3):1439-45.
117. Reitbauer S. Einfluss pharmazeutischer Hilfsstoffe auf die Plasmamembran von Caco-2 Zellmonolayern ermittelt durch Fluoreszenzdepolarisation. Basel: University of Basel; 2005.
118. Batrakova EV, Li S, Elmquist WF, Miller DW, Alakhov VY, Kabanov AV. Mechanism of sensitization of MDR cancer cells by Pluronic block copolymers: Selective energy depletion. *Br J Cancer* 2001;85(12):1987-97.
119. Imanidis G, Waldner C, Mettler C, Leuenberger H. An improved diffusion cell design for determining drug transport parameters across cultured cell monolayers. *J Pharm Sci* 1996;85(11):1196-203.
120. Nerurkar MM, Ho NF, Burton PS, Vidmar TJ, Borchardt RT. Mechanistic roles of neutral surfactants on concurrent polarized and passive membrane transport of a model peptide in Caco-2 cells. *J Pharm Sci* 1997;86(7):813-21.
121. Kastelova A, Dimova S, Nemery B. Effects of propranolol on xenobiotic enzyme activities in rat type II pneumocytes and alveolar macrophages in vivo. *Methods Find Exp Clin Pharmacol* 2003;25(10):797-802.
122. Mottier L, Moreno L, Alvarez L, Virkel G, Lanusse C. Measurement of triclabendazole and its metabolites in liver flukes: method development and full validation. *J Pharm Biomed Anal* 2004;35(5):991-9.
123. Virkel G, Lifschitz A, Sallovitz J, Pis A, Lanusse C. Assessment of the main metabolism pathways for the flukicidal compound triclabendazole in sheep. *J Vet Pharmacol Ther* 2006;29(3):213-23.
124. Liang E, Chessic K, Yazdanian M. Evaluation of an accelerated Caco-2 cell permeability model. *J Pharm Sci* 2000;89(3):336-45.
125. Hugger ED, Novak BL, Burton PS, Audus KL, Borchardt RT. A comparison of commonly used polyethoxylated pharmaceutical excipients on their ability to inhibit P-glycoprotein activity in vitro. *J Pharm Sci* 2002;91(9):1991-2002.
126. Herbette L, Katz AM, Sturtevant JM. Comparisons of the interaction of propranolol and timolol with model and biological membrane systems. *Mol Pharmacol* 1983;24(2):259-69.

127. Lecaillon JB, Godbillon J, Campestrini J, Naquira C, Miranda L, Pacheco R, et al. Effect of food on the bioavailability of triclabendazole in patients with fascioliasis. *Br J Clin Pharmacol* 1998;45(6):601-4.
128. Sugano K. Estimation of effective intestinal membrane permeability considering bile micelle solubilisation. *International Journal of Pharmaceutics* 2008;doi:10.1016/j.ijpharm.2008.10.001.
129. Avdeef A, Bendels S, Di L, Faller B, Kansy M, Sugano K, et al. Parallel artificial membrane permeability assay (PAMPA)-critical factors for better predictions of absorption. *J Pharm Sci* 2007;96(11):2893-2909.
130. Fagerholm U, Lennernaes H. Experimental estimation of the effective unstirred water layer thickness in the human jejunum, and its importance in oral drug absorption. *European Journal of Pharmaceutical Sciences* 1995;3(5):247-53.
131. Obata K, Sugano K, Saitoh R, Higashida A, Nabuchi Y, Machida M, et al. Prediction of oral drug absorption in humans by theoretical passive absorption model. *International journal of pharmaceutics* 2005;293(1-2):183-92. .
132. Sugano K, Nabuchi Y, Machida M, Aso Y. Prediction of human intestinal permeability using artificial membrane permeability. *Int J Pharm* 2003;257(1-2):245-51.
133. Larhed AW, Artursson P, Bjork E. The influence of intestinal mucus components on the diffusion of drugs. *Pharm Res* 1998;15(1):66-71.
134. Lai SK, O'Hanlon DE, Harrold S, Man ST, Wang YY, Cone R, et al. Rapid transport of large polymeric nanoparticles in fresh undiluted human mucus. *Proc Natl Acad Sci U S A* 2007;104(5):1482-7.
135. Norris DA, Sinko PJ. Effect of size, surface charge, and hydrophobicity on the translocation of polystyrene microspheres through gastrointestinal mucin. *J. Appl. Polym. Sci.* 1997;63(11):1481-1492.
136. Sanders NN, De Smedt SC, Demeester J. The physical properties of biogels and their permeability for macromolecular drugs and colloidal drug carriers. *J Pharm Sci* 2000;89(7):835-49.
137. Faassen F, Vogel G, Spanings H, Vromans H. Caco-2 permeability, P-glycoprotein transport ratios and brain penetration of heterocyclic drugs. *Int J Pharm* 2003;263(1-2):113-22.
138. Varma MV, Sateesh K, Panchagnula R. Functional role of P-glycoprotein in limiting intestinal absorption of drugs: contribution of passive permeability to P-glycoprotein mediated efflux transport. *Mol Pharm* 2005;2(1):12-21.
139. Shono Y, Nishihara H, Matsuda Y, Furukawa S, Okada N, Fujita T, et al. Modulation of intestinal P-glycoprotein function by cremophor EL and other surfactants by an in vitro diffusion chamber method using the isolated rat intestinal membranes. *J Pharm Sci* 2004;93(4):877-85.
140. Berginc K, Zakelj S, Levstik L, Ursic D, Kristl A. Fluorescein transport properties across artificial lipid membranes, Caco-2 cell monolayers and rat jejunum. *Eur J Pharm Biopharm* 2007;66(2):281-5.
141. Lee KJ, Johnson N, Castelo J, Sinko PJ, Grass G, Holme K, et al. Effect of experimental pH on the in vitro permeability in intact rabbit intestines and Caco-2 monolayer. *Eur J Pharm Sci* 2005;25(2-3):193-200.

142. Mahler HC, Printz M, Kopf R, Schuller R, Muller R. Behaviour of polysorbate 20 during dialysis, concentration and filtration using membrane separation techniques. *J Pharm Sci* 2008;97(2):764-74.

143. Van Veldhoven PP, Mannaerts GP. Inorganic and organic phosphate measurements in the nanomolar range. *Anal Biochem* 1987;161(1):45-8.

RESUME

Schneider Marcel

Pharmacist



Personal Details

Name:	Schneider Marcel
Date and place of birth:	29 April 1979, Langenthal
Nationality:	Swiss
Marital status:	Single
Current address:	Hauptstrasse 34, 4127 Birsfelden, Switzerland
Cell phone:	+41 79 729 26 80
Office phone:	+41 61 467 47 56
Phone :	+41 61 301 50 82
E-Mail:	marcel.schneider@unibas.ch

PhD Study

January 2005 – actual Date	PhD study at Institute of Pharmaceutical Technology (University of Basel) and at Institute Pharma Technology (University of Applied Sciences FHNW, Muttenz) under the supervision of Prof. Dr. Georgios Imanidis. Topic: Influence of lipid containing dosage forms on the absorption of lipophilic drugs in the Caco-2 cell model.
	Lectureship in practical courses of liquid and sterile dosage forms

Supervision of the following master theses

February 2007 – July 2007	„Einfluss von lipidhaltigen oralen Darreichungsformen auf die Absorption schwerlöslicher Wirkstoffe in Caco-2 Zellen“ (Sabrina Toscano).
January 2008 – June 2008	„Einfluss von lipidhaltigen oralen Darreichungsformen auf die Absorption schwerlöslicher Wirkstoffe in Caco-2 Zellen“ (Daniela Murer).

Presentations

September 9 – 12 2008	7 th biennial GPEN conference, GPEN 2008, at the University of Leuven (Leuven, Belgium) Podia presentation
October 25 – 27 2006	6 th biennial GPEN conference, GPEN 2006, at the University of Kansas (Lawrence, Kansas) Poster presentation

Education

October 1999 – November 2004	Pharmacy studies at University of Basel, Basel, Switzerland Master in Pharmaceutical Sciences and federal diploma as Pharmacist Final result state examination: 5.38 (maximum 6.00)
February 2004 – July 2004	Diploma thesis at Pentapharm GmbH, Aesch, Switzerland, under Supervision of Dr. Frank Gafner. Topic: „Antikoagulative Wirkung pflanzlicher Extrakte am Beispiel von Hypericum perforatum L.“ Final result practical diploma thesis: 5.5
September 2002	3 rd state examination („Assistentenprüfung für Apotheker“)
August 2001	2 nd state examination („Pharmazeutische Grundfächerprüfung“)
August 2000	1 st state examination („Naturwissenschaftliche Prüfung für Apotheker“)

August 1995 – July 1999 High school diploma (“Matura”) at Gymnasium Langenthal (specialization in latin “Typus B”). Final result: 4.23

Work Experience

December 2004 Temporary replacement at Apotheke Oensingen, S. Münch, Oensingen, Switzerland

September 2002 – March 2004 Temporary replacements at City Apotheke, Dr. D. Meier, Basel, Switzerland

March and September 2003 Temporary replacements at Dorfapotheke Meiringen, J. Schneider, Meiringen, Switzerland

September 2001 – September 2002 Practical year at City Apotheke, Dr. D. Meier, Basel, Switzerland

Additional Skills

Trainings

Spring Semester 2008 Seminar about scientific writing with Silvia Rogers, University of Basel

March 2007 Quality and GMP. Continuing education course of the Pharmacenter Basel-Zürich, Switzerland

March 2005 Method Development for GC und HPLC, Agilent Technologies (Schweiz) AG, Basel

Languages

German (native speaker)
English (fluent)
French (basic to good command)

PC Literacy

Proficient user

Applications

Good command of Microsoft Office applications

As a student and PhD student I have attended lectures and courses given by

Edwin Constable, Andreas Zuberbühler, Peter Strazewski, Urs Séquin, Peter C. Hauser, Peter C. Oelhafen, Gian Reto Plattner, Udo M. Spornitz, Konstantin Beier, Uwe Otten, Lukas Landmann, Daniel Haag-Wackernagel, Hansjakob Müller, Heinz Durrer, Alfred Fahr, Ruth U. Leu Marseiler, Peter Erb, Christoph Moroni, Alfons Hädener, Willi Hunziker, Niggi Iberg, Michael Kessler, Rudolf Bruppacher, Kurt Hersberger, Peter Huber, Axel Regeniter, Andre Scholer, Jürgen Drewe, Stefan Krähenbühl, Raymond Schlienger, Markus Lampert, Chritoph R. Meier, Stefan Mühlebach, Beat Ernst, Gert Folkers, Angelo Vedani, Jörg Huwyler, Willi Schaffner, Beat Meier, Karin Berger-Büter, Anna Seelig, Joachim Seelig, Hans Leuenberger, Georgios Imanidis, Dario Neri, Silvia Rogers, Theodor W. Güntert